Technical Report
TR-20-09
April 2020

Concrete caissons for 2BMA

Large scale test of design, material and construction method

Per Mårtensson
Carsten Vogt

SVENSK KÄRNBRÄNSLEHANTERING AB

SWEDISH NUCLEAR FUEL
AND WASTE MANAGEMENT CO

Box 3091, SE-169 03 Solna
Phone +46 8 459 84 00
skb.se

SVENSK KÄRNBRÄNSLEHANTERING

ISSN 1404-0344
SKB TR-20-09
ID 1697411
April 2020

Concrete caissons for 2BMA

Large scale test of design, material and construction method

Per Mårtensson, Svensk Kärnbränslehantering AB

Carsten Vogt, Betong och stålteknik

Keywords: Concrete, 2BMA, SFR, Repository, Caisson.

Abstract

In this report, experiences and results from the casting of a concrete caisson with the dimensions 18.1 × 9.36 × 4.6 meters in TAS08 in the Äspö Hard Rock Laboratory are presented. The work reported here covers all parts of the work from the initial design work and preparations prior to casting to long-term monitoring of the properties of the concrete caisson. The report also includes experiences from establishing and operating a mobile concrete production plant in the direct vicinity of the entrance to the Äspö tunnel.

Sammanfattning

I denna rapport presenteras erfarenheter och resultat från uppförande av en betongkassun med måtten 18,1 × 9,36 × 4,6 meter i TAS08 i Äspölaboratoriet. Arbetet som presenteras här innefattar samtliga delar från detaljerad design av kassunen och förberedelser inför gjutning till långtidsuppföljning av kassunens egenskaper. Rapporten redovisar även erfarenheter från uppförande och drift av en mobil betongstation i direkt anslutning till Äspölaboratoriets nedfartstunnel.

Contents

1 Introduction

1.1 The repository short-lived radioactive waste, SFR

The repository for short-lived radioactive waste, SFR has been in operation since 1988 and hosts operational waste from the Swedish nuclear power plants and from the other nuclear facilities. The repository includes underground waste vaults along with surface technical facilities. The waste vaults are located in granitic bedrock at a depth of about 60 meters below the Baltic Sea and are reached via two one-kilometre-long access tunnels from the ground surface.

The underground part of the existing facility, named SFR 1, consists of four 160-metre-long waste vaults and one 70-metre-high vault with a concrete silo with a total storage capacity of 63 000 m^3. The existing facility is shown in the top right part of Figure 1-1.

At present, plans are made to increase the storage capacity of SFR through the construction of 6 new waste vaults which will be located at a depth of 120 metres, i.e. at the same level as the bottom of the silo. These 6 waste vaults which are shown in the lower left part of Figure 1-1 will comprise of 4 vaults for low-level waste (2–5 BLA), one vault for intermediate level waste (2BMA) and one vault for reactor pressure vessels (BRT) each with a length of up to 275 meters. The work presented in this report relates primarily to 2BMA, see Section 1.2.

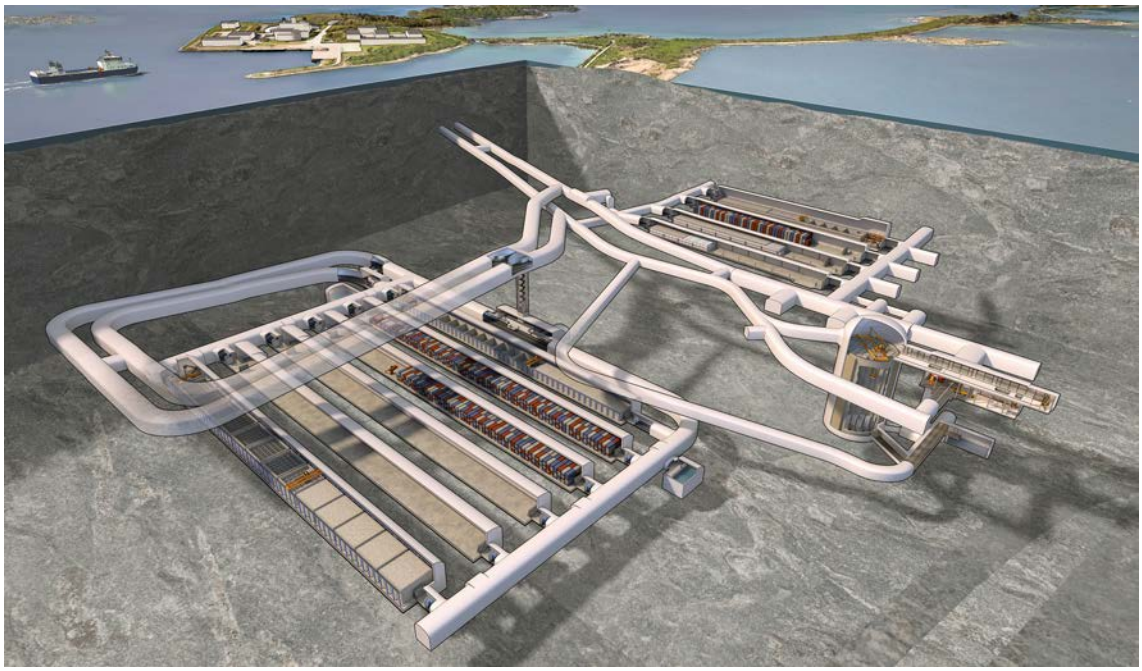

Figure 1-1. *An illustration of SFR. The existing facility is shown in the top right part and the planned extension in the lower left part of the illustration.*

1.2 The Rock vault for intermediate level waste, 2BMA

The rock vault for intermediate level waste, 2BMA will be in total about 275 meters long and contain a number of caissons in which the waste will be disposed, Figure 1-2. According to the present reference design the caissons shall have the dimensions of 18.1 × 18.1 × 9.0 meters, Figure 1-3, and be made from unreinforced concrete. The thickness of the walls and the base slab should be 680 mm and 600 mm respectively.

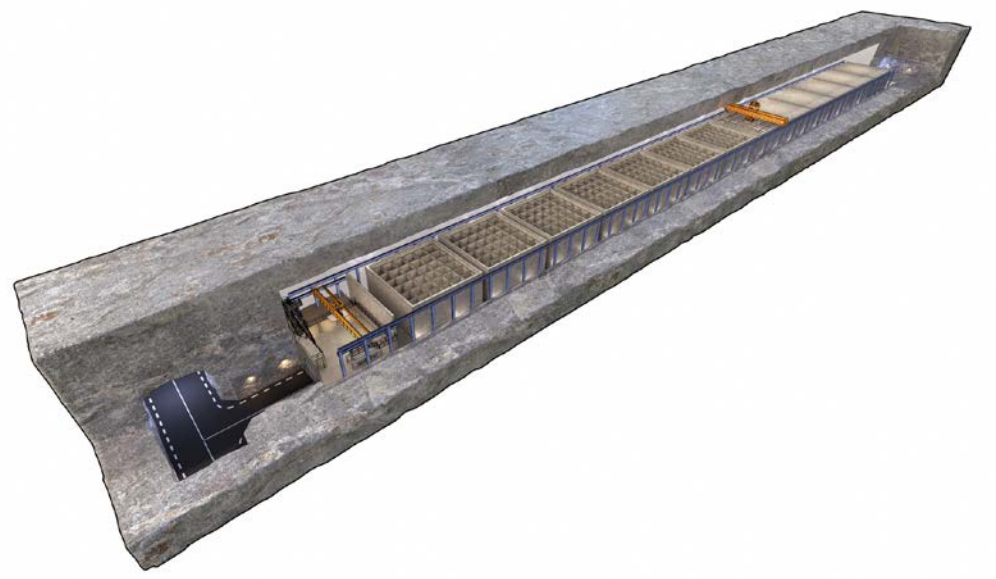

Figure 1-2. *The rock vault for intermediate level waste, 2BMA.*

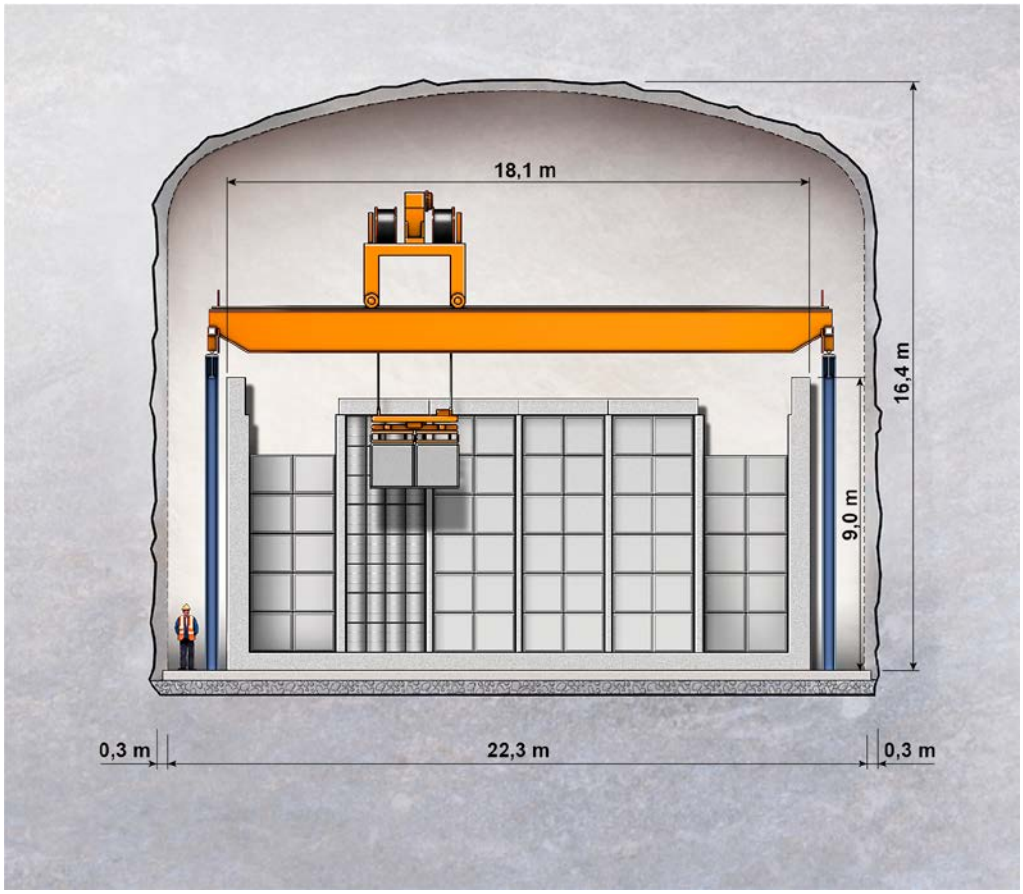

Figure 1-3. *Cross section of a caisson also showing the deposition of a waste container using an overhead crane.*

1.3 Material development

1.3.1 Prerequisites and requirements for concrete development

The following prerequisites and requirements apply regarding composition and properties of the concrete for the 2BMA concrete caissons.

Required properties of the fresh concrete

The following properties are required for the fresh concrete:

- **Setting time**: The setting of the concrete must be properly adjusted to avoid a high formwork pressure during casting of the walls but still long enough to facilitate proper homogenisation of the different concrete layers, thus avoiding unintended joints.
- **Workability**: The concrete must be pumpable for at least 3 hours from the time of production. Further, the concrete must also fill the mould completely so that no cavities are formed.
- **Stability**: Stone separation must not occur. Water separation may occur only to a very limited extent.
- **Pump ability**: The concrete should be pumpable and not separate during pumping.

Required properties of the hardened concrete

The following requirements apply:

- **Compressive strength:** The compressive strength at 90 days must exceed 50 MPa.
- **Tensile strength:** The tensile strength at 28 days must exceed 2.5 MPa.
- **Shrinkage:** Shrinkage should be minimized.
- **Internal strain:** Internal strain must be low to prevent the formation of cracks.
- **Porosity:** The concrete must have a low porosity in order to ensure a low hydraulic conductivity.

Prerequisites for choice of concrete components

The following conditions for selecting the concrete components must be considered:

- **Cement type**: The cement should be sulphate resistant, low alkali and have a low heat evolution.
- **Cement content**: Low cement content is preferred. However, the amount of paste in the concrete must not be reduced to the extent that the workability of the concrete is adversely affected.
- **Aggregates**: Aggregates produced from material that has emerged from the excavation of the repository should preferably be used. Natural sand and gravel should not be used.
- **W/C-ratio**: The water/cement ratio should preferably not exceed 0.50.
- **Admixtures (Liquid)**: Modern admixtures can be used but the amounts should be limited as far as possible.
- **Additives (Solid)**: Solid additives, such as different types of commercially available filler materials, can be used.

1.3.2 Summary of previous work conducted within the material development programme

Prior to the work presented in this report, several different studies which are briefly summarised in this section have been conducted. The focus in these studies have been the development of a concrete which fulfils the requirements presented in the preceding section but which can also be shown to ensure the post-closure safety of the repository.

Investigation of the suitability of the bedrock in SFR for aggregate production

The first part of the material development programme comprised an investigation of the bedrock in the future site for the SFR extension and evaluation of the possibility to use this rock for aggregate production for the concrete in 2BMA (Lagerblad et al. 2016).

Lagerblad et al. (2016) investigated samples from the bedrock of the present and the future repositories in the Forsmark area with focus on its suitability for aggregate production. The investigation showed that the excavated rock was acceptable, though not ideal and that suitable rock material would have to be selected during the excavation work whereas the less suitable material must be discarded. Lagerblad et al. (2016) also showed that there were quarries in the near region where rock material with similar properties as those of the material from the Forsmark area could be obtained for production of aggregates to be used in the material development programme.

Concrete development

The second part of the material development programme comprised development of a concrete with the desired properties.

In the development work Lagerblad et al. (2017) focused on the use of commercial filler materials as additives to compensate for the low cement content required to keep the heat of hydration at low levels. By the use of commercial fillers, aggregates entirely produced from crushed rock could be used and the workability of the fresh concrete acceptable. However, Lagerblad et al. (2017) also showed that commercial fillers made of fine grained lime stone could act as an accelerator during concrete hydration and both reduce the time until the concrete starts too harden as well as enhance the rate of hydration once hydration has been initiated. See also the following section.

The concrete finally recommended by Lagerblad et al. (2017) was based on the use of Degerhamn Anläggningscement from Cementa AB and aggregates obtained from crushed rock with similar properties as that expected to be obtained from the excavation of the repository. The mix design is presented in Table 1-1.

Table 1-1. Composition of the concrete recommended for use in 2BMA (Lagerblad et al. 2017).

Component	Products name/supplier	Amount (kg/m^3)
Cement	Degerhamn anläggningscement (CEM I)	320
Limestone filler	OmyaCarb 2GU (grain size: 2 μm)	130
Limestone filler	Myanit 10 (grain size: 10 μm)	33.3
Water		156.8
Aggregates 16–22 mm	Crushed rock	393.3
Aggregates 8–16 mm	Crushed rock	425.7
Aggregates 4–8 mm	Crushed rock	92.0
Aggregates 0–4 mm	Crushed rock	840.9
Superplasticiser	MasterGlenium Sky 558	1.30
Superplasticiser	Master Sure 910	1.70
Retarder	Master Set RT 401	0.96 (0.3 % of cement weight)

Large scale test of design and material

The third part of the material development programme comprised concrete production scale mixing, transport and pump tests at a commercial concrete production plant as well as casting of large concrete structures representative for the concrete caissons in 2BMA in a tunnel section at a depth of about 400 m below ground level in the Äspö Hard Rock Laboratory. In this work also aspects of design and engineering was included (Mårtensson and Vogt 2019).

The main conclusions from this work were that the concrete developed by Lagerblad et al. (2017) could be produced on a production scale and used for casting of large concrete structures. The study also showed that the hydraulic properties of the joints between different construction parts were similar to those of the bulk concrete. This indicates that the walls of the caissons could be cast subsequent to the base slab. This would make construction significantly simplified compared to the current reference method in which casting of the caisson in one uninterrupted sequence is required.

Long-term monitoring showed that the concrete structures were free from cracks still more than 1 year after casting and that the levels of internal strain were low. Here, it must be remarked that the monitoring period also included a period of 6 months during which the concrete structure was covered by a tarpaulin and dried out in an atmosphere with RH about 60 %.

However, Mårtensson and Vogt (2019) also showed that the concrete used in this test was sensitive to long transports and large problems with controlling the setting time of the concrete were encountered. For this reason Mårtensson and Vogt (2019) concluded that concrete production for future large scale experiments as well as construction of the caissons in 2BMA should utilise a concrete plant placed in the near vicinity of the tunnel entrance.

1.4 Programme for design and construction method

1.4.1 Prerequisites and requirements regarding design and construction method

The following prerequisites and requirements apply regarding design of the concrete caissons and choice of construction method. As a consequence of experiences made during previous work; these differ somewhat from the original prerequisites and requirements presented in Mårtensson and Vogt (2019).

- **Dimensions**: The dimensions of the concrete caissons are $18.1 \times 18.1 \times 9.0$ m. (l × w × h). Thickness of the walls and base slab is 680 mm and 600 mm respectively.
- **Formwork**: Casting of the concrete caissons should be done using a formwork designed without the use of form rods to avoid the risk for future formation of hydraulically conducting channels through the walls.
- **Casting**: Walls and base slab can be cast separately if it can be proven that the hydraulic properties of the joint are similar to those of the bulk concrete.
- **Foundation**: The foundation of the caissons must permit unrestricted movements of the caissons caused by e.g. shrinkage and expansion due to the annual variations of temperature and relative humidity in the repository or the concretes´ heat of hydration during casting.
- **Load cases**: The following dimensioning loads have been taken into account in the design and construction of the caissons;
  - Internal gas pressure due to gas formation from decomposition of waste.
  - Load from backfill material.
  - Load of waste.
  - Load of dropped waste container.
  - Accidental shock from overhead crane.
  - Load from falling block.
  - One-sided external water pressure during resaturation of the repository after closure.
- **Gas permeability**: No explicit requirements for the gas permeability of the concrete have been formulated. Instead, gas arising from corrosion of the waste, for example, will be expelled from the concrete structure through a dedicated gas-relief system.
- **Repository environment**: The concrete should be formulated with regard to the exposure class in the repository. Expected environment corresponds to marine environment.
- **Reinforcement**: No steel reinforcement can be used.

1.4.2 Summary of previous work conducted within the programme for design and construction method

The main focus of this programme was on engineering aspects related to the construction on the concrete caissons with particular emphasis on methods that could be utilised to avoid the formation of cracks during construction and operation. The programme has so far covered a number of topics and the results are briefly summarised below.

Foundation

In order reduce the risk of crack formation in the base slab due to a high degree of restraint between the foundation and the base slab of the caisson it was suggested to cover the concrete base slab that made up the foundation with a thick reinforced plastic foil (Mårtensson and Vogt 2019).

Visual inspections and results from the monitoring system showed that no cracks had formed in the concrete during the first 2 years after casting. Instead, measurements of the external dimensions indicated global shrinkage of the concrete structure. It was thus concluded that the use of this type of foundation was a suitable tool to reduce the risk for crack formation.

Formwork design

From the original requirements it was identified that casting of walls and base slab in one uninterrupted sequence should be utilised in order to avoid hydraulically conducting joints called for the use of a suspended formwork system. However, this also required that the base slab formwork was at least partly covered with board. This was motivated with an identified risk that the wet concrete in the walls would exert a pressure on the not yet hardened concrete in the base slab and push it out of the formwork. In the work presented by Mårtensson and Vogt (2019) it was therefore decided to investigate the consequences of this by completely covering the base slab during casting of the part denoted “Section 1”.

Experiences from this work showed that covering the base slab caused major problems during casting. This was caused by both the unexpectedly fast setting of the concrete but also that a covered formwork with openings for concrete pouring required that the concrete hose was moved more or less continuously in order to homogeneously fill the formwork. However, in spite of large efforts, the surface of the base slab was very rough with many parts with poor filling and air blisters.

The conclusions from this work was therefore that covering the entire formwork of a full scale caisson would require very careful adjustments of the setting time of the concrete but also tremendous efforts during casting. For this reason, covering the formwork of the base slab could not be recommended. This suggests that casting the walls and the base slab in one uninterrupted sequence according to the tested method would be associated with large risks and other options should therefore be sought for.

Sequential casting of base slab and walls

The main concern related to sequential casting of base slab and walls was related to the risk for early formation of cracks in the walls caused by restrained shrinkage of the concrete upon cooling. However, concerns were also made that the joint between the walls and the base slab should constitute a hydraulically conducting zone due to poor adhesion between these two parts as well as high porosity of the concrete in this region.

In the work presented by Mårtensson and Vogt (2019) it was therefore decided to investigate the consequences of sequential casting of base slab and walls by casting a second wall denoted “Section 2” on top of the base slab of Section 1.

Short- and long-term monitoring of the results from casting of Section 2 showed that no cracks were formed in the walls or in the base slab during the first 24 months after casting. Further, measurements showed that the hydraulic conductivity of the joint was similar to that of the bulk concrete, implying that no hydraulically conducting zone had been formed in or close to the joint. It was thus concluded that sequential casting of walls and base slab is a feasible method to be used during construction of a concrete caisson.

1.5 Purpose and goal of the work presented in this report

The main purposes of the work presented in this report are the following:

- To conduct a large scale concrete production test to verify consistent quality.
- To perform a production scale test casting of a concrete caisson representative of the concrete caissons for 2BMA.
- To verify that restraint between the foundation and the caisson base slab can be mitigated by founding the caissons on a smooth concrete slab covered with plastic sheet in order to reduce the adhesion between these parts.
- To investigate the effects of warming the base slab prior to casting of the walls as a means to mitigate the effect of temperature shrinkage of the walls after casting.
- To study the hydraulic properties of the joint between the base slab and the walls of the concrete caisson.
- To perform long term follow-up of the properties of the caisson and the effect of the climate in the repository on these properties.
- To develop methods for sealing the holes from the tie rods and study the hydraulic properties of the sealed holes.

1.6 Purpose and scope of this report

The purpose of this report is to present the results from the work covered by the bullet points presented in Section 1.5. It is further the purpose of this report to recommend a method for erecting the base slab and outer walls of the caissons in the future 2BMA. The report does, however, not cover construction methods and materials for the inner walls. This will be reported elsewhere.

1.7 Structure of this report

The report is divided into 13 chapters and 5 appendices with the following content:

Chapter 1: Chapter 1 presents a background to the work presented in this report. Here concrete pre-requisites and requirements as well as short descriptions of the material and technology development programmes are found.

Chapter 2: Chapter 2 presents the suggested design of the concrete caisson to be cast in TAS08 in the Äspö laboratory. The work starts with an analysis of the available space in TAS08 as well as of the restraint situation in a full scale caisson.

Chapter 3: Chapter 3 presents the instrumentation used in the long-term monitoring of the concrete properties. Here the different sensors and their positions in the concrete structure are presented.

Chapter 4: Chapter 4 presents the preparations in TAS08 prior to casting.

Chapter 5: Chapter 5 presents the above ground preparations, including commissioning of the concrete production plant, material handling and mixing tests.

Chapter 6: Chapter 6 presents test castings which were performed in order to verify a correct function of the strain transducers.

Chapter 7: Chapter 7 presents the casting of the base slab of the caisson including all steps from formwork design through casting but also including post casting inspection and material investigations.

Chapter 8: Chapter 8 presents the casting of the walls of the concrete caisson including all steps from formwork design through casting but also including post casting inspection and material investigations.

Chapter 9: Chapter 9 presents work conducted in order to investigate the possibility to remove the plastic tubes used to cover the tie rods used to keep the wall formwork together and the subsequent filling of the holes with a cementitious grout.

Chapter 10: Chapter 10 presents the results from the long-term monitoring programme of the base slab.

Chapter 11: Chapter 11 presents the results from the long-term monitoring programme of the walls.

Chapter 12: Chapter 12 presents a summary of the work presented in this report.

Chapter 13: Chapter 13 finally presents the conclusions from this work and gives recommendations regarding materials and methods to be used for construction of the caissons in 2BMA. Also additional future work is discussed.

Appendix A: Appendix A presents raw data from the truck mixers showing the amount of each component in each concrete mix.

Appendix B: Appendix B presents measurements of thermal expansion of concrete specimens.

Appendix C: Appendix C presents heat calculations and thermal risk calculations.

Appendix D: Appendix D presents computation details for the base slab.

Appendix E: Appendix E presents computation details for the walls.

2 Design of the concrete caisson

In this chapter the design of the concrete caisson to be cast in a side tunnel (TAS08) at Äspö Hard Rock Laboratory is described.

2.1 Prerequisites

2.1.1 Location and dimensions of TAS08

TAS08 is situated in TASU at a depth of approximately 410 m below ground in Äspö hard rock laboratory, Figure 2-1. The dimensions of TAS08 are 26.5 × 15.5 meters (Figure 2-2) with a maximum height of about 7 meters in the centre of the tunnel. However, closer to the walls the height is only 4–5 meters, Figure 2-5.

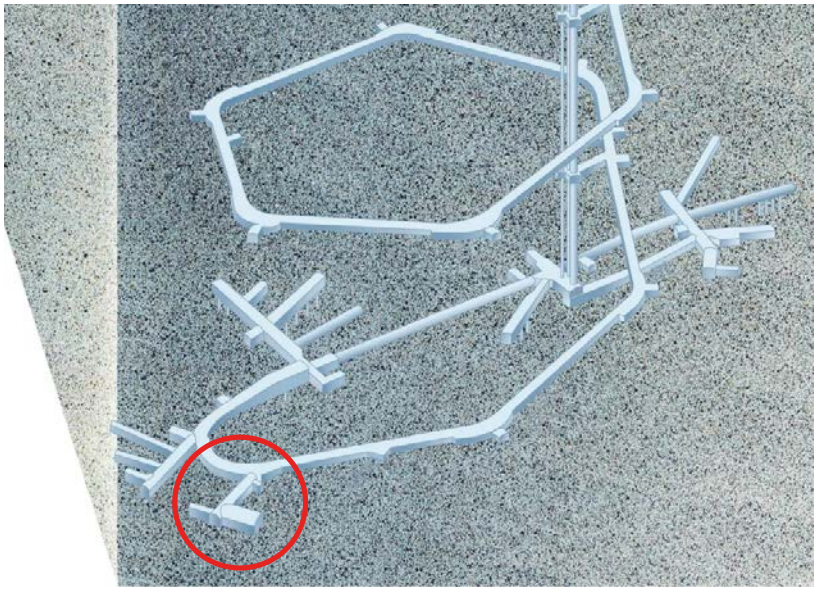

Figure 2-1. *Overview of the underground part of the Äspö Hard Rock Laboratory. TAS08 is the widest of the shorter tunnels in the red circle.*

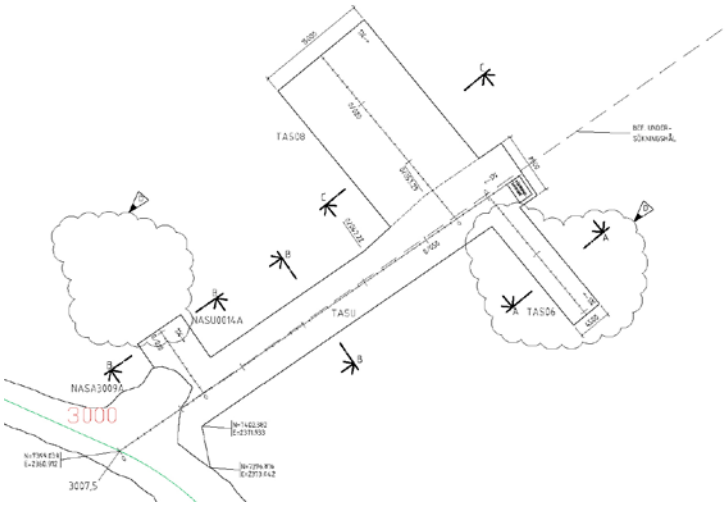

Figure 2-2. *Location and dimensions of TAS08.*

2.1.2 Tunnel climate

The annual variations in temperature and relative humidity in the main tunnel at a distance of about 100 meters from TAS08 are shown in Figure 2-3.

As can be seen from Figure 2-3, annual temperature variations are small, while the relative humidity varies somewhat more. From the raw data from the measurement system, the mean values are:

- Temperature: 15.7 °C
- Relative humidity: 83.9 %

2.1.3 Foundation for the concrete caisson

In order to allow for casting of a caisson with maximum height, the foundation should be as low as possible. In principle, there are two alternatives: casting an unreinforced concrete slab directly on the rock floor or using the more traditional design where a reinforced concrete slab is cast on a layer of draining material.

Here, the foundation should be constructed using the method that allows for the highest caisson to be cast, also taking into consideration the need for sufficient working space during this work. For that reason, it was decided that the foundation should constitute a concrete slab which was cast directly onto the rock floor and that the rock floor prior to this should be cleaned from all rock debris from the excavation of TAS08. See also Chapter 4.

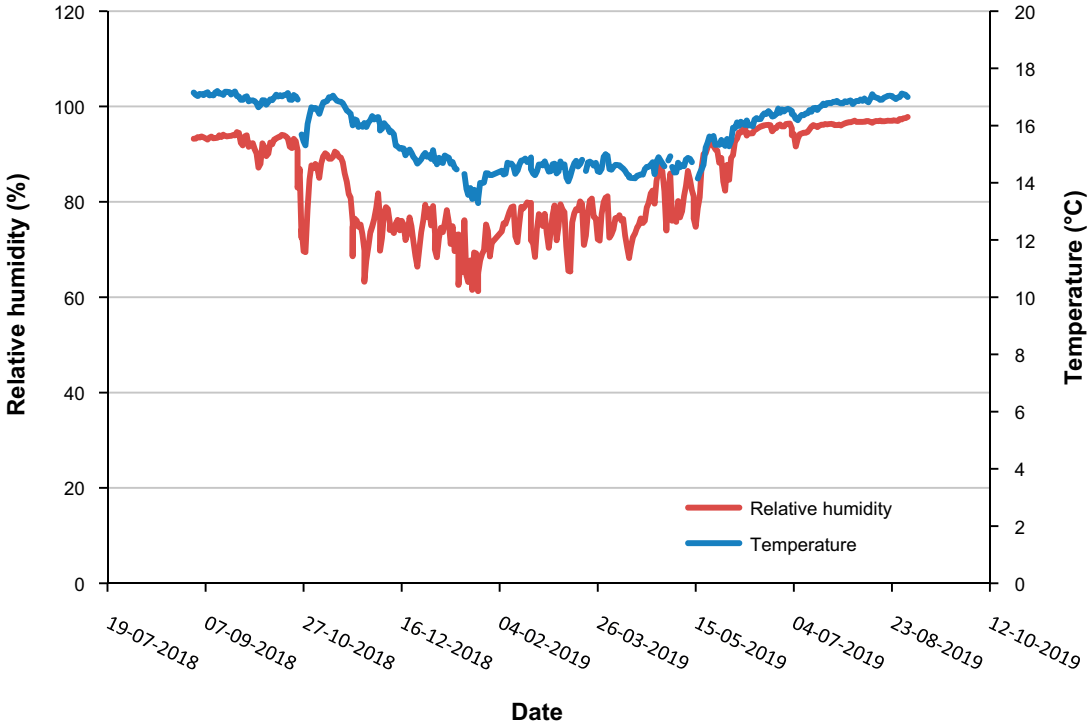

Figure 2-3. *Temperature and relative humidity in the main tunnel at a distance of about 100 meters from TAS08.*

2.1.4 Available space for casting of caisson in TAS08

From 3D-laser scanning of TAS08, the maximum dimensions of TAS08 were estimated to 26.5 × 15.5 × 7 m. However, the available volume is only about 24 m in length, 14 m in width and 5–6 m in height.

The end wall of TAS08 must be available for other experiments with a space requirement of approximately 3–4 m from the end wall. No additional requirements on availability of the side walls were presented to this project. This gives an available length and height for casting of about 20 × 4.6 meters respectively, Figure 2-4.

Further, a certain work space between the top of the wall and the tunnel roof of about 1.5 meters is required, red areas in Figures 2-4 and 2-5. This leaves a height of about 4.6 m and a width of 10–11 m for the test casting, see Figure 2-5.

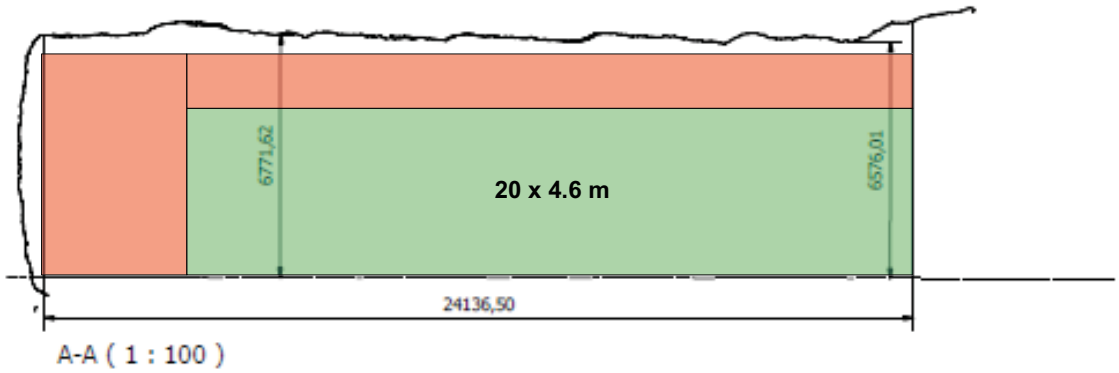

Figure 2-4. *Available length and height for casting of the caisson (green) and required working space (red). Not to scale.*

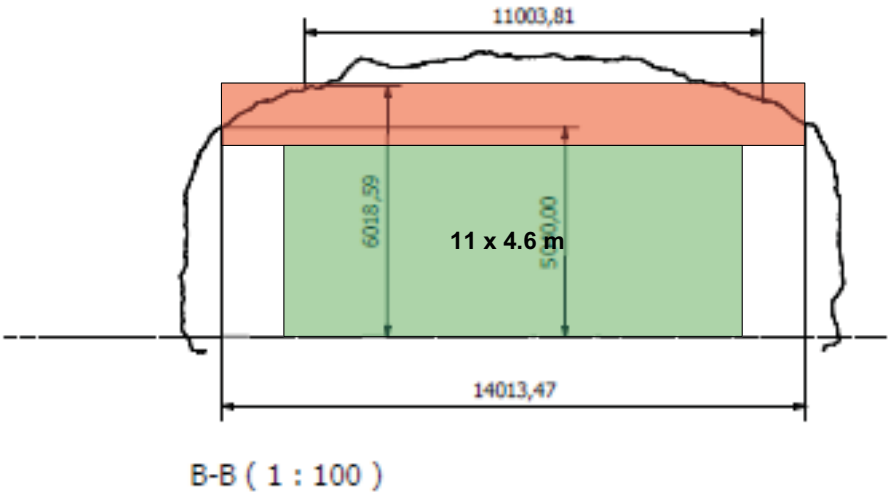

Figure 2-5. *Available width and height for casting of the caisson (green) and required working space (red). Not to scale.*

2.2 Design and dimensions of the concrete caisson

In the previous section, an estimate of the available space for the casting of the concrete caisson in TAS08 was presented. As the dimensions of TAS08 do not allow for a casting of a full-scale caisson, the dimensions of the caisson have to be adjusted to the available space. In order for the caisson in TAS08 to be representative for the full-scale caissons in terms of temperature evolution and levels of internal strain scaling need to be carefully calculated.

The available space in TAS08 allows for casting of a caisson, of which the length of one side equals that of the full-scale caisson. However the limited height of TAS08 only allows for a maximum height of the caisson of 4.6 meters. In order to obtain a similar degree of restraint in the test casting as in the future 2BMA caissons, a similar length: height-ratio (L/H) is desired. As 4.6 meters roughly equals half of the height of the full-scale caisson, the width of the caisson in TAS08 should be roughly half the width of the full-scale caissons.

According to the reference design the dimensions of the caissons should be 18.1×18.1× 9.0 meters. A rough estimation of the degree of restraint in wall-on-slab structures is based on the free L/H. The free width of the walls of a full-scale caisson is $18.1 - 2 \times 0.68 = 16.74$ m where 0.68 meters is the thickness of the walls. The height of the walls above the base slab is $9 - 0.6 = 8.4$ m where 0.6 meters corresponds to the thickness of the base slab. This gives a free L/H of 1.99 for the walls.

Applying this principle to the shorter walls and keeping the L/H identical, a free wall height of 4 m and a L/H of $1.99 \approx 2$ gives a outer width of the caisson of 2 × (height of the caisson) + 2 × (thickness of the walls which in numbers give a width of $(2 \times 4) + (2 \times 0.68) = 9.36$ m.

This means that the outer dimensions of the caisson of $18.1 \times 9.32 \times 4.6$ m give 2 walls with the same length as the caissons in the future 2BMA and 2 walls the same free L/H as the 2BMA caissons. These dimensions also provide for sufficient working space in TAS08, Figures 2-6 and 2-7.

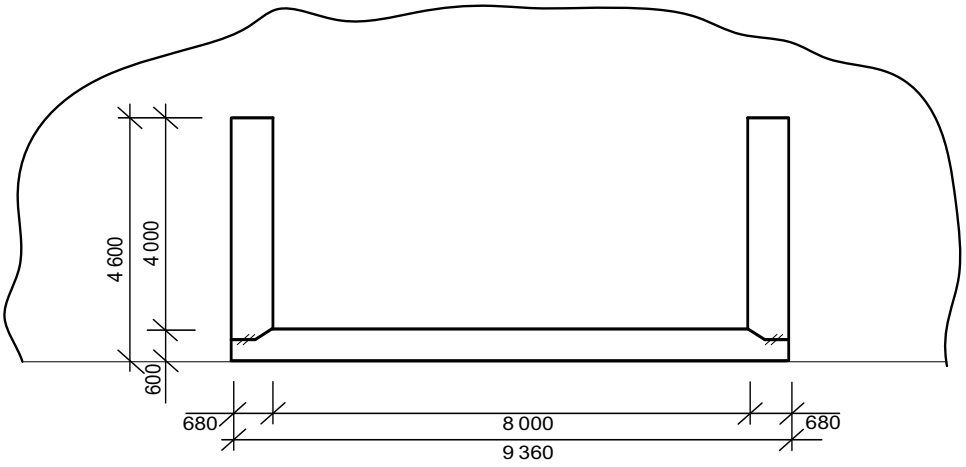

Figure 2-6. *Width of the caisson.*

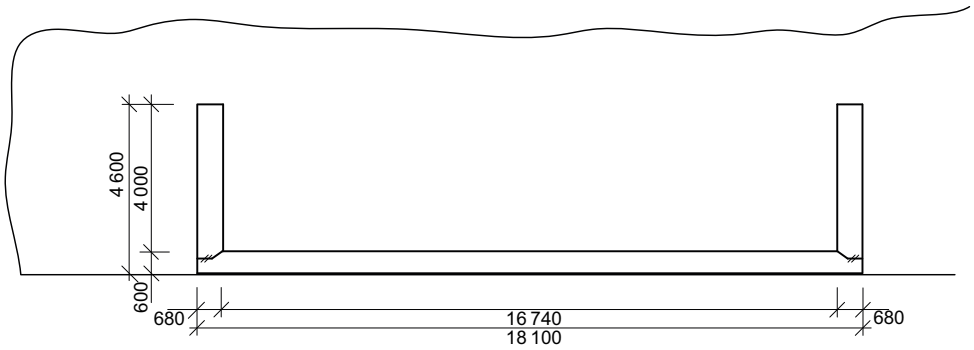

Figure 2-7. *Length of the caisson.*

2.2.1 Design details

The use of unreinforced concrete stipulates the need to reduce stress peaks, likely to occur at corners and changes of dimensions. Therefore, the basic design stipulates a casting joint between slab and wall that is partly inclined, see Figure 2-8. Also, the inner corner of the outer walls shall be executed with chamfers, 150 mm at an angle of 45° (Könonen and Olsson 2017).

2.2.2 Joint seals

Mårtensson and Vogt (2019) showed that the hydraulic properties of the joint between the base slab and the wall (denominated *Section 2*) were in the same range as those of the bulk concrete. This could motivate the exclusion of the joint seal in the future full-scale caisson. However, in order to further strengthen the basis for a future decision on the use of joints seals, it was decided that joint seals should be used also here. Joint seals made of 300 mm wide and 1.5 mm thick copper sheets were therefore placed in the joint between the base slab and the walls as illustrated in Figure 2-9.

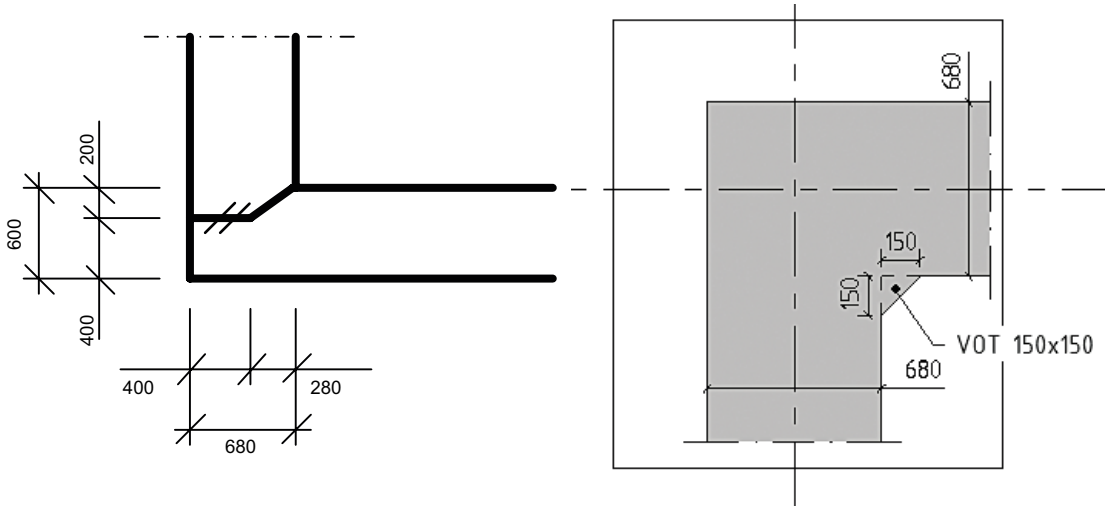

Figure 2-8. *Details showing the joint between the slab and the wall (left) and a chamfer in corner of the outer walls.*

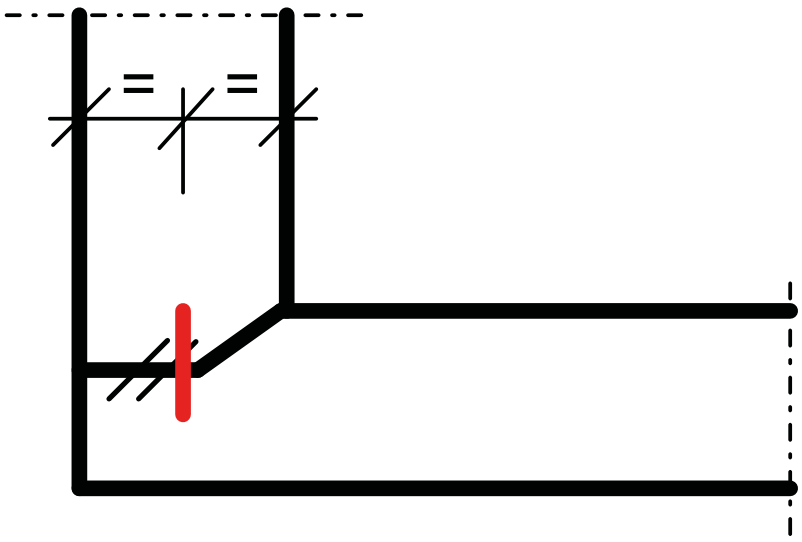

Figure 2-9. *Placement of joint seals in the joint between the base slab and the walls.*

2.3 Formwork design

Based on the results from the previous casting in TAS05 (Mårtensson and Vogt 2019) it was early decided that the caisson should be erected according to standard principles by first casting the base slab and later the walls. The time between casting of slab and walls would be expected to be about 5 weeks, i.e. enough for the concrete to harden and preparations for wall casting to be made.

2.3.1 Base slab

The formwork for the base slab was designed according to standard principles with supports against the adjacent rock wall and secured by bolts into the underlying concrete foundation.

However, in addition to the standard formwork, also on-site built formwork for the recess in the position of the future walls was constructed. This also allows for the fastening of the joint seals.

The formwork pressure from the fresh concrete was expected to be low and no additional measures other than those normally used were expected.

2.3.2 Walls

It was early decided to use a lightweight framed formwork or board framework manufactured on site.

However, the requirements emanating from the analysis of the post closure safety of the repository states that form rods must not be used in the formwork and that any kind of cast-in steel components should be avoided in the repository structures in 2BMA. With these requirements a formwork which is supported against the adjacent rock wall and/or against a supporting construction frame placed on the base slab must be used.

However, due to the limited space available in TAS08 the use of large lifting devices such as those required to handle supporting construction frames were not possible. It was therefore decided to use a traditional formwork system with tie rods of steel and some additional braces. However, in order to be able to remove the tie rods after casting additional plastic tubes were installed in order to ensure that the tie rods did not come in contact with the wet concrete.

Even though this is a deviation from the basic design it was acknowledged that the advantages clearly outweighed the disadvantages. The use of tie rods allowed for a larger caisson to be cast safely, which will increase the similarity to the full-scale caisson. The installation of the required sensors was also simplified when tie rods are available. Also, the use of protective plastic tubes ensures that the temperature sensors are isolated from the highly heat conducting steel tie rods. Most importantly, the tie rods will not influence the behaviour of the caisson in any way with respect to temperature evolution, strain, change of dimension or change of humidity.

The major disadvantage is that a formwork supported by supporting construction frames as required in the future 2BMA will not be tested in practice. However, since the dimensions of the current caisson (mainly height) differ from the full-scale caisson it would not have been a completely representative test in any case.

3 Instrumentation

In order to be able to follow the evolution of the concrete properties; the caisson was instrumented with different types of sensors to log temperature, relative humidity, internal strain and changes of external dimensions. During casting, also the formwork pressure was monitored in order to ensure a safe casting.

In this chapter, the instrumentation program of the caisson is presented. The setup is based on experiences from the previous work by Mårtensson and Vogt (2019). The programme includes a certain redundancy of the instrumentation system.

3.1 Temperature

Two types of sensors were used for temperature registration. Ready-to-use sensors of the PT 100 type (platinum temperature sensor according to EN 60751) were used for the logging of the ambient temperature and heat of hydration of the hardening concrete was measured using simple type T (Cu-CuNi) thermocouples. A double setup was used for redundancy. A total of 16 thermocouples were considered sufficient for monitoring the heat evolution of the concrete and pre-heating of the slab.

Additionally, the temperature was measured at the position of the strain gauges. The placement of the temperature sensors (except the ones included in the strain gauges) is shown in Figure 3-1.

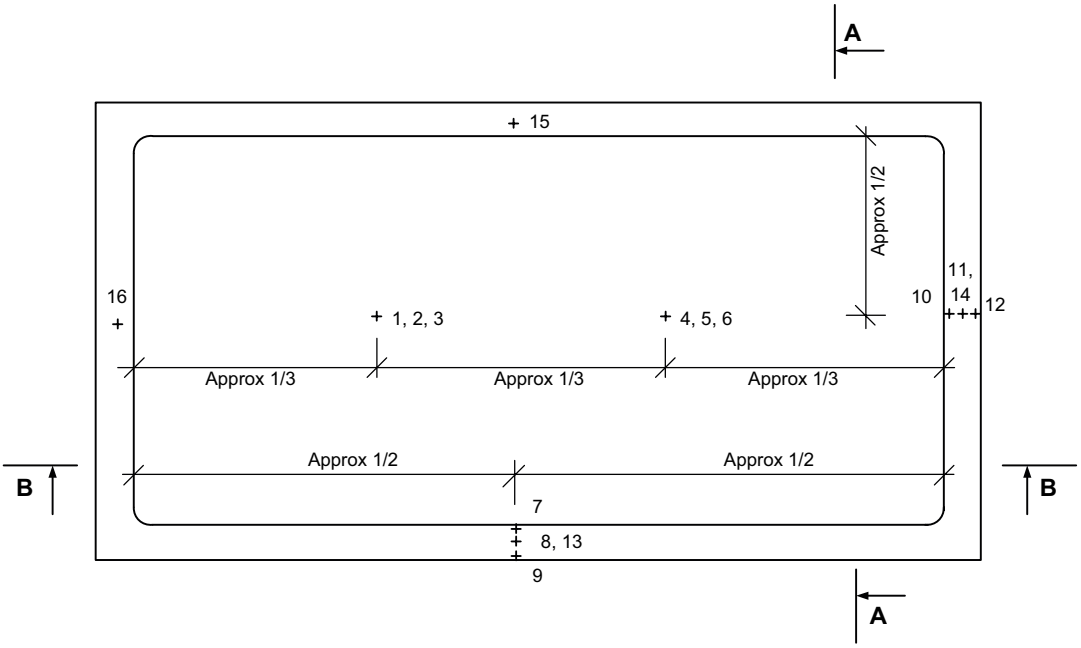

Figure 3-1. *Continuing.*

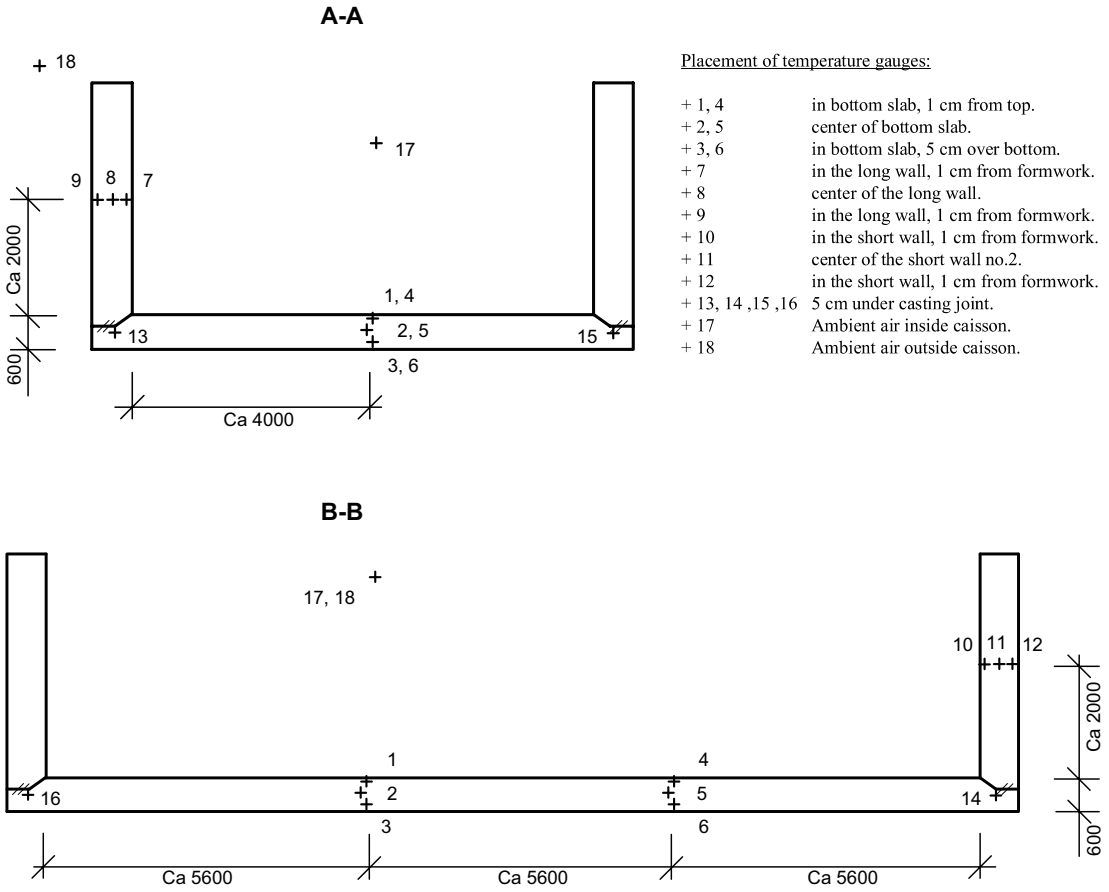

Figure 3-1. *Placement of temperature gauges. The topmost illustration shows the caisson from above whereas the middle and lower illustrations show side-view images of the caisson.*

3.2 Internal strain

3.2.1 Strain transducers

Ready to use strain gauge transducer

There is a wide selection of ready-to-use strain transducers commercially available. The strain gauges work according to different principles. Three different types used in civil engineering are strain gauge transducer, vibrating wire transducer and fibre optic sensing. Based on the experiences in TAS05, strain gauge transducers were also used here.

Strain gauge transducers work with strain gauges attached to a medium (usually some type of metal rod with attached end caps) and an outer sealing, see Figure 3-2. When the metal rod is subjected to forces and is deformed, the strain gauge inside the transducer will deform as well and the resulting change in voltage can be related to the strain. The commonly used transducers have measuring lengths from 30 mm to 200 mm. This type of sensor with a measuring length of 100 mm was also used in the previous work by Mårtensson and Vogt (2019).

Manufactured strain transducers

Manufactured strain transducers are basically up-scaled strain gauge transducers and have been successfully created and installed in previous projects. These transducers have typical measuring lengths of 2 meters. The longer measuring distance reduces the number of required channels for data recording. Additionally, the probability of directly measuring “over” an eventual crack increases with increasing length of the transducer. Figure 3-3 shows a manufactured strain transducer prior to installation.

Figure 3-2. *Strain gauge transducer.*

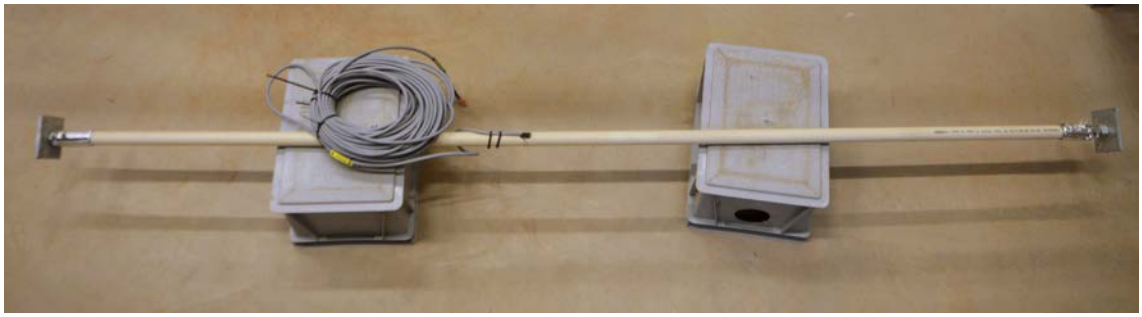

Figure 3-3. *Manufactured strain transducer.*

Setup

A total of 8 manufactured strain gauge transducers each with a length of 2 500 mm and 6 commercial strain gauges with a length of 200 mm were used to monitor the internal strains in the caisson. Figures 3-4, 3-5 and 3-6 show the placement of the strain transducers in the concrete caisson.

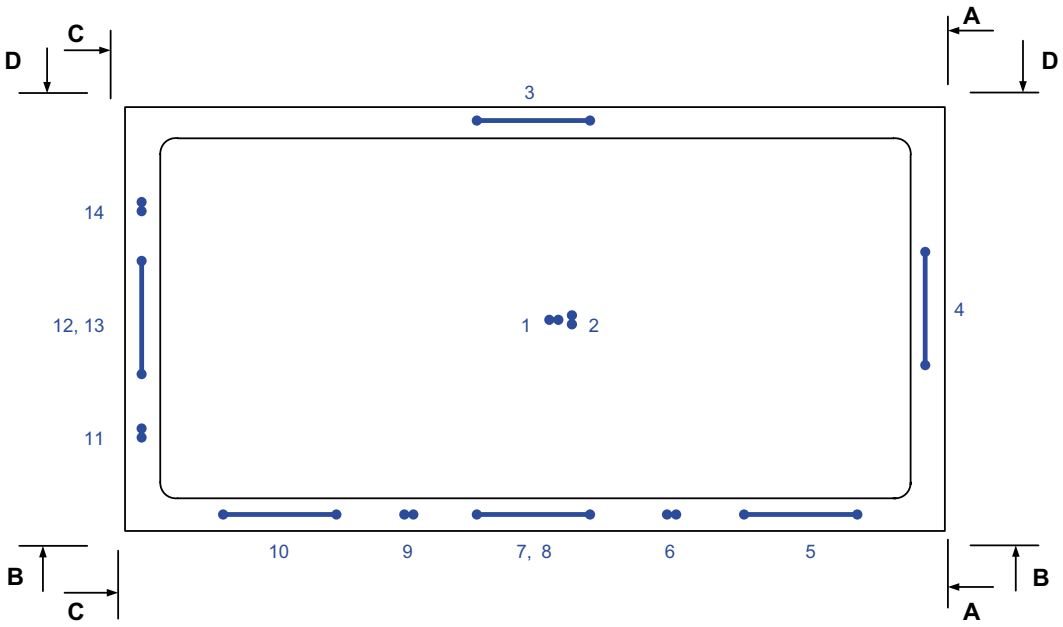

Figure 3-4. *Top-view illustration of the caisson showing the placement of the strain transducers.*

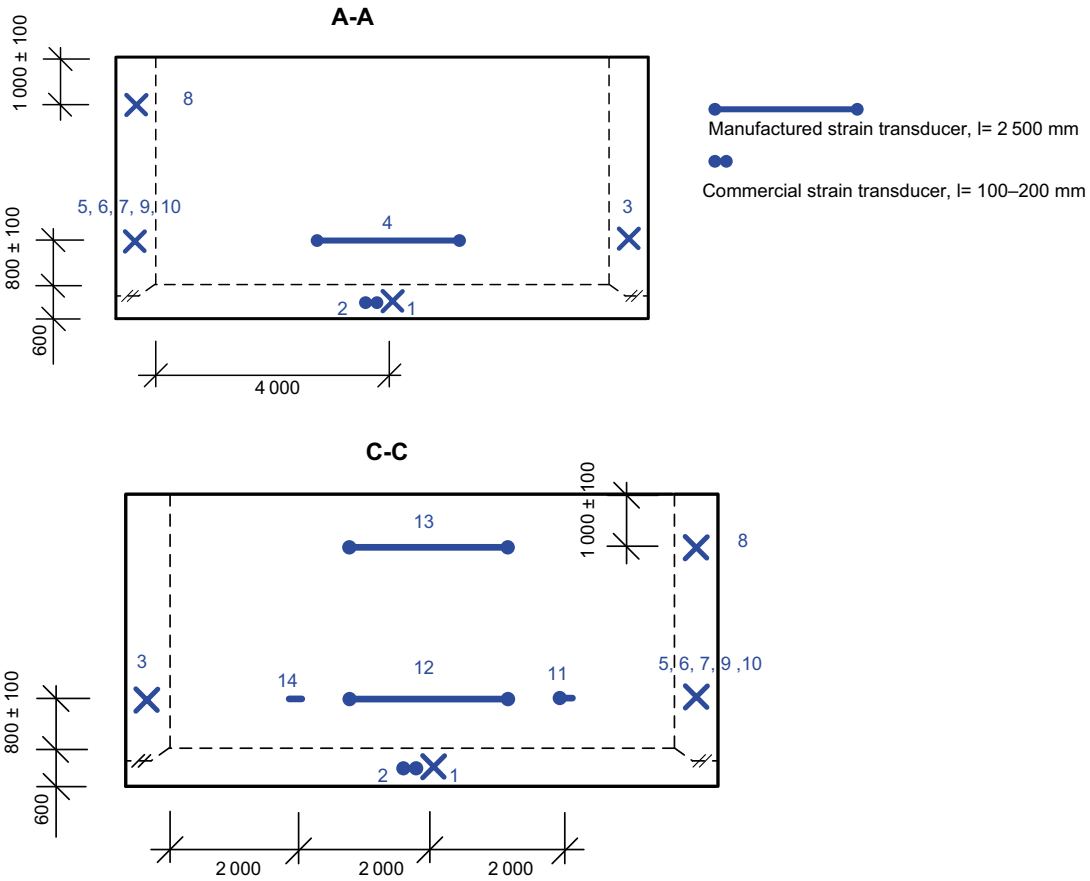

Figure 3-5. *Side-view illustration of the two short walls of the caisson showing the placement of the strain transducers.*

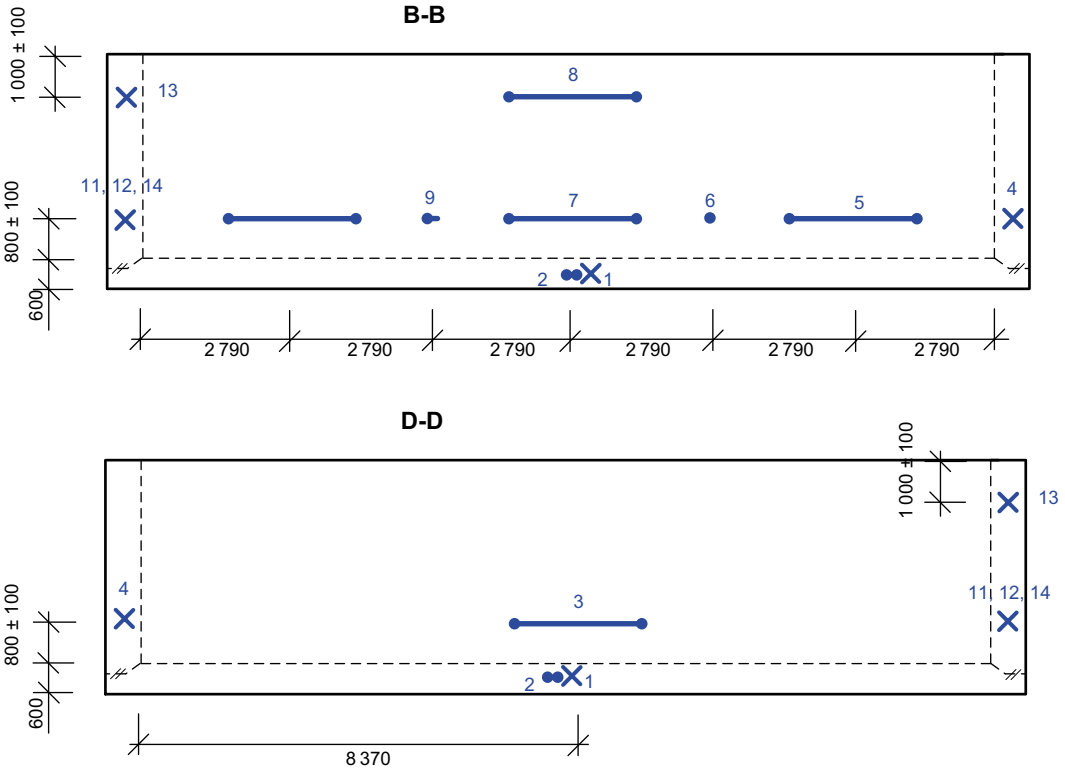

Figure 3-6. *Side-view illustration of the two long walls of the caisson showing the placement of the strain transducers.*

3.3 External dimensions

Measurements of the external dimensions of the caisson were made using external LVDT sensors (Linear Variable Differential Transformer).

A total of 4 LVDT sensors, arranged as displayed in Figure 3-7, were used to monitor the external dimensions of the caisson. Sensors 1 and 2 were installed on supporting bars attached directly to the foundation prior to start of the heating of the base slab in order to monitor the dimensional changes of the base slab during heating. These were also used for long-term monitoring of the dimensional changes in the base slab due to cooling and drying caused by climate variations in the tunnel during which the changes were compared with changes higher up on the walls, sensors 3 and 4.

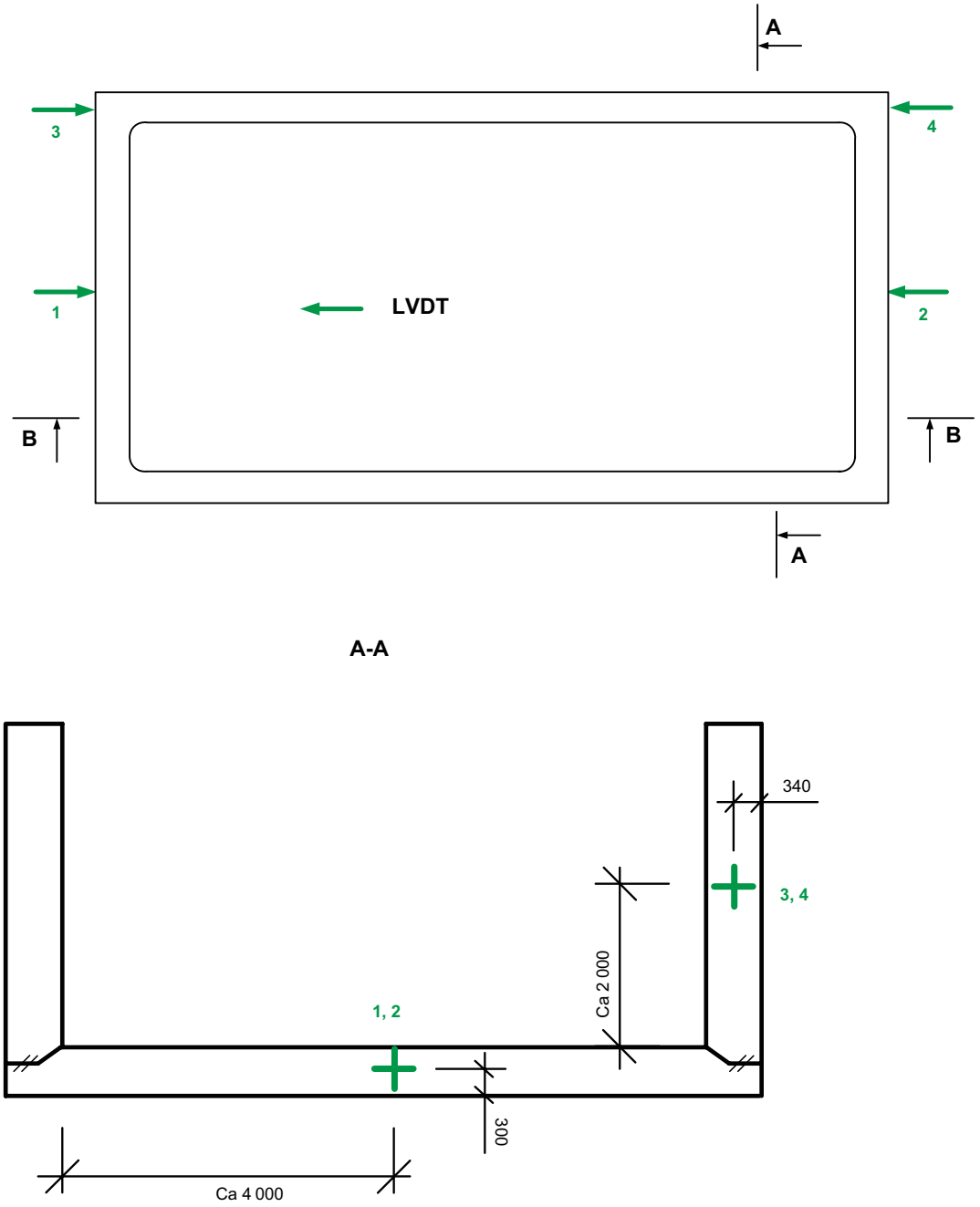

Figure 3-7. *Placement of the LVDT sensors. The upper illustration shows the caisson from above whereas the lower illustrations show side-view images of the caisson.*

3.4 Formwork pressure

Formwork pressure is usually monitored using (i) load cells attached in between formwork and tie rods, (ii) strain gauges attached to the tie rods or (iii) pressure cells installed in the formwork itself. The last method was used when casting the dome plug in the Dome Plug experiments (Grahm et al. 2015).

When using monitoring methods (i) and (ii) the evaluation of the results and their relationship to actual formwork pressure is rather difficult. This is due to the fact that a formwork is a hyperstatic system. The redistribution of loads between individual tie rods as a result of deformations is difficult to assess due to often uneven formwork stiffness. Also, the influence of individual pre-stressing levels of the tie rods complicates the evaluation.

Therefore, the use of pressure cells installed in the formwork and in direct contact with the concrete (method iii), which monitors the pressure of concrete on the formwork is much easier to evaluate. Limitations are mainly the use of very stiff concrete since contact between concrete and pressure cell is essential. Also, reasonably stiff formwork is required. Figure 3-8 shows a pressure cell installed in a formwork. Figure 3-9 shows the setup for the pressure cells in the formwork of the walls to the caisson in TAS08.

Figure 3-8. *A pressure sensor installed in the formwork of the Dome Plug at Äspö. From Grahm et al. (2015).*

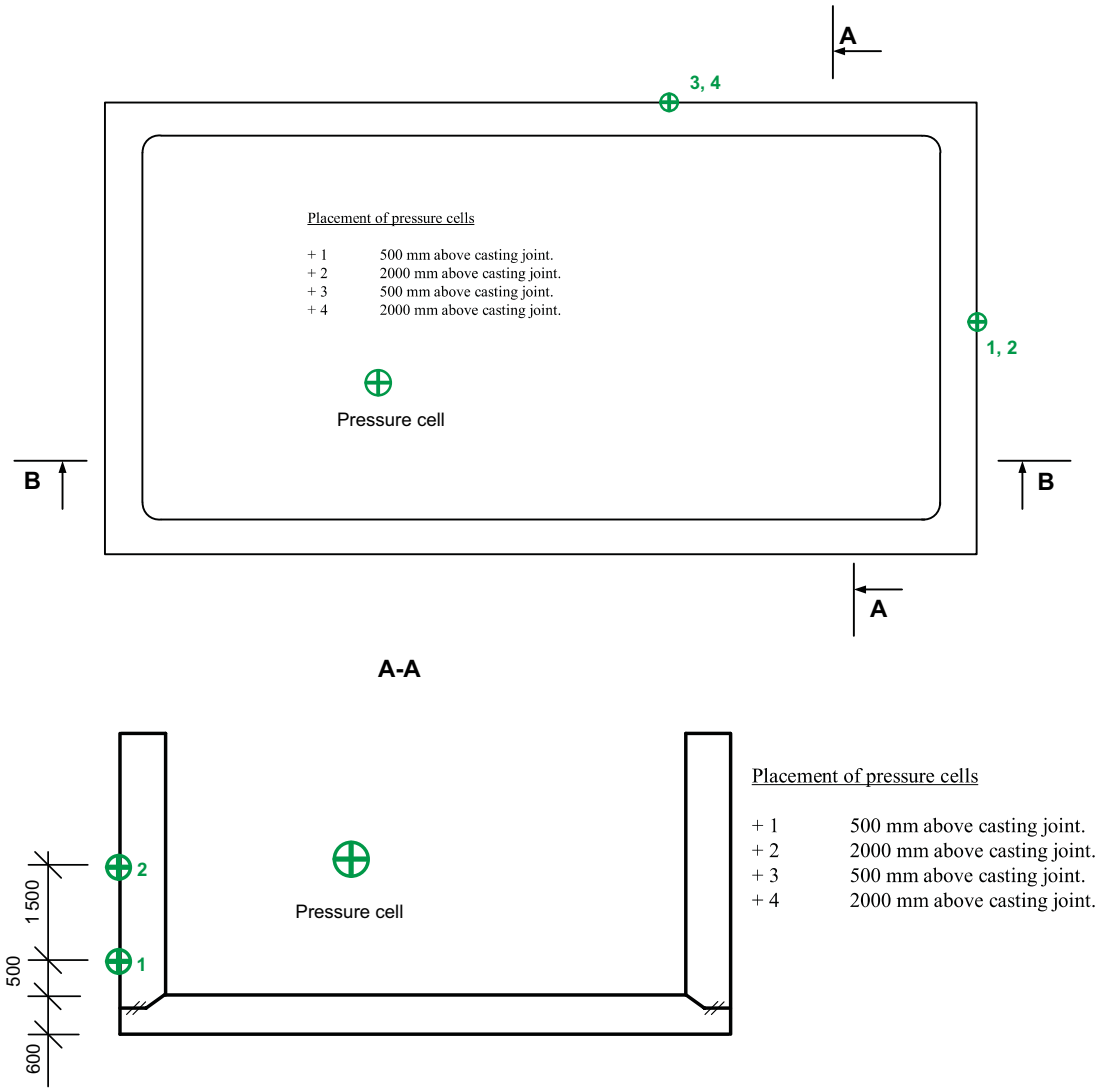

Figure 3-9. *Placement of the pressure cells for monitoring the formwork pressure. The upper illustration shows the caisson from above whereas the lower illustrations show side-view images of the caisson.*

3.5 Relative Humidity

The shrinkage of the concrete (which can be related to the relative humidity in the concrete) is one of the most important load independent deformation mechanisms which may lead to undesirable cracks.

Humidity sensors were installed in drilled holes in the walls and base slab of the caisson once the formwork had been disassembled. The sensors were placed as far from the casting joints and edges as possibly suitable. This was motivated by that closer to edges, drying occurs in 3 dimensions and the results could be flawed.

A total number of 5 humidity sensors were used and placed as shown in Figure 3-10. Additionally, the relative humidity of the ambient air was also monitored.

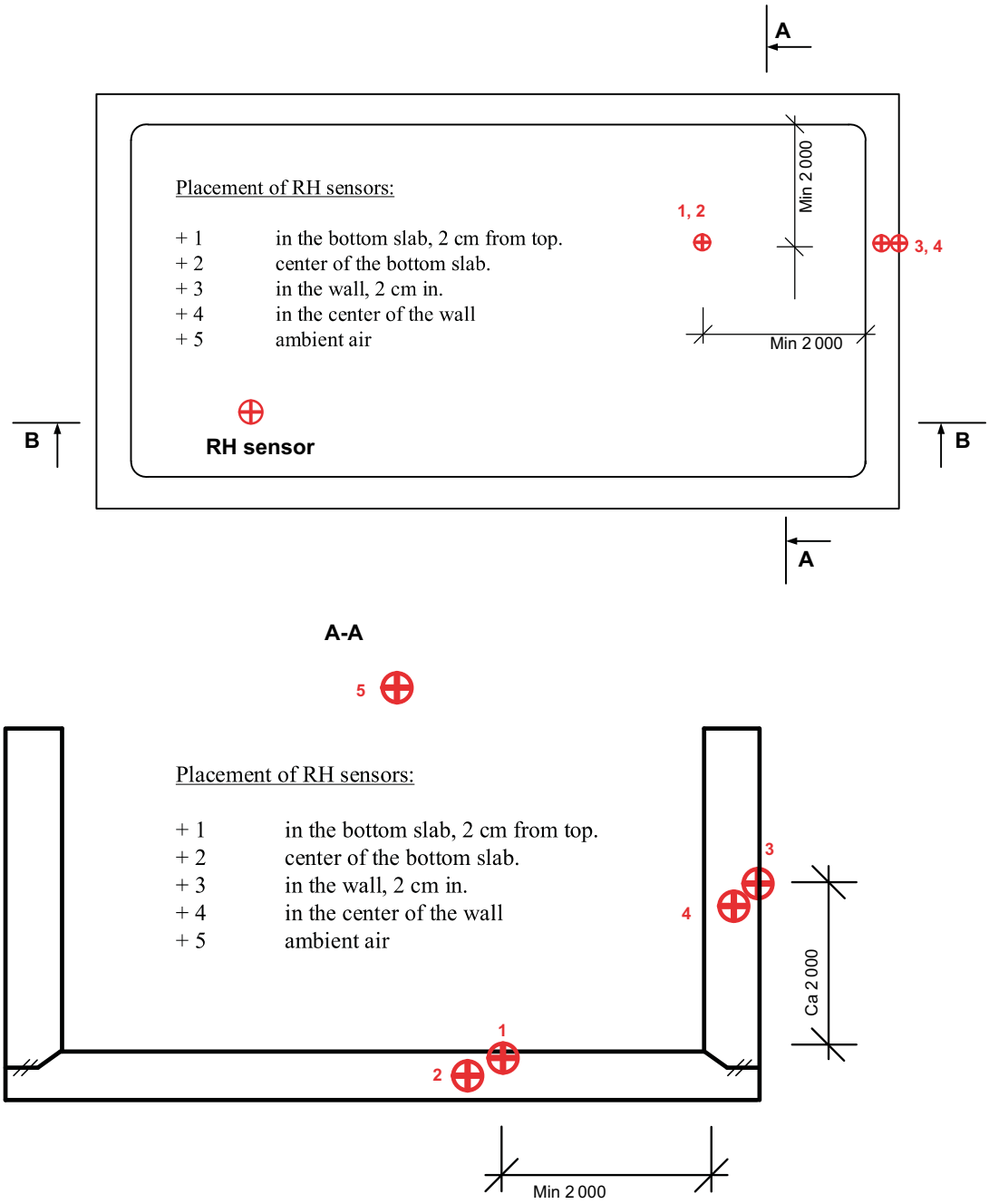

Figure 3-10. *Placement of the RH sensors. The upper illustration shows the caisson from above whereas the lower illustrations show side-view images of the caisson.*

3.6 Data acquisition and storage

A system for data acquisition and storage was also installed to collect the signals from the different sensors. The system was installed in a closed cabinet in order to protect the sensible equipment from the rather harsh environment.

The system was adjusted to the demands of a long-term measurement where a high sampling frequency was not required.

3.7 Instrumentation for control of strain transducers

In order to ensure the reliability of the strain transducers, 2 test castings were performed. The tests each comprised 2 beams with the dimensions 500 × 500 × 4 000 mm, one with plain wooden formwork and one with insulated formwork (100 mm insulation), Figure 3-11. The test castings were done in TAS08 and TAS05 respectively and both temperature and internal strain were measured.

Expectedly, the setup should result in zero strain even though a slight increase in compression due to autogenous shrinkage could occur. The results are presented in Chapter 6.

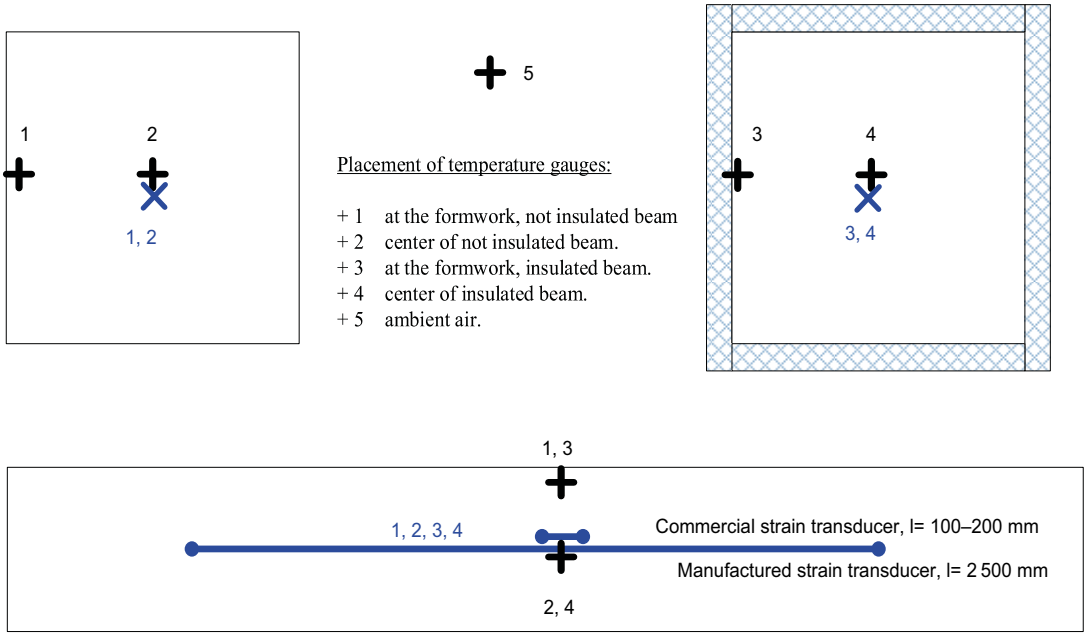

Figure 3-11. *Instrumentation of test casting.*

3.8 Summary of the installed sensors

The type and number of sensors are summarised in Table 3-1. The presented instrumentation is based on the experiences from the instrumentation of the components in TAS05 and includes a certain degree of redundancy.

Table 3-1. The installed sensors.

To be recorded	Number of sensors	Duration	Sensor type
Ambient temperature	2	Long term	PT 100
Heat of hydration	16 + 5*	Short term	Type T thermocouple
Temperature at strain transducers	6	Long term	Included in the strain transducer
Internal strain	8 + 2*	Long term	Manufactured strain gauge transducers
Internal strain	6 + 2*	Long term	TML KM 100 with temperature registration
External deformation	4	Long term	HBM WA-T 10 mm
Formwork pressure	4	Short term	Wika S10
Humidity	5	Long term	Jumo 907021

* For test casting aiming to verify the function of the strain transducers.

4 Preparations in TAS08

In this chapter, the preparations made in TAS08 prior to casting are described. These preparations mainly included casting of the foundation on which the caisson should be erected but also work in order to ensure a safe working environment were undertaken.

4.1 Prerequisites

Since the excavation, TAS08 had been empty and unused. No cleansing of the floor had been undertaken and the floor was covered with a layer of stone / gravel of varying composition, Figure 4-1. The lighting was a little limited as well as the ventilation.

Figure 4-1. *TAS08 at project start.*

4.2 Preparations

Prior to the commencement of work, rock reinforcement, lighting and ventilation were checked. Some additional lighting was installed but otherwise TAS08 was considered safe and to provide a healthy working environment.

4.3 Removal of rock debris from the rock floor

The first step in the preparatory work comprised removal of the rock debris from the floor of TAS08. Initially, mechanical equipment was used to remove as much as possible of the rock debris. In subsequent steps the rock floor was flushed with large amounts of water in order to remove the remaining material to expose the bare rock, Figure 4-2.

Figure 4-2. *All rock debris in TAS08 has been removed and the bare rock exposed.*

4.4 Casting of concrete slab

Due to the large roughness in the rock floor, the casting was carried out in the following 3 steps:

- Filling of the largest pits in the outer part of TAS08.
- Filling of the largest pits in the inner part of TAS08.
- Casting of the top layer of the slab.

4.4.1 Concrete

The concrete was nominally class C40/50 and was delivered by *AB Högsby grus och betong*.

4.4.2 Filling of the largest pits in the outer part of TAS08

For filling of the largest pits in the outer part of TAS08 about 40 m^3 of concrete was used. Concrete was poured directly onto the rock floor from the truck by use of its chute, Figure 4-3. The concrete was moderately vibrated during the casting process.

Figure 4-3. *Filling of the largest pits in the outer part of TAS08.*

4.4.3 Filling of the largest pits in the inner part of TAS08

Filling of the largest pits in the inner part of TAS08 was carried out in the same manner as for the outer part. Here, the concrete trucks parked on the newly cast concrete in the outer part of TAS08 during casting. Afterwards more or less the entire rock floor was covered with a relatively thick concrete layer, Figure 4-4.

4.4.4 Casting of the top layer of the slab

Casting of the top layer of the slab comprised a total of about 50 m^3 of concrete (class C40/50).

The casting was carried out mostly using a pump located in adjacent tunnel (TASU), Figure 4-5. However, the last part was poured directly from the concrete truck using the truck's chute.

Figure 4-4. *After filling of the largest pits also in the inner part of TAS08 and formwork construction for casting of the top layer.*

Figure 4-5. *Casting of the top layer of the slab.*

4.4.5 Trowelling of the concrete surface

Trowelling of the concrete surface started already before casting was completely finished, Figure 4-6. This was a consequence of the unexpectedly fast setting of the concrete which required trowelling to be started before the concrete had hardened completely. In spite of this, the surface finish of the slab after trowelling did not comply with the requirements, Figure 4-7.

Besides the rather rough surface finish, inspections also revealed that the slab was not level but contained depressions with a depth of up to a few centimetres over an area of a couple of square metres. After the slab was trowelled, it was covered with a plastic sheet to prevent dehydration, Figure 4-7.

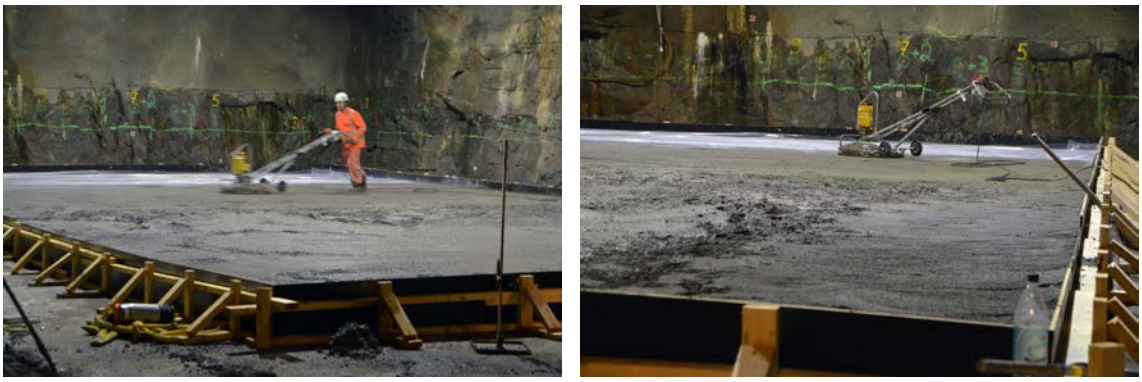

Figur 4-6. *Trowelling of the concrete slab.*

Figure 4-7. *Surface finish of the trowelled concrete.*

4.4.6 Grinding of the surface of the concrete slab

As a final step, the slab was grinded in order to improve its surface finish and planarity. Grinding dramatically improved the surface finish of the slab. However, inspections a few weeks post grinding revealed that the (now water-filled) depressions had not been sufficiently remedied, Figure 4-8.

The inspections also showed that the depressions contained large amounts of precipitates. However, the type of precipitation was not studied. The main options would be NaCl/$CaCl_2$ from rock drainage or $CaCO_3$ formed through a reaction between cement leachates and CO_2.

Figure 4-8. *The concrete slab after grinding.*

4.5 Casting of ramp

As a last step, a small ramp from TASU and up against the concrete slab was constructed for easy access during formwork construction, Figure 4-9.

Figure 4-9. *All is ready.*

5 Commissioning and operation of the concrete production plant

The concrete production plant was commissioned one week ahead of casting of the base slab.

5.1 Concrete production site

The mobile concrete production plant was established on a surface in immediate access to the entrance to the tunnel of the Äspö Hard Rock Laboratory, Figure 5-1. The surface is covered with asphalt and there is also access to the electric grid, water and a place for washing trucks and other equipment.

Figure 5-1. *The area in connection with the entrance to the tunnel of the Äspö Hard Rock Laboratory, which is visible in the upper middle of the image. (Google earth.)*

5.2 The concrete production plant

The concrete production plant included the following equipment:

- 2 silos, each with a capacity of 50 metric tons (Section 5.2.1).
- 2 truck mixers, each with a capacity of 5 m^3 (Section 5.2.2).
- 1 water tank with a volume of about 10 m^3 provided with a high-capacity pump.
- 1 container for the staff but also containing various types of smaller equipment.

5.2.1 The silos

The silos were each about 10 meter tall and equipped with a feeder screw for filling the truck mixers as well as vent with dust filter at the top, Figure 5-2.

5.2.2 Truck mixers

The concrete was mixed in two truck mixers, each with a maximum capacity of 5 m^3, Figure 5-3. Each truck mixer is equipped with a control system, built-in load cells for weighing of material and a loading bucket for loading of aggregate material, Figure 5-3.

5.2.3 Construction of ramp

For the reloading of concrete from the truck mixers to the transport trucks a ramp was constructed. The ramp was demarcated by concrete blocks on 2 sides and a gravel embankment on the third. The space between these boundaries was filled with crushed rock and gravel. The final height and total length of the ramp were 3.2 meters and about 30–40 meters respectively, Figure 5-4.

5.2.4 Aggregate storage areas

Storage areas for the 4 different aggregate fractions were prepared in close proximity to the concrete production plant. The fraction that constituted the largest part, 0–4 mm, was laid on the asphalt against the fence facing the tunnel entrance while the other fractions were placed on a gravel surface against the gravel embankment, Figure 5-5. The fractions were separated with concrete elements to prevent mixing.

Figure 5-2. *The two silos, each with a capacity of 50 tonnes.*

Figure 5-3. *One of the two truck mixers during filling of gravel into the mixer.*

Figure 5-4. *The ramp.*

Figure 5-5. *Storage areas for the 4 different aggregate fractions.*

5.3 Commissioning of the concrete production plant

5.3.1 Assembling of the equipment

The equipment was delivered on trucks and included 2 silos, water tank (Figure 5-7), a container with various equipment and 2 truck mixers. Once the silos were erected and assembled, the surface underneath them was covered with a layer of gravel to facilitate cleaning once the work was finished, Figure 5-6.

5.3.2 Filling of the silos

The silos were filled with cement and limestone from bulk car, Figure 5-8. Cement was delivered from Degerhamn and limestone filler from Omya. Both silos were filled to their maximum capacity.

Figure 5-6. *The silos have been erected and assembled and a layer of gravel has been laid out for protection of the asphalt surface.*

Figure 5-7. *The water tank was placed near the silos. In the tank was a powerful pump for quick filling of the truck mixers which could be started and stopped by means of an electric switch attached to the post in the left part of the image.*

Figure 5-8. *Filling of the cement silo.*

5.4 Deliveries of aggregate materials

Aggregate materials were delivered by truck over a couple of days. The fraction 0–4 mm was delivered from Rollsmo, southwest of Kalmar, while other fractions were delivered from Flivik about 30 km from Äspö. The choice of Rollsmo as the supplier of the finest fraction was motivated by the fact that this material was used in the previous work (Mårtensson and Vogt 2019), while it is also the fraction that has the greatest impact on the concrete's fresh properties. Other fractions do not have the same effect, and they could therefore be replaced by equivalent material from another nearby supplier.

5.5 Operating the concrete plant

5.5.1 Handling of water and admixtures

Water was fed directly into the mixer through a hose. The admixtures were manually measured in graded containers, mixed in a bucket and finally manually fed into the mixer, Figure 5-9.

Figure 5-9. *Feeding water and admixtures (in the bucket) into the truck mixer.*

5.5.2 Handling of aggregates

Aggregates were handled by means of the truck mixer´s own loading bucket which fed the aggregates directly into the mixer, Figure 5-10.

5.5.3 Handling of cement and limestone filler from the silos

Cement and limestone (OmyaCarb 2GU) were fed directly into the truck mixer from the silos by means of electrically operated feeder screws, Figure 5-11. The amounts of material were controlled by the truck mixers´ built-in load cells.

Figure 5-10. *Feeding aggregates (0–4 mm) into the truck mixer.*

Figure 5-11. *Feeding cement into the truck mixer.*

5.5.4 Handling of limestone filler from sacks

The amount of Myanit 10 was not large enough to motivate the use of a silo. Instead, sacks of Myanit 10 were emptied directly into the loading bucket of the truck mixers as shown in Figure 5-12.

5.5.5 Concrete testing at the production site

Once all components had been fed into the truck mixer, the concrete was mixed for about 5 minutes. Before the concrete could be poured into the transport truck, slump and sometimes also temperature were measured. Sampling was done directly from the mixers at the top of the ramp and slump was measured immediately before emptying the concrete into the transport trucks, Figure 5-13.

Figure 5-12. *Filling the loading bucket of the truck mixer with Myanit 10 and feeding of the mixer.*

Figure 5-13. *Concrete sampling and slump measurement.*

5.5.6 Pouring the concrete into the transport trucks

When the concrete had been approved, the concrete was poured directly into the transport truck, Figure 5-14. Once the transport truck was full (corresponding to 7 m^3) it proceeded immediately to TAS08.

Figure 5-14. *The truck mixer is positioned for pouring of the concrete into the transport truck.*

5.6 Adjustments of the concrete mix design

5.6.1 Original concrete mix design

The concrete mix design was the same as the one previously developed by Lagerblad et al. (2017) and further tested by Mårtensson and Vogt (2019). Table 5-1 shows the original mix design prior to adjustments, including also the type of material/supplier used in this work.

Table 5-1. The original concrete mix design prior to adjustments.

Component	Products name/supplier	Amount (kg/m^3)
Cement	Degerhamn anläggningscement (CEM I)	320
Limestone filler	OmyaCarb 2GU (grain size: 2 mm)	130
Limestone filler	Myanit 10 (grain size: 10 mm)	33.3
Water		156.8*
Aggregates 16–22 mm	Flivik (Crushed rock)	393.3
Aggregates 8–16 mm	Flivik (Crushed rock)	425.7
Aggregates 4–8 mm	Flivik (Crushed rock)	92.0
Aggregates 0–4 mm	Rollsmo (Crushed rock)	840.9
Superplasticiser	MasterGlenium Sky 558	1.30
Superplasticiser	Master Sure 910	1.70
Retarder	Master Set RT 401	0.96 (0.3 % of cement weight)

* Water in admixtures not included.

5.6.2 Mixing tests

Mixing tests began approximately 36 hours before planned casting of the base slab.

The concrete was mixed in the 2 truck mixers in batches of 3.5 m^3. Manufacturing was carried out according to standard procedures for this type of plant. Cement and OmyaCarb 2GU were added from each silo and water from the tank. Admixtures and Myanit 10 were added manually while aggregates were added using the mixer's loading bucket. The amounts of aggregates were slightly adjusted due to a small difference in density between the aggregates used here and the ones used by Mårtensson and Vogt (2019). A small adjustment of the mix design was also made in order to customize the mix design to a number of full sacks of Myanit 10 and thus avoid weighing of the material.

Mix #1

Mix #1 followed the original mix design with the adjustments of the solid components mentioned above. The components were added in the following order: water (w/c: 0.50), admixtures, cement, limestone, aggregates (smallest first and then the larger fractions). Data are shown in Table 5-2.

Table 5-2. Data from Mix #1.

Time after WAT*(min)	Temperature (°C)	Adjustments	Slump (mm)	Comment
30	18.4	Added 1 dm^3 sky 558 to 3.5 m^3 concrete		Concrete too stiff. Extra SP added
55			140	
120	14.4		100	
165	13.0		0	Concrete very stiff

* WAT: Water Addition Time.

The concrete was very stiff and was not considered to be able to pump.

When the mixer was emptied, it appeared that there was some paste left in the bottom which was not completely mixed with the aggregates. The mixing sequence was therefore not considered to be well adapted to the current type of mixer.

Mix #2

Mix #2 followed the original mix design with the adjustments of the solid components mentioned above. The components were added in the following order: water (w/c: 0.50), admixtures, cement, limestone, aggregates (smallest first and then the larger fractions). The difference between Mix #1 and 2 was that 0.3 % retarder was used in Mix #2. Data are shown in Table 5-3.

Table 5-3. Data from Mix #2.

Time after WAT (min)	Temperature (°C)	Adjustments	Slump (mm)	Comment
30	17.9		80	
85	13.7		50–60	
105	14.4			The concrete was rather stiff but slump was not measured

When the mixer was emptied, it appeared that there was some paste left in the bottom which was not completely mixed with the aggregates. The mixing sequence was therefore not considered well adapted to the current type of mixer.

Mix #3

Mix #3 followed the original mix design with the adjustments of the solid components mentioned above. The amounts of retarder and Sky 558 were 0.3 % and 0.6 % of the cement weight respectively. The components were added in the following order: Water (w/c: 0.50), admixtures, aggregates 16–22 mm, cement, limestone, remaining aggregates in the order 0–4, 4–8 and 8–16 mm. Data are shown in Table 5-4.

Table 5-4. Data from Mix #3.

Time after WAT (min)	Temperature (°C)	Adjustments	Slump (mm)	Comment
30	17.4		165	
119	14.4		180–200	The concrete appears more fluid as mixing proceeds

Observations indicate that the truck mixers are not efficient enough to mix the concrete according to the original mix design in the required time. After standard mixing time – about 5 minutes – the concrete is very stiff and it is judged that it will not be able to empty the concrete from the truck mixers in less than 20 minutes. However, after about 30 minutes mixing, the properties of the concrete are according to the requirements.

Mix #4

Mix #4 followed the original mix design with the adjustments of the solid components mentioned above. The amounts of retarder and Sky 558 were 0.3 % and 0.4 % of the cement weight respectively. The components were added in the following order: water, admixtures, aggregates 16–22 mm, cement, limestone, remaining aggregates. The amount of water was increased to w/c: 0.52. Data are shown in Table 5-5.

Table 5-5. Data from Mix #4.

Time after WAT (min)	Temperature (°C)	Adjustments	Slump (mm)	Comment
60			80	The concrete appears more fluid as mixing proceeds.

The concrete was still judged too stiff after standard mixing time.

Mix #5

Mix #5 followed the original mix design with the adjustments of the solid components mentioned above. The amounts of retarder and Sky 558 were 0.3 % and 0.5 % of the cement weight respectively. The components were added in the following order: water, admixtures, aggregates 16–22 mm, cement, limestone, remaining aggregates. The amount of water was increased to w/c: 0.54. Data are shown in Table 5-6.

Table 5-6. Data from Mix #5.

Time after WAT*(min)	Temperature (°C)	Adjustments	Slump (mm)	Comment
20	18.1		180	
95	21		150	

Mix #5 could be mixed efficiently during the standard mixing time for the truck mixers and the properties of the fresh concrete were according to requirements.

5.6.3 Final production test

The final step in the adjustment of the concrete mix design comprised a final production test with both truck mixers in order to gain an understanding of the plant's delivery capacity and capacity to maintain a consistent quality.

Two truck mixers with concrete were prepared according to the mix design presented in Table 5-7.

Table 5-7. Concrete mix design used in the final production test.

Component	Product name/supplier	Amount (kg/m^3)
Cement	Degerhamn anläggningscement	320
Limestone filler	OmyaCarb 2GU (grain size: 2 μm)	130
Limestone filler	Myanit 10 (grain size: 10 μm)	34.3
Water		169.4*
Aggregates 16–22 mm	Flivik (Crushed rock)	383.5
Aggregates 8–16 mm	Flivik (Crushed rock)	415.1
Aggregates 4–8 mm	Flivik (Crushed rock)	89.7
Aggregates 0–4 mm	Rollsmo (Crushed rock)	819.9
Superplasticiser	MasterGlenium Sky 558	1.60
Superplasticiser	Master Sure 910	1.70
Retarder	Master Set RT 401	0.96

* Water in admixtures not included.

The different components were added in the following order

1. Water and admixtures
2. Aggregates 16–22 mm
3. Cement
4. Fillers
5. Aggregates 0–4 mm
6. Aggregates 4–8 mm
7. Aggregates 8–16 mm

Water and cement were mixed at 3:00 pm and Table 5-8 shows measured data from both truck mixers. In total, it took less than 30 minutes from the adding of water and admixtures to the first truck mixer until both mixers had emptied their cargo in the transport truck. Given the intended casting schedule with the delivery of a truck every 30 minutes, this capacity was approved. The test also showed that the properties of the fresh concrete were according to the requirements and it was therefore decided that the base slab should use the concrete mix design used in the production test.

Table 5-8. Data from the final production test.

Time	Temperature (°C)	Slump (mm)	Comment
3:15	20.6	220	Truck mixer 1
3:20	20.2	200	Truck mixer 2
4:15		210	Truck mixer 1
5:00		210	Truck mixer 1

6 Control of strain transducers

In order to check the function of the strain gauges, 2 separate castings were made, each comprising two beams with the dimensions 0.5 × 0.5 × 4 meters. Of the 2 moulds, one was insulated with about 100 mm foam plastic/ styrofoam whereas no insulation was used in the second one. In the first test the same concrete as used for casting of the base slab was used whereas the second test utilised standard concrete without limestone filler. The set-up of the sensor system of the beams is presented in Section 3.7.

Expectedly, the setup should result in zero strain regardless of type of concrete used even though a slight increase in compression due to autogenous shrinkage could occur. The results from these tests could therefore be used as a baseline level in the evaluation of the results from casting of the caisson.

6.1 Casting of beams using 2BMA concrete

6.1.1 Casting

Casting of the 2 beams using 2BMA concrete was carried out immediately after casting of the base slab. The same type of concrete was used for both the beams and the slab. The moulds were placed adjacent to the base slab and the sensor system was connected to the same data collection system as used for the sensors from the base slab, Figure 6-1.

Figure 6-1. *Casting of the beams using 2BMA concrete.*

6.1.2 Results

Internal strain and temperature

In Figures 6-2 and 6-3, temperature and internal strain in the concrete in the uninsulated and insulated moulds are shown. A comparison of these figures shows that the initial evolution of temperature and strain is equivalent in the two moulds but also that the maximum temperature and the maximum compressive stresses are higher in the insulated mould than in the uninsulated. The figures also show that the concrete in the insulated mould cools much slower than the concrete in the uninsulated mould, which is also reflected in the strain evolution.

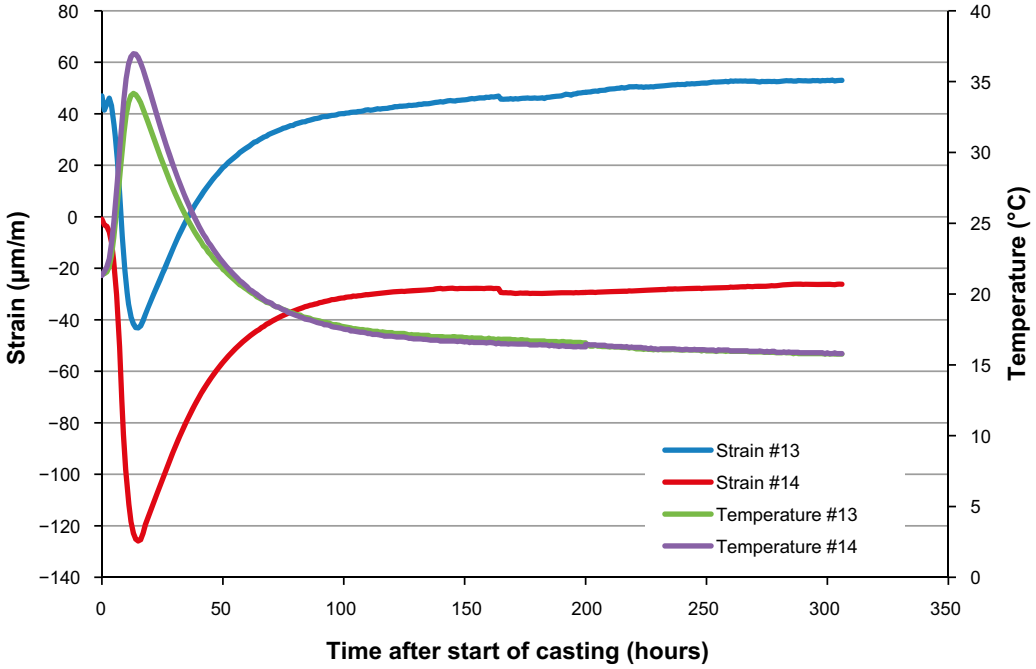

Figure 6-2. *Internal strain and temperature in the uninsulated beam during the first 300 hours after casting.*

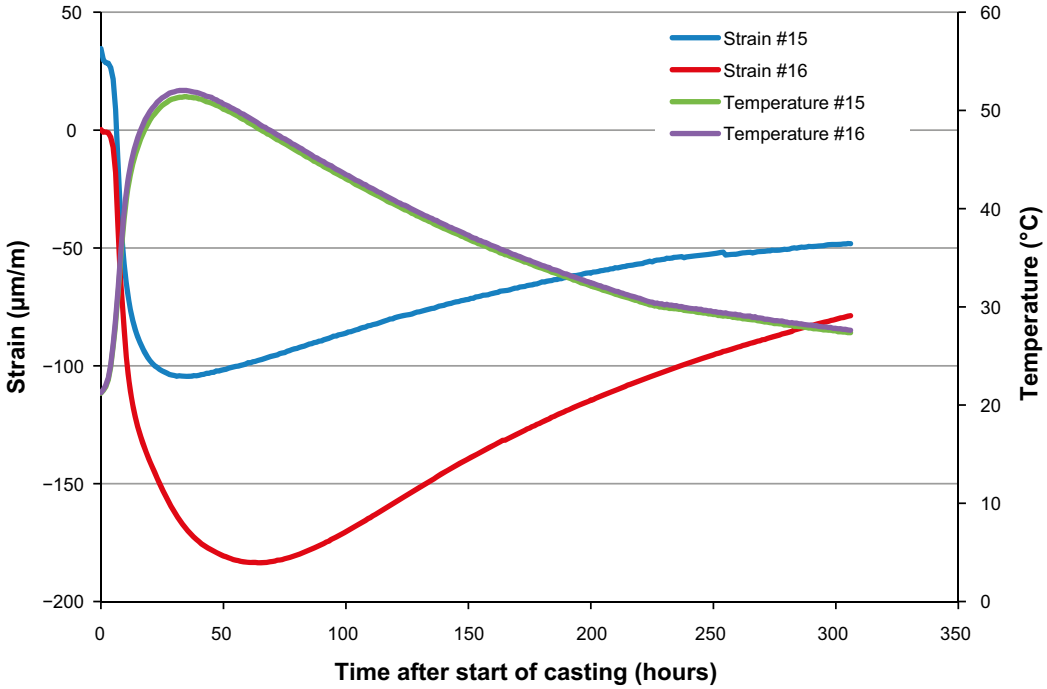

Figure 6-3. *Internal strain and temperature in the insulated beam during the first 300 hours after casting.*

Material structure

In order to ensure that the concrete was homogeneous, specimens were extracted from the beams by means of core drilling. Each core was 500 mm long with a diameter of 100 mm. An overview image of one of the cores is shown in Figure 6-4 and details showing a rather frequent occurrence of smaller pores in Figure 6-5.

Summary

The results from this test show that the strain levels were far higher than expected due to the presumed unrestrained situation in the moulds. The photographs show frequent occurrence of smaller pores in the concrete but the possible influence of this has not been clarified. In order to ensure that the results were not caused by some unique properties of the 2BMA concrete it was decided to repeat this experiment using standard concrete not containing any limestone filler, Section 6.2.

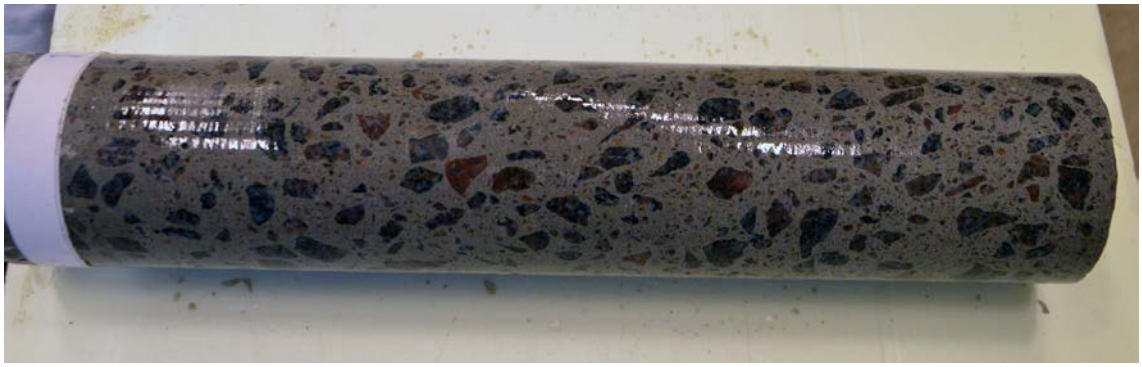

Figure 6-4. *An overview picture showing one of the cores. The core is 500 mm long and 100 mm in diameter.*

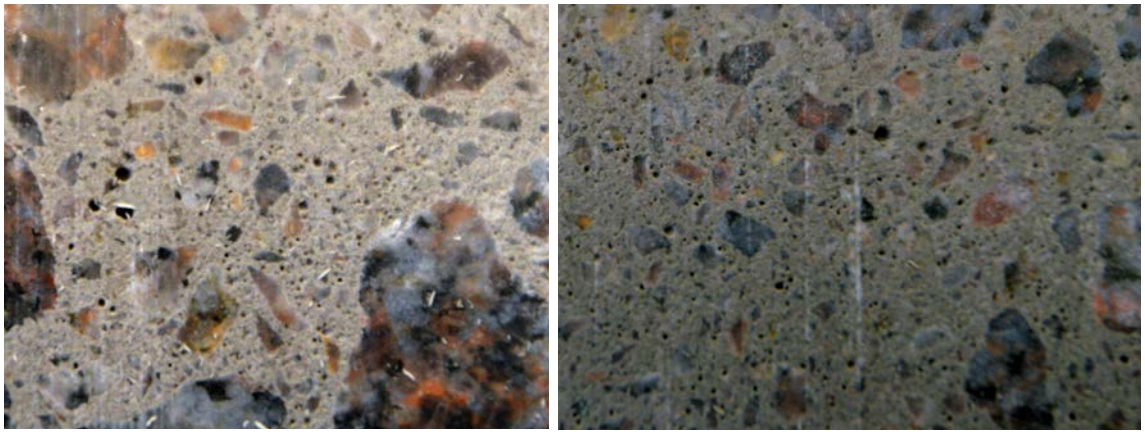

Figure 6-5. *Images in higher magnification showing the presence of smaller pores in the surface of the core.*

6.2 Casting of beams with standard concrete

Casting of the 2 beams using standard concrete was carried out about 6 months after casting of the caisson walls. As mentioned in Section 6.1.2, the main purpose of this experiment was to ensure that the 2BMA concrete did not possess any unique features that caused the unexpected strain evolution.

6.2.1 Casting

Casting was carried out using standard C40/50 concrete delivered by *AB Högsby grus och betong*.

The moulds were placed in TASP and the sensor system was connected to the same control system as used during casting of concrete structures in TAS05 (Mårtensson and Vogt 2019), Figure 6-6. Concrete was poured directly into the moulds using the truck's own chute and vibration was carried out using a standard concrete poker.

6.2.2 Results

Temperature and internal strain

In Figures 6-7 and 6-8, temperature and internal strain in the concrete in the uninsulated and insulated moulds are shown. A comparison of these figures shows that the initial evolution of temperature and strain is equivalent in the two moulds but also that the maximum temperature and the maximum compressive stresses are higher in the insulated mould than in the uninsulated. The figures also show that the concrete in the insulated mould cools much slower than the concrete in the uninsulated mould, which is also reflected in the strain evolution. The somewhat unconventional temperature evolution (second temperature peak) in the insulated mould is explained by the fact that the mould was not covered by insulation until the day after casting was carried out.

Figure 6-6. *Casting of the beams using standard concrete.*

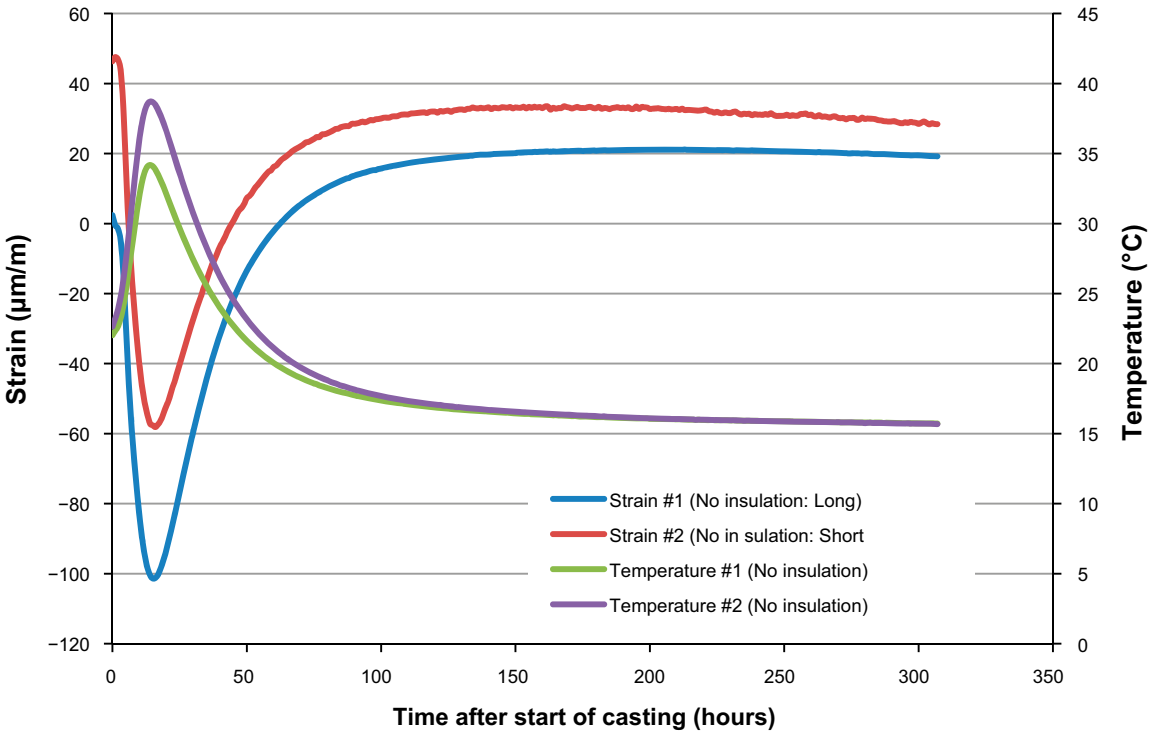

Figure 6-7. *Evolution of temperature and strain in the concrete in the uninsulated mould.*

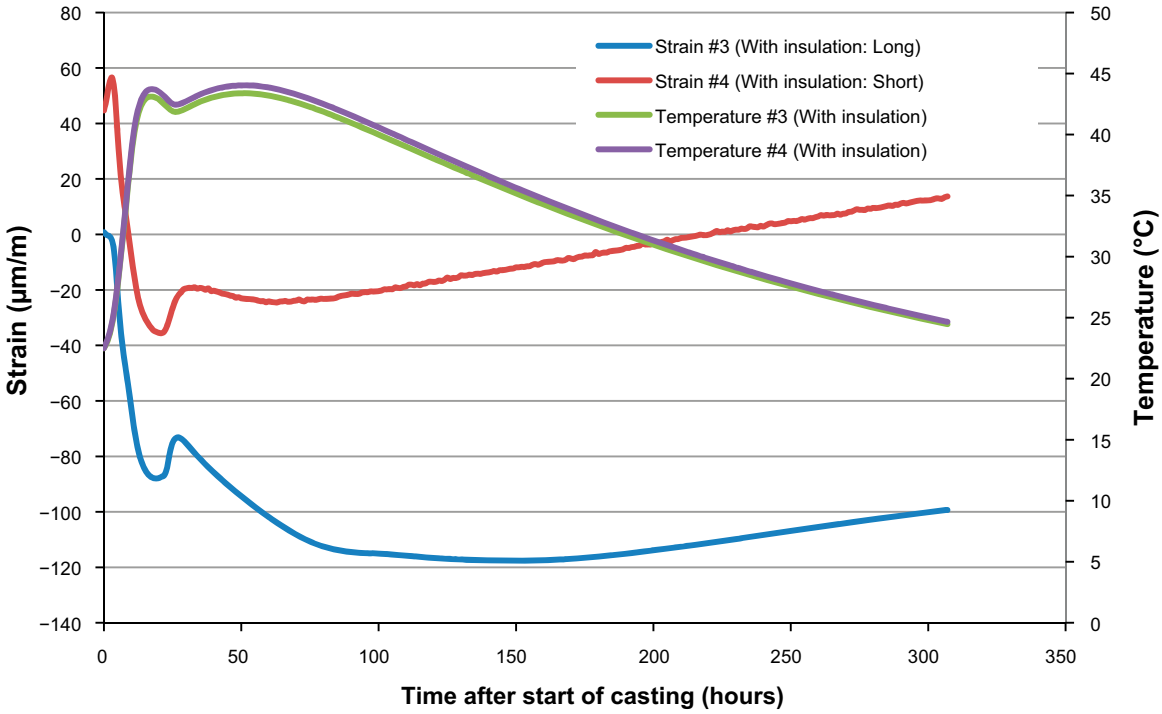

Figure 6-8. *Evolution of temperature and strain in the concrete in the insulated mould.*

Material structure

In order to ensure that the concrete was homogeneous, specimens were extracted from the beams by means of core drilling. Each core was 500 mm long with a diameter of 100 mm. An overview image of one of the cores is shown in Figure 6-9 and details in Figure 6-10. Figure 6-9 shows that the concrete is homogeneous with a similar distribution of aggregates and paste throughout the specimen. Figure 6-10 shows that also the standard concrete contains a number of small pores; however somewhat less frequently occurring than in the 2BMA concrete. On the other hand, the number of larger pores was higher in the standard concrete than in this 2BMA concrete.

Summary

The results presented in this section were again unexpected and the strain levels were far higher than expected due to the presumed unrestrained situation in the moulds and the use of standard concrete. The photographs show the occurrence of smaller and larger pores but nothing that can explain the high levels of strain in the concrete.

Given previously made assumptions that the concrete, when cast completely without any restraint, should be more or less stress-free, these results were undeniably unexpected. Although the limited study presented in this chapter shows that the concrete developed by SKB for use in erecting the caissons in 2BMA behaves as a standard concrete, it does not explain the high initial compressive stresses measured in previously completed castings (Mårtensson and Vogt 2019). However, the conclusion from these tests are that the initial high compressive stresses are not an unique feature of the 2BMA concrete but also occurs when standard concrete is used.

Figure 6-9. *An overview picture showing one of the cores. The core is 500 mm long and 100 mm in diameter.*

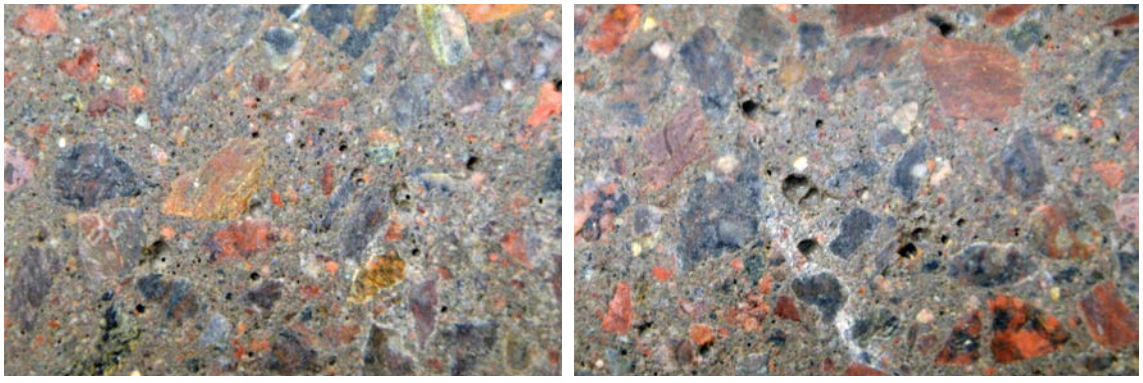

Figure 6-10. *Images in higher magnification showing the presence of smaller pores in the surface of the core.*

7 Casting of base slab

In this chapter the casting of the base slab of the concrete caisson – also including all preparations – is described. For casting of foundation, means to ensure a healthy working environment in TAS08 etc, see Chapter 4.

7.1 Manufacturing of the joint seals

The joints seals were made from 1.5 mm thick and 1 000 mm wide copper sheets which were cut to a width of 333 mm and then welded together into the desired length, Figure 7-1.

Figure 7-1. *A copper joint seal.*

7.2 Formwork construction

The formwork was based on the use of a traditional lightweight formwork (Doka) which was mounted directly on the foundation concrete, Figure 7-2. In addition, the formwork also included purpose-built details for the wall recess as shown in Figure 7-3. This part was manufactured on site using wood and board and also fitted the joint seals as shown in the figures.

Figure 7-2. *An overview picture of the formwork for the base slab.*

Figure 7-3. *Details of the on-site built formwork for the recess, also showing details on how the joint seal was mounted in the formwork.*

7.3 Construction of working platform

To facilitate the casting, a removable platform was constructed. The platform comprised a central footbridge supported by steel rods mounted in the foundation and wooden beams that stretched between the footbridge and the formwork, Figure 7-4.

The construction of the platform required that approximately 20 metal rods be drilled into the foundation. The rods were protected with plastic tubes for easy removal as casting progressed. When the base slab was ready, only the protective plastic tubes remained. These are not considered to have an effect on the levels of stress in the base slab. However, for construction of 2BMA, other methods have to be used or methods to remove the protective tubes and sealing of the holes developed. See also Chapter 9.

Figure 7-4. *The central footbridge of the platform used during casting of the base slab.*

7.4 Emplacement of the adhesion reducing plastic sheet

In order to eliminate adhesion between the foundation and the base slab, a plastic sheet was placed on the foundation prior to casting of the base slab. The sheet (Figure 7-4) was emplaced late in the process in order to prevent any damages during construction of formwork and working platform.

7.5 Installation of the sensor system

In this section, details on the installation of the sensor system in the base slab are described. For information about the types of sensors used and their positions in the base slab, see Chapter 3.

7.5.1 Embedded sensors

Temperature and strain

Temperature sensors and strain transducers were mounted on or between rods fastened in the foundation of the base slab, Figure 7-5, according to the set-up shown in Chapter 3. The cables were fastened against the plastic sheet and collected into a bundle through the formwork and into the control cabinet.

Figure 7-5. *A short strain transducer mounted between 2 of the rods that were used to support the footbridge of the working platform.*

7.5.2 Sensors installed after casting

Linear Variable Differential Transformers (LVDT)

About 4 weeks after casting of the base slab Linear Variable Differential Transformers (LVDT) were mounted in the positions shown in Section 3.3, Figure 7-6.

Relative humidity sensors

RH sensors were mounted in drilled holes in the base slab a couple of days after casting of the walls in the positions shown in Section 3.5, Figure 7-7. The upper part of the holes were sealed with silicon but care was taken not to fill the entire hole in order to avoid affecting the measurements.

Figure 7-6. *LVDT mounted through the formwork against the base slab.*

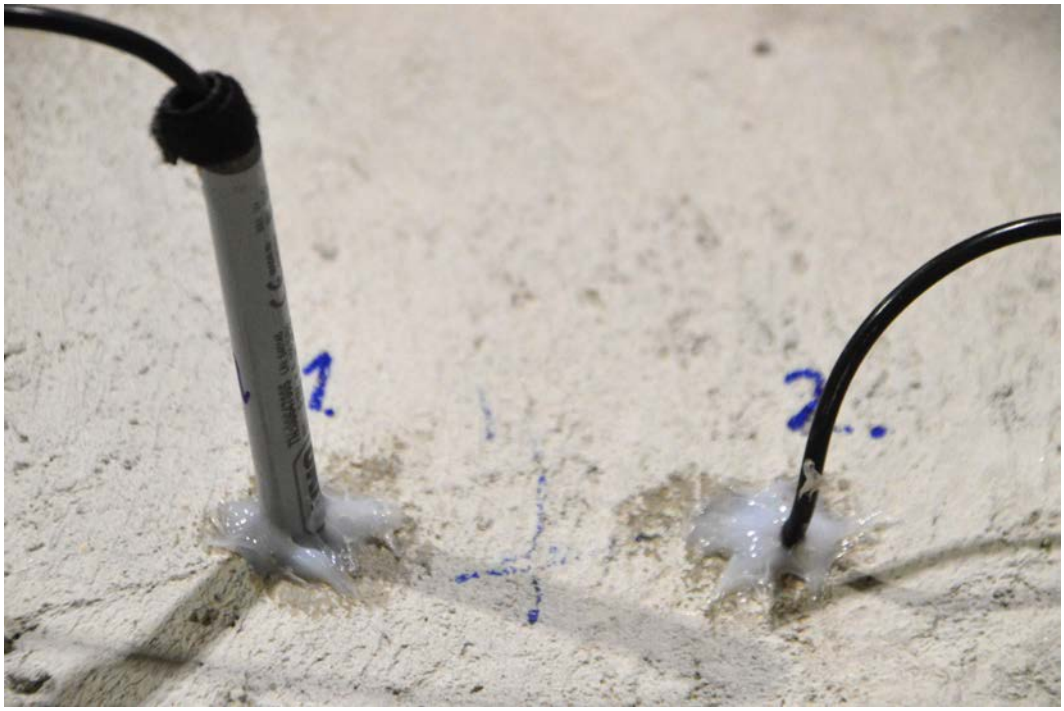

Figure 7-7. *RH sensors mounted in the base slab.*

7.5.3 Control cabinet

All cables were collected into a bundle pulled through the side of the formwork and into the control cabinet where the data collection equipment was placed, Figure 7-8.

Figure 7-8. *The cables were collected into one bundle connected to the control cabinet through a hole in the formwork.*

7.6 Concrete production and transport

7.6.1 Concrete production

The concrete was produced in the concrete production plant according to the method outlined in Section 5.6.3. In total, about 100 m^3 of concrete was produced and transported to the casting site in trucks, each carrying about 7 m^3. The concrete plant in full operation is shown in Figure 7-9.

Figure 7-9. *The concrete plant in full production.*

7.6.2 Concrete mix design

The concrete was mixed according to the mix design shown in Table 7-1 and the different components were added according to the sequence shown below the table. This is the same mix design and order of addition as used in the final production test, Section 5.6.3.

Table 7-1. Concrete mix design used.

Component	Product name/supplier	Amount (kg/m^3)
Cement	Degerhamn anläggningscement	320
Limestone filler	OmyaCarb 2GU (grain size: 2 μm)	130
Limestone filler	Myanit 10 (grain size: 10 μm)	34.3
Water	Tap water	169.4*
Aggregates 16–22 mm	Flivik (Crushed rock)	383.5
Aggregates 8–16 mm	Flivik (Crushed rock)	415.1
Aggregates 4–8 mm	Flivik (Crushed rock)	89.7
Aggregates 0–4 mm	Rollsmo (Crushed rock)	819.9
Superplasticiser	MasterGlenium Sky 558	1.60
Superplasticiser	Master Sure 910	1.70
Retarder	Master Set RT 401	0.96

*Water in admixtures not included.

The different components were added in the order outlined below and the amounts of each component according to data from the truck mixers built-in weighing systems are shown in Table A-8.

1. Water and admixtures
2. Aggregates 16–22 mm
3. Cement
4. Fillers
5. Aggregates 0–4 mm
6. Aggregates 4–8 mm
7. Aggregates 8–16 mm

The difference between target amounts and actual amounts for water, cement and aggregates is displayed in Figure A-1, A-2 and A-3 in Appendix A. According to SIS (2013), the tolerance of the batching process is ± 3 % for cement, water and total amount of aggregates. There are no requirements on the tolerance for the individual aggregate fractions.

Figure A-1 shows that the deviations for cement and aggregate are within the limits. For water, the tolerance is not met for 4 batches. However, less water is added than stipulated which results in lower w: c ratio. This is on the safe side regarding strength but with possible negative impact on workability.

The largest differences were recorded for aggregate fraction 4–8 mm, generally on the plus-side, Figure A-2 and A-3. This is explained by the fact that the total amount of 4–8 mm aggregate is only 315 kg per batch of concrete and therefore already a relatively small extra amount gives a large deviation (in per cent).

7.6.3 Concrete testing at production site

In connection with concrete production, the temperature, slump and, in some cases, also air content were measured, Table 7-2. Data from the truck mixers weighing system showing variations between the different mixes are presented in Appendix A.

Table 7-2. Concrete properties at production site.

Truck*	Water Addition time	Time for sampling	Temperature (°C)	Slump (mm)	Air content (%)
1a	07:05	07:20	19.0	200	3.3
1b	07:10	07:30	14.0	180	
2a	07:30	07:50	15.8	170	
2b	07:35	08:00	14.4	240	
3a	08:00	08:20	15.8	200	
3b	08:05	08:25	16.3	240	
4a	08:30	08:45	17.0	210	
4b	08:35	08:50	16.4	200	
5a	08:50	09:10	16.6	160	2.2
5b	08:55	09:20	16.2	210	
6a	09:20	09:35	17.5	140	
6b	09:25	09:40	17.5	210	
7a	09:40	10:05	17.0	170	
7b	09:45	10:10	16.9	230	
8a	10:15	10:35	17.8	160	
8b	10:20	10:40	17.8	200	
9a	10:45	11:00	17.5	160	
9b	10:50	11:05	18.0	190	
10a	11:10	11:30	17.8	160	
10b	11:15	11:35	18.0	200	
11a	11:40	12:00	18.0	180	3.0
11b	11:45	12:05	18.1	200	
12a	12:10	12:50	19.5	200	
12b	12:15	12:55	19.5	220	
13a	13:15	13:50	19.1	210	
13b	13:20	13:55	19.4	240	
14a	14:20	14:40	18.0	220	
14b	14:25	14:45	18.4	220	

* a and b corresponds to the two truck mixers.

7.7 Casting

7.7.1 Equipment

Concrete pump

During casting, the pump shown in Figure 7-10 was used. Attached to the pump was a 4” rubber hose which was connected to a concrete distributor used to distribute the concrete within the mould, Figure 7-11.

Figure 7-10. *The concrete pump that was used during casting. It can be noted that the mast could not be used due to limited space. Instead, the hose was directly connected to the pump.*

Concrete distributor

The concrete distributor consists of a number of steel pipes, which can be electrically operated, thus replacing the mast connected to the pump when casting is carried out in spaces where the use of the pump´s mast is not possible.

When casting the base slab, the use of the concrete distributor, Figure 7-11, was not really required since casting could have been carried out with the hose directly from the pump. However, in order to reduce the need for heavy handling of the hose as well as to gain experience prior to casting of walls it was decided to also use it during casting of the base slab.

Figure 7-11. *The concrete distributor.*

7.7.2 Concrete testing and casting of specimens for property control

Slump

Slump was measured upon arrival of the concrete transport trucks to the main tunnel, TASU. For all trucks, the concrete fulfilled the requirements and no adjustments were made, Table 7-3.

Table 7-3. Concrete slump at arrival at the casting site.

Truck #	Water Addition time	Time for measurement	Slump (mm)
1	07:05	08:00	220
2	07:30	08:30	210
3	08:00	09:00	240
4	08:30	09:28	220
5	08:50	09:57	210
6	09:20	10:26	220
7	09:40	10:59	210
8	10:15	11:25	210
9	10:45	11:52	210
10	11:10	12:40	210
11	11:40	12:59	220
12	12:10	13:48	210
13	13:15	14:23	200
14	14:20	15:20	220

Manufacturing of specimens for control of the properties of the hardened concrete.

During control of the properties of the fresh concrete, specimens were cast for later measurement of the concrete's compressive strength and shrinkage, Figure 7-12.

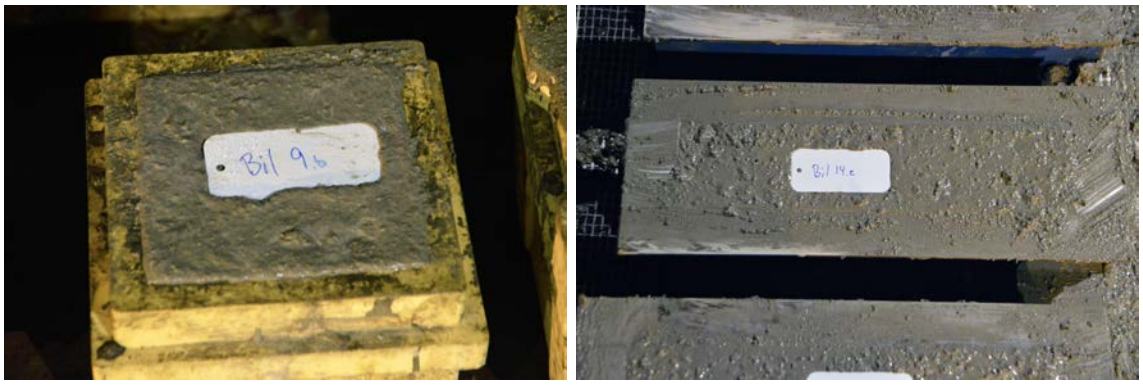

Figure 7-12. *Specimens for measurement of compressive strength (left) and shrinkage (right).*

7.8 Schedule for casting of the base slab

Casting began just after 8:00 AM on Wednesday October 17, 2018. Before that, hoses and concrete distributor were lubricated by means of cement slurry. The casting schedule is shown in Table 7-4.

Table 7-4. Schedule for casting of the base slab.

Truck #	Water addition time (WAT)	Pumping starts	Truck empty	Total time from WAT for truck mixer #1 until transport truck was empty	Comment
1	07:05	08:01	08:20	1 h 25 min	Somewhat hard to pump
2	07:30	08:28	08:52	1 h 22 min	
3	08:00	08:56	09:20	1 h 20 min	
4	08:30	09:31	09:49	1 h 19 min	Concrete distributor moved
5	08:50	09:54	10:16	1 h 26 min	
6	09:20	10:25	10:43	1 h 23 min	Concrete distributor moved
7	09:40	10:57	11:15	1 h 35 min	
8	10:15	11:22	11:42	1 h 27 min	Concrete distributor moved
9	10:45	12:05	12:30	1 h 45 min	
10	11:10	12:40	12:52	1 h 30 min	About 4 m^3 discarded. Hard to pump.
11	11:40	12:56	13:36	1 h 56 min	
12	12:10	13:46	14:03	1 h 53 min	
13	13:15	14:21	14:40	1 h 25 min	
14	14:20	15:18	15:52	1 h 32 min	

As can be seen from Table 7-4, the work proceeded relatively quickly with an average time from mixing water and cement until the transport truck was empty of approximately 90 minutes. For a couple of trucks at the end, however, it took a little bit longer due to the relocation of the concrete distributor, which meant that the concrete at the end became a little bit harder to pump. To catch up with the casting it was decided to discard approximately 4 m^3 of concrete in the tenth truck. At the end, emptying took a little longer due to adjustment of the surface of the slab. A series of images showing the different stages of the casting process is shown in Figures 7-13 to 7-15.

Figure 7-13. *Initially, the concrete is laid out in a 30–40 cm thick layer in the inner part. The concrete flow ability was high and the front became quite long and flat.*

Figure 7-14. *As casting proceeded, the footbridge was removed and the surface of the slab trowelled.*

Figure 7-15. *Towards the end of the casting, several activities were carried out simultaneously. While casting was still in progress in the outer parts, disassembling of the footbridge and trowelling was carried out in the inner parts.*

7.9 Post treatment and preliminary inspection

Coverage and watering

Once casting was finished, the surface was trowelled, sprinkled with water and covered with a plastic sheet. The following morning, more water was sprinkled onto the base slab after which the slab was covered again, Figure 7-16.

Figure 7-16. *The base slab has been sprinkled with water and covered with a plastic sheet.*

Disassembling the formwork

Disassembling of the formwork was carried out a couple of days after casting. At this time only the part of the formwork that covered the recess was removed. The remaining part of the formwork was left to be used as a basis for building the formwork for the walls.

Visual inspection immediately after demoulding

Immediately after demoulding, an inspection was conducted in which the physical result of the casting was examined. The focus here was on surface imperfections, form filling and appearance of the concrete/copper sheet interface. An overview image also showing that formwork construction for the casting of the walls has been initiated is shown in Figure 7-17.

Figure 7-17. *The base slab after partial disassembling of the formwork and start of erection of formwork to the walls.*

7.10 Detailed inspection

7.10.1 Base slab

An overview of the interior of the caisson is shown in Figure 7-18 (left image) and details of the base slab in Figure 7-18 (right image). The surface is planar but rather coarse as there was no need for a very smooth surface. It should be noted that inspection of the entire base slab could not be carried out before casting of the walls as the base slab was used for material storage or covered with heating mats.

7.10.2 Joint against future walls

As shown in Figure 7-19, filling of the recess varied from excellent to poor. Filling was complete in at least 95 % but in some parts filling was poor as shown in the right image in Figure 7-19. These imperfections are probably due to a combination of the fact that the distance between the joint seal and the foundation was limited and thus obstructive to concrete flow and the fact that the formwork in this section was completely covered making vibration and inspections difficult. Since the unfilled parts will be filled when the walls are cast, they are not considered critical to the hydraulic properties of the caisson. However, investigations of the hydraulic properties of the joint itself may prove the joint seals unnecessary. See also Section 8.10.4.

7.10.3 Joint seals

In connection with casting of the base slab, preparations were made for casting of the walls by embedding joint seals made of copper sheets in a recess in the base slab, Figures 7-19 and 7-20. The focus of the inspection after the casting was on how well the concrete was connected to the joint seal. The connection between joints and concrete was as shown in the pictures good and no gaps were found. Adhesion was not evaluated at this stage.

Figure 7-18. *An overview image of the interior of the concrete caisson and details of the surface.*

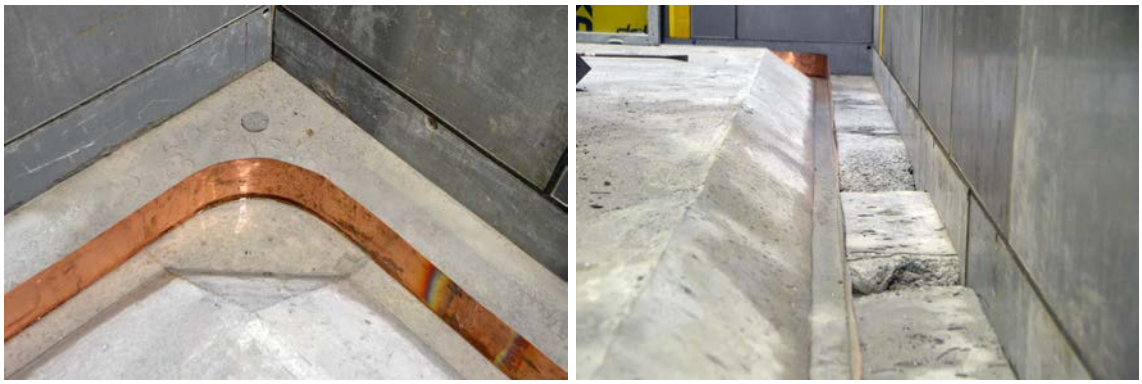

Figure 7-19. *Images showing the joint against the walls in more detail. Note some positions with poor fill.*

Figure 7-20. *The joint seal cast into the base slab.*

7.11 Crack monitoring

Visual inspections of the base slab with focus on the occurrence of cracks have been carried out from disassembling of the formwork and onwards. To date (October 2019) no cracks have yet been found.

7.12 Concrete properties

7.12.1 Compressive strength

28 days compressive strength

28 days compressive strength was measured on cubes cast from concrete from 4 of the trucks delivering concrete to the base slab, Table 7-5.

Table 7-5. 28 days compressive strength for the concrete to the base slab.

Specimen	Truck #	Weight (g)	Density (kg/m^3)	Force (kN)	Compressive strength (MPa)
1a	1	8052	2378	1084	48.0
1b	1	7985	2358	996	44.1
1c	1	8053	2373	1059	46.8
5a	5	8175	2406	955	42.2
5b	5	8164	2400	1018	44.9
5c	5	8169	2396	-	-
9a	9	8114	2391	1178	52.1
9b	9	8133	2394	1181	52.2
9c	9	8182	2408	1211	53.5
13a	13	7894	2319	1016	44.8
13b	13	8036	2381	922	41.0
13c	13	8096	2375	1113	49.0

From Table 7-5, the average compressive strength of the 11 samples is 47.1 MPa with a spread between 41.0 and 53.5 MPa. This can be compared with the values from the casting of Section 2 of the concrete structure in TAS05 with an average of 49.6 MPa and a variation from 46.3 to 53.1 MPa (Mårtensson and Vogt 2019).

The lower average compressive strength in this work compared to data presented by Mårtensson and Vogt (2019) is likely due to the higher water: cement ratio used in this work. The reason for the larger spread is however more difficult to determine and several causes can be identified. The data presented in Appendix A, Figure A-5, show that the water: cement ratio is rather stable and rather on the lower side than on the higher side of the stipulated value. For that reason, these variations cannot be explained by large variations in the w: c ratio between the different batches. Instead it can be speculated that the large differences between samples from different trucks but also from samples from the same truck has been caused during sample preparation and testing. However, this can only be speculated upon and no conclusive evidence can be presented.

6 months compressive strength

Six months of compressive strength was measured on ∅ 100 mm cores from the beams used to verify the function of the strain transducers, Section 6-1. The results are presented in Table 7-6. Samples labelled 1–3 come from the uninsulated mould and samples labelled A–C come from the insulated mould.

Tabell 7-6. 6 months compressive strength for the concrete to the base slab.

Core	Diameter (mm)	Length (mm)	Density (kg/m^3)	Force (kN)	Compressive strength (MPa)
1	99.9	96.2	2320	484	61.2
2	99.9	98.0	2320	528	67.0
3	99.9	95.7	2320	510	64.5
A	99.9	99.8	2330	377	48.1
B	99.9	91.2	2290	555	69.0
C	99.9	93.8	2310	497	62.5

As shown in Table 7-6, the compressive strength continued to increase during the period after 28 days and is for all samples except one higher than 60 MPa with an average value of 64.8. This exceeds with a good margin the requirement of 50 MPa after 90 days. In the calculation of the average value, sample A was excluded as it was considered not representative for this concrete. This was motivated by the fact that the large difference could only have occurred due to poor handling of the specimen in the lab as the same concrete was used to cast all specimens.

The average value can be compared with the corresponding values for the casting carried out in TAS05 (Mårtensson and Vogt 2019) which were 67.7 MPa for the concrete used when casting Section 1 and 67.8 MPa for the concrete for Section 2. The slightly lower strength in the current samples compared to previous samples can probably be explained by higher nominal water: cement ratio in the concrete used in this work compared to the previous work.

7.12.2 6 months splitting tensile strength

6-months splitting tensile strength was measured on ∅ 100 mm cores from the beams used to control the strain transducers, Section 6.1. The results are presented in Table 7-7.

Table 7-7. 6-months splitting tensile strength for concrete to the base slab.

Core	Diameter (mm)	Length (mm)	Weight (g)	Density (kg/m^3)	Force (kN)	Splitting tensile strength (MPa)
1	99.9	98.0	1777	2310	65.9	4.30
2	99.9	99.2	1817	2340	67.3	4.30
3	99.8	94.2	1717	2330	68.4	4.62
A	99.9	97.0	1765	2320	79.5	5.20
B	100.0	100.1	1831	2330	84.5	5.35
C	99.9	99.5	1826	2340	71.2	4.55

As can be seen from Table 7-7, the splitting tensile strength varies between 4.30 and 5.35 MPa with an average value of 4.72 MPa. The average value can be compared with the corresponding value from the casting of a monolith in the CBI's backyard, which was done as a final test in the first part of the material development program (Lagerblad et al. 2017). In that study, an average value of 5.43 MPa was obtained. The slightly lower strength of the samples in this study compared to previous samples can probably be explained by a higher nominal w:c ratio used in this work compared to the previous work, 0.50 and 0.53 respectively. See also Section 8.10.2.

7.12.3 Shrinkage

Casting of the beams for shrinkage measurements was done using concrete from transport truck #14 as shown in Figure 7-21 and the results are presented in Figure 7-22. Two different methods were used in the measurements, Swedish standard SS 137215 (SIS 2000) and for specimens sealed to prevent drying.

As can be seen from Figure 7-22, the drying shrinkage is the dominant part of the total shrinkage of the concrete used here. This could imply that the formation of cracks in 2BMA can be considerably limited by choosing a high humidity climate in the repository. However, this will be contrasted with the fact that other installations can benefit from a drier climate.

Figure 7-21. *Concrete beam for shrinkage measurements made in connection with casting.*

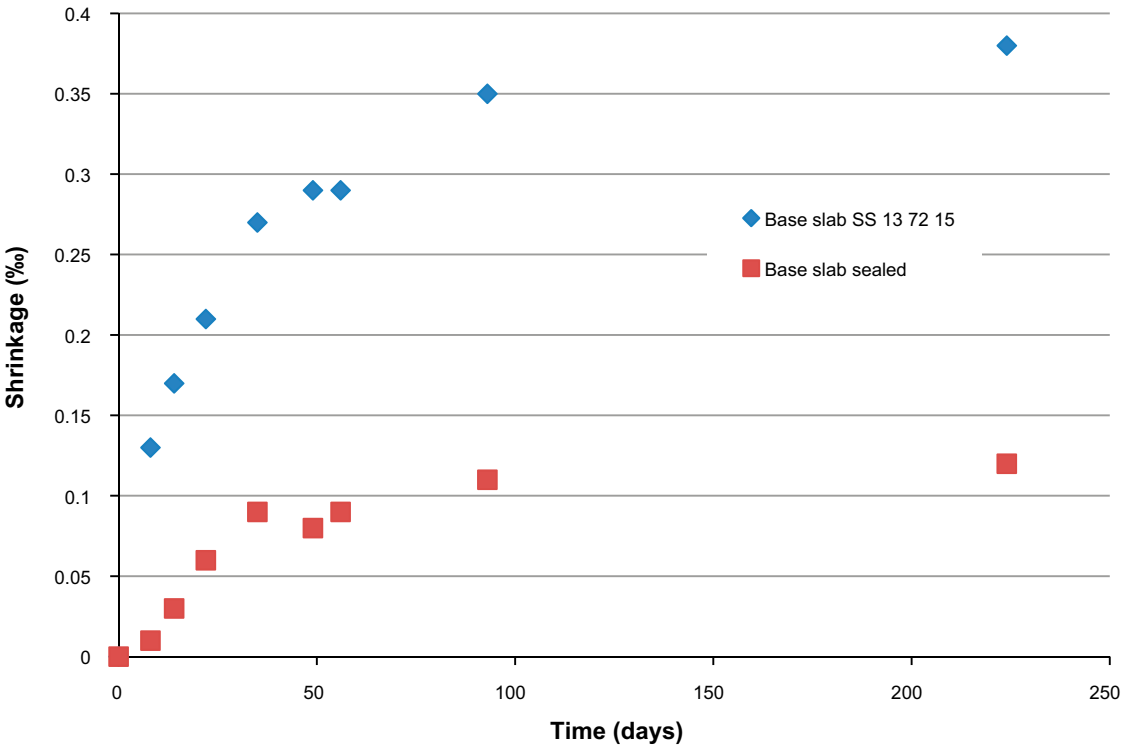

Figure 7-22. *Results from shrinkage measurements using concrete from casting of the base slab.*

7.12.4 Hydraulic conductivity

See Section 8.10.4.

7.13 Casting of the base slab – Summary

In this section the most important experiences from the casting of the base slab of the concrete caisson are presented (Section 7.13.1) as well as a summary of the material properties, Section 7.13.2. Over all, all parts of the work were carried out according to plans and the material properties were as expected.

7.13.1 Implementation

Formwork construction

The formwork was constructed according to requirements. The part of the formwork that formed the recess and held the joint seal took some time to construct but the quality of the work was very high.

Mounting the sensors and wiring

Mounting of sensors was performed after the formwork was erected. The mounting went well and the sensors were fastened in various parts of the formwork.

Concrete production and transport

Concrete production and transport worked very well. Concrete quality was consistent and no adjustments had to be made prior to casting. The average time from mixing cement and water in the first truck mixer until the transport truck had been emptied was about 90 minutes.

Casting

The casting proceeded as planned. However, moving and lifting of the concrete distributor took some time, and in the end that about 4 m^3 of concrete had to be discarded in order to catch up with the casting schedule again.

Working environment

The environment in the tunnel was fine. This was also the case for the concrete production plant as the weather this day was sunny with a nice 15 °C.

7.13.2 Material properties

Concrete composition

Variations in concrete composition between the different mixes were small as shown by the data presented in Appendix A. The relatively large variations for the 4–8 mm aggregate fraction are explained by the low amount of this material type.

Properties of the fresh concrete

The concrete was not exceptionally easy to pump and occasionally the pump pressure increased above 40 bars. Once the concrete was in the mould, it flowed very well and a long rather flat front was formed and for that reason a somewhat stiffer concrete would have been preferred. However, this is not considered feasible due to pumpability reasons.

Properties of the hardened concrete

The properties of the hardened concrete were studied by means of several different methods with the following results:

- 28 days compressive strength varied between 41.0 and 53.5 MPa with an average of 47.1 MPa. After 6 months the average compressive strength had increased to 64.8 MPa with a spread from 61.2 to 69.0, one outlier excluded.
- 6 months splitting tensile strength was measured using cores extracted from the beams used to verify a correct function of the strain transducers. The average splitting tensile strength was 4.72 MPa with a spread between 4.30 and 5.35 MPa.
- Concrete shrinkage was measured according to SIS (2000) where the specimens were stored in a climate room with RH 50 % but also on sealed specimens which were sealed in butyl tape to prevent dehydration. After 224 days, total shrinkage was 0.38 ‰ and 0.12 ‰ respectively for the 2 methods indicating that drying shrinkage is the dominating process.

8 Casting of walls

In this chapter the casting of the walls of the concrete caisson – also including all preparations – is described. For casting of foundation, means to ensure a healthy working environment in TAS08 etc, see Chapter 4. For casting of base slab: see Chapter 7.

8.1 Formwork construction

The formwork was designed for a formwork pressure of about 60 kN/m^2. The design pressure was based on the assumption of a concrete with plastic consistency (not flowable or SCC), setting time of 4–5 hours and a maximum casting rate of 0.5 m/h.

Assembling the formwork required about 3 weeks for completion. The formwork comprised a standard light weight system which was held together by steel tie rods protected by plastic tubes and which therefore could be removed after completion of casting. As mentioned in Section 1.4.1, steel tie rods should preferably not be used in the caissons in 2BMA in order to avoid the formation of hydraulically conducting zones once the tie rods degrade and supporting construction frames should be used instead.

However, in this work supporting construction frames could not be used due to the fact that very limited space in TAS08 made the use of the large lifting devices required to handle these not possible and the use of steel tie rods was therefore accepted. This decision was also supported by the fact that the use of tie rods was not anticipated to influence the outcome of this work.

A photograph of the formwork just prior to completion is shown in Figure 8-1 and a tie rod and plastic tube are shown in Figure 8-2.

Figure 8-1. *An overview image of the formwork just prior to completion.*

Figure 8-2. *A tie rod which is protected by a plastic tube in the upper part of the formwork.*

8.2 Platform

In order to facilitate the casting process, a platform (steel system) was constructed entirely covering the area surrounded by the formwork of the walls, Figure 8-3. This platform was also used as a foundation for the concrete distributor used to distribute the concrete into the formwork. Note the limited space above the formwork.

Figure 8-3. *The concrete distributor has been lifted onto the platform.*

8.3 Emplacement of heating mats

In order to reduce the degree of restraint between the base slab and the walls due to temperature shrinkage of the walls a time after casting, it was decided that the base slab should be heated prior to casting of the walls. Through heating, the base slab was expected to expand a part. Then – through controlled cooling after completion of the casting of the walls – the base slab would slowly return to its original dimensions at approximately the same rate as the walls and the risk of cracking thus be reduced.

A week before the casting of the walls, heating mats and insulation were placed over the entire surface of the base slab, Figure 8-4. Heating mats and insulation were also placed inside the long sides of the formwork while – due to insufficient number of heating mats – only insulation was placed in the short sides of the walls. The effect of heating is discussed in Section 10.2.

Figure 8-4. *Heating mats have been placed over the entire base slab with insulation covering the inner parts.*

8.4 Installation of the sensors

The design of the sensor system is presented in Chapter 3.

8.4.1 Embedded sensors

Temperature and strain

The sensors for follow-up of temperature and strain in the walls were mounted in the formwork and attached to the plastic tubes covering the tie rods just before completion of the formwork, Figure 8-5.

All cables from the sensor system were laid on the concrete surface of the joint between the walls and the base slab inside the wall and then pulled out through the formwork in a single bundle to the control cabinet, Figure 7-8.

Figure 8-5. *Strain transducers mounted in the form rods inside the formwork.*

Formwork-pressure sensors

In addition to the strain and temperature sensors, 2 formwork-pressure sensors were also mounted in the formwork at about 0.48 and 1.48 meters above the base slab. The main function of these sensors was to control the formwork pressure during the casting and ensure that the pressure did not exceed the design pressure and also to follow the setting of the concrete. The pressure sensors were removed the day after completion of casting.

8.4.2 Sensors mounted after casting

Linear Variable Differential Transformers

Linear Variable Differential Transformers (LVDT) were installed a few weeks after disassembling of the formwork, Figure 8-6. The sensors were mounted on a supporting steel construction made of square steel tubes which was secured with bolts into the concrete foundation, Section 4.4. This means that no part of the supporting steel construction was in contact with any part of the caisson.

Relative humidity sensors

Sensors for measuring the relative humidity of the concrete were mounted in the concrete after disassembling of the formwork. The sensors were placed at 2 different depths by drilling holes into the concrete. The holes were sealed to the outside with silicon to prevent any direct influence from the tunnel climate; see also figure 7-7.

8.4.3 Control cabinet

See Section 7.5.3.

Figure 8-6. *LVDT-sensor mounted against the top part of the wall.*

8.5 Concrete production and transport

8.5.1 Concrete production

The concrete was produced in the concrete production plant according to the method outlined in Section 5.6.3. In total, about 150 m^3 of concrete was produced and transported to the casting site in trucks, each carrying about 7 m^3.

8.5.2 Adjustments of the concrete mix design

Prior to the casting of the walls, tests with the aim of identifying the need for adjustments of the concrete mix design were carried out. This was called for because the outside temperature was only about +3 °C compared to +15 °C when casting the base slab. The need for adjustments was also motivated by the fact that a very good control of the setting was required in order to ensure sufficient homogenisation of the different concrete layers but also to avoid an excessive formwork pressure.

The concrete was mixed in the 2 truck mixers in batches of 3.5 m^3 according to the previously used procedure. The tests showed that the optimum casting properties for casting of walls according to the intended plan were obtained if the retarder was excluded but the mix design was otherwise left unchanged. It was therefore decided that the casting of the caisson's walls should be carried out with the mix design in Table 8-1.

Table 8-1. Concrete mix design for the walls.

Component	Product name/supplier	Amount (kg/m^3)
Cement	Degerhamn anläggningscement	320
Limestone filler	OmyaCarb 2GU (grain size: 2 µm)	130
Limestone filler	Myanit 10 (grain size: 10 µm)	34.3
Water		169.4*
Aggregates 16–22 mm	Flivik (Crushed rock)	383.5
Aggregates 8–16 mm	Flivik (Crushed rock)	415.1
Aggregates 4–8 mm	Flivik (Crushed rock)	89.7
Aggregates 0–4 mm	Rollsmo (Crushed rock)	819.9
Superplasticiser	MasterGlenium Sky 558	1.60
Superplasticiser	Master Sure 910	1.70
Retarder	Master Set RT 401	-

*Water in admixtures not included.

The different components were added in the order outlined below and the actual amounts of each component according to data from the truck mixers´ built-in weighing systems are shown in Table A-13.

1. Water and admixtures
2. Aggregates 16–22 mm
3. Cement
4. Fillers
5. Aggregates 0–4 mm
6. Aggregates 4–8 mm
7. Aggregates 8–16 mm

The difference between target amounts and actual amounts for water, cement and aggregates is displayed in Figure A-6, A-7 and A-8 in Appendix A. According to SIS (2013), the tolerances of the batching process are ± 3 % for cement, water and total aggregates. There are no requirements on the tolerance for the individual aggregate fractions. Figure A-6 shows that the tolerance for cement and aggregate is within the limits. For water, the tolerance is not met for three batches. With one exception, less water is added than required according to mix design which results in lower w/c (safe side regarding strength, workability may be influenced negatively). The largest differences were again recorded for aggregate fraction 4–8 mm, generally on the plus-side. See Section 7.6.2 for details.

On average, the difference between target amounts and actual amounts for all batches was −0.2 % for water, +0.8 % for cement and +0.7 % for total aggregates. This is very high precision again, considering the manual control of the weighing process in the truck mixers and displays the skill of the operators.

8.5.3 Concrete testing at production site

During concrete production, the temperature, slump and, in some cases, also air content were measured, Table 8-2. Data from the truck mixers weighing system showing variations between the different mixes are presented in Appendix A.

Table 8-2. Concrete properties at the time of production.

Truck #	Water addition time	Testing time	Temperature (°C)	Slump (mm)	Air content (%)
1a	07:10	07:26	7.8	200	
1b	07:15	07:30	7.6	180	
2a	07:30	07:50	8.1	190	
2b	07:40	07:55	8.0	210	
3a	07:55	08:15	9.1	200	3.1
3b	08:05	08:20	8.7	210	
4a	08:20	08:50	9.5	200	
4b**	08:30	08:55	9.1	220	
5a	08:55	09:25	9.3	220	
5b	09:05	09:30	9.4	220	
6a	09:35	09:55	8.8	220	
6b	09:40	10:00	9.3	230	
7a	10:00	10:25	10.1	160	
7b	10:05	10:30	10.0	160	3.5
8a	10:35	10:55	10.1	220	
8b	10:40	11:00	10.0	230	
9a	11:05	11:25	10.4	210	
9b	11:10	11:30	9.7	190	
10a	11:35	11:50	9.6	220	
10b	11:35	12:00	10.6	200	
11a	12:05	12:25	9.5	230	
11b	12:10	12:30	9.8	220	
12a	12:30	12:55	10.0	230	
12b	12:35	13:00	11.2	210	3.2
13a	13:05	13:20	9.9	220	
13b	13:10	13:25	9.5	220	
14a	13:25	13:50*	10.5	240	
14b	13:30	13:55	10.3	210	
15a*	13:55	14:20	11.3*	210	
15b	14:00	14:25	12.5	210	
16a	14:30	14:50	12.3	230	
16b	14:35	15:00	11.5	220	
17a	15:00	15:25	12.1	240	
17b	15:05	15:30	11.3	240	
18a	15:35	15:55	10.7	180	
18b	15:40	16:00	12.2	210	
19a	16:00	16:25	12.2	210	3.1
19b	16:10	16:30	12.5	190	
20a	16:30	16:55	11.5	210	
20b	16:40	17:00	11.0	220	
21a	17:05	17:30	10.9	200	
21b	17:10	17:35	10.6	210	
22a	17:35	17:55	10.3	220	
22b	17:40	18:00	11.7	210	

* At 13:50 about 9 metric tons of cement was delivered into the silo. Concrete temperatures indicate that the new cement was being used from truck #15a.
** From truck #4b additional 0.01 % of the cement weight of Sky 558 was added.

8.6 Casting

8.6.1 Equipment

The same equipment as used for casting of the base slab was used also here. See Section 7.7 for details.

8.6.2 Quality control at the casting site

Slump

On arrival at the main tunnel TASU, the concrete slump was measured, Table 8-3. For all trucks the properties were according to requirements and no adjustments were necessary.

Table 8-3. Slump on arrival at the casting site.

Truck #	Water addition time	Measurement time	Slump (mm)
1	07:10	08:02	200
2	07:30	08:37	220
3	07:55	09:08	230
4	08:20	09:32	220
5	08:55	09:59	220
6	09:35	10:24	240
7	10:00	10:57	220
8	10:35	11:23	220
9	11:05	11:50	210
10	11:35	12:25	230
11	12:05	12:52	220
12	12:30	13:24	230
13	13:05	13:54	235
14	13:25	14:20	230
15	13:55	14:52	225
16	14:30	15:27	220
17	15:00	16:01	230
18	15:35	16:24	220
19	16:00	17:00	220
20	16:30	17:38	220
21	17:05	17:57	220
22	17:35	18:37	220

Manufacturing of specimens for quality control

During control of the properties of the fresh concrete, specimens were also produced for later measurement of the concrete's compressive strength and shrinkage, Figures 8-7 and 8-8.

Figure 8-7. *Specimens for control of compressive strength.*

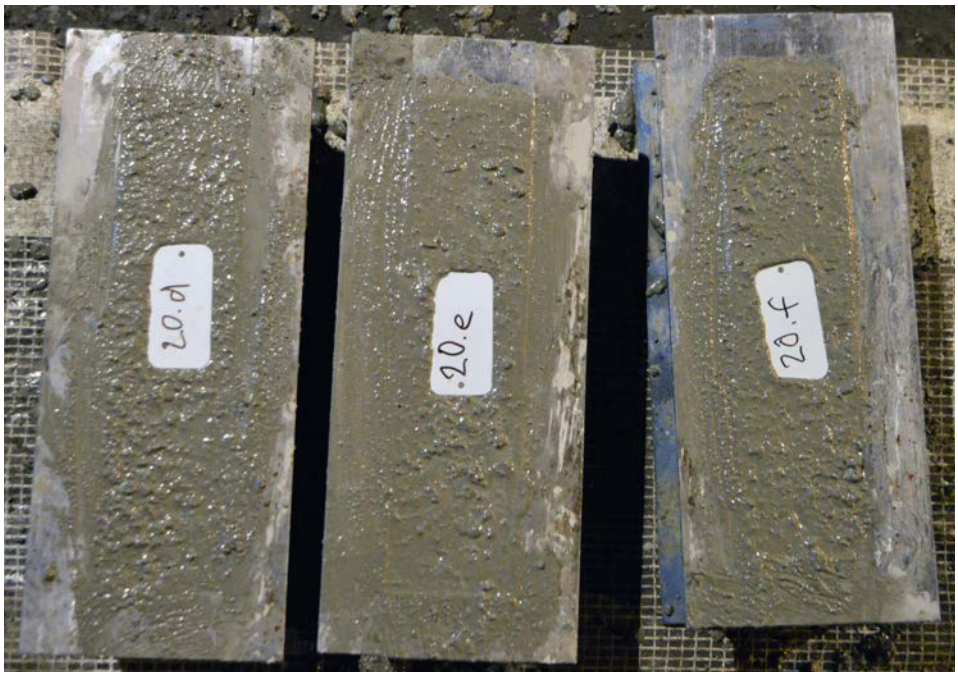

Figure 8-8. *Specimens for control of shrinkage.*

8.6.3 Schedule for casting of the walls

Casting was carried out with an increment of about 400 mm per hour, corresponding to about 14 m^3 or 2 trucks per hour. Prior to start of casting the pipes and hoses were lubricated with cement slurry. The casting schedule is presented in Table 8-4.

Table 8-4. Schedule for casting of the walls.

Truck #	Water addition time	Pumping starts	Truck empty	Time from mixing until transport truck was empty
1	07:10	08:02	08:29	1 h 19 min
2	07:30	08:35	09:01	1 h 31 min
3	07:55	09:06	09:24	1 h 29 min
4	08:20	09:30	09:53	1 h 33 min
5	08:55	09:59	10:15	1 h 20 min
6	09:35	10:20	10:35	1 h
7	10:00	10:55	11:11	1 h 11 min
8	10:35	11:21	11:40	1 h 05 min
9	11:05	11:48	12:10	1 h 05 min
10	11:35	12:21	12:38	1 h 03 min
11	12:05	12:50	13:11	1 h 06 min
12	12:30	13:20	13:40	1 h 10 min
13	13:05	13:49	14:07	1 h 02 min
14	13:25	14.17	14:36	1 h 11 min
15	13:55	14:48	15:05	1 h 10 min
16	14:30	15:21	15:34	1 h 04 min
17	15:00	15:56	16:14	1 h 14 min
18	15:35	16:20	16:33	0 h 58 min
19	16:00	16:55	17:18	1 h 18 min
20	16:30	17:32	17:48	1 h 18 min
21	17:05	17:51	18:18	1 h 13 min
22	17:35	18:30	No data	

As can be seen from Table 8-4, the work proceeded relatively quickly with a time from mixing water and cement in the first truck mixer until the transport truck was emptied of between 60 and 90 minutes. A comparison with the schedule for casting of the base slab (Table 7-4) shows that casting of walls was about 20 minutes faster for each truck than for casting of the base slab. Figure 8-9 show the placement of concrete as well as vibration.

8.6.4 Formwork pressure

The formwork pressure was measured at two levels in formwork, 0.48 and 1.48 meters above the top of the base slab. As shown in Figure 8-10, the maximum pressure was 28 kPa, which was about half of the design pressure. Considering also the fact that both placement of the concrete as well as homogenisation of the successive layers were easily carried out this shows that the concrete setting was very well optimized for this casting.

Figure 8-9. *Placement of the concrete and vibration in the upper part of the wall.*

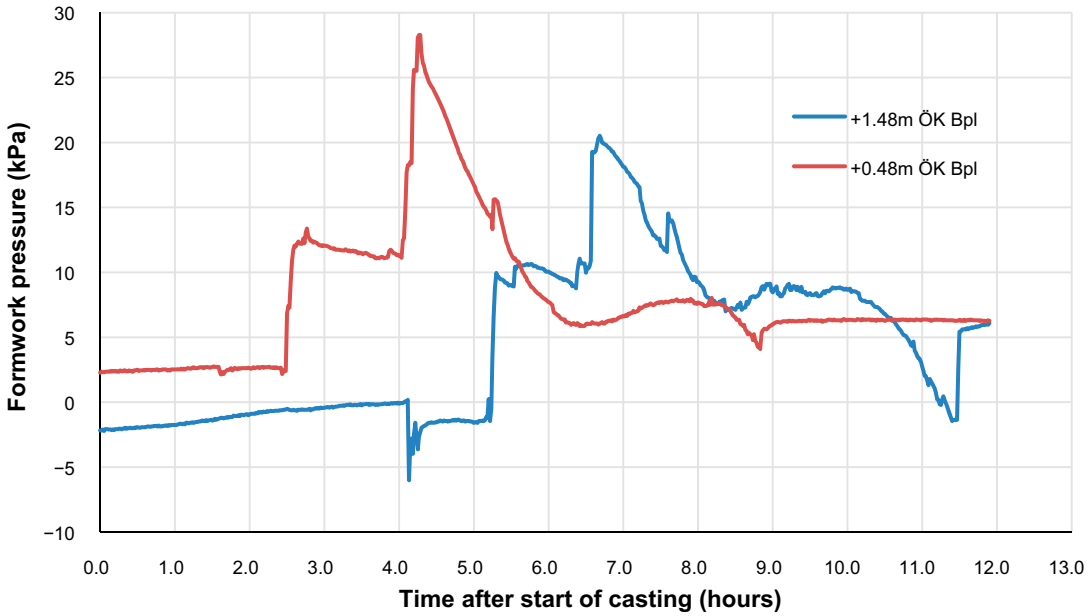

Figure 8-10. *Formwork pressure at 2 different levels. Please note that casting started at time 30 minutes in this diagram.*

8.7 Post treatment and preliminary inspection

Covering

As a final step, the concrete surface was covered with a plastic sheet, Figure 8-11.

Disassembling of the formwork

Disassembling of the formwork started 1 week after casting was finished.

Visual inspection immediately after disassembling of the formwork

Immediately after disassembling of the formwork, an inspection was conducted in which the physical result of the casting was examined. The focus here was on surface properties, the presence of air bubbles or other imperfections and the occurrence of cracks. Figure 8-12, shows the caisson after dismantling of the formwork.

Figure 8-11. *The top surface of the concrete has been covered with a plastic foil.*

Figure 8-12. *The caisson after dismantling of the formwork.*

8.8 Detailed inspection

8.8.1 Walls

The walls were smooth and fine but with some colour variations and only a few smaller blisters. An overall view of the wall towards TASU is shown in Figure 8-12 and details are shown in Figure 8-13.

Figure 8-13. *The picture on the left shows a protective tube for a tie rod and the one on the right shows a colour change in the wall caused by the use of concrete from 2 different trucks. In the right image, the contrast has been enhanced compared to the original image.*

8.8.2 Joint between base slab and walls

The appearance of the joints on the outside was affected by incomplete filling of parts of this section during casting of the base slab, Section 7.10.1. Figure 8-14 shows the appearance of a perfectly executed joint (left image) and a joint with poor filling in this section of the base slab (right image).

Figure 8-15 shows the joint's appearance on the interior of the caisson. The left image shows a corner and the right image the joint on one of the sides. From these images it is noted that a small amount of cement paste penetrated under the bottom edge of the formwork and out onto the base slab.

However, these are very small quantities which have no effect other than that it is not possible to precisely study the transition between the wall and the base slab in this zone. The properties of the joint will therefore need to be investigated through studies of cores extracted from this zone.

Figure 8-14. *Joint between the base plate and wall in an area with the correct casting of the base slab (left) and in an area with poor filling in this section of the base slab.*

Figure 8-15. *Visual appearance of the joint on the inside of the concrete caisson.*

8.9 Crack monitoring

Visual inspections of the caisson with a focus on the occurrence of cracks were carried out on a weekly basis from the time of disassembling of the wall formwork. At the time of writing (roughly one year after casting of the walls) no cracks have been detected in the walls or in the base slab.

8.10 Material properties

8.10.1 Compressive strength

28 days compressive strength

28 days compressive strength was measured on cubes manufactured during casting of the walls and the results are presented in Table 8-5.

Table 8-5. 28 days compressive strength for the concrete to the caisson walls.

Specimen	Truck #	Weight (g)	Density (kg/m^3)	Force (kN)	Compressive strength (MPa)
2a	2	8073	2392	1087.3	48.3
2b	2	7846	2325	1064.4	47.3
2c	2	8016	2367	1123.4	49.8
7a	7	7977	2363	1100.1	48.9
7b	7	7986	2369	1117.8	49.7
7c	7	8073	2376	912.6	40.3
12a	12	7992	2368	979.8	43.5
12b	12	7917	2338	1000.9	44.3
12c	12	8115	2405	822.7	36.6
18a	18	8016	2375	1045.9	46.5
18b	18	8026	2362	917.3	40.5
18c	18	8059	2388	987.5	43.9

From the values presented in Table 8-5, the average compressive strength is 45 MPa with a spread between 36.6 and 49.8 MPa. This can be compared to the average from the casting of the base slab which was 47.1 MPa with a variation between 41.0 and 53.5 MPa and the average from the casting of Section 2 in TAS05 which was 49.6 MPa with a spread between 46.3 and 53.1 MPa.

Thus, it is seen here that both the highest and the lowest values when casting the walls are lower than the corresponding values in previous castings. In addition, the spread between the highest and lowest values in this casting is almost twice as large as when casting in TAS05 when a “real” concrete station is used. Compared to the casting of the base slab, the spread is comparable but still unexpectedly high. For a discussion on possible causes of these results, see Section 7.12.1.

6 months compressive strength

6 months compressive strength was measured on cores from different parts of the walls of the caisson. As shown in Table 8-6, the strength growth continued during the period after 28 days and the average value after about 6 months is 55.8 MPa with a rather large spread between 49.0 and 61.0 MPa. These values are lower than the 6 months compressive strength for concrete from the base slab but the reason is unknown. A comparison between Table A-5 and A-10 show that the water: cement ratio is similar for concrete used in the walls and the base slab respectively.

Table 8-6. 6 months compressive strength for the concrete to the caisson walls.

Specimen	Density (kg/m^3)	Force (kN)	Compressive strength (MPa)	Comment
F08000013-1	2310	429.0	55.5	
F08000013-2	2320	433.6	56.5	
F08000008-1	2310	477.2	61.0	In the joint
F08000008-2	2280	454.0	58.0	In the joint
F08000010-1	2300	425.2	55.0	In the joint
F08000010-2	2280	444.9	58.0	In the joint
F08000011-1	2310	377.7	49.0	
F08000011-2	2310	408.0	53.0	

8.10.2 6 months splitting tensile strength

6 months splitting tensile strength was measured on cores from different parts of the walls of the caisson. The results are presented in Table 8-7.

Table 8-7. 6 months splitting tensile strength for cores from the caisson walls.

Specimen	Density (kg/m^3)	Splitting tensile strength (MPa)	Comment
F08000013-1	2310	3.70	
F08000013-2	2320	4.20	
F08000008-1	2310	3.60	In the joint
F08000008-2	2280	2.40	In the joint
F08000010-1	2300	2.25	In the joint
F08000010-2	2280	3.45	In the joint
F08000011-1	2310	4.40	
F08000011-2	2310	2.80	

From the values presented in Table 8-7, the average splitting tensile strength is 3.0 MPa. However, it should be noted that half of the samples come from the joint between the base slab and the wall. For the pure bulk concrete, the average splitting tensile strength is 3.8 MPa.

These values can be compared with the corresponding values for concrete from the base slab, Section 7.12.2 which were significantly higher with an average value of 4.7 MPa and a spread between 4.3 and 5.3 MPa. Also, Lagerblad et al. (2017) reported splitting tensile strength on concrete samples from a monolith cast in the CBI's backyard of 5.4 MPa, which is considerably higher than measured in this work.

8.10.3 Shrinkage

Shrinkage was measured according to SIS (2000) but also using sealed samples which did not permit drying shrinkage using specimens manufactured from concrete from truck #20, Figure 8-16.

As can be seen from Figure 8-17, the drying shrinkage is the dominant part of the total shrinkage of the concrete used here. However, whereas shrinkage according to SS 13 72 15 (SIS 2000) is basically the same as for concrete from the base slab, the shrinkage for sealed samples is in principle zero here compared to about 0.1 ‰ for concrete from the base slab.

Figure 8-16. *A concrete beam for shrinkage measurements made of concrete from transport truck #20.*

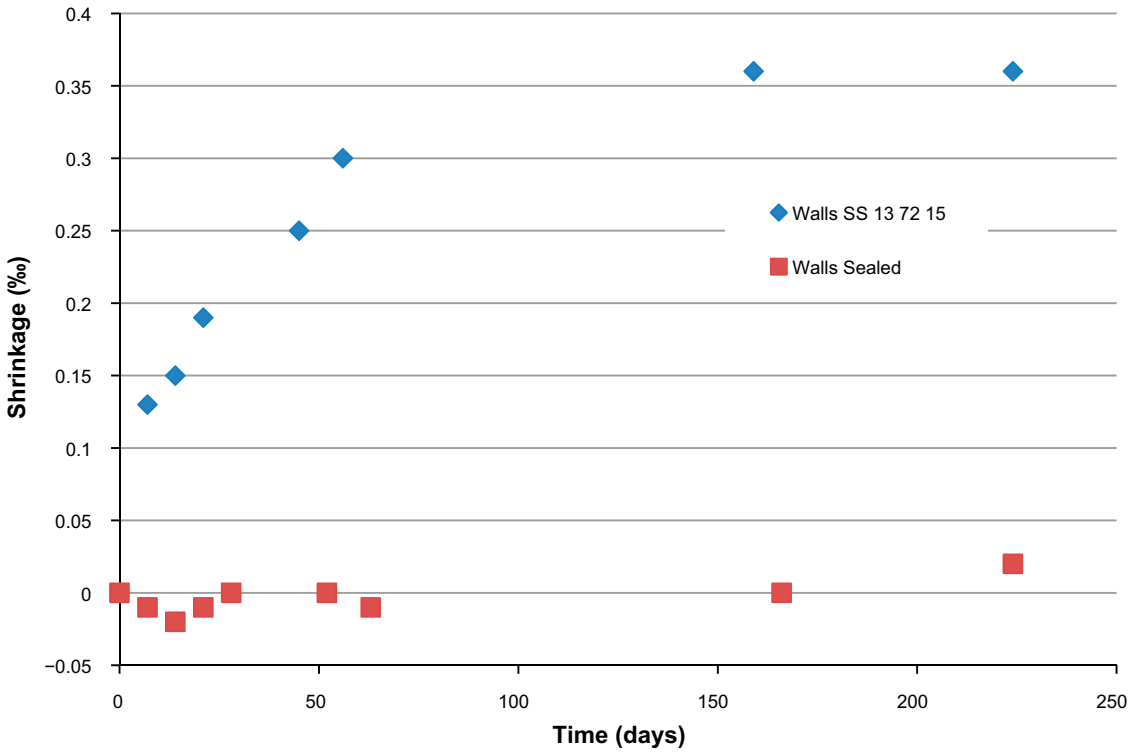

Figure 8-17. *Results from shrinkage measurements using concrete from casting of the walls.*

8.10.4 Hydraulic conductivity

Hydraulic conductivity was measured on cores obtained from different parts of the caisson with focus on the comparison of cores extracted from the centre of the wall and from the joint between the base slab and the walls respectively. Figure 8-18 shows holes for drilled cores in the joint between the base slab and the wall and Table 8-8 presents data from the measurement of hydraulic conductivity in the different parts of the caisson.

Table 8-8. Hydraulic conductivity for bulk specimens and specimens from the joint.

Specimen	Hydr. cond. [m/s]	Direction of drilling	Comment
F08000008a	5.4×10^{-8}	Across the core	In the joint
F08000008b	3×10^{-11}	Across the core	In the joint
F08000011 IN	1×10^{-11}	Along the core	Centre of wall
F08000013	3×10^{-12}	Along the core	Centre of wall

From Table 8-8, the hydraulic conductivity of specimen F08000008b is similar to that of the bulk concrete whereas it is much higher for specimen F08000008a even though these have been extracted from the same original core. The most likely reason for this is the presence of some weak part in the joint due to poor surface preparation of the joint prior to casting of the walls. This conclusion is supported by the fact that specimen F08000010 which was extracted from a nearby position separated completely in the joint during specimen preparation.

These results confirms the findings presented by Mårtensson and Vogt (2019) that the joint between the walls and the base slab will not constitute a hydraulically conducting zone as long as the surface is properly prepared prior to casting of the walls. The findings that the hydraulic conductivity of the joint between the walls and the base slab is similar to that of the bulk concrete would also support the conclusion that joint seals will not be required in the future caissons in 2BMA.

Figure 8-18. *Holes after extraction of cores from the joint between the base slab and one of the walls.*

8.11 Casting of the walls – Summary

In this section the most important experiences from the casting of the walls of the concrete caisson are presented (Section 8.11.1) as well as a summary of the material properties, Section 8.11.2. Over all, all parts of the work were carried out according to plans but concrete strength were a little lower than expected with a larger spread between the individual values than observed during previous work.

8.11.1 Implementation

Formwork construction

The formwork was very well built and the preparations for casting complete. The formwork was designed for a maximum pressure of 60 kPa which gave a good margin to the maximum formwork pressure during casting which was only 28 kPa.

Installation of the sensors and handling of cables

Installation of the sensors was performed after assembling of the formwork. The installation went well and the sensors were secured in the plastic tubes that protected the form rods.

Concrete production and transport

Concrete production and transport worked very well. Concrete quality was consistent and no adjustments had to be made prior to casting.

Casting

Casting of the walls was performed entirely according to plans with an average time from concrete mixing until the transport truck was empty of about 70 minutes. The handling of the concrete hose and distributor worked very well. A comment from the staff was that the casting would not have been possible without the distributor as the hose was far too heavy to handle under such an extensive casting.

Working environment

The working environment was good in the tunnel, although it became quite hot at the workplace. Above ground it was cloudy and +3–4 ºC which was really good for being late November. Slight rainfall fell during the night and the morning before casting but no rain during the day.

Disassembling of the formwork

The formwork was disassembled without any major problems. The main problems being those related to the limited space for lifting of equipment and formwork parts.

8.11.2 Concrete properties

Concrete composition

Variations in concrete composition between the different mixes were small as shown by the data presented in Appendix A. The relatively large variations for the 4–8 mm aggregate fraction are explained by the low amounts of this material type.

Properties of the fresh concrete

The properties of the fresh concrete were very well adjusted for casting of the walls with only minor variations of the concrete slump and required pump pressure. Concrete setting permitted complete homogenisation of the different concrete layers but was still fast enough to ensure that the formwork pressure was well below the design pressure of the formwork.

Properties of the hardened concrete

The properties of the hardened concrete were studied by means of several different methods with the following results:

- 28 days compressive strength varied between 36.6 and 49.8 MPa with an average of 45 MPa. After 6 months the average compressive strength had increased to 55.8 MPa with a spread from 49.0 to 61.0 MPa.
- 6 months splitting tensile strength was measured using cores extracted from different parts of the walls. The average splitting tensile strength of bulk concrete was 3.8 MPa with a spread between 2.80 and 4.40 MPa.
- Concrete shrinkage was measured according to SIS (2000) where the specimens were stored in a climate room with RH 50 % but also on specimens which were sealed to prevent dehydration. After 224 days, total shrinkage was 0.36 ‰ and 0.02 ‰ respectively for the 2 methods indicating that drying shrinkage is the dominating shrinkage process.
- Hydraulic conductivity of specimens from the central parts of the walls was 1×10^{-11} to 3×10^{-12} m/s whereas corresponding values for the joint between the base slab and the walls was about 5×10^{-11} m/s. Unfortunately the number of specimens had to be limited due to the very long measuring time and limited availability of equipment.

9 Grouting of holes at the position of the tie rods in the caisson walls

9.1 Background/Overview

According to the initial requirement (Section 1.4) the formwork should be constructed without the use of tie rods but instead supporting construction frames should be used where the formwork could not be supported against adjacent bedrock. However, as noted in Section 2.3.2 the use of a formwork without tie rods was not possible in this work due to the very limited space for lifting of large construction parts available in TAS08 and the use of tie rods was therefore a requirement to facilitate this work. Also, the use of tie rods was not expected to influence the outcome of this test casting.

As the use of tie rods dramatically simplifies formwork construction compared to formwork construction using supporting construction frames discussions concerning the possibility to remove the plastic tubes and fill the holes with a grout were initiated. In these discussions, it was decided to perform a small-scale test of the concept using the equipment available at the Äspö laboratory. If this showed promising results, a production test should be performed in order to further develop material and method for grouting of the holes.

9.2 Concept test

The concept test was focused on three main issues; (i) investigating methods for removing the plastic tubes from the holes in the concrete walls, (ii) finding a suitable material for grouting of the holes and (iii) evaluating the hydraulic conductivity of the grouted holes in order to verify that the concept was promising enough for further development work to be carried out.

9.2.1 Methods

The concept test comprised a total of 15 holes in different parts of the caisson walls, Figure 9-1. The work included several steps, which are described in the following sections.

Figure 9-1. *Some of the holes used in the concept test have been covered with a wooden board with a hole provided with a plastic hose for injection of the grout.*

Extraction of the plastic tubes

The first attempts to remove the plastic tubes were conducted using either a standard cemented carbide drill (diameter approximately 30 mm and length 800 mm) alone or in combination with a special drill made for this work.

Surprisingly, drilling was considerably more troublesome than expected. When drilling with the special tool, the high heat output caused the plastic to melt and stick to the drill which made it difficult to use. When using the cemented carbide drill for concrete / stone the drill did not follow the direction of the hole which resulted either in the formation of 2 holes on the inside of the caisson, Figure 9-2, left image or in a keyhole shaped hole, Figure 9-2, right image. However, also holes where the plastic tube was successfully removed were produced by this method but these had been prepared for grouting and covered with a wooden board at the time the holes were documented.

In addition, breakouts of concrete were noted adjacent to the holes on the inside of the caisson, Figure 9-2.

Mounting of mould

Wooden boards, each provided with a hole and a flexible plastic hose were fixed against both the inside and outside surfaces of the caisson walls and sealed with silicone, Figure 9-3. The purpose of the flexible hose was to allow some overfilling of the holes and prevent the formation of a gap in the upper part of the hole.

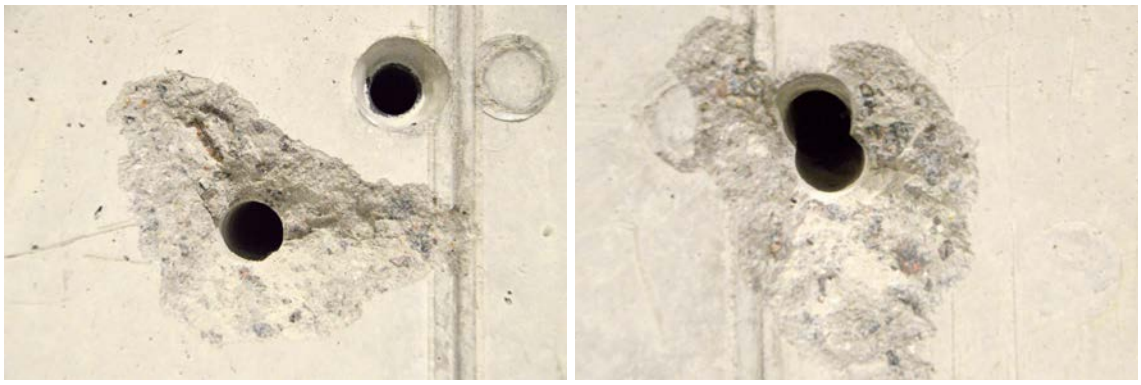

Figure 9-2. *Holes on the inside of the caisson showing both that drill has not followed the direction of the holes but also large breakouts at the concrete surface.*

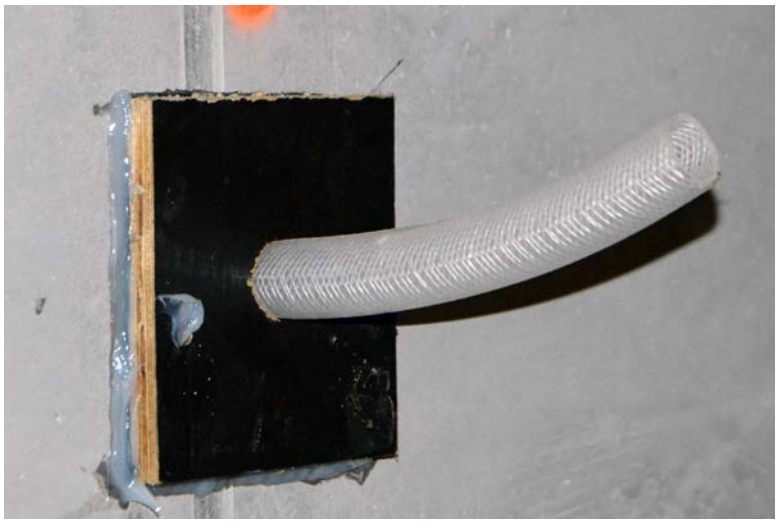

Figure 9-3. *The wooden board provided with a flexible hose mounted on the surface of the caisson wall.*

Wetting

To prevent dehydration of the grout inside the hole, the holes were filled with water a few days before the grouting was to be carried out. Both filling and emptying of the holes were carried out without problems.

Mixing of grout

Grout (Bemix A3 from Finja) which was mixed with a hand-held mixer in a larger barrel was used, Figure 9-4. The grout was mixed according to instructions on the package with 2.9 litres of water per 25 kg of dry material, Figure 9-5, giving it an almost liquid consistency.

Figure 9-4. *Mixing of grout.*

Figure 9-5. *Front and back of the package for Bemix A3 ready-mixed powder.*

Grouting

Shortly before grouting, the holes were emptied of the remaining water.

Grouting was carried out with a hand-held pump, Figure 9-6. The pump was filled by dipping the tip into the grout, after which the grout was sucked into the cylinder. The tip of the pump was then pushed into the hose after which the grout was pressed into the hole, Figure 9-6.

Grouting was quick and easy and only took a few minutes per hole with one or two refills of the pump for each hole. When the grout level was sufficiently high in the plastic hose on the inside of the caisson, grouting was stopped and the grout left to harden, Figure 9-7.

Figure 9-6. *Grouting the hole with a hand-held injection pump.*

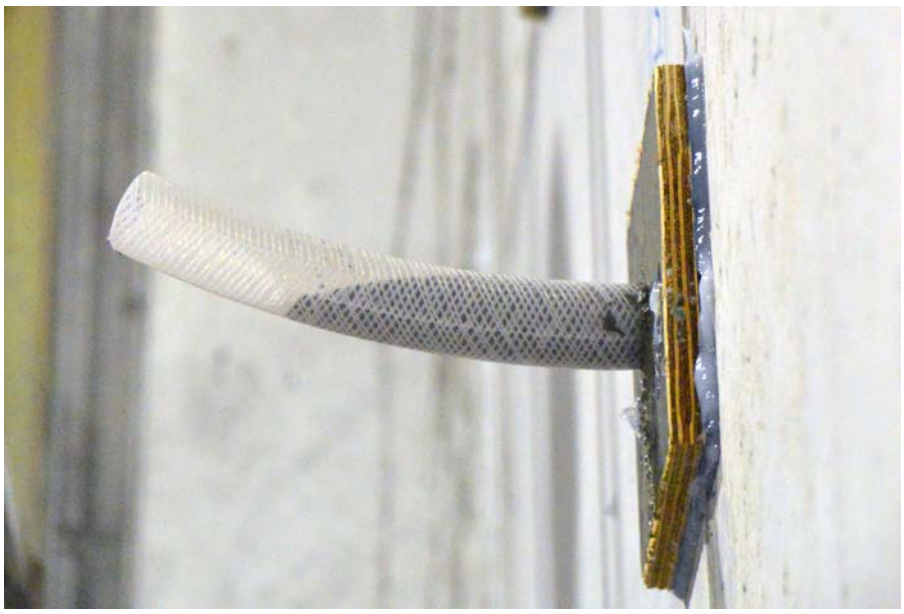

Figure 9-7. *The hole is filled and grouting stopped.*

9.2.2 Specimen preparation and analyses

Core drilling

About 6 weeks after grouting the grouted holes were over-cored with ∅ 100 mm core drill from the outside of the caisson, after which the cores were covered in plastic prior to evaluation to be performed, Figure 9-8.

Specimen preparation

The cores (length 680 mm) were first divided into two shorter sections, of which one was split along its central axis for visual inspection while the other was used for measurements of hydraulic conductivity.

Figure 9-8. *Cores waiting for evaluation.*

9.2.3 Evaluation

Evaluation comprised visual inspections and documentation of the cores as well as measurements of the hydraulic conductivity of the some of the specimens as summarised below.

Visual inspection

Visual inspection of the injected holes showed that some holes were completely filled with grout, Figure 9-9 (left image) whereas in others a large void that penetrated the entire thickness of the wall was observed, Figure 9-10. The images also show some separation of the grout manifested in a layer of cement paste on the top of the grout, Figure 9-9 (right image). This should suggest that too much water was used when mixing the grout even though the specifications on the package was followed. Overall, grouting was unsuccessful in too many holes for the concept test to be considered a success.

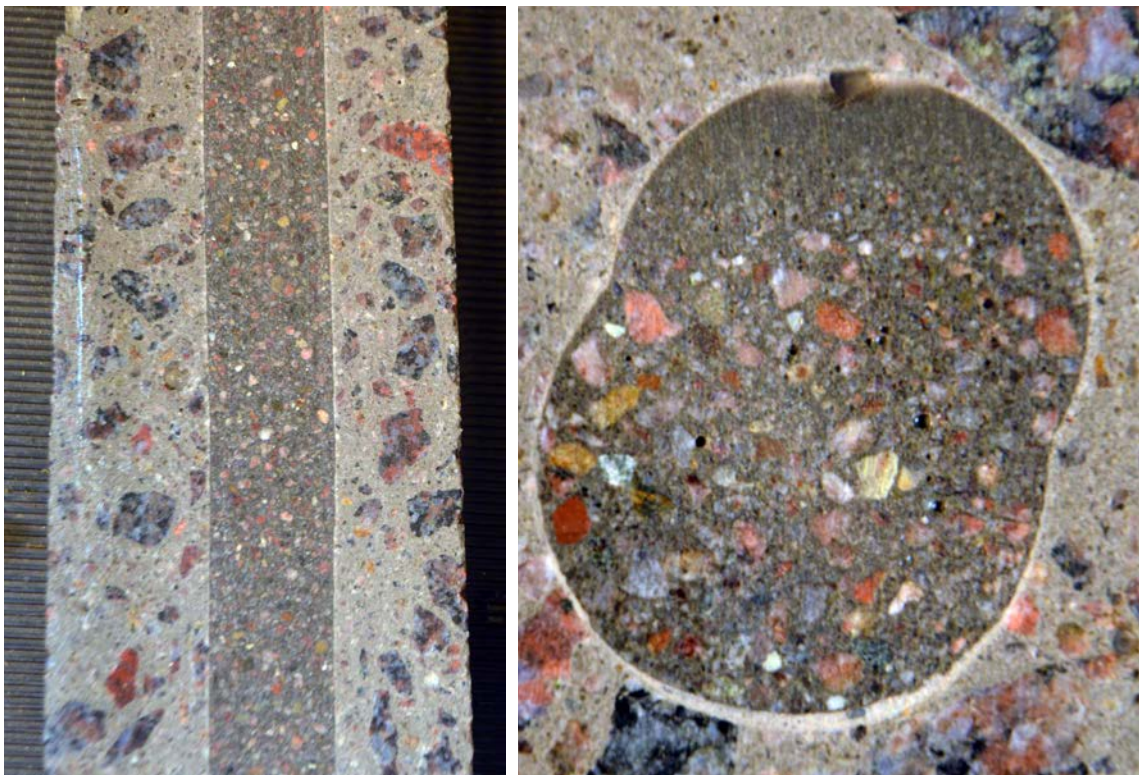

Figure 9-9. *Successful grouting (left image) and grouting with separation layer (right image).*

Figure 9-10. *Failed grouting.*

Hydraulic conductivity

The hydraulic conductivity was measured for some of the specimens and the results are shown in Table 9-1. From this table it is clear that for specimens for which grouting was successfully done; the hydraulic conductivity is similar to that of the bulk concrete. However, of the total of 7 grouted holes, 5 contained a penetrating pore and only 2 were without pores. For specimens with penetrating pores, the hydraulic conductivity was more or less infinite. For that reason, only one of the cores containing a penetrating pore was quickly checked after which all cores with pores were discarded.

Table 9-1. Hydraulic conductivity of grouted holes and bulk concrete as a reference.

Specimen	Hydr. cond. [m/s]	Comment
F08000002 B	-	Penetrating pore, not tested
F08000002 M	-	Penetrating pore, not tested
F08000002 T	3×10^{-12}	-
F08000003 B	-	Penetrating pore, not tested
F08000003 M	7×10^{-12}	-
F08000003 T	1×10^{-11}	-
F08000011 IN	1×10^{-11}	Bulk concrete
F08000013	3×10^{-12}	Bulk concrete

Position in the core. B = Inside, M = Middle, T = Outside.

9.2.4 Concept test – Summary and conclusions

The concept test presented in this section comprised two parts, removal of plastic tubes and grouting, which are shortly summarised below.

Removal of plastic tubes

Removal of the plastic tubes was much more troublesome than expected and at this stage it is concluded that the methods used in the concept test were unsuitable for the purpose.

Grouting of the holes

The most important result from the grouting test is that the hydraulic conductivity of holes that have been successfully grouted is in par with the hydraulic conductivity of the bulk concrete. However, as also shown here, only a few holes were successfully grouted and in many holes, a void that penetrated the entire thickness of the wall was formed in the upper part of the hole. Also in many holes, a separation layer containing mainly cement paste was formed in the upper part of the grout.

It was believed that both the voids and the separation layer could be attributed to the choice of method for grouting as the hand held pump required the use of a very fluid grout. With the excellent hydraulic properties of the successfully grouted holes in consideration, it was therefore decided to perform a production test with improved material and equipment.

9.3 Production test

A few months after the concept test was completed, a production test was carried out. This test comprised both development of material and method for grouting but also of equipment and method for removal of the plastic tubes from the concrete wall.

9.3.1 Extraction of the plastic tubes

With the experiences of the concept test in fresh memory, it was decided to change strategy for method of extracting the plastic tubes. Instead of drilling, the work was directed to methods where the tubes were instead first heated to obtain a slight shrinkage and then pulled out of the walls by means of an extraction tool.

Heating

In all parts of the production test, heating was done using a standard hot air gun. In order to evenly distribute the heat within the entire plastic tube, a perforated steel tube equipped with a funnel was inserted into the tube during heating, Figure 9-11.

Extraction of the tubes

Several different tests were carried out during the development of the extraction tool finally leading to the design shown in Figure 9-12.

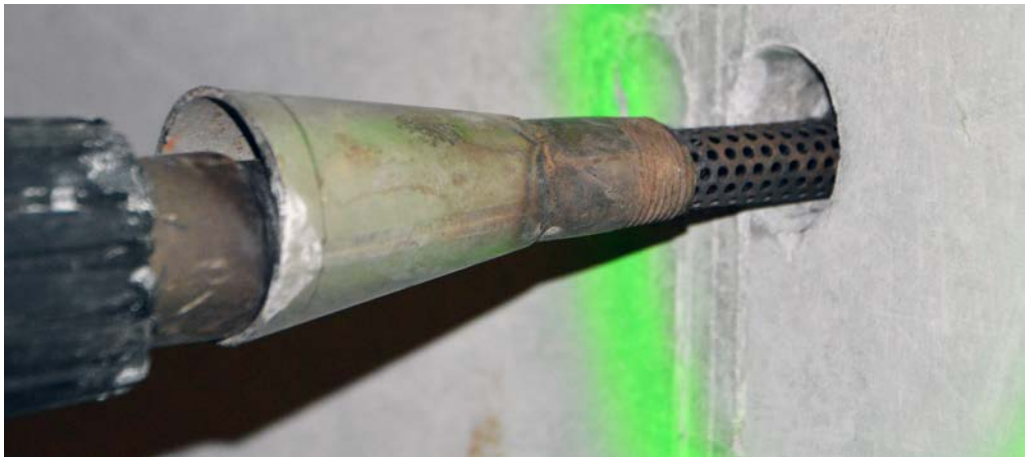

Figure 9-11. *The hot air gun and perforated steel tube used to heat the plastic tube prior to extraction.*

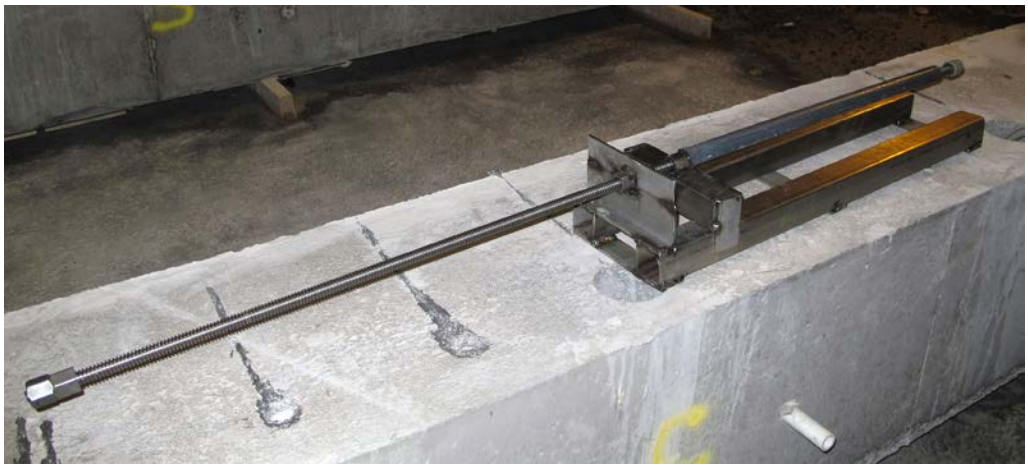

Figure 9-12. *The extraction tool used to extract the plastic tubes from the concrete walls.*

The tool is mounted against the concrete wall after which the threaded rod is inserted all the way through the tube. On the inside of the concrete wall the threaded rod is provided with a stopper which transfers the force from the rod to the plastic tube. Once the tool is mounted, the threaded tube is rotated using a handheld wrench, an electric screwdriver or the like.

During the development work of the extraction tool, several plastic tubes were extracted from the concrete wall. In some cases the tubes were easily extracted while in others more force was required.

However, during the final tests which were conducted in order to investigate the capacity of the extraction process several problems were encountered. These resulted in a very low capacity of the extraction process but also that some plastic tubes could not be extracted and remained stuck in the hole. Based on these experiences it was concluded that using plastic tubes to protect the tie rods during casting is a less suitable method and other types of tubes have to be searched for or entirely other concepts for formwork construction used.

Figure 9-13. *The stopper used to transfer the force from the threaded rod to the plastic tube.*

Figure 9-14. *The extraction tool has been mounted against the concrete wall (left image) and the tube extracted (right image).*

9.3.2 Grouting

Grouting was carried out using a purpose bought *Spray boy*, Figure 9-15. Initially tests were carried out in the test hall in order to ensure the function of the equipment. This was followed by grouting tests during which 30 500 mm long (∅ 30 mm) holes which had been drilled in a concrete beam were grouted using an injection grout.

Testing the Spray boy

The initial tests were done using Weber concrete for underwater casting. This was motivated by the fact that a parallel project on borehole sealing was carried out in which this equipment was also planned to be used. The work proceeded according to expectations and after a few tests the spray boy was also considered safe for use in the grouting tests.

Figure 9-15. *The Spray boy used in the production test.*

Mixing tests and tests of hoses and grouting pipes

As in the concept test, Bemix A3 was used also in the production test. The material has a low shrinkage which makes it suitable for use in filling holes with strict requirements on low permeability.

Mixing test #1

25 kg of Bemix A3 powder was mixed with 2.8 litres of water using a hand held mixer in a large barrel adjacent to the Spray boy. After mixing, the properties of the fresh grout looked OK and it was decided to continue with a pump test using a 10 meters. rubber hose and a steel pipe aimed for use during grouting, Figure 9-16.

Prior to pumping, a cement slurry was pumped through the system for lubrication and prevention of clogging. Once no more slurry remained the grout was poured into the mixer. Initially, pumping proceeded at a very low pressure but suddenly, the pressure rose to 50 bar and pumping was immedietely stopped.

The equipment was dismantled and cleaned. It was realised that the reduction from ∅ 25 mm to ∅ 14 mm from the rubber hose to the grouting pipe was too abrubt and clogging therefore occurred in the transission beween these parts. It was therefore decided to discard the grouting pipe from further tests.

Figure 9-16. *The steel pipe aimed for use during grouting.*

Mixing test #2

The mixer was filled with 2.55 litres of water and then powder was added. The mix was a bit stiff and water and more powder was added to a total of 2.85 litres of water to 25 kg of powder. The grout looked OK and the pump started. As in the previous test, pumping proceeded initially at a low pressure but suddenly the pressure increased to 50 bars and pumping was stopped and cleaning commenced.

During cleaning, large amounts of gravel was found in different parts of the system, indicating that separation of the grout had occurred. Also, during emptying of the systems, cubes for measurements of compressive strength were made. However, about an hour later, separation was observed also here with a 10 mm layer of water on top of a layer of cement paste and mainly gravel in the bottom of the cube. It was thus concluded that too much water had been used and that additional tests were required.

Mixing test #3

25 kg of powder was carefully mixed with 2.7 litres of water using a hand held mixer in a large barrel. After mixing, cubes were cast for possible testing of compressive strength but as this was late in the day no pump test was carried out. The grout was found to be stable and no separation was observed. It was therefore decided to carry out a pump test, the first thing the morning after.

Mixing test #4

25 kg of powder was carefully mixed with 2.7 litres of water using a hand held mixer in a large barrel. Simultaneously, cement slurry was mixed in the Spray boy and pumped through the system to prevent clogging during pumping of the grout. This time a short 25 mm standard water hose was used instead of the 10 m rubber hose as the plans were to use that during grouting, Figure 9-17.

Initially, pumping was carried out without any hose (Figure 9-17, left image). However, as the pressure was very low, the hose was connected (Figure 9-17 right image). Pumping proceeded at a pressure of about 2 bars and no separation was observed. It was therefore decided to relocate and perform the final grouting test.

Figure 9-17. *Pumping of Bemix A3 without and with a short hose.*

Preparations

In total about 30 ∅ 30 mm holes were drilled in the beams previously made for control of the function of the strain transducers using standard concrete, Section 6.2. The holes were sealed on one side of the beams as shown in Figure 9-18.

Mixing

25 kg of Bemix A3 was mixed with 2.7 litres of water using a hand held mixer in a large barrel, Figure 9-19. The grout looked a little loose and some more powder was therefore added to improve the stability of the grout and prevent separation. Approximately 2.65 litres of water was used for 25 kg of powder. The grout lasted about 18 holes after which more somewhat stiffer material was mixed according to the same principle.

Figure 9-18. *The concrete beams used in the grouting tests.*

Figure 9-19. *Mixing of grout.*

9.3.3 Grouting and plugging

The grout was poured into the mixer and mixed a short while before pumping started. A 3 metre long hose of the same type as tested in mixing test #4 was used. The hose was inserted all the way into the hole before the pump started and grouting thus made from the inside and out. Each hole took about 10 seconds to fill and in all, the 30 holes required not more than 30 minutes for completion; mixing included. The pressure in the pump was very low and grouting proceeded without any mishaps, Figure 9-20.

After grouting, the holes were plugged with a small piece of an insulating mattress as shown in the left image in Figure 9-21. The method worked OK but a plug (wood, cork or rubber) would probably have been a more suitable alternative.

Figure 9-20. *Grouting.*

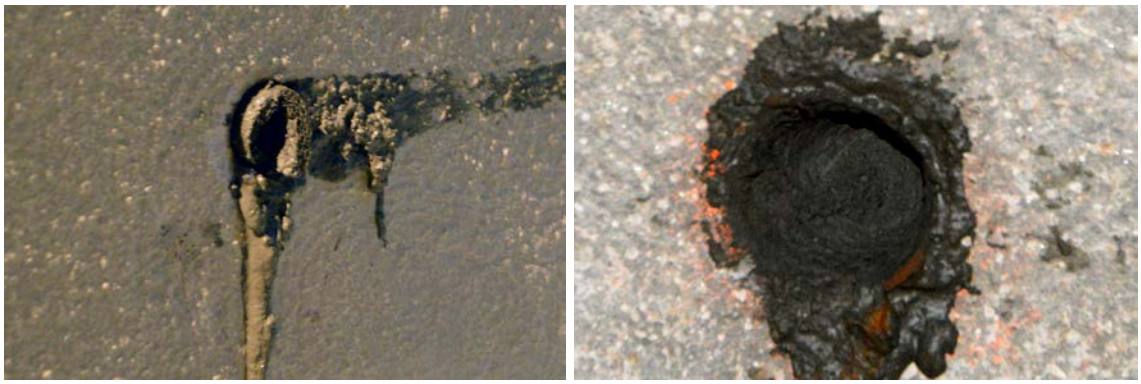

Figure 9-21. *Holes with plug (left image) and about an hour later after the plug has been removed (right image).*

9.3.4 Over coring

Over coring of a total of 10 grouted holes (5 in each beam) was carried out with a ∅ 100 mm core drill through the entire thickness of the beams. After drilling, the cores were wrapped in plastic, labelled and then placed on a pallet for transport up to the test hall, Figure 9-22.

9.3.5 Core sectioning

The cores were sectioned using a water-cooled circular saw. The cores were first divided into two parts of equal lengths after which one half was split along its axis to obtain a long cross-section of the grouted hole, Figure 9-23.

Figure 9-22. *The cores.*

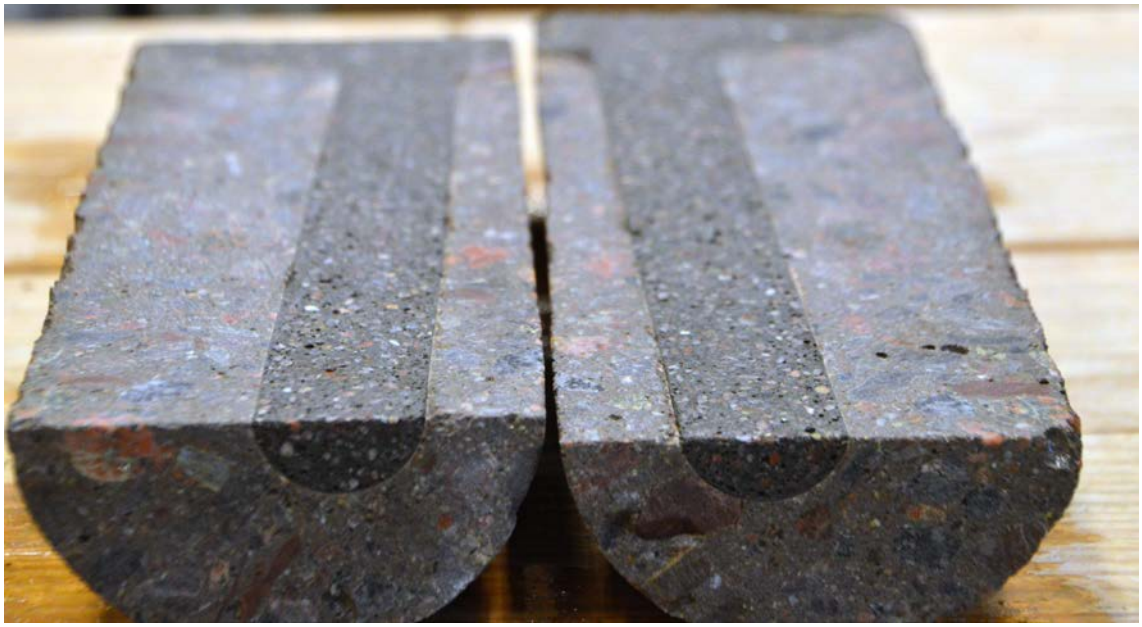

Figure 9-23. *A core after sectioning.*

9.3.6 Analyses

The samples were analysed by visual inspection and documented by photography. In some cases also the hydraulic conductivity of the samples was measured.

9.3.7 Evaluation

Visual inspection

In Figure 9-24 and 9-25 different cross sections of a number of the grouted holes are shown.

From the images shown in Figure 9-24 and 9-25 it is found that the filling capacity has been much improved compared to the concept test and all holes were completely filled with grout. Further, a comparison with Figure 9-9 also shows that the stability of the grout is much better with no signs of separation.

However, as shown in Figure 9-24 and 9-25 s, the porosity of the grout is much larger in these specimens than in the corresponding samples from the concept test, Figure 9-9. The reason for this is unclear but it is not unlikely that it is related to the very fast grouting of these holes compared to the concept test or by the method used for mixing the grout. Further work will be required for full understanding.

Figure 9-24. *Cross sections of some of the cores extracted from the concrete beams used in the production test.*

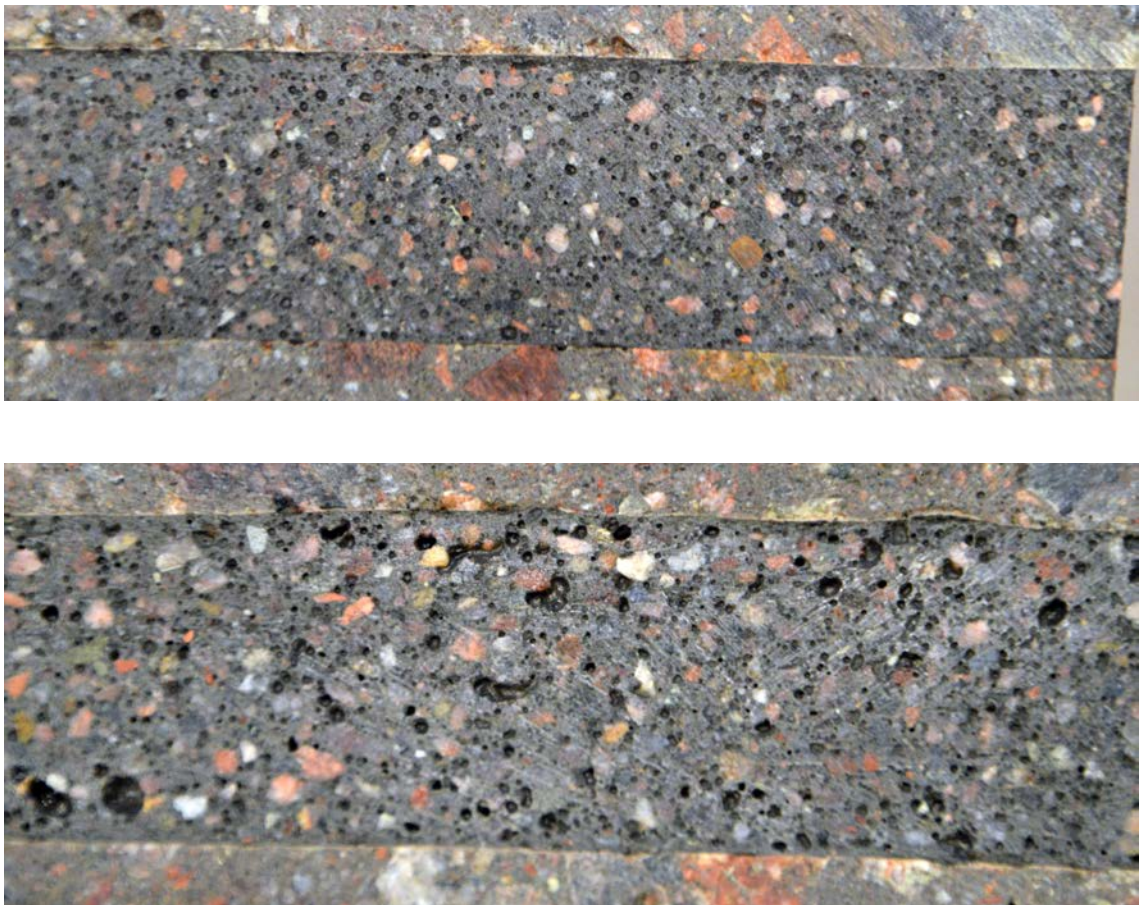

Figure 9-25. *Cross sections showing 2 of the cores from the production test.*

Hydraulic conductivity

The hydraulic conductivity was measured for some of the specimens and the results are shown in Table 9-2. From this table it is clear that the high porosity of the specimens is reflected also in that the hydraulic conductivity is 2–3 orders of magnitude higher than the stipulated value.

Table 9-2. Hydraulic conductivity of grouted holes and bulk concrete as a reference.

Specimen	Hydraulic conductivity [m/s]	Comment
C	2.3×10^{-7}	Grouted hole
E	1.6×10^{-8}	Grouted hole
3	3.8×10^{-8}	Grouted hole
5	-	Grouted hole. Flow not stable
F08000011 IN	1×10^{-11}	Bulk concrete
F08000013	3×10^{-12}	Bulk concrete

Position in the core. B = Inside, M = Middle, T = Outside.

9.3.8 Production test – Summary and conclusions

The production test presented in this section comprised two parts, extraction of the plastic tubes and grouting, which are shortly summarised below.

Extraction of the plastic tubes

Extraction of the plastic tubes by means of the method used in the production test had a rather low capacity and in some cases it was not possible to extract the tubes even though extensive heating was carried out prior to extraction. The method used is therefore considered not suitable for use during construction of the concrete caissons in the future 2BMA and other materials and/or methods have to be sought for.

Grouting of the holes

Grouting of the holes using the spray boy was efficient and had a high capacity. The hardened grout filled the holes entirely but the porosity of the grout was very high which was also reflected in a high hydraulic conductivity of the grouted holes.

From the results it can be concluded that grouting of the holes can be done with a high capacity but that the hydraulic conductivity of the grouted holes does not comply with requirements. Further development work will thus be required if tie rods are to be used in formwork construction for the 2BMA caissons.

10 Base slab – Monitoring programme

This chapter presents the results from the long-term monitoring of the base slab. The results are presented separately for 3 different time periods; (i) the first 4 weeks after casting, (ii) during heating of the base slab prior to casting of the walls and (iii) the remaining period. Corresponding results for the walls are presented in Chapter 11.

10.1 The first 4 weeks until heating of the base slab

10.1.1 Temperature

Figure 10-1 shows the temperature evolution during the first 100 hours after start of casting and Figure 10-2 shows also the following 500 hours.

As shown in the figures, the temperature of the concrete was about 16 °C at the time of start of casting (compare Table 7-2) and about 20 hours after casting started a maximum of about 41 °C was reached. The concrete then cooled slowly and about 3 weeks after casting, the temperature had assumed that prevailing in the surrounding rock vault. As expected, the highest temperatures were observed in the central parts of the base slab, whereas the temperatures were lower close to its top and underside.

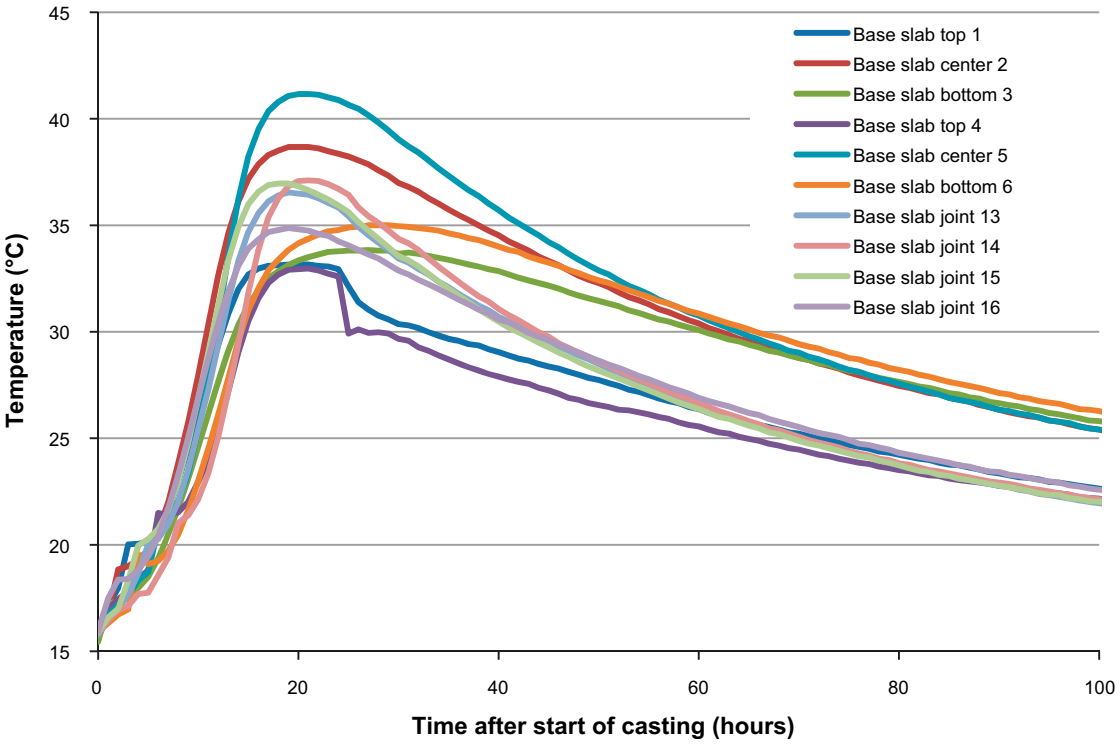

Figure 10-1. *Temperature evolution in the base slab during the first 100 hours after casting.*

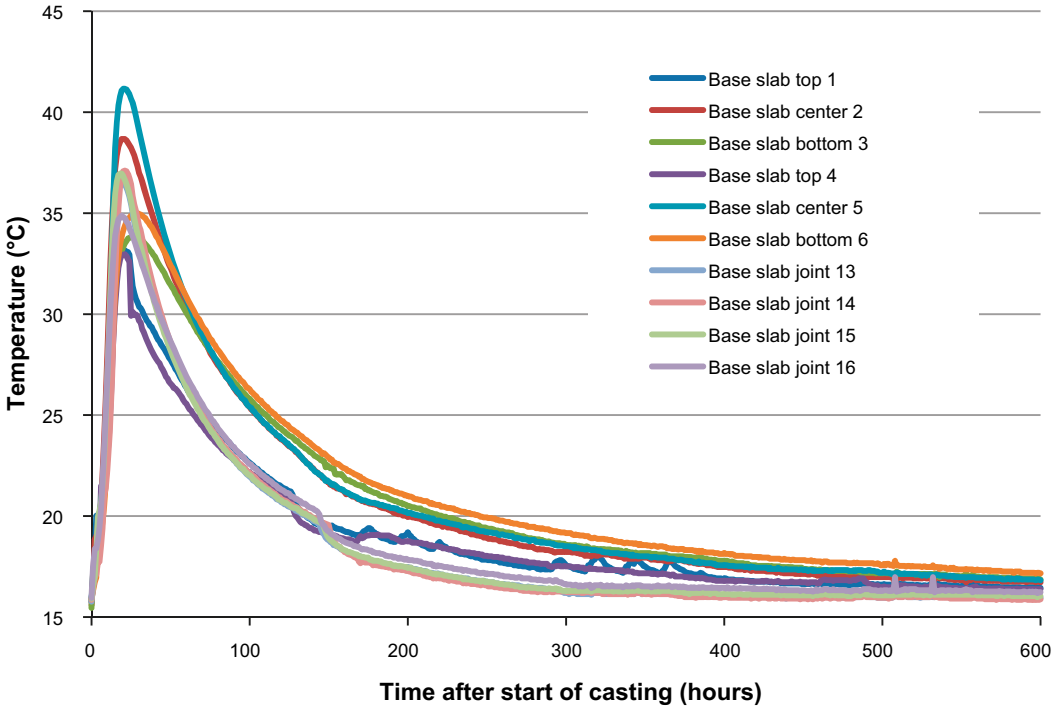

Figure 10-2. *Temperature evolution in the base slab during the first 600 hours after casting, corresponding to a period of 25 days.*

10.1.2 Internal strain

Figure 10-3 shows the levels of internal strain during the first 100 hours after the casting was started, while Figure 10-4 also shows the following 500 hours. For both measurement positions, tensile strain is observed in the still relatively plastic concrete immediately after casting started. This is followed by increasing compressive strain in connection with the temperature increase caused by cement hydration. Following this is a decrease in compressive strain as the concrete cools. From about 300 hours after casting started, low levels of tensile strain are observed in the positions of the two sensors. A comparison between Figure 10-1 and 10-3 shows that maximum compressive strain is obtained at the about the same time as the maximum concrete temperature, Table 10-1.

Table 10-1. Time for maximum temperature and compressive strain in the base slab.

Sensor	Time for maximum temperature (hours after casting)	Time for maximum compressive strain (hours after casting)
1	19–21	20
2	19–21	23

10.1.3 Relative humidity

The relative humidity in the base slab was not measured during this period.

10.1.4 External dimensions

External dimensions in the base slab were not measured during this period.

10.1.5 Crack monitoring

No cracks were observed in the base slab during the first 4 weeks after casting.

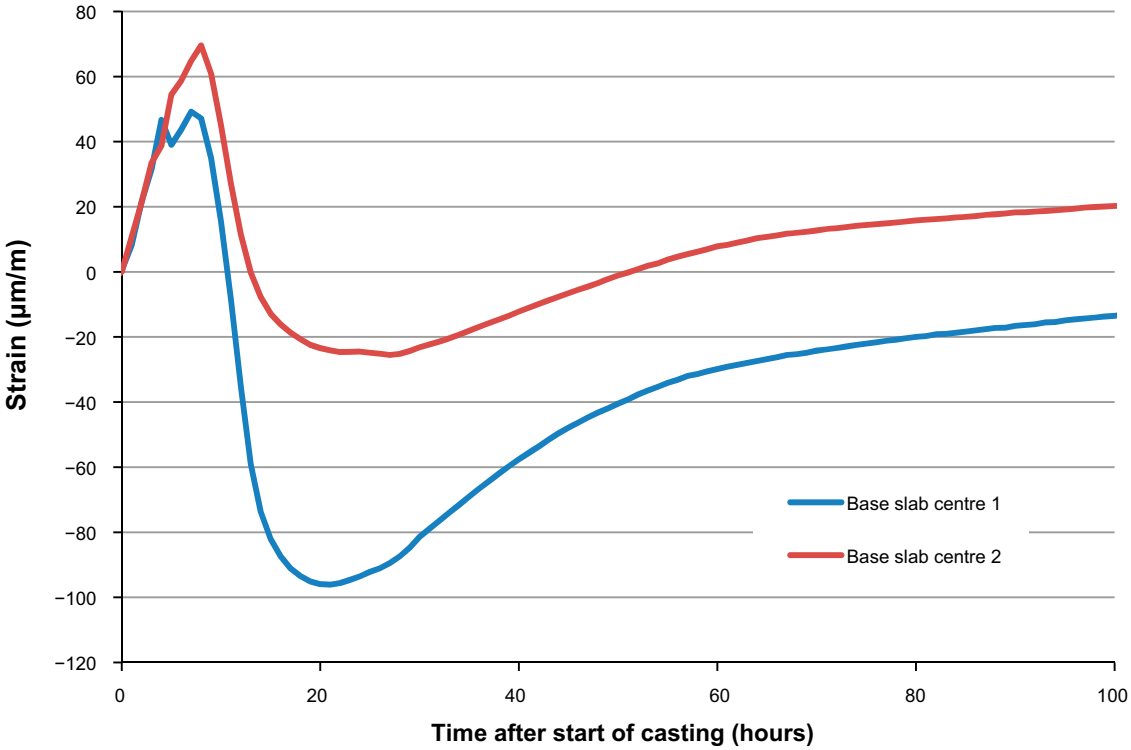

Figure 10-3. *Internal strain in the centre of the base slab during the first 100 hours after start of casting.*

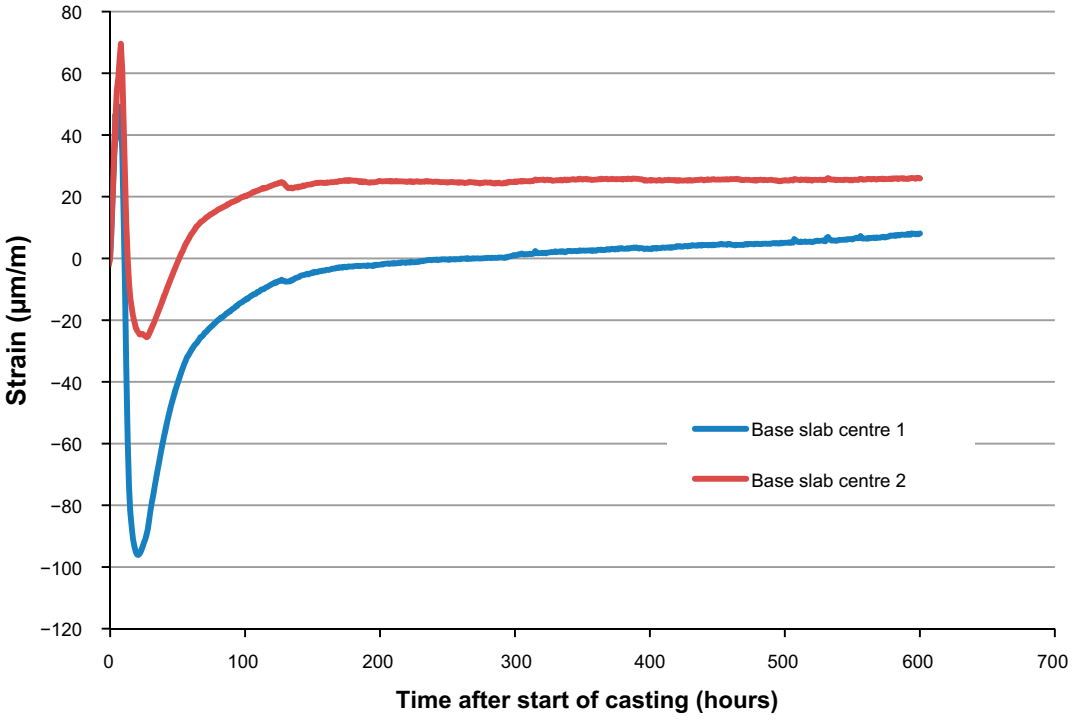

Figure 10-4. *Internal strain in the centre of the base slab during the first 600 hours after start of casting.*

10.2 During heating of the base slab prior to casting of walls

10.2.1 Temperature

Figure 10-5 shows the temperature evolution in the base slab from start of heating until about one week after casting of the walls. From Figure 10-5, the temperature at the start of the casting (168 hours after start of heating) was just below 39 °C at the surface of the slab and about 29 °C at its underside. Sensors 14 and 16 showing low temperatures in the joint are placed in the joint on the short sides of the caisson, which were only insulated. Heating inside the formwork of the long sides was stopped at about 145 hours after start of heating in order to be able to close the formwork completely before casting as shown by sensors #13 and #15.

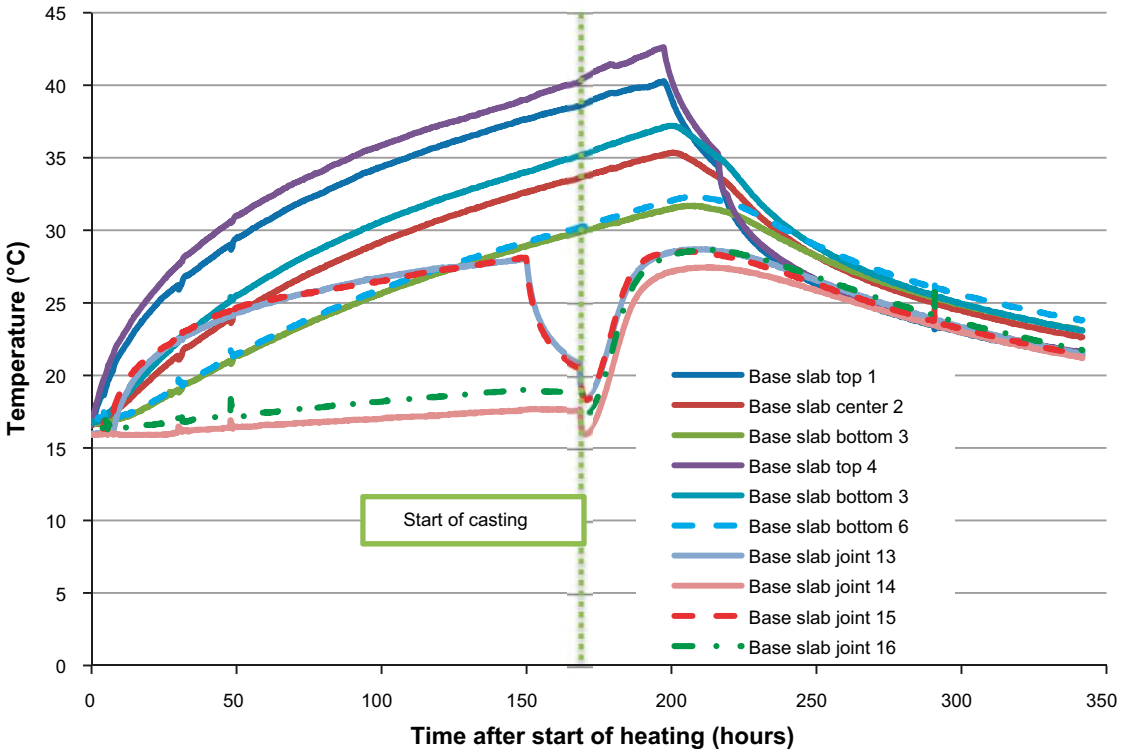

Figure 10-5. *Temperature in the base slab from start of heating until about 1 week after casting. Casting started 168 hours after start of heating (Vertical green dotted line) and the heaters were turned off the day after casting.*

10.2.2 Internal strain

Figure 10-6 shows internal strain in the base slab from the start of the heating to about 120 hours after casting of the walls.

From Figure 10-6, the levels of compressive strain in the base slab increased upon heating. Once the concrete started to cool after the casting compressive strain again decreased and already about 150 hours after the casting, the strain situation was approximately the same as when the heating started.

10.2.3 Relative humidity

The relative humidity of the concrete in the base slab was not measured during this period.

10.2.4 External dimensions

Measurement of the base slab's external dimensions was started 2 days before start of heating of the base slab.

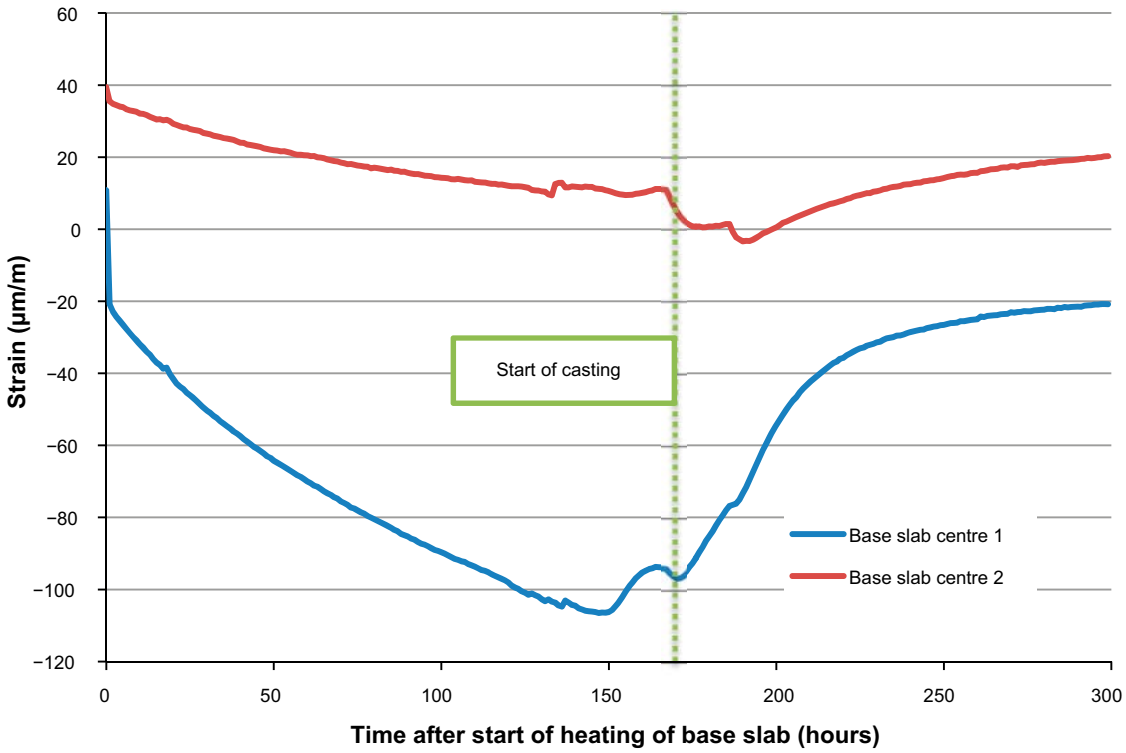

Figure 10-6. *Internal strain in the base slab from start of heating of the base slab until about 120 hours after casting of the walls was completed. Start of casting is represented by the dotted green vertical line.*

Figure 10-7 shows that the total expansion of the base slab was approximately 2.4 mm at about 2 days after casting considering also the disturbances of the signals during the first 50 hours of heating. As shown in Figure 3-7, LVDT 1 and LVDT 2 are places on opposite sides of the base slab which means that the total expansion is the sum of the signals from the 2 sensors.

Of this, the expansion caused by heating of the slab prior to casting was about 1.6 mm, corresponding to the values at about 168 hours after start of heating. This was slightly less than the calculated value (3.6 mm). A plausible explanation for this is an uneven temperature distribution in the base slab and that the colder parts restricted expansion of the warmer parts. However, as shown in Appendix B the linear coefficient of thermal expansion (CTE) was somewhat lower in beams made from the same concrete as used in the base slab than the value used in the estimate prior to heating. For that reason, expansion caused by heating was somewhat overestimated during planning of the heating.

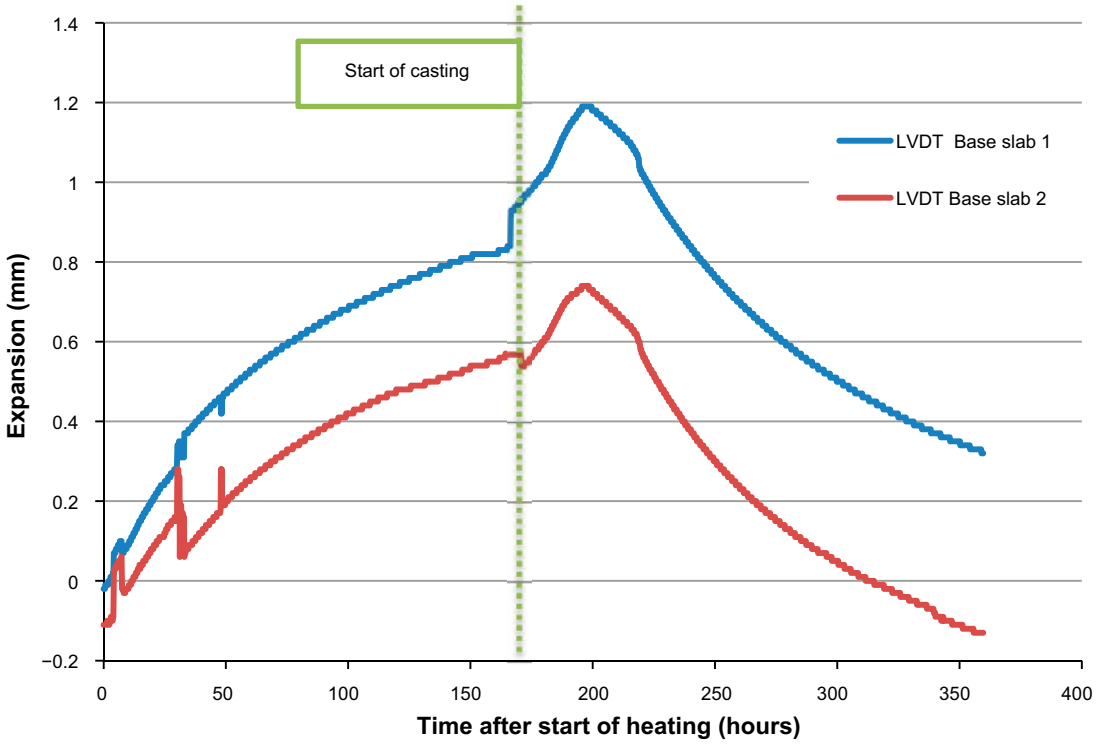

Figure 10-7. *Expansion and contraction of the base slab from start of heating until about one week after casting of the walls. Start of casting is represented by the dotted green vertical line.*

10.3 Long-term evolution

10.3.1 Temperature

Figure 10-8 shows the temperature evolution in the base slab during the first 4 months after casting of the base slab, corresponding approximately to about 3 months after casting the walls of the caisson.

The figure clearly shows the temperature effects of the concrete´s heat of hydration during casting as well as of the heating prior to the casting of the walls. However, after cooling down after casting the walls, no further temperature changes occur.

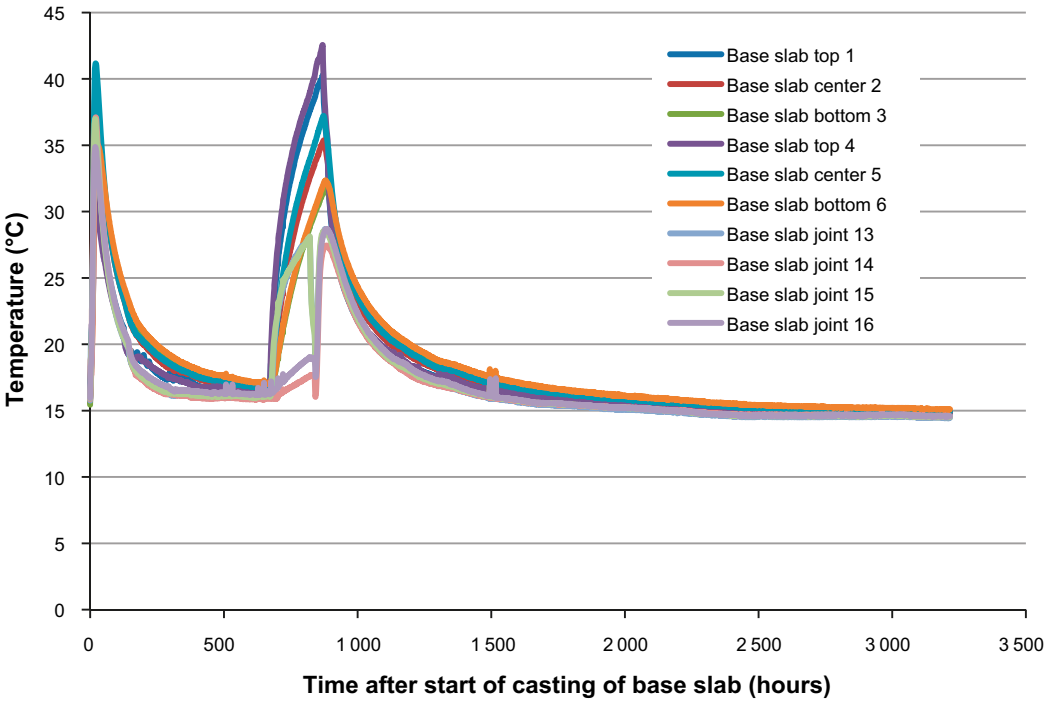

Figure 10-8. *Temperature evolution in the base slab during the first 4 months after casting of the base slab.*

10.3.2 Internal strain

The internal strain in the base slab until about 8 months after casting is shown in Figure 10-9. For the base slab, high levels of compressive strain are shown in connection with casting of the base slab but also during the heating of the base slab before casting the walls. With time, the concrete cools and the base slab reaches an almost strain-free state.

10.3.3 Relative humidity

The relative humidity of the concrete was monitored from approximately two months after casting of the base slab. As shown in Figure 10-10, the function of the sensors does not seem to have been completely satisfactory. Unfortunately, this is a commonly experienced problem for RH sensors in this type of environment as also reported by Mårtensson and Vogt (2019).

10.3.4 External dimensions

As shown in Figure 10-11, changes in the external dimensions of the base slab during the period up to July 09 2018 have been very small with a total net shrinkage of about 0.2 mm. This value is obtained as the difference between the initial value of −0.4 mm in December and the minimum value of −0.6 mm from the end of May. With a total length of the base slab of 18 meters, this corresponds to 0.01 ‰.

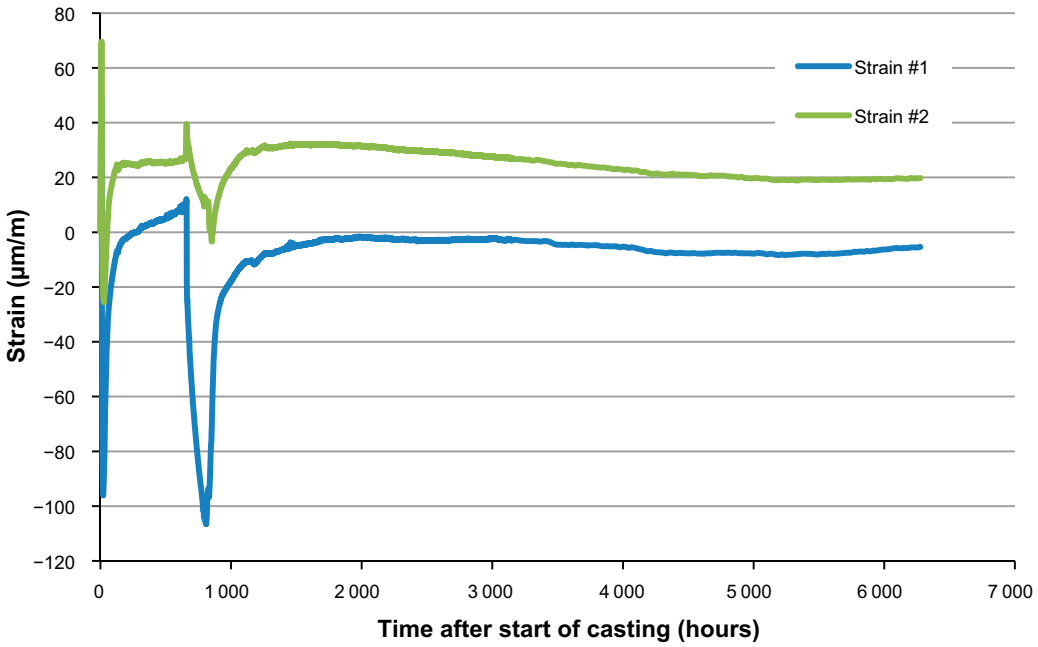

Figure 10-9. *Internal strain in the base slab during the first 6 200 hours after casting, corresponding to the period up to July 2019.*

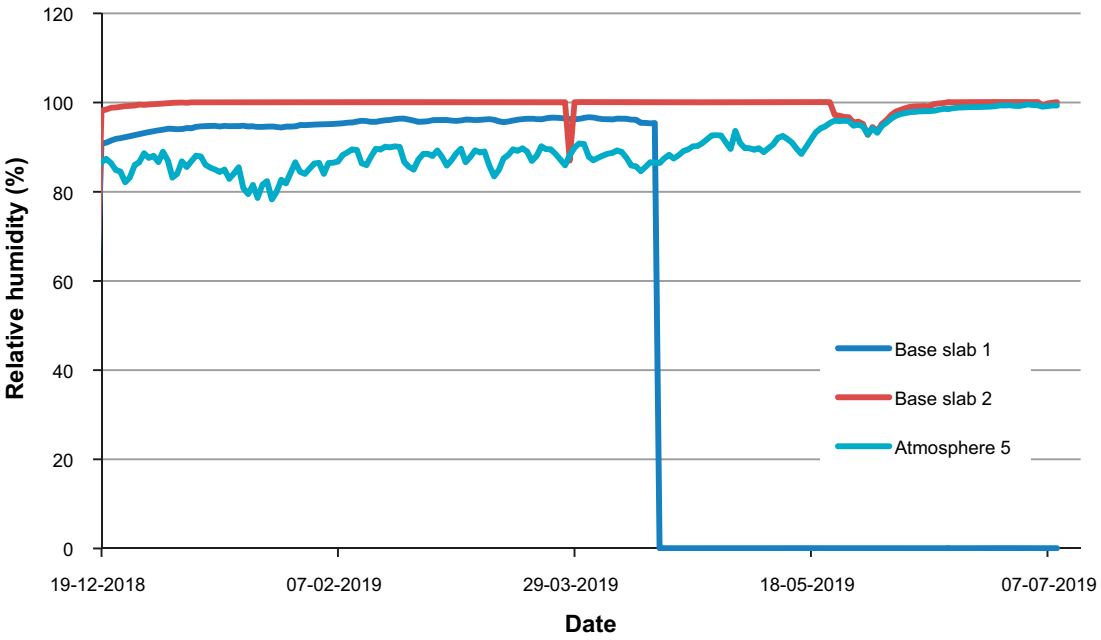

Figure 10-10. *Relative humidity in the concrete of the base slab from 19-12-2018 until 09-07-2019.*

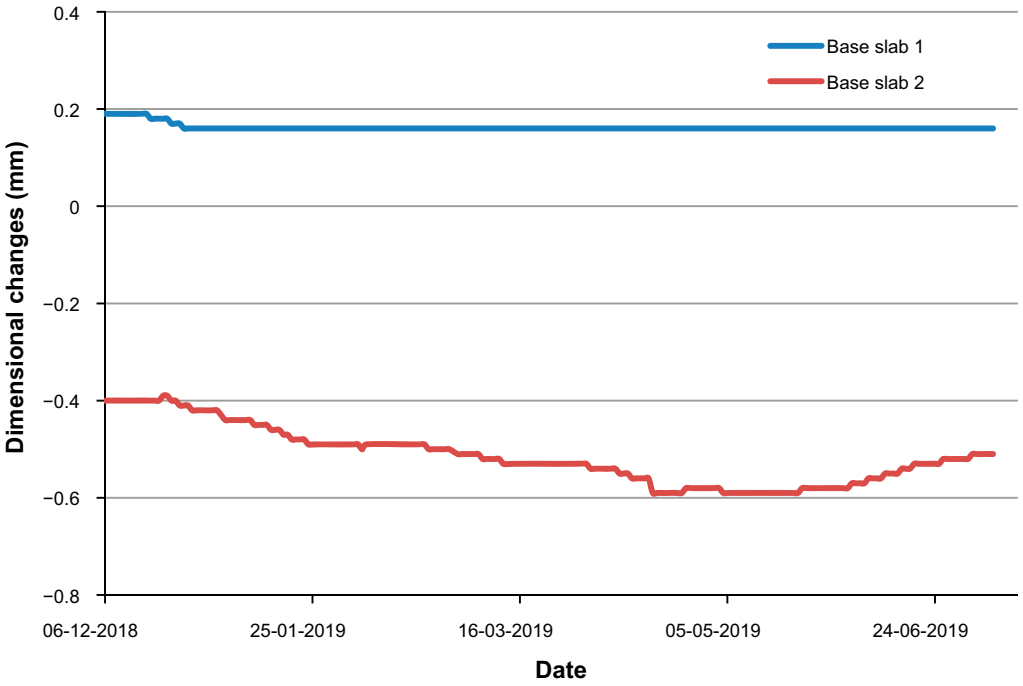

Figure 10-11. *Changes in the external dimensions of the base slab during the period from 06-12-2018 until 09-07-2019.*

10.3.5 Crack monitoring

No cracks were observed in the base slab until early October 2019, i.e. 11 months after casting of the base slab.

10.4 Monitoring of the base slab – Summary

In this chapter the results from the long-term monitoring programme of the base slab covering the period from the day of casting in mid-October 2018 until July 2019. The following observations have been made:

- **Temperature –** After an early and rather fast temperature increase during hydration with a maximum temperature in the centre of the slab of about 41 °C the temperature soon cooled down and after a few weeks the temperature of the concrete structure had returned to that prevailing in the tunnel. Prior to casting of the walls, the base slab was heated by means of heating mattresses covered with insulating mats and during this period the temperature reached a maximum of about 43 °C.
- **Internal strain –** The internal strain in the concrete has been monitored by means of 2 strain transducers. Both of these show a similar pattern with a sharp increase in compressive strain during the very early hydration period. This is followed by a period where the compressive strain is reduced. After about 6 months after casting only very low levels of strain are observed where one sensor show tensile strain and the other compressive strain.
- **Relative humidity –** The monitoring of the relative humidity has suffered from malfunctioning of several of the RH sensors. Those that have been functioning have shown that the relative humidity in the concrete is between 95 and 100 %.
- **External dimensions –** The external dimensions of the base slab were monitored from about 1 month after casting. The general observation is that the external dimensions have followed the temperature and relative humidity in the concrete. Heating of the base slab prior to casting of the walls and the heat generated during the following casting caused a total expansion of about 2.4 mm in the base slab. Following this period, changes in external dimensions due to the annual changes in temperature and relative humidity in the tunnel have been very limited.
- **Crack formation –** No cracks were observed in the concrete during the first 11 months following casting of base slab.

11 Walls – Monitoring programme

In this chapter the results from the long-term monitoring of the properties of the walls are presented. The results are presented separately for 2 different time periods; (i) the first 4 weeks after casting and (ii) the remaining period. Corresponding results from the base slab are presented in Chapter 10.

11.1 The first 4 weeks after casting of the walls

11.1.1 Temperature

As shown in Figures 11-1 and 11-2, an early temperature decrease is noted when the cool concrete reaches the temperature sensors, a few hours after casting has begun. About 6 hours later, the temperature starts to increase again as the exothermic chemical reactions in the concrete start up properly. However, as indicated by the formwork pressure sensors, Figure 8-10, the concrete has set already at this stage.

Almost 40 hours after casting started, the maximum temperature is 43 °C in the central parts of the wall, after which the concrete starts to slowly cool. The time to reach maximum temperature in the walls is almost twice as long as for the base slab. This was surprising as the concrete in the base slab contained some retarder whereas the concrete for the wall did not. However, the cement used in the walls had been stored in the cement silo for about 5 weeks which may have made it less reactive than the very fresh cement used for casting of the base slab. Also, when casting of the walls no retarder was used contrary to when casting the base slab. Commonly, cement reactions are very fast once the effect of the retarder is lost compared to when no retarder is used. A possible explanation could also be the lower concrete temperature during casting of the walls than when casting the base slab, about 8–12 ºC (Table 8-2) compared to 14–19 ºC (Table 7-2) for the concrete to the base slab. However, this small difference is not likely to be responsible for the entire difference.

Approximately 600 hours (corresponding to 25 days) after the casting had taken place, the temperature in the wall has returned to that prevailing in the tunnel.

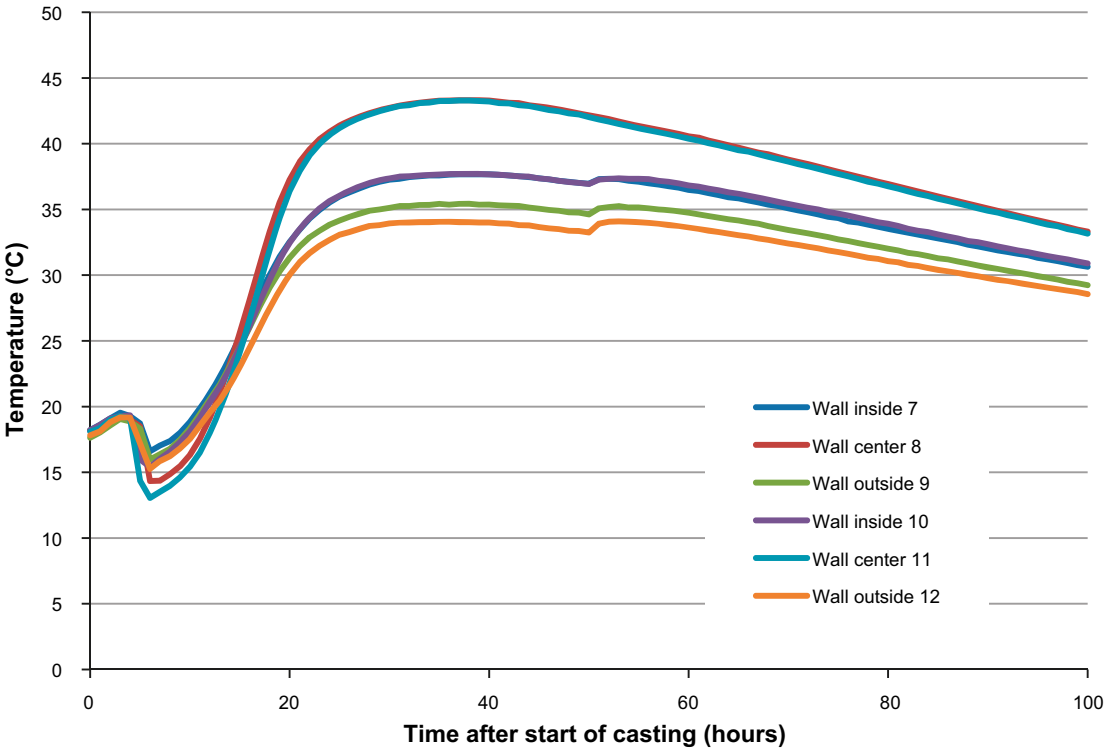

Figure 11-1. *Temperature evolution in the walls during the first 100 hours after start of casting.*

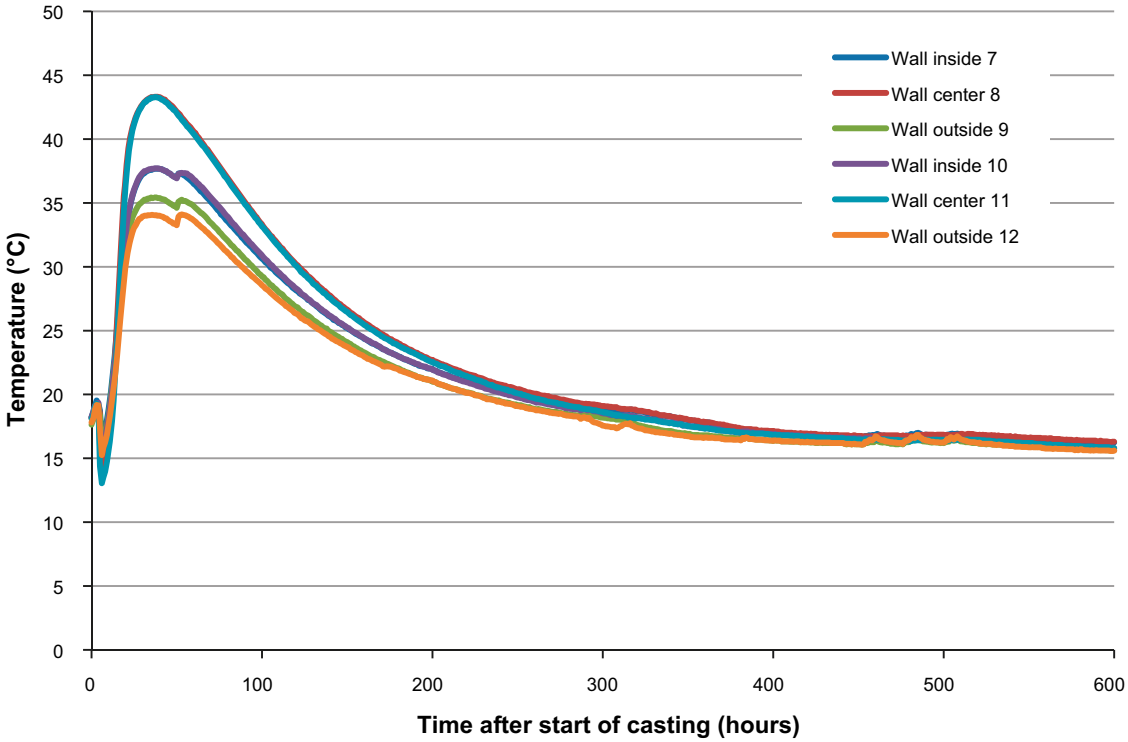

Figure 11-2. *Temperature evolution in the walls during the first 600 hours after start of casting.*

11.1.2 Internal strain

The levels of internal strain in the walls of the caisson were monitored using a large number of strain transducers. The positions of the different strain gauges can be found in Figures 3-4 and 3-5.

Short wall 800 mm above joint

Figures 11-3 and 11-4 show compilations of internal strain 800 mm above the joint between the short walls and the base slab during the first 100 and 600 hours after casting started respectively. The evolution of the strain situation is similar to that in the base slab with early high levels of compressive strain followed by reduced levels as the concrete cools. Tensile strain is, however, not observed during this period.

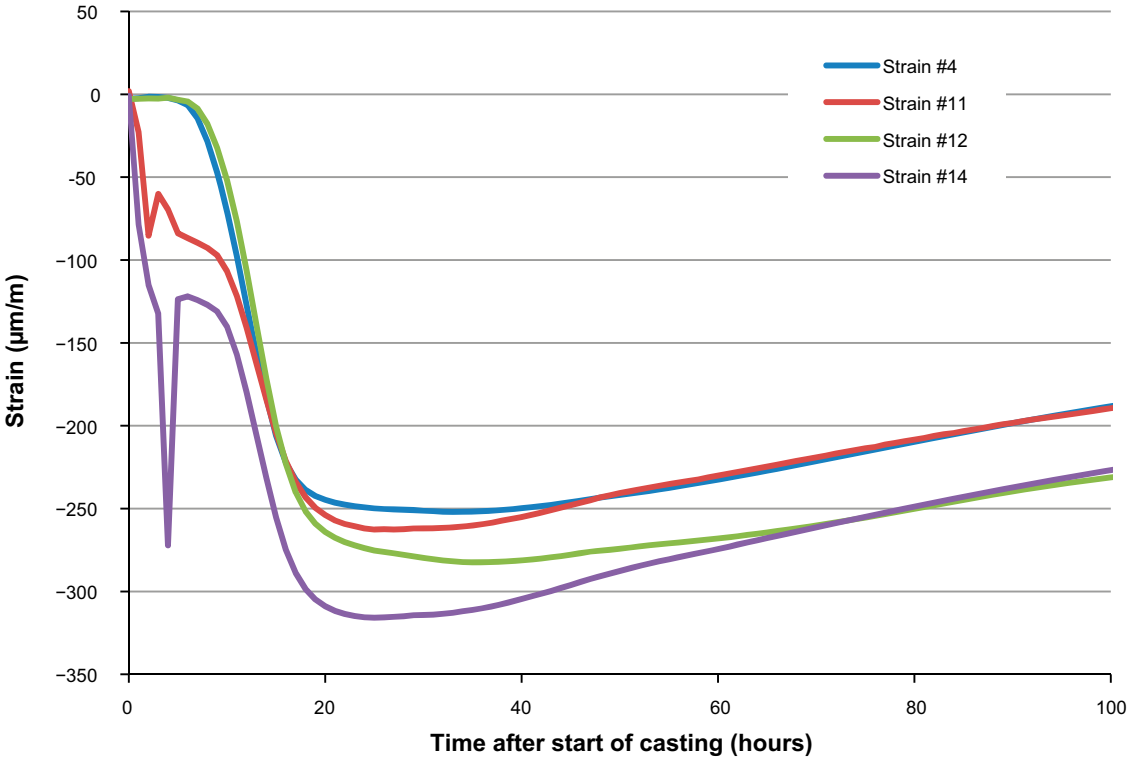

Figure 11-3. *Compilation of internal strain during the first 100 hours after start of casting in different positions 800 mm above the joint between the base slab and the short walls.*

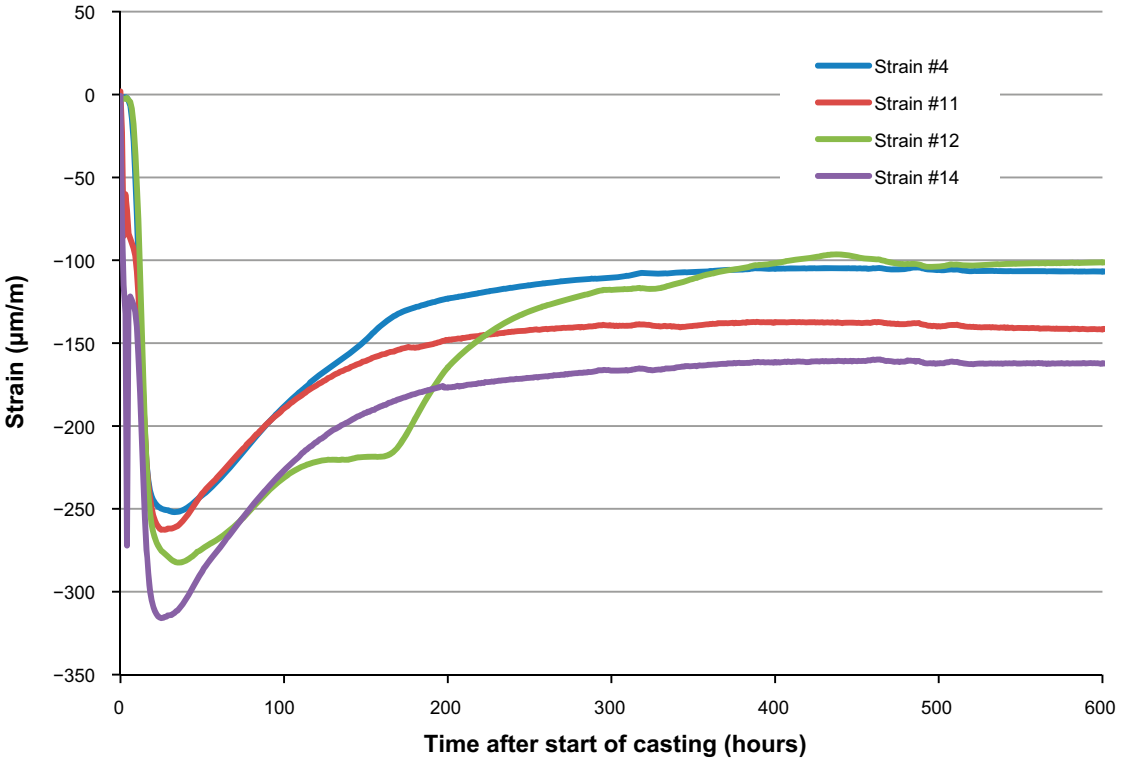

Figure 11-4. *Compilation of internal strain during the first 600 hours after start of casting in different positions 800 mm above the joint between the base slab and the short walls.*

The relationship between strain and temperature evolution is shown in Figure 11-5 as a representative example for all positions in the concrete caisson. As shown there, strain and temperature follows a similar trend over time represented by increased levels of compressive train with increasing temperature. As the concrete cools some time after casting, the levels of compressive strain are reduced and eventually only low levels of strain remain.

As previously observed the evolution of internal strain in the walls follows the temperature evolution as shown in Figure 11-5.

Long wall 800 mm above joint

Figures 11-6 and 11-7 show compilations of internal strain 800 mm above the joint between the long walls and the base slab during the first 100 and 600 hours after casting started respectively. Also in this part of the wall, the strain evolution follows the familiar pattern and is not further discussed here.

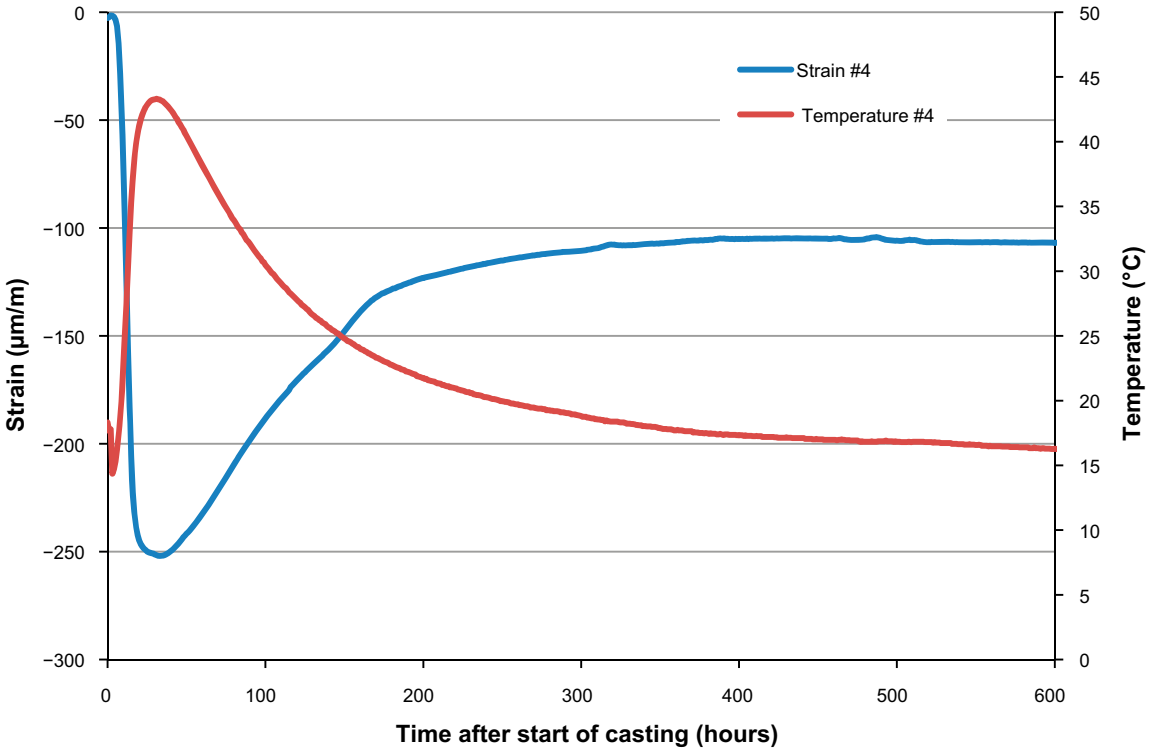

Figure 11-5. *Internal strain and temperature during the first 600 hours after start of casting in position #4 800 mm above the joint between the base slab and the short wall.*

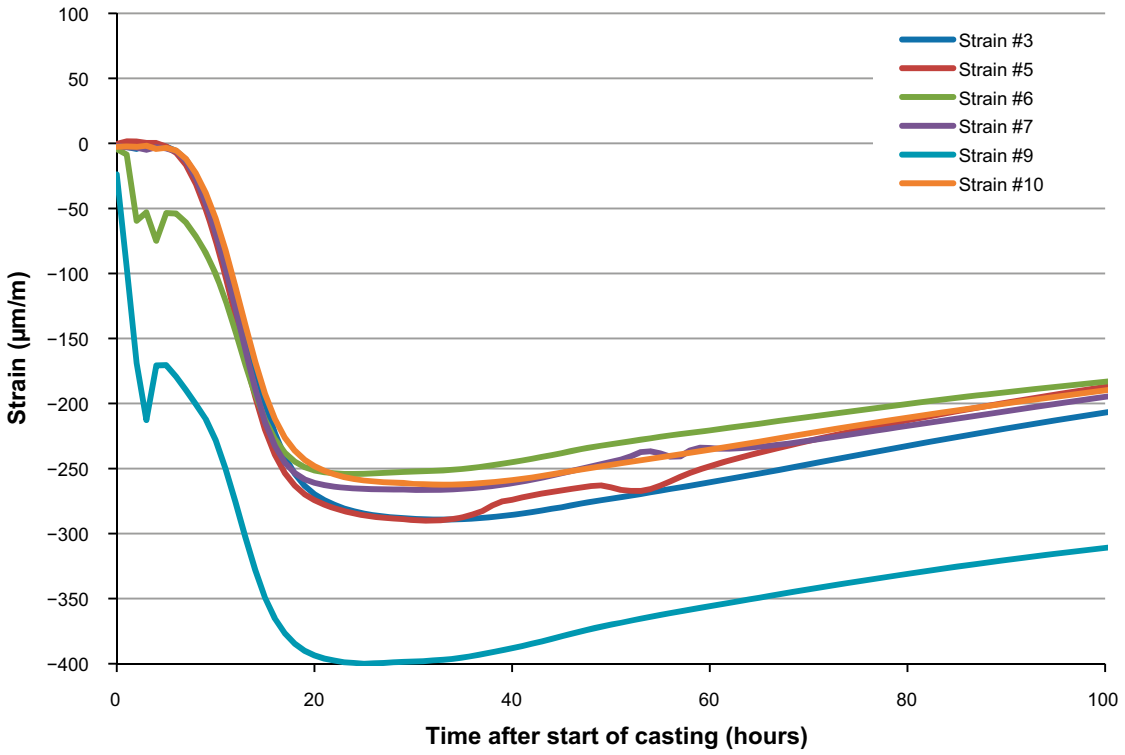

Figure 11-6. *Compilation of internal strain during the first 100 hours after start of casting in different positions 800 mm above the joint between the base slab and the long walls.*

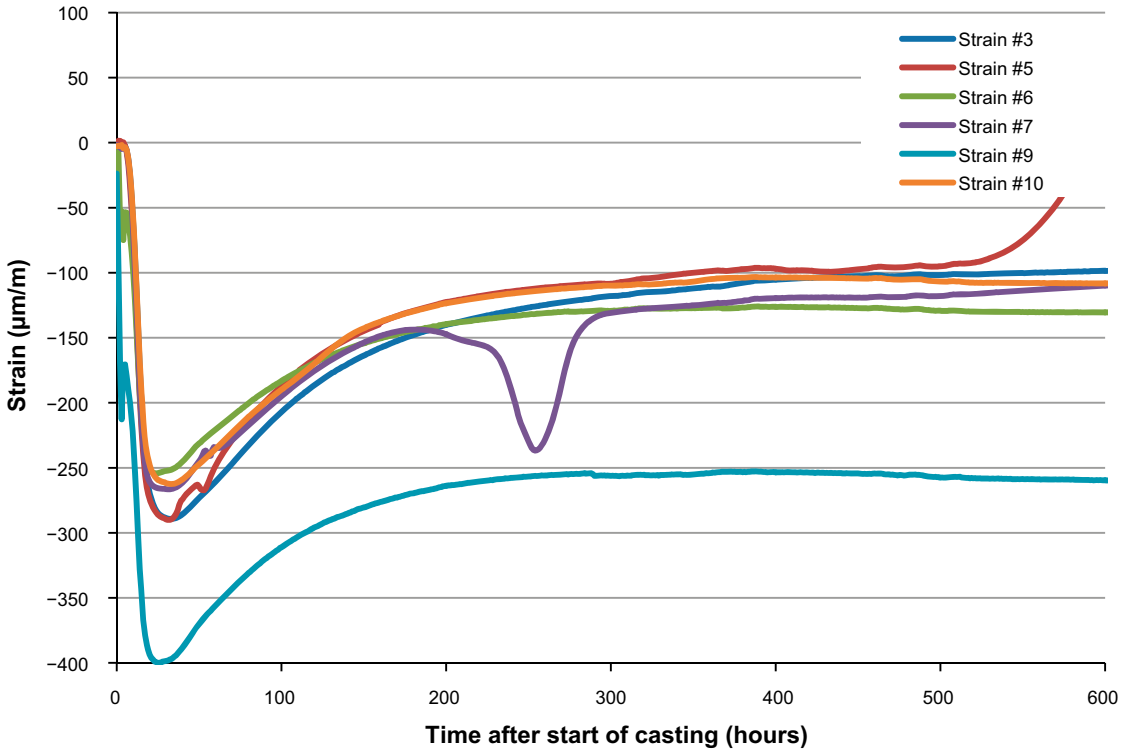

Figure 11-7. *Compilation of internal strain during the first 600 hours after start of casting in different positions 800 mm above the joint between the base slab and the long walls.*

1 000 mm beneath the top of the short wall

Figure 11-8 shows internal strain and temperature during the first 600 hours after casting started 1 000 mm below the top edge of the short wall. In this position, the temperature measurement did not work for the first 120 hours after casting, giving the temperature curve a strange appearance. Otherwise, the appearance of the curves is familiar and not further discussed here.

1 000 mm beneath the top of the long wall

Figure 11-9 shows internal strain and temperature during the first 600 hours after casting started 1 000 mm beneath the top of the long wall. Also here the trends follow the familiar pattern and are not further discussed.

In summary, the follow-up of temperature and internal strain in the walls during the first 600 hours after casting of the of the walls follow the similar trends as in the previous work reported by Mårtensson and Vogt (2019) as well as in base slab (Chapter 10) and beams made for control of the strain gauges, Chapter 6.

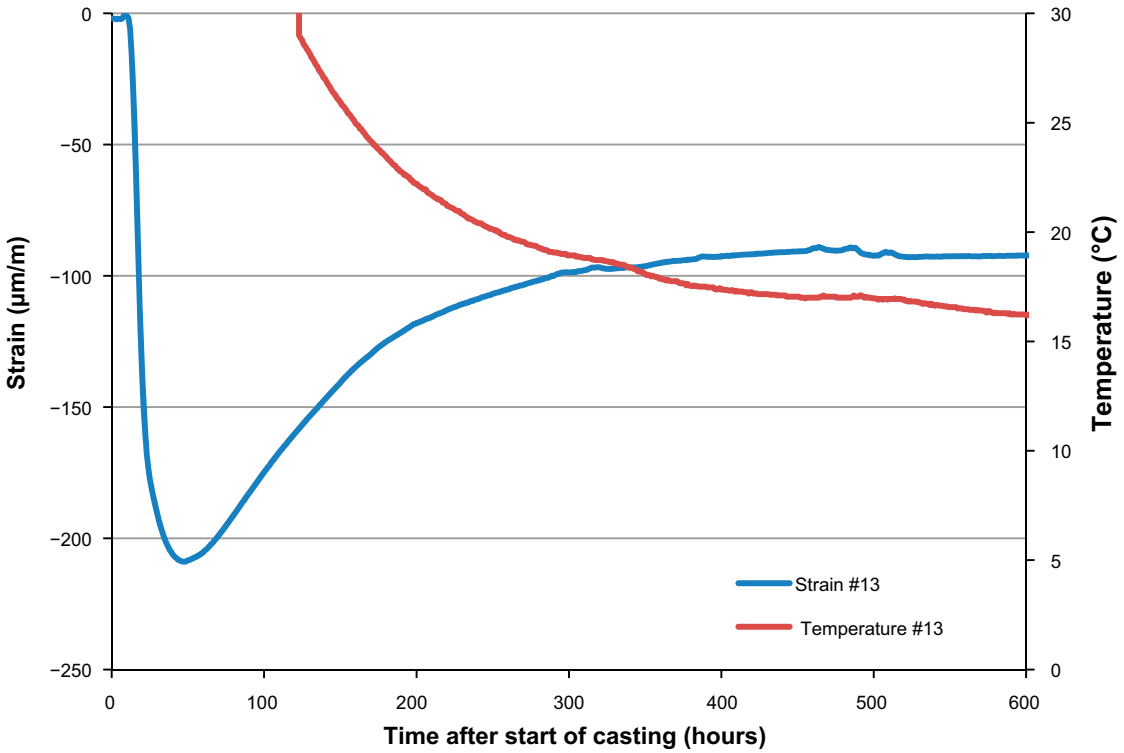

Figure 11-8. *Internal strain and temperature during the first 600 hours after start of casting in position #13 1 000 mm beneath the top of the short wall.*

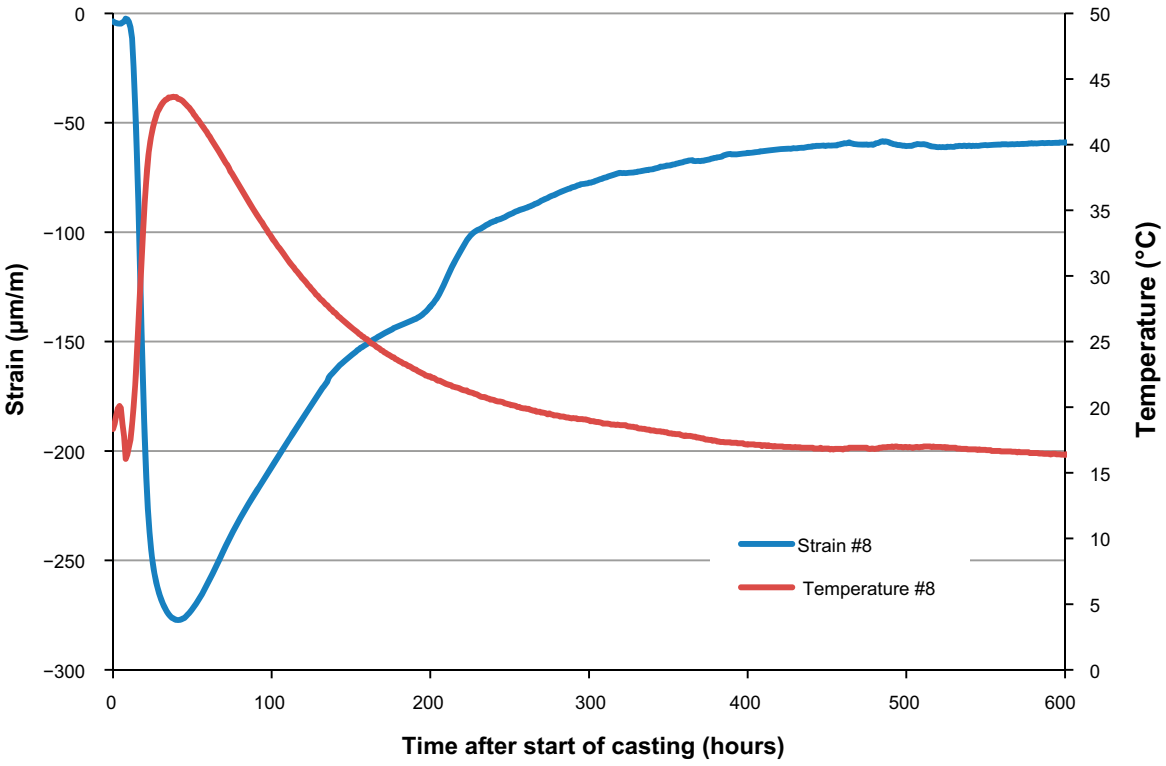

Figure 11-9. *Internal strain and temperature during the first 600 hours after start of casting in position # 8 1 000 mm beneath the top of the long wall.*

11.1.3 Relative humidity

Monitoring of the relative humidity of the concrete was started approximately 4 weeks after casting, and the results are therefore reported in Section 11.2.3.

11.1.4 External dimensions

Monitoring of the external dimensional changes in the walls of the caisson was started a little more than 4 weeks after casting and the results are therefore reported in Section 11.2.4.

11.1.5 Crack monitoring

No cracks were observed in the walls during this period.

11.2 Long-term evolution

11.2.1 Temperature

Figure 11-10 shows the temperature evolution in the walls during the first 3 months after casting. As expected, after cooling down after casting of the walls, the temperature in the concrete follows that of the rock vault.

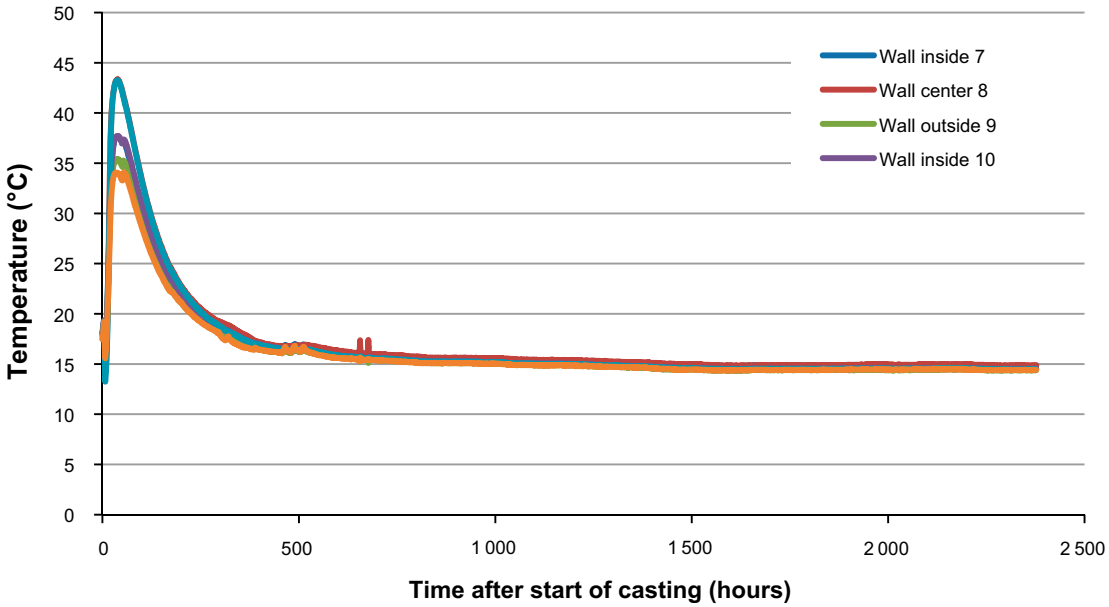

Figure 11-10. *Temperature evolution in the walls during the first 3 months after casting.*

11.2.2 Internal strain

Short wall 800 mm above joint

Figure 11-11 shows a compilation of the internal strain in the short wall 800 mm above the joint between the wall and the base slab during the first 7 months after casting. As shown in this figure, strain levels vary only little after the initial large variations. Here, though, sensor #4 varies in an unexpected way for which no explanation has been found.

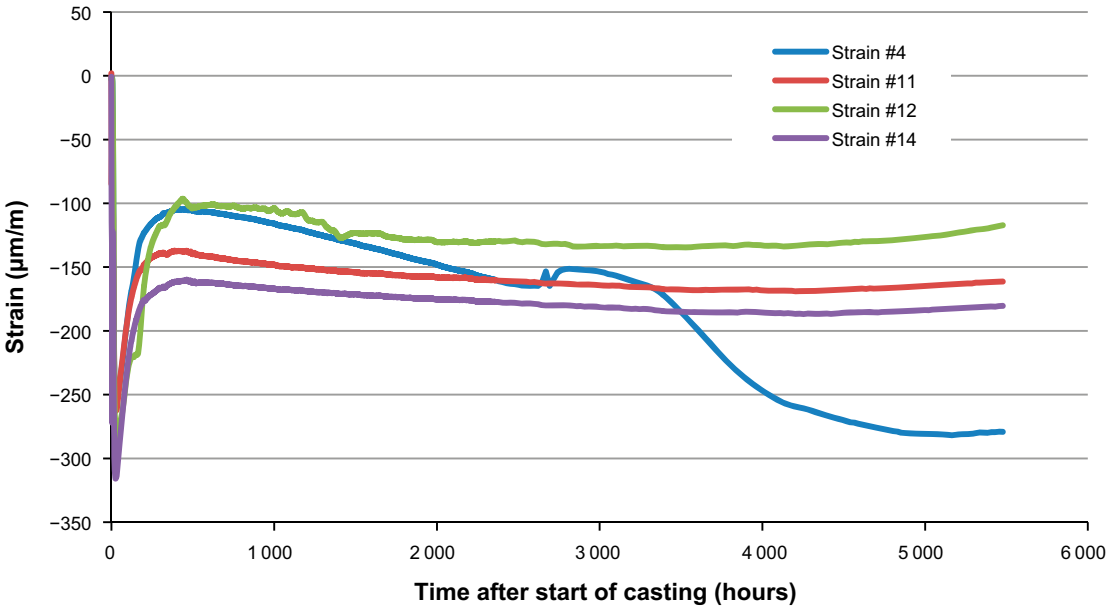

Figure 11-11. *Compilation of the internal strain in 4 different positions in the short wall 800 mm above the joint between the base slab and the short wall during the first 7 months after casting.*

Long wall 800 mm above joint

Figure 11-12 shows a compilation of the internal strain in the long wall 800 mm above the joint between the wall and the base slab during the first 7 months after casting. As shown in this figure, strain levels vary only little after the initial large variations. The cause of the variations shown by sensors #5 and #10 is unclear.

1 000 mm beneath the upper edge of the short wall

Figure 11-13 shows internal strain and temperature in a position 1 000 mm beneath the upper edge of the short wall. Note that the temperature sensor did not work for the first 120 hours after casting. Also the response from the strain gauge is awkward but the reason is unclear. At this position, about 3 meters from the joint, levels of strain should be low and only very small variations should be expected due to the low degree of restraint.

1 000 mm beneath the upper edge of the long wall

Figure 11-14 shows internal strain and temperature in position #8 1 000 mm below the top edge of the long wall during the first about 7 months after casting. The variations in strain and temperature are, as expected, small after the initial 1 000 hours after casting.

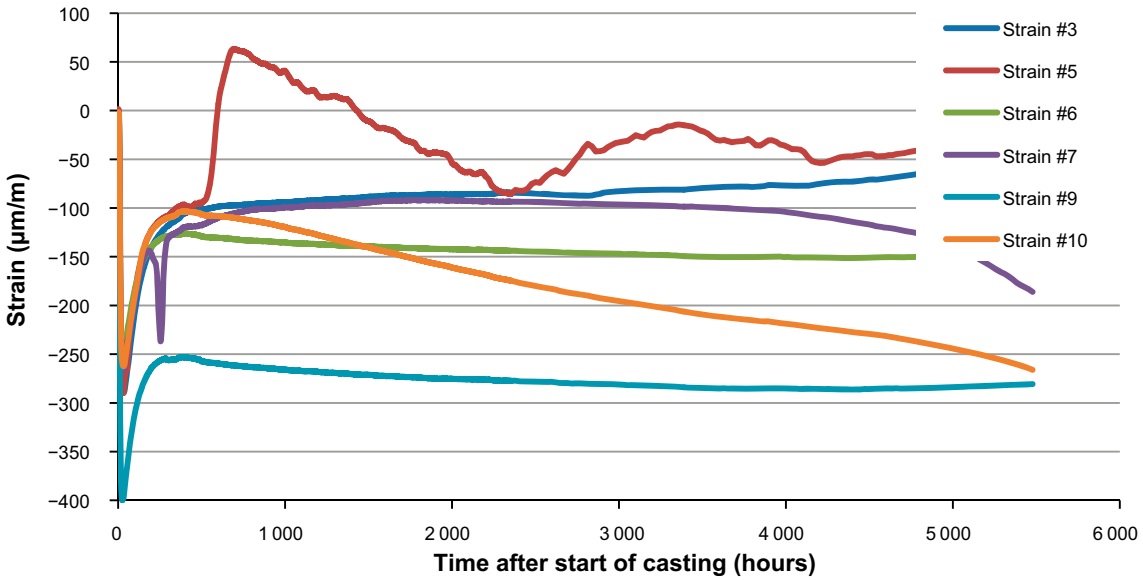

Figure 11-12. *Compilation of the internal strain in 6 positions in the long wall 800 mm above the joint between the base slab and the wall.*

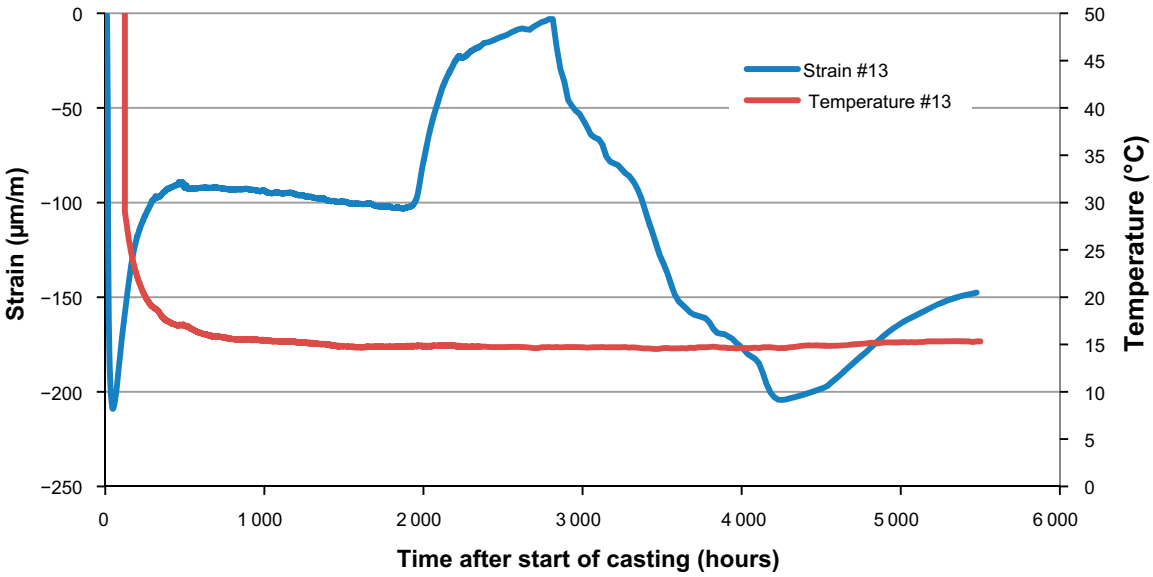

Figure 11-13. *Internal strain and temperature 1 000 mm beneath the upper edge of the short wall during the first 7 months after casting.*

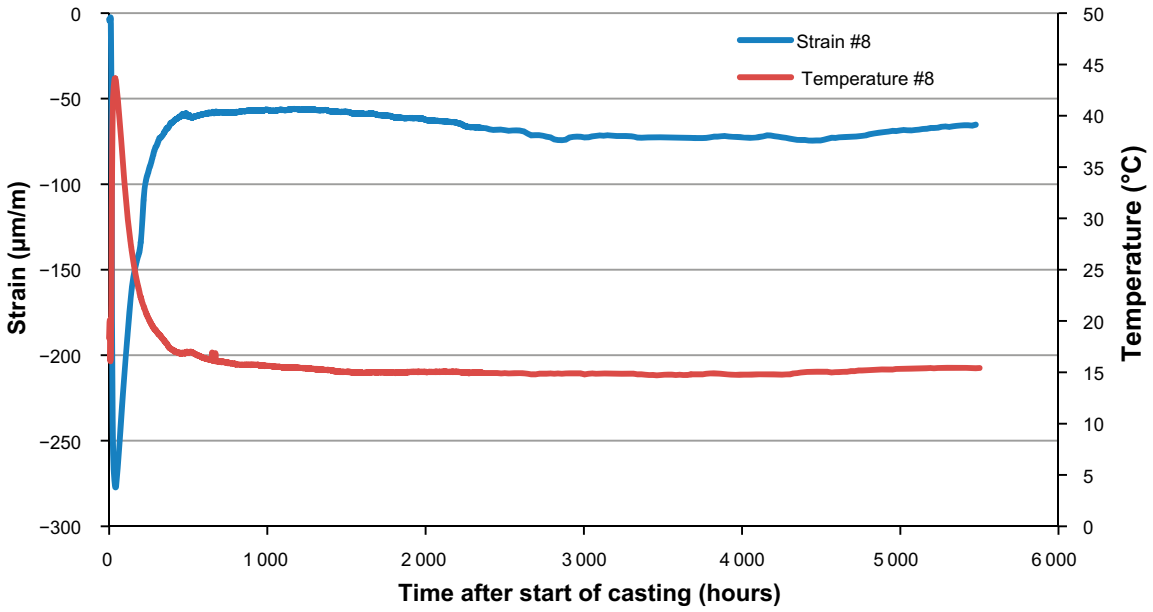

Figure 11-14. *Internal strain and temperature 1 000 mm beneath the upper edge of the long wall during the first 7 months after casting.*

11.2.3 Relative humidity

Measurements of the relative humidity in various parts of the concrete were started 4 weeks after casting of the walls. Figure 11-15 shows that the relative humidity in the centre of the wall (Wall 3) and close to the surface (Wall 4) is close to 100 % about 6 months after casting. However, some concern must be raised on the function of sensor #4 which expectedly should have shown reducing RH during the dry period of the year; compare sensor "Atmosphere 5". See also Section 10.3.3.

11.2.4 External dimensions

Measurement of external dimensions of the walls was started with LVDT sensors beginning 16-12-2018 and the results are shown in Figure 11-16. The positions of the sensors are shown in Figure 3-3. Dimensional changes in the base slab are reported in Section 10.3.4.

Figure 11-16, shows certain levels of shrinkage during the dry winter and early spring followed by expansion of the caisson from early may and onward as temperature and humidity increase; compare Figure 2-3.

The total shrinkage – obtained from adding the values from the 2 sensors – is estimated to 0.45 mm which distributed over the total length of 18 meters, gives a shrinkage of 0.025 ‰.

This can be compared with Section 8.10.3, where shrinkage of beams made of the same concrete as used for casting of the walls was studied. For samples stored according to SIS (2000) and for sealed samples shrinkage after 224 days was 0.36 ‰ and 0.02 ‰ respectively. Thus, the shrinkage observed for the walls is similar to that of sealed specimens, which can be explained by the high humidity in the rock vault which prevents extensive dehydration.

It should finally be noted that the fact that the LVDT sensors were mounted a few weeks after casting may have meant that the actual shrinkage is somewhat larger since some of the initial shrinkage may have occurred before these sensors were mounted.

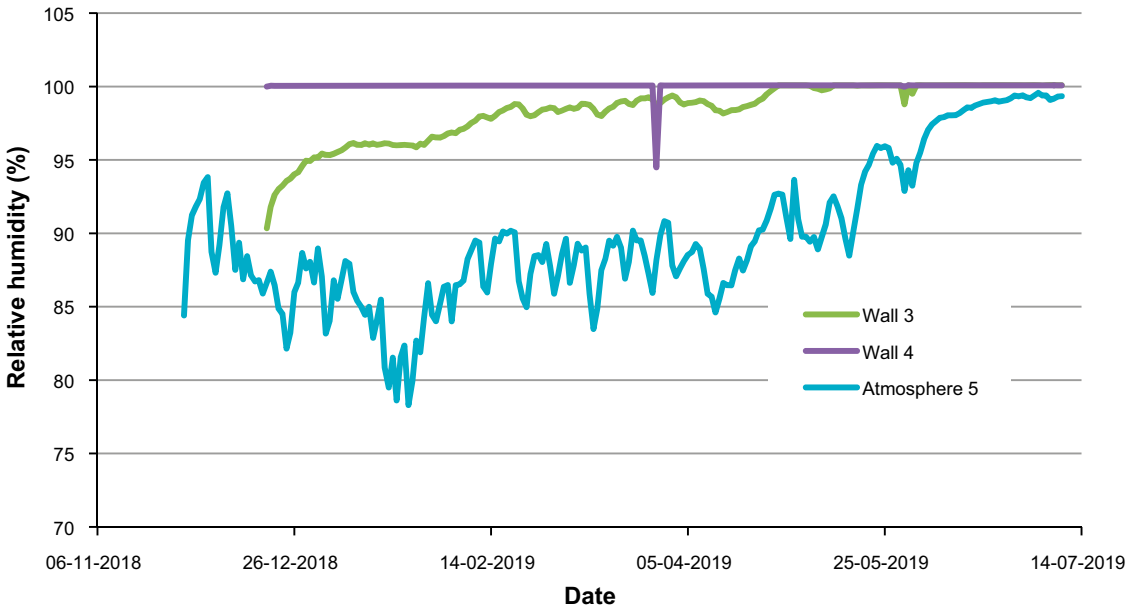

Figure 11-15. *Relative humidity in the wall of the concrete caisson and the surrounding atmosphere until mid-July 2019.*

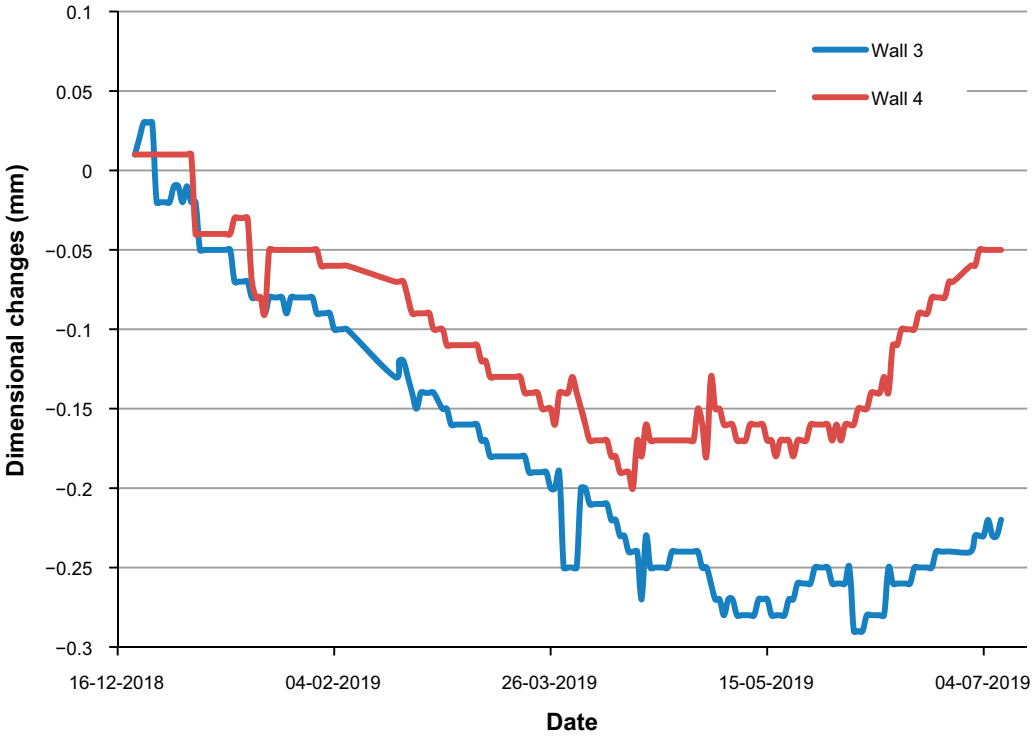

Figure 11-16. Changes in external dimensions of the walls of the concrete caisson until July 2019.

11.2.5 Crack monitoring

About 1 year after casting of the walls, no cracks had yet been found in the caisson walls.

11.3 Monitoring of the walls – Summary

In this chapter the results from the long-term monitoring programme of the caisson walls covering the period from the day of casting in mid-November 2018 until the autumn of 2019 has been presented. The following observations have been made:

- **Temperature –** After an early and rather fast temperature increase during hydration with a maximum temperature in the centre of the structure of about 43 °C the concrete soon cooled down and followed that of the tunnel.
- **Internal strain –** Typically all of strain transducers show a sharp increase in compressive strain during the very early hydration period. This is followed by a period where the compressive strain is reduced and about 6 months after casting only very low levels of strain are observed. See Appendix C for a discussion regarding strain measurement and comparison with simulations.
- **Relative humidity –** Relative humidity is high but measurements have suffered from malfunction of many of the sensors. This is a commonly experienced problem with RH sensors in this type of environment.
- **External dimensions –** The external dimensions of the walls were monitored from about 1 month after casting. The general observation is that the external dimensions have followed the climate in the tunnel with shrinkage during the cool and dry winter and early spring followed by small expansion during late spring and summer.
- **Crack formation –** No cracks have been observed in the concrete during the first 11 months after casting of the walls.

12 Summary

12.1 Overview

The work presented in this report has comprised construction and long-term monitoring of the properties of a concrete caisson with the dimensions 18.1 × 9.36 × 4.6 metres with thickness of base slab and walls of 0.60 and 0.68 metres respectively. The dimensions correspond to ¼ of the caissons in the future 2BMA whereas concrete thicknesses of the different parts are the same as planned for the 2BMA caissons.

The casting was divided into two steps where the first comprised casting of the base slab and the second step the walls. Prior to casting of the base slab a concrete foundation slab was cast directly onto the bare rock floor. This slab was also covered with a plastic sheet to reduce the adhesion between the foundation and the caisson base slab.

The concrete used in these experiments had previously been developed and tested by Lagerblad et al. (2017) and tested in a large scale test by Mårtensson and Vogt (2019). The concrete is based on Degerhamn Anläggningscement from Cementa AB and the crushed rock aggregates. Additionally also rather large amounts of commercial limestone filler is used in order to obtain the desired workability of the concrete.

The concrete was produced in a mobile concrete production plant placed just at the entrance to the Äspö Hard Rock laboratory where casting was performed. The concrete was transported to the site by means of standard concrete trucks.

Below follows short summaries of the different parts of the work presented in this report. Conclusions, recommendations and suggestions for future work are presented in Chapter 13.

12.2 Preparations

Prior to casting of the caisson preparations in TAS08 were made in order to ensure a healthy and safe working environment and to prepare the foundation for the caisson.

The foundation comprised a concrete slab which was cast directly onto the bare rock floor. Casting was carried out in 3 steps and comprised in total about 150 m^3 of concrete delivered by *AB Högsby Grus och Betong*. After casting and trowelling, the surface was also grinded in order to obtain the desired surface finish.

12.3 Base slab

The base slab was cast in mid-October 2018 and comprised about 100 m^3 of concrete produced in a mobile concrete production plant placed just next to the entrance to the Äspö tunnel.

Implementation

The formwork was constructed according to requirements. The part of the formwork that formed the recess and held the joint seal took some time to construct but the quality of the work was very high. In parallel with formwork construction, the sensors were mounted in bars secured in the foundation.

Concrete production and transport worked very well with consistent concrete quality and an average time from mixing concrete in the first truck mixer until the transport truck had been emptied was about 90 minutes.

However, moving and lifting of the concrete distributor required some additional efforts which delayed the casting a little and forced a few of the concrete trucks to wait a little longer before being emptied. This meant that the concrete became a little more difficult to pump and that about 4 m^3 had to be discarded in order to catch up with the casting schedule again.

Properties of the fresh concrete

The properties of the fresh concrete were consistent and according to the requirements throughout the casting. Slump varied from 210 mm to 240 mm with an average of about 220 mm. In spite of an occasionally rather high pump pressure (up to 40 bars) the concrete was very flow able once delivered into the mould. This caused some problems as a long rather flat front which required casting and post treatment to be done in parallel on different parts of the base slab was formed.

Properties of the hardened concrete

The properties of the hardened concrete were studied using several methods and the following results obtained:

Compressive strength – The 28 days compressive strength varied between 41.0 and 53.5 MPa with an average of 47.1 MPa. After six months the compressive strength had increased to an average of 64.8 MPa with a variation from 61.2 to 69.0 MPa.

Splitting tensile strength – 6-months splitting tensile strength was measured on ∅ 100 mm cores from the beams used to control the strain transducers. The average splitting tensile strength was 4.72 MPa, with a spread from 4.3 to 5.35 MPa.

Shrinkage – Concrete shrinkage was measured according to SIS (2000) where samples were stored in a climate room with RH 50 % but also on sealed samples where dehydration was prevented. After 224 days, total shrinkage was 0.38 ‰ and 0.12 ‰, respectively for these methods. This indicates that dehydration shrinkage is the dominant shrinkage process.

Long-term monitoring

The following observations were made during the long-term monitoring:

Temperature – After an early and rather fast temperature increase during hydration with a maximum temperature in the centre of the slab of about 41 °C the concrete cooled slowly and soon returned to that of the tunnel.

Internal strain – Internal strain varied from high compressive strain during the very early hydration period to very low levels of strain from about 1 month after casting and onwards.

Relative humidity – The relative humidity in the different parts of the base has varied between 95 and 100 %. However, monitoring has suffered from malfunctioning of several of the RH sensors.

External dimensions – Changes in external dimensions of the base slab have been very small apart from the expansion caused by heating of the base slab prior to casting of the walls. Once heating was turned off, the base slab contracted to its original dimensions.

Crack formation – No cracks were observed in the concrete during the first 11 months following casting of base slab.

12.4 Walls

The walls were cast in mid-November 2018 and comprised about 150 m^3 of concrete produced in a mobile concrete production plant placed just next to the entrance to the Äspö tunnel.

Implementation

The formwork was very well built and the preparations for casting complete. The formwork was designed for a maximum pressure of 60 kPa. This can be compared with the maximum formwork pressure during casting which was 28 kPa. Installation of the sensors was performed after assembling of the formwork. The installation went well and the sensors were secured in the plastic tubes that protected the form rods from the fresh concrete.

Concrete production and transport worked very well with consistent concrete quality with an average time from mixing concrete in the first truck mixer until the transport truck had been emptied of about 70 minutes.

The handling of the concrete hose and distributor worked very well. A comment from the staff was that the casting would not have been possible without the distributor as the hose was far too heavy to handle under such an extensive casting.

Properties of the fresh concrete

The properties of the fresh concrete were consistent and according to the requirements throughout the casting. Slump varied from 200 mm to 240 mm with an average of about 225 mm. The setting of the concrete was very well adjusted for the purpose. This was manifested in that consecutive layers of concrete could be homogenised while the formwork pressure still did not exceed 30 kPa.

Properties of the hardened concrete

The properties of the hardened concrete were studied using several methods and the following results obtained:

Compressive strength – The 28 days compressive strength varied between 36.6 and 49.8 MPa with an average of 45 MPa. After 6 months the compressive strength had increased to 55.8 MPa with a variation between 49 and 61 MPa.

Splitting tensile strength – 6 months splitting tensile strength was measured on Æ 100 mm cores from different parts of the caisson walls. The average splitting tensile strength was 3.8 MPa, with a spread from 2.8–4.4 MPa.

Shrinkage – Concrete shrinkage was measured according to SIS (2000) where samples were stored in a climate room with RH 50 % but also on sealed samples where dehydration was prevented. After 224 days, total shrinkage was 0.36 ‰ and 0.02 ‰, respectively for these methods. This indicates that dehydration shrinkage is the dominant shrinkage process.

Long-term monitoring

The following observations were made during the long-term monitoring:

Temperature – After an early and rather fast temperature increase during hydration with a maximum temperature in the centre of the structure of about 43 °C the concrete soon cooled down and followed that of the tunnel.

Internal strain – Internal strain varied from high compressive strain during the very early hydration period to very low levels of strain from about 1 month after casting and onwards.

Relative humidity – Relative humidity is high in the concrete but measurements have suffered from malfunction of the sensors. This is a commonly experienced problem with RH sensors in this type of environment.

External dimensions – The external dimensions of the walls were monitored from about 1 month after casting. The general observation is that the external dimensions have followed the climate in the tunnel with shrinkage during the cool and dry winter and early spring followed by small expansion during late spring and summer.

Crack formation – No cracks were observed in the concrete during the first 11 months after casting of the walls.

12.5 Sealing of holes caused by the tie rods

Sealing of the holes in the concrete walls caused by the plastic tubes that covered the tie rods comprised first removing the plastic tubes and then grouting the holes. The work started with a very simple concept test with the purpose of evaluating the possibility to achieve the desired hydraulic conductivity of the grouted holes. This was followed by a production test during which equipment and methods were further developed.

Extraction of the plastic tubes

Extraction of the plastic tubes by means of any of the methods tested had a rather low capacity and in some cases in the production test it was not possible to extract the tubes even though extensive heating was carried out prior to extraction. None of the methods used is therefore considered suitable for use during construction of the concrete caissons in the future 2BMA and other materials and/or methods have to be sought for.

Grouting of the holes

Grouting of the holes using a spray boy was efficient and had a high capacity. The hardened grout filled the holes entirely but the porosity of the grout was very high which was also reflected in a high hydraulic conductivity of the grouted holes.

From the results it can be concluded that grouting of the holes can be done with a high capacity but that the hydraulic conductivity of the grouted holes does not comply with requirements. Further development work will thus be required if tie rods are to be used in formwork construction for the 2BMA caissons.

13 Conclusions, recommendations and future work

13.1 Conclusions

The following conclusions can be drawn from the results presented in this report:

- Concrete production was successfully carried out in mobile truck mixers with consistent properties of the fresh concrete but with somewhat larger variations in the properties of the hardened concrete compared to when concrete was produced in a standard concrete production plant (Mårtensson and Vogt 2019). In order to avoid inconsistent quality of the hardened concrete in the engineered barrier system, care must be taken when certifying the concrete production plant.
- The very short transport time from concrete production to the casting site was a key success factor in this work and allowed for careful adjustments of the properties of the fresh concrete and its setting time.
- In this work it was verified that the hydraulic properties of the joint between the base slab and the walls are similar to those of the bulk concrete. With these results it can be concluded the walls and base slab can be cast separately and also that joint seals will not be required in the caissons in 2BMA. However, careful preparation of the joint prior to casting of the walls is required to obtain the desired properties.
- The properties of the fresh and hardened concrete are in accordance with requirements presented in Section 1.3. Also considering the results from the long-term monitoring it can be concluded that it is suitable for casting of the caissons in 2BMA.
- The foundation used in these experiments comprised a levelling concrete slab with a smooth surface finish on which a reinforced plastic foil had been placed in order to promote unrestrained shrinkage of the concrete structures. From the results obtained up to 1 year after casting of Section 1, this combination has fulfilled these requirements and no cracks have yet been identified.

Altogether the results presented in this report verify that the previously developed and tested concrete can be used for construction of the future caissons in 2BMA.

13.2 Recommendations and requirements

It is recommended that…

- The concrete mix design shown in the table below is used in the production of the caissons in 2BMA. Slight adjustments are allowed in order to handle variations in outside temperature, detailed properties of the aggregate materials, availability of admixtures over time and the different requirements from casting the base slab and the walls.

Table 13.1. Recommended concrete mix design to be used for casting of the concrete caissons in 2BMA.

Component	Products name/supplier	Amount (kg/m^3)
Cement	Anläggningscement (CEM I)	320
Limestone filler*	OmyaCarb 2GU (grain size: 2 mm)	130
Limestone filler*	Myanit 10 (grain size: 10 mm)	33.3
Water		156.8
Aggregates 16–22 mm	Crushed rock	393.3
Aggregates 8–16 mm	Crushed rock	425.7
Aggregates 4–8 mm	Crushed rock	92.0
Aggregates 0–4 mm	Crushed rock	840.9
Superplasticiser*	MasterGlenium Sky 558	1.30
Superplasticiser*	Master Sure 910	1.70
Retarder*	Master Set RT 401	0.96 (0.3 % of cement weight)

* As it is considered unlikely that products with these specific product names will be available during the entire period of construction, other products are likely to be used instead and slight adjustments of the mix design are therefore anticipated.

- The different components should be added in the order outlined below if the same type of equipment is used. However, for other methods of concrete production, other mixing sequences may be more suitable.
  1. Water and admixtures
  2. Aggregates 16–22 mm
  3. Cement
  4. Fillers
  5. Aggregates 0–4 mm
  6. Aggregates 4–8 mm
  7. Aggregates 8–16 mm
- The concrete is produced in a concrete production plant in the near vicinity of the entrance tunnel to the repository in order for accurate control of the properties of the fresh concrete. This is further supported by the requirement that all aggregates used in the concrete should be made from crushed rock from the excavation of the repository and that long transports must be avoided.
- The properties of the excavated rock are carefully tested and its suitability for aggregate production determined.
- The foundation constitutes a concrete slab with a smooth surface. This slab should also be covered with a plastic sheet prior to casting of the base slab in order to reduce adhesion between the foundation and the slab and allow for unrestricted shrinkage and expansions caused by temperature and humidity variations in the rock vault.
- Base slab and walls are cast on different occasions separated by a time period of at least 5 weeks.
- Tie rods or the like are used during construction of the formwork. However, detailed specifications on which system to use need to be carefully investigated and tested prior to construction. See also Section 13.3.1.
- Joint seals are not placed in the joint between the walls and the base slab.

It is required that…

- The joint surface between the base slab and the walls is carefully cleansed prior to casting of the walls in order to ensure that not dust or any loose particles are left but also in order to remove the topmost cement surface to expose the aggregate particles.
- The base slab is heated at least 1 week prior to casting of the walls in order to reduce the degree of restraint between these 2 construction parts during the cooling of the walls after casting and hydration. The exact heating time to ensure sufficient expansion of the base slab must be calculated prior to start of heating.

13.3 Future work

In this section identified remaining work that needs to be undertaken prior to construction of the caissons in 2BMA is presented.

13.3.1 Formwork construction

The required initial state of the concrete caissons specifies that no hydraulically conducting zones are present in any of the construction parts of the concrete caissons. Initially this specified the use of a suspended formwork and that tie rods were not allowed. In this work tie rods were used due to lack of space in the rock vault to handle the components required for a fully suspended formwork utilising also external support beams.

In this work, tests have been undertaken in order to remove the plastic tubes that protected the tie rods from the fresh concrete and to fill the holes with grout.

However, as the project was not fully successful in this work a new or modified concept for formwork construction has to be evaluated. The 2 possible options identified at this stage are 1) replacing the plastic protective tubes with tubes made of another type of material which can either be easily removed or left in the concrete or 2) use a suspended formwork system with external supporting beams as initially required.

If tie rods or the like are still identified as the primary option, also further development of grout and method for grouting of the holes in the caisson walls need to be further developed and tested and the properties verified.

13.3.2 Construction of inner walls

Method for construction of inner walls has not been a part of this project. However, as the inner walls have the important function of supporting the outer walls from external forces caused during backfilling and resaturation of the rock vault their design and method of construction have to be carefully tested and evaluated.

References

SKB's (Svensk Kärnbränslehantering AB) publications can be found at www.skb.com/publications. SKBdoc documents will be submitted upon request to document@skb.se.

Arizona Leisure, 2018. Construction history of Hoover Dam – A brief overview of Hoover Dam construction. Available at: http://www.arizona-leisure.com/hoover-dam-building.html

Bamforth P B, 2007. Early-age thermal crack control in concrete. CIRIA C660, CIRIA, London.

Eckfeldt L, 2005. Möglichkeiten und Grenzen der Berechnung von Rissbreiten in veränderlichen Verbundsituationen. PhD thesis. Technische Universität Dresden (In German.)

Grahm P, Malm R, Eriksson D, 2015. System design and full-scale testing of the Dome Plug for KBS-3V deposition tunnels. Main report. SKB TR-14-23, Svensk Kärnbränslehantering AB.

Hedlund H, 2000. Hardening concrete: measurements and evaluation of non-elastic deformation and associated restraint stresses PhD thesis. Luleå University of Technology, Sweden.

Hösthagen A, 2017. Thermal crack risk estimation and material properties of young concrete, Lic. thesis. Luleå University of Technology, Sweden.

Jonasson J-E, Wallin K, Emborg M, Gram A, Saleh I, Nilsson M, Larson M, Hedlund H, 2001. Temperatursprickor i betongkonstruktioner: handbok med diagram för sprickriskbedömning inklusive åtgärder för några vanliga typfall. LTU rapport 2001:14, Luleå University of Technology, Sweden. (In Swedish.)

Jonasson J-E, Wallin K, Nilsson M, 2009. Gjutning av vägg på platta – Studier av sprickrisker orsakat av temperaturförloppet vid härdningen. Luleå: Luleå University of Technology. (In Swedish.)

Könönen M, Olsson D, 2018. 2BMA – analys av konstruktionsstyrande lastfall och olyckslaster. SKBdoc 1609765 ver 1.0, Svensk Kärnbränslehantering AB. (In Swedish.)

Lagerblad B, Golubeva M, Cirera Rui J, 2016. Lämplighet för krossberg från Forsmark och SFR att användas som betongballast. SKB P-16-13, Svensk Kärnbränslehantering AB. (In Swedish.)

Lagerblad B, Rogers P, Vogt C, Mårtensson P, 2017. Utveckling av konstruktionsbetong till kassunerna i 2BMA. SKB R-17-21, Svensk Kärnbränslehantering AB.

Leonhardt F, 1988. Cracks and crack control in concrete structures. PCI Journal 33, 124–145.

Ljungkrantz C, Möller G, Petersons N (eds), 1994. Betonghandbok Material. 2nd ed. Solna: Svensk byggtjänst. (In Swedish.)

Löfquist B, 1946. Temperatureffekter i hårdnande betong (Temperature effects in hardening concrete). PhD thesis. Chalmers tekniska högskola, Kungliga Vattenfallsstyrelsen, Stockholm. (In Swedish.)

Mårtensson P, Vogt C, 2019. Concrete caissons for 2BMA. Large scale test of design and material. SKB TR-18-12, Svensk Kärnbränslehantering AB.

Neville A M, 1995. Properties of concrete. 4th ed. Harlow: Longman Group.

SIS, 2000. SS 13 72 15: Betongprovning – Hårdnad betong – Krympning (Concrete testing – Hardened concrete – Shrinkage). Stockholm: Swedish Standards Institute. (In Swedish.)

SIS, 2013. SS-EN 206:2013: Betong – Fordringar, egenskaper, tillverkning och överensstämmelse (Concrete – Specifcation, performance, production and conformity). Stockholm: Swedish Standards Institute. (In Swedish.)

Springenschmid R, 1998. Prevention of thermal cracking in concrete at early ages: state-of-the-art report prepared by RILEM Technical Committee 119 Avoidance of Thermal Cracking in Concrete at Early Ages. London: E & FN Spon.

Vogt C, Lagerblad B, Wallin K, Baldy F, Jonasson J-E, 2009. Low pH self-compacting concrete for deposition tunnel plugs. SKB R-09-07, Svensk Kärnbränslehantering AB.

Vogt C, Hedlund H, Wallin K, Baldy F, Pettersson D, 2010. Beständiga undervattensgjutna konstruktioner. SBUF project 11940. Available at: https://sbuf.se/Projektsida?project=a5153380-9a34-43d9-b003-697eb91f2bca (In Swedish.)

Appendix A

Data from concrete production

The truck mixers are equipped with a logging system to trace the amount of material in the batches of concrete produced. The data was evaluated and the differences between target amounts and actual amounts for most of the components in the mixes are displayed below. Observe that the admixtures were measured and added manually. Thus, the amount of admixture is not included in the logged data. Also, one type of limestone filler was added from the silo while the other type was added manually into the loading bucket of the truck mixers. Therefore, the amount of limestone filler that was recorded is not correct in many cases and is excluded from the evaluation.

A1 Base slab

A1.1 Difference between target amounts and actual amounts

The difference between target amounts and actual amounts for water, cement and aggregates is displayed in Figure A-1, A-2 and A-3 below. According to SIS (2013), the tolerance of the batching process is ± 3 % for cement, water and total aggregates. There are no requirements on the tolerance for the individual aggregate fractions.

Figure A-1 shows that the deviations for cement and aggregate are within the limits. For water, the tolerance is not met for 4 batches. However, less water is added than stipulated which results in lower w:c ratio. This is on the safe side regarding strength but with possible negative impact on workability.

The largest differences were recorded for aggregate fraction 4–8 mm, generally on the plus-side, Figure A-2 and A-3. This is explained by the fact that the total amount of 4–8 mm aggregate is only 315 kg per batch of concrete and therefore already a relatively small extra amount gives a large deviation (in per cent). Also, the volume of the truck mixers´ loading bucket is 650 litres and as the operator only gets a reading of the added amount of material once it has entered the drum (load cells weigh the drum and not the loading bucket) high precision is difficult to achieve. The operator usually balances the total amount of aggregate with the final fraction, thus the low tolerance for total aggregates.

On average, the difference between target amounts and actual amounts for all batches was −1.4 % for water, +0.3 % for cement and +0.6 % for total aggregates. This is very high precision, considering the manual control of the weighing process in the truck mixers and displays the skill of the operators.

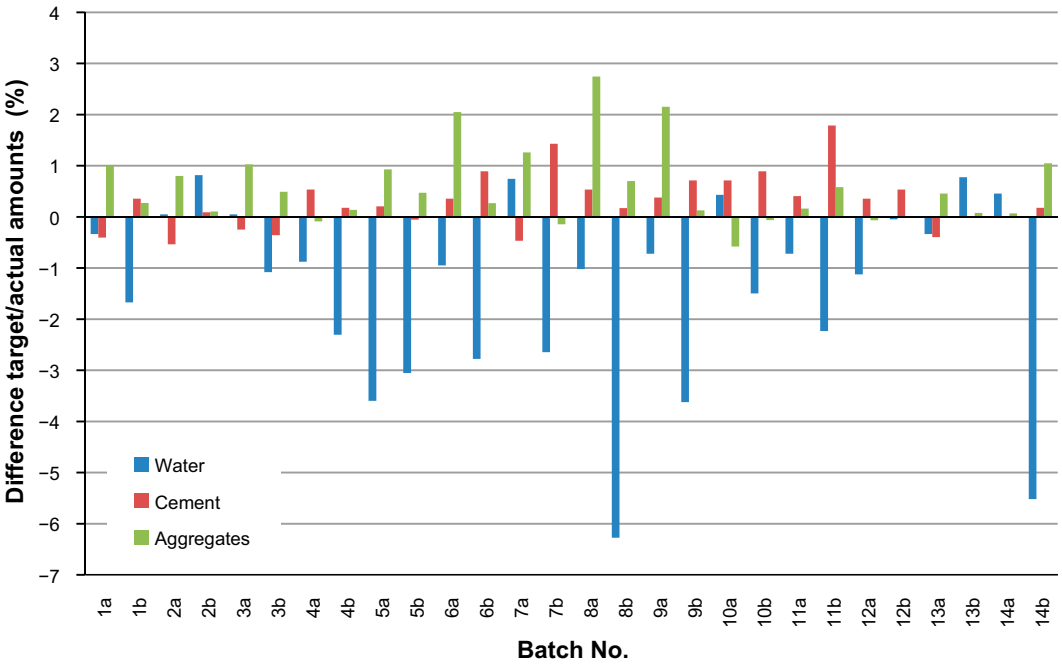

Figure A-1. *Difference between actual and target amount for water, cement and total amount of aggregates in the individual concrete batches for the base slab.*

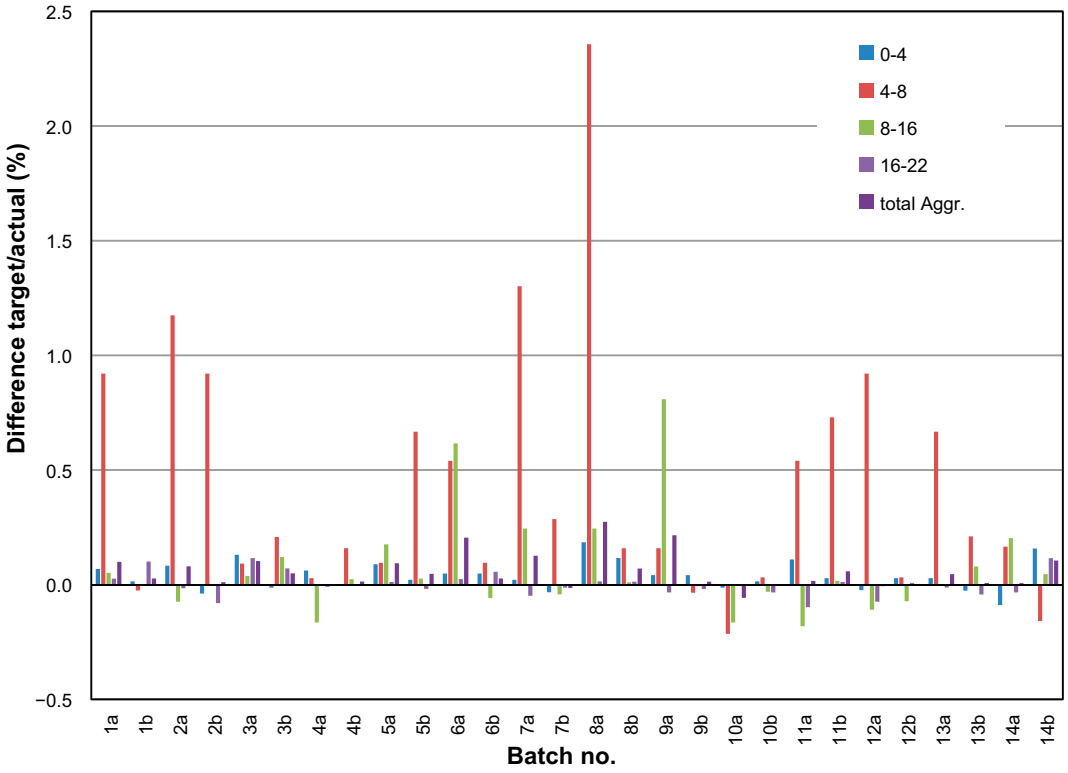

Figure A-2. *Difference between actual and target amount for the individual aggregate fractions in the individual batches for the base slab.*

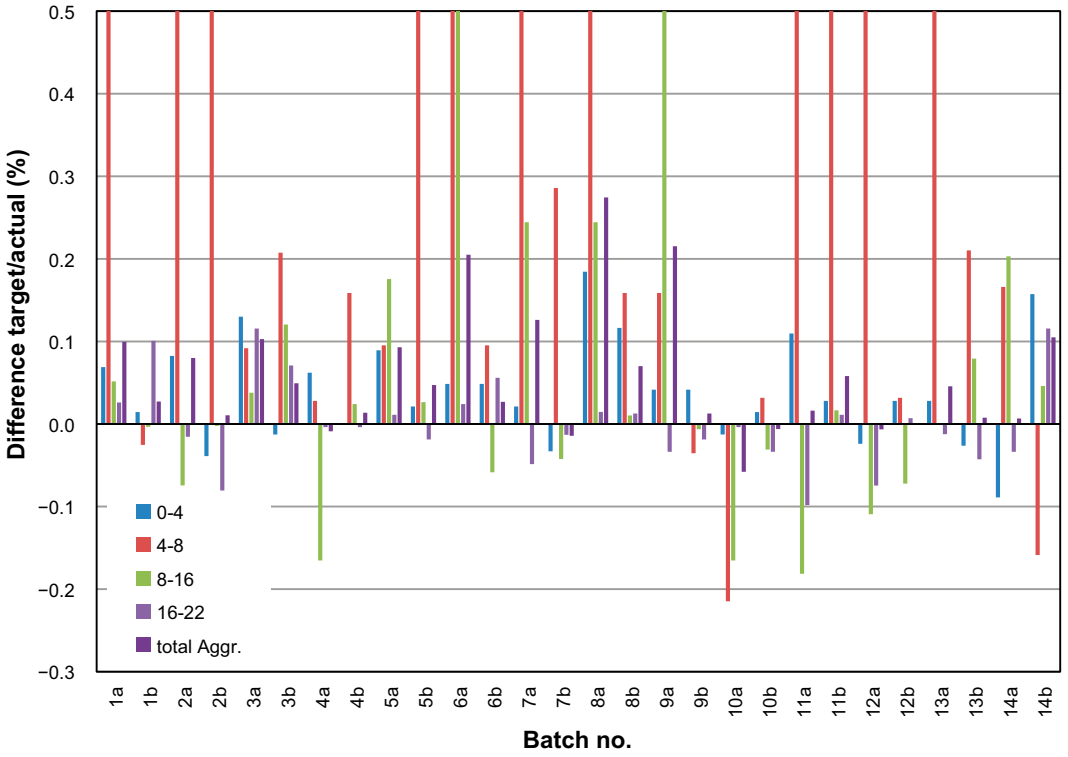

Figure A-3. *Difference between actual and target amount for the individual aggregate fractions in the individual batches for the base slab. Different scale compared to Figure A-2 but same data.*

A1.2 Water cement ratio for batches and transport trucks

The water-cement ratio was calculated for the individual batches of concrete and for the delivery trucks (each containing two batches) assuming that the two batches were intermixed to a certain degree in the delivery trucks. Figure A-4 shows the w/c of the individual batches. 4 batches had a w/c slightly above the stipulated value of 0.54. Two batches were combined in one delivery truck. Figure A-5 shows that only two trucks had a w/c which was marginally higher than 0.54. This is very high precision under the circumstances.

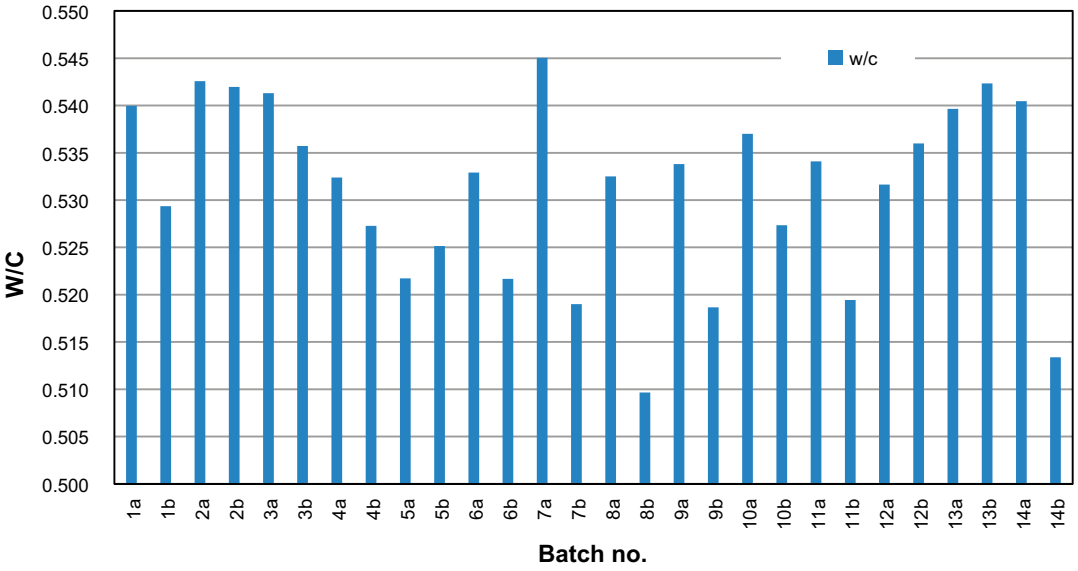

Figure A-4. *Water-cement ratio for the individual batches.*

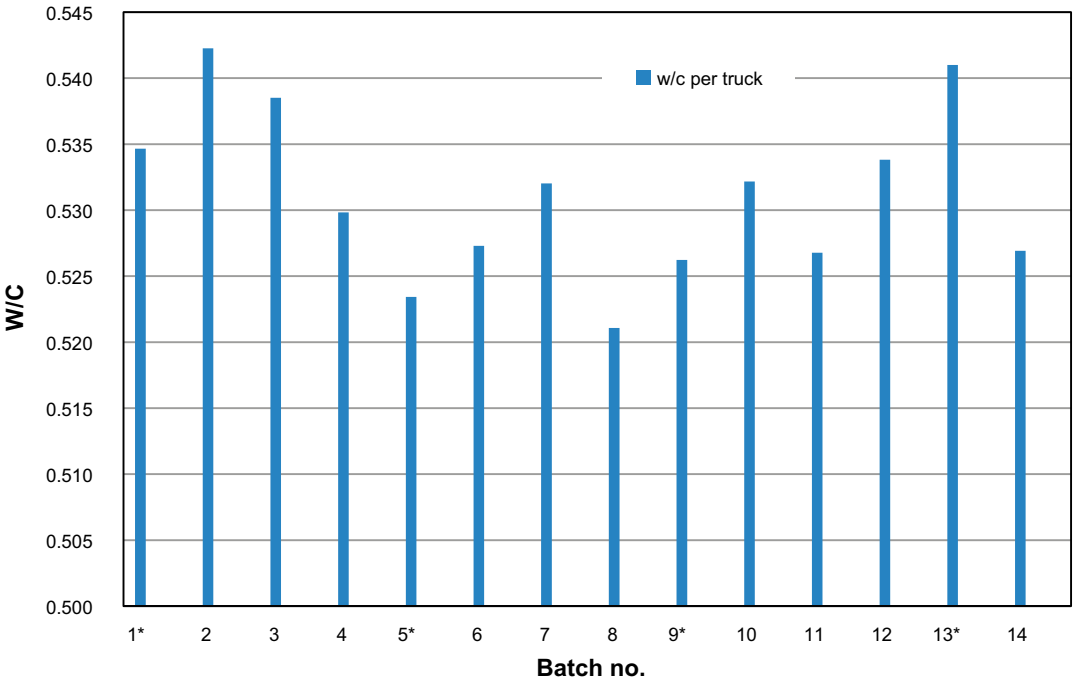

Figure A-5. *Water-cement ratio for the transport trucks. Trucks marked with * were tested on strength.*

A2 Walls

A2.1 Difference between target amounts and actual amounts

The difference between target amounts and actual amounts for water, cement and aggregates is displayed in Figure A-6, A-7 and A-8 below. According to SIS (2013), the tolerances of the batching process are ± 3 % for cement, water and total aggregates. There are no requirements on the tolerance for the individual aggregate fractions. Figure A-6 shows that the tolerance for cement and aggregate is within the limits. For water, the tolerance is not met for three batches. With one exception, less water is added than required according to mix design which results in lower w/c (safe side regarding strength, workability may be influenced negatively). The largest differences were again recorded for aggregate fraction 4–8 mm, generally on the plus-side. For an explanation, see Section A1.1.

On average, the difference between target amounts and actual amounts for all batches was −0.2 % for water, +0.8 % for cement and +0.7 % for total aggregates. This is very high precision again, considering the manual control of the weighing process in the truck mixers and displays the skill of the operators.

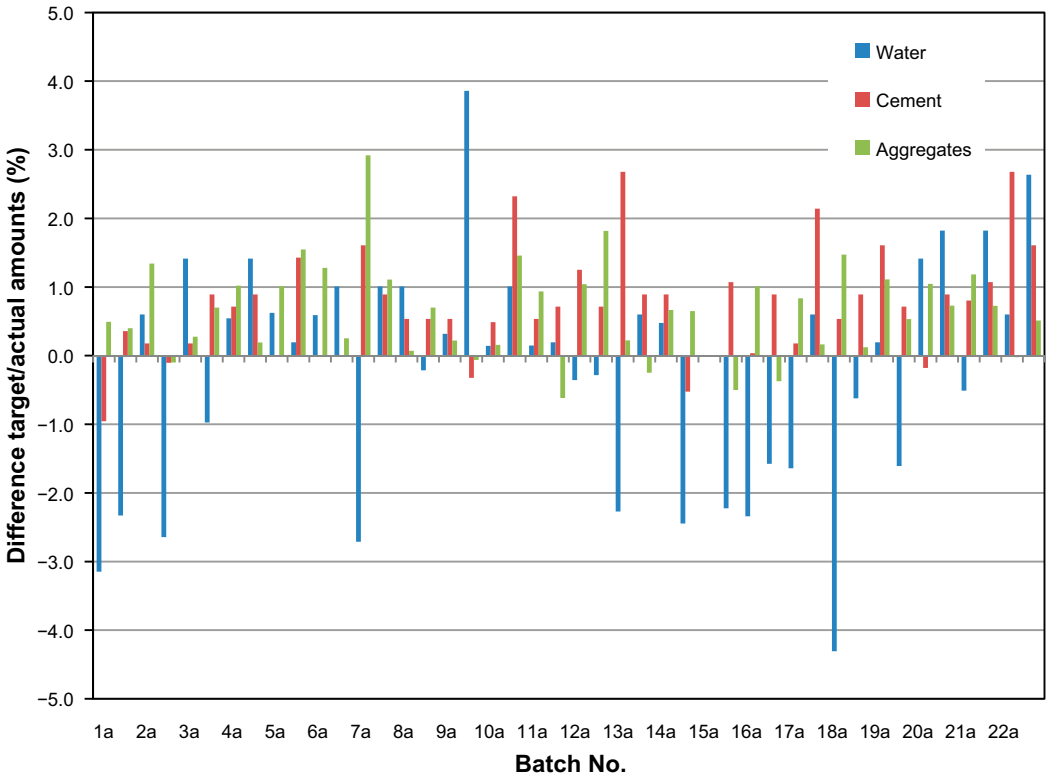

Figure A-6. *Difference between actual and target amount for water, cement and total amount of aggregates in the individual concrete batches for the walls. Data is missing for batch 15a.*

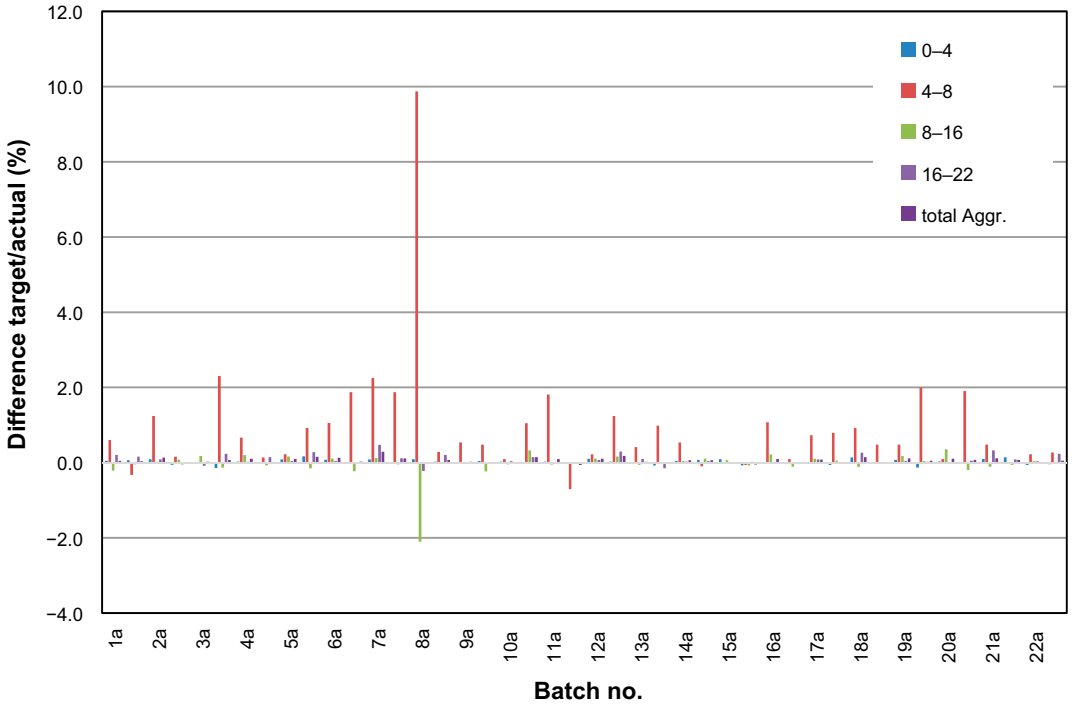

Figure A-7. *Difference between actual and target amount for the individual aggregate fractions in the individual batches for the walls. Data is missing for batch 15a.*

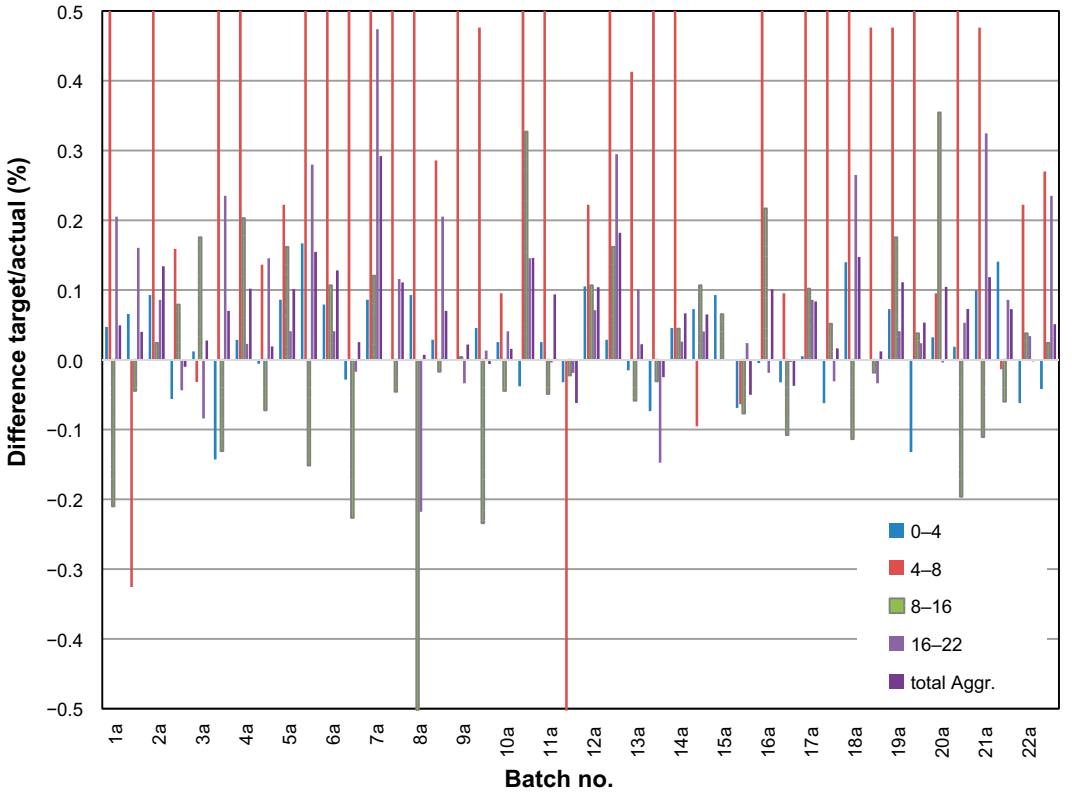

Figure A-8. *Difference between actual and target amount for the individual aggregate fractions in the individual batches for the walls. Different scale compared to Figure A-7 but same data. Data is missing for batch 15a.*

A2.2 Water cement ratio for batches and transport trucks

The water-cement ratio was calculated for the individual batches of concrete and for the delivery trucks (each containing two batches). One may assume that the two batches were intermixed to a certain degree in the delivery trucks. Figure A-9 shows the w/c of the individual batches. Three batches had a w/c slightly above the stipulated value of 0.54. Two batches were combined in one delivery truck. Figure A-10 shows that only two trucks had a w/c which was marginally higher than 0.54.

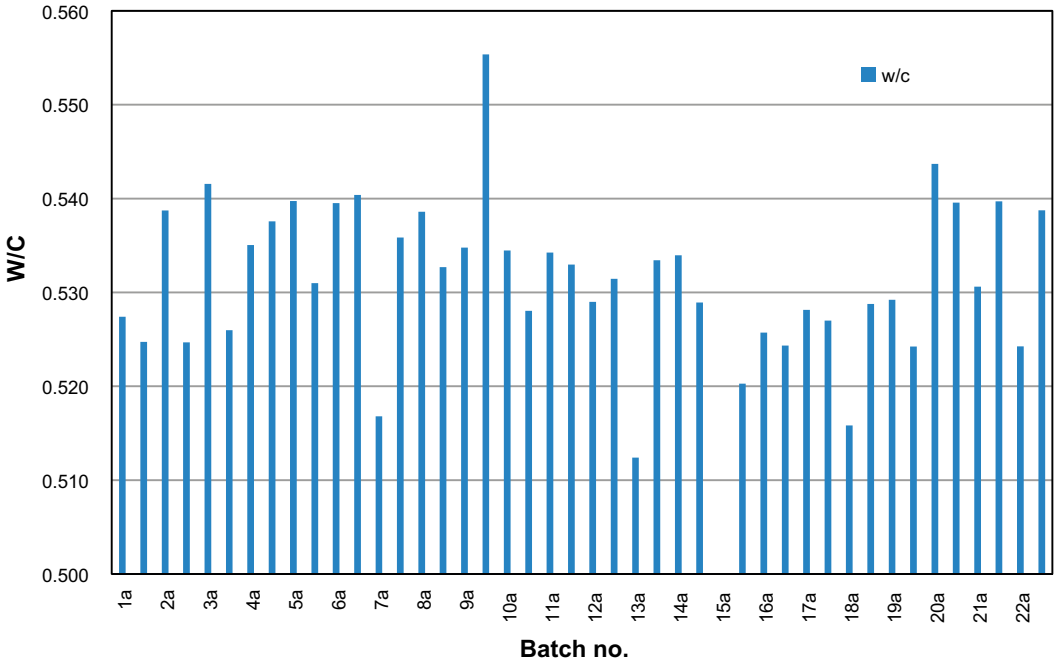

Figure A-9. *Water-cement ratio for the individual batches. Data is missing for batch 15a.*

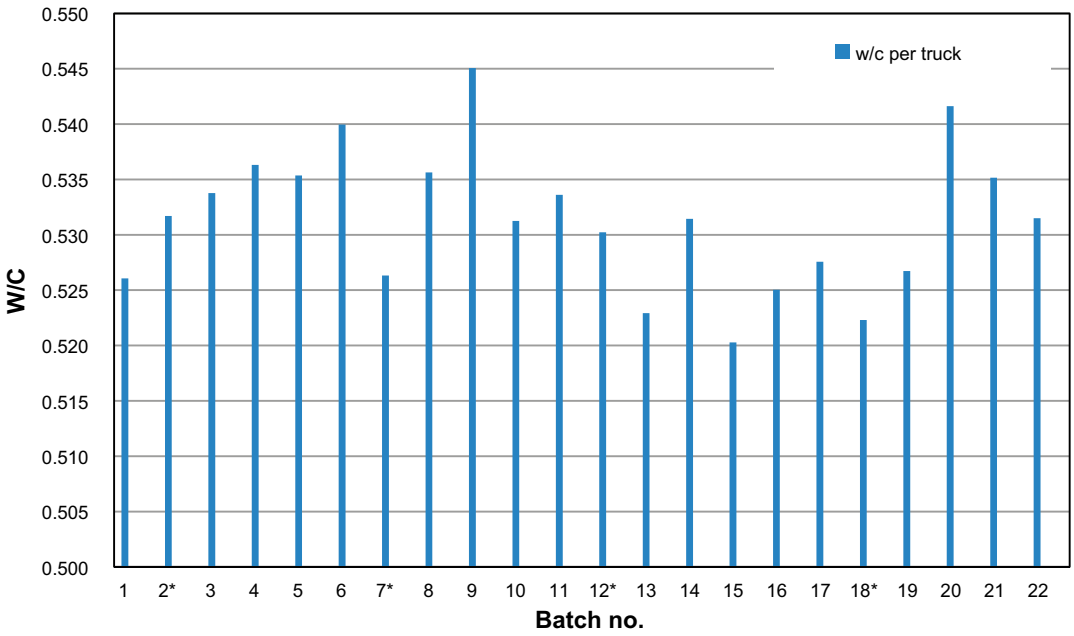

Figure A-10. *Water-cement ratio for the transport trucks. Trucks marked with * were tested on strength.*

A3 Data from concrete production

A3.1 Data from the truck mixers during the trial mixes

Table A-1. General information.

Batch	Truck mixer	Batch ID	Date*	Time
1	1	349	15-10-2018	15:31
2	1	354	16-10-2018	09:52
3	2	172	16-10-2018	10:46
4	2	173	16-10-2018	12:52
5	1	356	16-10-2018	13:55
6	2	174	16-10-2018	14:56
7	1	357	16-10-2018	15:14
8	1	376	19-11-2018	13:09
9	1	378	20-11-2018	08:12
10	2	193	20-11-2018	09:58

*Note that batches 1–7 were mixed prior to casting of the slab and batches 8–10 prior to casting of the walls.

Table A-2. Target amounts of concrete components in the different batches.

				Aggregates (mm)								
Batch	Water	Cem.	Fill.	0–4	4–8	8–16	16–22	Total	Moist. (%)**	Moist. (kg)	w/c*	w/c
1	469.04	1120	575	3006.5	322	1480.5	1368.5	6177.5	2.75	80.5	0.491	0.501
2	469.04	1120	575	3006.5	322	1480.5	1368.5	6177.5	2.75	80.5	0.491	0.501
3	489.15	1120	575	3010.9	322	1480.5	1368.5	6181.9	2.9	84.8	0.513	0.523
4	519.75	1120	575	2941.8	315	1452.5	1340.5	6049.8	2.5	71.8	0.528	0.539
5	476.35	1120	575	2999.2	322	1480.5	1368.5	6170.2	2.5	73.2	0.491	0.501
6	519.75	1120	575	2941.8	315	1452.5	1340.5	6049.8	2.5	71.8	0.528	0.539
7	519.75	1120	575	2941.8	315	1452.5	1340.5	6049.8	2.5	71.8	0.528	0.539
8	519.75	1120	575	2941.8	315	1452.5	1340.5	6049.8	2.5	71.8	0.528	0.539
9	519.75	1120	575	2941.8	315	1452.5	1340.5	6049.8	2.5	71.8	0.528	0.539
10	505.4	1120	575	2956.1	315	1452.5	1340.5	6064.1	3	86.1	0.528	0.539

*w/c excluding water of admixtures.
**Moisture content is calculated only for the 0.4 mm aggregate fraction and used to calculate the amount of water to be added.

Table A-3. Actual amounts of concrete components in the different batches.

				Aggregates (mm)								
Batch	Water	Cem.	Fill.	0–4	4–8	8–16	16–22	Total	Moist. (%)**	Moist. (kg)	w/c*	w/c
1	459.3	1119	552	3012	338	1458	1367.0	6175.1	2.75	80.6	0.482	0.493
2	480.0	1128	574	2967	458	1684	1359.3	6468.3	2.75	79.4	0.496	0.507
3	494.0	1092	575	3018	370	1490	1390	6268.2	2.9	85.1	0.530	0.541
4	519.2	1113	575	3012	400	1450	1356	6218	2.5	73.5	0.533	0.543
5	474.1	1126	582	3000	330	1486	1376	6192	2.5	73.2	0.486	0.497
6	540.0	1115	575	2948	330	1444	1350	6072	2.5	71.9	0.549	0.560
7	525.0	1142	564	2936	336	1456	1335.5	6063.5	2.5	71.6	0.522	0.533
8	500.3	1130	578	2930	330	1452	1340	6052	2.5	71.4	0.506	0.517
9	499.2	1119	550	2948	320	1443	1340	6052.0	2.5	71.9	0.510	0.521
10	489.5	1109	575	2970	334	1422	1368	6094	3	86.5	0.519	0.530

*w/c excluding water of admixtures.
**Moisture content is calculated only for the 0.4 mm aggregate fraction.

Table A-4. Differences between target and actual amount (kg).

			Aggregates				
Batch	**Water**	**Cement**	**0–4 mm**	**4–8 mm**	**8–16 mm**	**16–22 mm**	**Total**
1	−9.8	−0.8	5.5	16.0	−22.5	−1.4	−2.4
2	11.0	8.0	−39.5	136.0	203.5	−9.2	290.9
3	4.9	−28.0	7.1	48.2	9.5	21.5	86.3
4	−0.6	−7.1	70.3	85.0	−2.5	15.5	168.3
5	−2.3	6.0	0.8	8.0	5.5	7.5	21.9
6	20.3	−4.9	6.3	15.0	−8.5	9.5	22.3
7	5.3	22.0	−5.8	21.0	3.5	−5.0	13.8
8	−19.5	10.0	−11.8	15.0	−0.5	−0.5	2.3
9	−20.6	−0.9	6.3	5.7	−9.2	−0.5	2.3
10	−15.9	−10.7	13.9	19.0	−30.5	27.5	29.9

Table A-5. Differences between target and actual amounts (%).

			Aggregates				
Batch	**Water**	**Cement**	**0–4 mm**	**4–8 mm**	**8–16 mm**	**16–22 mm**	**Total**
1	−2.1	−0.1	0.2	5.0	−1.5	−0.1	0.0
2	2.3	0.7	−1.3	42.2	13.7	−0.7	4.7
3	1.0	−2.5	0.2	15.0	0.6	1.6	1.4
4	−0.1	−0.6	2.4	27.0	−0.2	1.2	2.8
5	−0.5	0.5	0.0	2.5	0.4	0.5	0.4
6	3.9	−0.4	0.2	4.8	−0.6	0.7	0.4
7	1.0	2.0	−0.2	6.7	0.2	−0.4	0.2
8	−3.7	0.9	−0.4	4.8	0.0	0.0	0.0
9	−4.0	−0.1	0.2	1.8	−0.6	0.0	0.0
10	−3.1	−1.0	0.5	6.0	−2.1	2.1	0.5
MIN	−4.0	−2.5	−1.3	1.8	−2.1	−0.7	0.0
MAX	3.9	2.0	2.4	42.2	13.7	2.1	4.7

A3.2 Data from the truck mixers during production of concrete to the base slab of the caisson

Table A-6. General information.

Batch	Truck mixer	Batch ID	Date	Time
1a	2	176	17-10-2018	07:07
1b	1	359	17-10-2018	07:25
2a	2	177	17-10-2018	07:31
2b	1	360	17-10-2018	07:51
3a	2	178	17-10-2018	08:03
3b	1	361	17-10-2018	08:22
4a	2	179	17-10-2018	08:28
4b	1	362	17-10-2018	08:51
5a	2	180	17-10-2018	08:53
5b	1	363	17-10-2018	09:18
6a	2	181	17-10-2018	09:19
6b	1	364	17-10-2018	09:42
7a	2	182	17-10-2018	09:45
7b	1	365	17-10-2018	10:05
8a	2	183	17-10-2018	10:13

Batch	Truck mixer	Batch ID	Date	Time
8b	1	366	17-10-2018	10:30
9a	2	184	17-10-2018	10:43
9b	1	367	17-10-2018	11:03
10a	2	185	17-10-2018	11:11
10b	1	368	17-10-2018	11:34
11a	2	186	17-10-2018	11:41
11b	1	369	17-10-2018	12:01
12a	2	187	17-10-2018	12:11
12b	1	370	17-10-2018	12:32
13a	2	188	17-10-2018	13:17
13b	1	371	17-10-2018	13:34
14a	2	189	17-10-2018	14:29
14b	1	372	17-10-2018	14:45

Table A-7. Target amounts of concrete components in the different batches of concrete to the base slab.

				Aggregates (mm)								
Batch	Water	Cem.	Fill.	0–4	4–8	8–16	16–22	Total	Moist. (%)**	Moist. (kg)	w/c*	w/c
1a	519.75	1120	575	2942	315	1453	1341	6050	2.5	71.7	0.528	0.539
1b	519.75	1120	575	2942	315	1453	1341	6050	2.5	71.7	0.528	0.539
2a	519.75	1120	575	2942	315	1453	1341	6050	2.5	71.7	0.528	0.539
2b	519.75	1120	575	2942	315	1453	1341	6050	2.5	71.7	0.528	0.539
3a	519.75	1120	575	2942	315	1453	1341	6050	2.5	71.7	0.528	0.539
3b	519.75	1120	575	2942	315	1453	1341	6050	2.5	71.7	0.528	0.539
4a	519.75	1120	575	2942	315	1453	1341	6050	2.5	71.7	0.528	0.539
4b	519.75	1120	575	2942	315	1453	1341	6050	2.5	71.7	0.528	0.539
5a	519.75	1120	575	2942	315	1453	1341	6050	2.5	71.7	0.528	0.539
5b	519.75	1120	575	2942	315	1453	1341	6050	2.5	71.7	0.528	0.539
6a	519.75	1120	575	2942	315	1453	1341	6050	2.5	71.7	0.528	0.539
6b	519.75	1120	575	2942	315	1453	1341	6050	2.5	71.7	0.528	0.539
7a	519.75	1120	575	2942	315	1453	1341	6050	2.5	71.7	0.528	0.539
7b	519.75	1120	575	2942	315	1453	1341	6050	2.5	71.7	0.528	0.539
8a	519.75	1120	575	2942	315	1453	1341	6050	2.5	71.7	0.528	0.539
8b	519.75	1120	575	2942	315	1453	1341	6050	2.5	71.7	0.528	0.539
9a	519.75	1120	575	2942	315	1453	1341	6050	2.5	71.7	0.528	0.539
9b	519.75	1120	575	2942	315	1453	1341	6050	2.5	71.7	0.528	0.539
10a	519.75	1120	575	2942	315	1453	1341	6050	2.5	71.7	0.528	0.539
10b	519.75	1120	575	2942	315	1453	1341	6050	2.5	71.7	0.528	0.539
11a	519.75	1120	575	2942	315	1453	1341	6050	2.5	71.7	0.528	0.539
11b	519.75	1120	575	2942	315	1453	1341	6050	2.5	71.7	0.528	0.539
12a	519.75	1120	575	2942	315	1453	1341	6050	2.5	71.7	0.528	0.539
12b	519.75	1120	575	2942	315	1453	1341	6050	2.5	71.7	0.528	0.539
13a	519.75	1120	575	2942	315	1453	1341	6050	2.5	71.7	0.528	0.539
13b	519.75	1120	575	2942	315	1453	1341	6050	2.5	71.7	0.528	0.539
14a	519.75	1120	575	2942	315	1453	1341	6050	2.5	71.7	0.528	0.539
14b	519.75	1120	575	2942	315	1453	1341	6050	2.5	71.7	0.528	0.539

*w/c excluding water of admixtures.
**Moisture content is calculated only for the 0.4 mm aggregate fraction and used to calculate the amount of water to be added.

Table A-8. Actual amounts of concrete components in the different batches of concrete to the base slab.

				Aggregates (mm)								
Batch	**Water**	**Cem.**	**Fill.**	**0–4**	**4–8**	**8–16**	**16–22**	**Total**	**Moist. (%)****	**Moist. (kg)**	**w/c***	**w/c**
1a	518	1115.5	575	2962	344	1460	1344	6110	2.5	72.2	0.529	0.540
1b	511.1	1124	560	2946	314	1452	1354	6066	2.5	71.9	0.519	0.529
2a	520	1114	575	2966	352	1442	1338	6098	2.5	72.3	0.532	0.543
2b	524	1121	560	2930	344	1452	1330	6056	2.5	71.5	0.531	0.542
3a	520	1117.2	575	2980	318	1458	1356	6112	2.5	72.7	0.530	0.541
3b	514.1	1116	526	2938	322	1470	1350	6080	2.5	71.7	0.525	0.536
4a	515.2	1126	575	2960	316	1429	1340	6044	2.5	72.2	0.522	0.532
4b	507.8	1122	570	2942	320	1456	1340	6058	2.5	71.8	0.517	0.527
5a	501.1	1122.3	575	2968	318	1478	1342	6106	2.5	72.4	0.511	0.522
5b	503.9	1119.4	576	2948	336	1456	1338	6078	2.5	71.9	0.514	0.525
6a	514.8	1124	575	2956	332	1542	1344	6174	2.5	72.1	0.522	0.533
6b	505.3	1130	566	2956	318	1444	1348	6066	2.5	72.1	0.511	0.522
7a	523.6	1114.8	575	2948	356	1488	1334	6126	2.5	71.9	0.534	0.545
7b	506	1136	558	2932	324	1446	1339	6041	2.5	71.5	0.508	0.519
8a	514.4	1126	575	2996	389	1488	1342	6216	2.5	73.1	0.522	0.532
8b	487.1	1121.9	558	2976	320	1454	1342	6092	2.5	72.6	0.499	0.510
9a	516	1124.2	575	2954	320	1570	1336	6180	2.5	72.0	0.523	0.534
9b	500.9	1128	556	2954	314	1452	1338	6057	2.5	72.0	0.508	0.519
10a	522	1128	575	2938	308	1428	1340	6015	2.5	71.7	0.526	0.537
10b	512	1130	548	2946	316	1448	1336	6046	2.5	71.9	0.517	0.527
11a	516	1124.5	575	2974	332	1426	1327	6059	2.5	72.5	0.523	0.534
11b	508.1	1140	564	2950	338	1455	1342	6085	2.5	72.0	0.509	0.519
12a	513.9	1124	575	2935	344	1437	1331	6046	2.5	71.6	0.521	0.532
12b	519.5	1126	566	2950	316	1442	1341	6049	2.5	72.0	0.525	0.536
13a	518	1115.6	575	2950	336	1453	1339	6077	2.5	72.0	0.529	0.540
13b	523.8	1120	548	2934	322	1464	1335	6054	2.5	71.6	0.532	0.542
14a	522.1	1120	575	2916	320	1482	1336	6054	2.5	71.1	0.530	0.540
14b	491.1	1122	566	2988	310	1459	1356	6113	2.5	72.9	0.503	0.513

*w/c excluding water of admixtures.
** Moisture is calculated only for the 0–4 mm aggregate fraction.

Table A-9. Differences between target and actual amounts (kg) for the concrete to the base slab.

			Aggregates				
Batch	**Water**	**Cement**	**0–4 mm**	**4–8 mm**	**8–16 mm**	**16–22 mm**	**Total**
1a	−1.8	−4.5	20.3	29.0	7.5	3.5	60.3
1b	−8.7	4.0	4.3	−0.8	−0.5	13.5	16.5
2a	0.3	−6.0	24.3	37.0	−10.8	−2.1	48.4
2b	4.3	1.0	−11.4	29.0	−0.3	−10.8	6.4
3a	0.3	−2.8	38.3	2.9	5.5	15.5	62.1
3b	−5.6	−4.0	−3.8	6.5	17.5	9.5	29.8
4a	−4.6	6.0	18.3	0.9	−24.0	−0.5	−5.4
4b	−12.0	2.0	0.3	5.0	3.5	−0.5	8.3
5a	−18.7	2.3	26.3	3.0	25.5	1.5	56.3
5b	−15.9	−0.6	6.3	21.0	3.8	−2.5	28.6
6a	−4.9	4.0	14.3	17.0	89.5	3.2	124.0
6b	−14.4	10.0	14.3	3.0	−8.5	7.5	16.3
7a	3.9	−5.2	6.3	41.0	35.5	−6.5	76.3
7b	−13.8	16.0	−9.8	9.0	−6.2	−1.8	−8.7
8a	−5.3	6.0	54.3	74.3	35.5	1.9	165.9
8b	−32.6	1.9	34.3	5.0	1.5	1.7	42.4

			Aggregates				
Batch	**Water**	**Cement**	**0–4 mm**	**4–8 mm**	**8–16 mm**	**16–22 mm**	**Total**
9a	−3.8	4.2	12.3	5.0	117.5	−4.5	130.3
9b	−18.8	8.0	12.3	−1.1	−0.9	−2.5	7.7
10a	2.3	8.0	−3.8	−6.8	−24.0	−0.5	−35.0
10b	−7.8	10.0	4.3	1.0	−4.5	−4.5	−3.8
11a	−3.8	4.5	32.3	17.0	−26.3	−13.2	9.7
11b	−11.6	20.0	8.3	23.0	2.4	1.5	35.1
12a	−5.8	4.0	−7.1	29.0	−15.9	−10.0	−3.9
12b	−0.3	6.0	8.3	1.0	−10.5	0.9	−0.3
13a	−1.8	−4.4	8.3	21.0	0.0	−1.7	27.6
13b	4.0	0.0	−7.8	6.6	11.5	−5.7	4.6
14a	2.4	0.0	−26.2	5.2	29.5	−4.5	4.1
14b	−28.7	2.0	46.3	−5.0	6.7	15.5	63.4

Table A-10. Differences between target and actual amounts (%) for the concrete to the base slab.

			Aggregates				
Batch	**Water**	**Cement**	**0–4 mm**	**4–8 mm**	**8–16 mm**	**16–22 mm**	**Total**
1a	−0.3	−0.4	0.7	9.2	0.5	0.3	1.0
1b	−1.7	0.4	0.1	−0.3	0.0	1.0	0.3
2a	0.0	−0.5	0.8	11.7	−0.7	−0.2	0.8
2b	0.8	0.1	−0.4	9.2	0.0	−0.8	0.1
3a	0.0	−0.2	1.3	0.9	0.4	1.2	1.0
3b	−1.1	−0.4	−0.1	2.1	1.2	0.7	0.5
4a	−0.9	0.5	0.6	0.3	−1.7	0.0	−0.1
4b	−2.3	0.2	0.0	1.6	0.2	0.0	0.1
5a	−3.6	0.2	0.9	1.0	1.8	0.1	0.9
5b	−3.1	−0.1	0.2	6.7	0.3	−0.2	0.5
6a	−0.9	0.4	0.5	5.4	6.2	0.2	2.0
6b	−2.8	0.9	0.5	1.0	−0.6	0.6	0.3
7a	0.7	−0.5	0.2	13.0	2.4	−0.5	1.3
7b	−2.6	1.4	−0.3	2.9	−0.4	−0.1	−0.1
8a	−1.0	0.5	1.8	23.6	2.4	0.1	2.7
8b	−6.3	0.2	1.2	1.6	0.1	0.1	0.7
9a	−0.7	0.4	0.4	1.6	8.1	−0.3	2.2
9b	−3.6	0.7	0.4	−0.4	−0.1	−0.2	0.1
10a	0.4	0.7	−0.1	−2.1	−1.7	0.0	−0.6
10b	−1.5	0.9	0.1	0.3	−0.3	−0.3	−0.1
11a	−0.7	0.4	1.1	5.4	−1.8	−1.0	0.2
11b	−2.2	1.8	0.3	7.3	0.2	0.1	0.6
12a	−1.1	0.4	−0.2	9.2	−1.1	−0.7	−0.1
12b	0.0	0.5	0.3	0.3	−0.7	0.1	0.0
13a	−0.3	−0.4	0.3	6.7	0.0	−0.1	0.5
13b	0.8	0.0	−0.3	2.1	0.8	−0.4	0.1
14a	0.5	0.0	−0.9	1.7	2.0	−0.3	0.1
14b	−5.5	0.2	1.6	−1.6	0.5	1.2	1.0
MIN	−6.3	−0.5	−0.9	−2.1	−1.8	−1.0	−0.6
MAX	0.8	1.8	1.8	23.6	8.1	1.2	2.7
AVG	−1.4	0.3	0.4	4.3	0.6	0.0	0.6

A3.3 Data from the truck mixers during production of concrete to the walls of the caisson

Table A-11. General information.

Batch	Truck mixer	Batch ID	Date	Time
1a	2	195	21-11-2018	07:26
1b	1	380	21-11-2018	07:28
2a	1	381	21-11-2018	07:53
2b	2	196	21-11-2018	08:08
3a	1	382	21-11-2018	08:17
3b	2	197	21-11-2018	08:30
4a	1	383	21-11-2018	08:44
4b	2	198	21-11-2018	08:56
5a	1	384	21-11-2018	09:14
5b	2	199	21-11-2018	09:19
6a	1	385	21-11-2018	09:50
6b	2	200	21-11-2018	09:54
7a	2	202	21-11-2018	10:14
7b	1	386	21-11-2018	10:19
8a	2	203	21-11-2018	10:45
8b	1	387	21-11-2018	10:54
9a	1	388	21-11-2018	11:18
9b	2	204	21-11-2018	11:20
10a	1	389	21-11-2018	11:42
10b	2	205	21-11-2018	11:46
11a	1	390	21-11-2018	12:18
11b	2	206	21-11-2018	12:18
12a	1	391	21-11-2018	12:42
12b	2	207	21-11-2018	12:42
13a	1	392	21-11-2018	13:13
13b	2	208	21-11-2018	13:13
14a	1	393	21-11-2018	13:35
14b	2	209	21-11-2018	13:38
15a	1	394	21-11-2018	14:05
15b	2	210	21-11-2018	14:07
16a	1	395	21-11-2018	14:41
16b	2	211	21-11-2018	14:44
17a	1	396	21-11-2018	15:13
17b	2	212	21-11-2018	15:15
18a	1	397	21-11-2018	15:47
18b	2	213	21-11-2018	15:50
19a	1	398	21-11-2018	16:17
19b	2	214	21-11-2018	16:18
20a	1	399	21-11-2018	16:46
20b	2	215	21-11-2018	16:48
21a	1	400	21-11-2018	17:02
21b	2	216	21-11-2018	17:19
22a	1	402	21-11-2018	17:49
22b	2	217	21-11-2018	17:50

Table A-12. Target amounts of concrete components in the different batches for the walls.

				Aggregates (mm)								
Batch	**Water**	**Cem.**	**Fill**	**0–4**	**4–8**	**8–16**	**16–22**	**Total**	**Moist. (%)****	**Moist. (kg)**	**w/c***	**w/c**
1a	505.4	1120	575	2956	315	1453	1341	6064	3	86.1	0.528	0.539
1b	491.05	1120	575	2970	315	1453	1341	6078	3.5	100.5	0.528	0.536
2a	491.05	1120	575	2970	315	1453	1341	6078	3.5	100.5	0.528	0.536
2b	491.05	1120	575	2970	315	1453	1341	6078	3.5	100.5	0.528	0.536
3a	491.05	1120	575	2970	315	1453	1341	6078	3.5	100.5	0.528	0.536
3b	491.05	1120	575	2970	315	1453	1341	6078	3.5	100.5	0.528	0.536
4a	491.05	1120	575	2970	315	1453	1341	6078	3.5	100.5	0.528	0.536
4b	491.05	1120	575	2970	315	1453	1341	6078	3.5	100.5	0.528	0.536
5a	491.05	1120	575	2970	315	1453	1341	6078	3.5	100.5	0.528	0.536
5b	491.05	1120	575	2970	315	1453	1341	6078	3.5	100.5	0.528	0.536
6a	491.05	1120	575	2970	315	1453	1341	6078	3.5	100.5	0.528	0.536
6b	491.05	1120	575	2970	315	1453	1341	6078	3.5	100.5	0.528	0.536
7a	491.05	1120	575	2970	315	1453	1341	6078	3.5	100.5	0.528	0.536
7b	491.05	1120	575	2970	315	1453	1341	6078	3.5	100.5	0.528	0.536
8a	491.05	1120	575	2970	315	1453	1341	6078	3.5	100.5	0.528	0.536
8b	491.05	1120	575	2970	315	1453	1341	6078	3.5	100.5	0.528	0.536
9a	491.05	1120	575	2970	315	1453	1341	6078	3.5	100.5	0.528	0.536
9b	491.05	1120	575	2970	315	1453	1341	6078	3.5	100.5	0.528	0.536
10a	491.05	1120	575	2970	315	1453	1341	6078	3.5	100.5	0.528	0.536
10b	491.05	1120	575	2970	315	1453	1341	6078	3.5	100.5	0.528	0.536
11a	491.05	1120	575	2970	315	1453	1341	6078	3.5	100.5	0.528	0.536
11b	491.05	1120	575	2970	315	1453	1341	6078	3.5	100.5	0.528	0.536
12a	491.05	1120	575	2970	315	1453	1341	6078	3.5	100.5	0.528	0.536
12b	491.05	1120	575	2970	315	1453	1341	6078	3.5	100.5	0.528	0.536
13a	491.05	1120	575	2970	315	1453	1341	6078	3.5	100.5	0.528	0.536
13b	491.05	1120	575	2970	315	1453	1341	6078	3.5	100.5	0.528	0.536
14a	491.05	1120	575	2970	315	1453	1341	6078	3.5	100.5	0.528	0.536
14b	491.05	1120	575	2970	315	1453	1341	6078	3.5	100.5	0.528	0.536
15a	491.05	1120	575	2970	315	1453	1341	6078	3.5	100.5	0.528	0.536
15b	491.05	1120	575	2970	315	1453	1341	6078	3.5	100.5	0.528	0.536
16a	491.05	1120	575	2970	315	1453	1341	6078	3.5	100.5	0.528	0.536
16b	491.05	1120	575	2970	315	1453	1341	6078	3.5	100.5	0.528	0.536
17a	491.05	1120	575	2970	315	1453	1341	6078	3.5	100.5	0.528	0.536
17b	491.05	1120	575	2970	315	1453	1341	6078	3.5	100.5	0.528	0.536
18a	491.05	1120	575	2970	315	1453	1341	6078	3.5	100.5	0.528	0.536
18b	491.05	1120	575	2970	315	1453	1341	6078	3.5	100.5	0.528	0.536
19a	491.05	1120	575	2970	315	1453	1341	6078	3.5	100.5	0.528	0.536
19b	491.05	1120	575	2970	315	1453	1341	6078	3.5	100.5	0.528	0.536
20a	491.05	1120	575	2970	315	1453	1341	6078	3.5	100.5	0.528	0.536
20b	491.05	1120	575	2970	315	1453	1341	6078	3.5	100.5	0.528	0.536
21a	491.05	1120	575	2970	315	1453	1341	6078	3.5	100.5	0.528	0.536
21b	491.05	1120	575	2970	315	1453	1341	6078	3.5	100.5	0.528	0.536
22a	491.05	1120	575	2970	315	1453	1341	6078	3.5	100.5	0.528	0.536
22b	491.05	1120	575	2970	315	1453	1341	6078	3.5	100.5	0.528	0.536

*w/c excluding water of admixtures.
**Moisture content is calculated only for the 0.4 mm aggregate fraction and used to calculate the amount of water to be added.

Table A-13. Actual amounts of concrete components in the different batches to the walls.

				Aggregates (mm)								
Batch	**Water**	**Cem.**	**Fill**	**0–4**	**4–8**	**8–16**	**16–22**	**Total**	**Moist. (%)*****	**Moist. (kg)**	**w/c***	**w/c**
1a	489.5	1109.3	575.0	2970.0	334.0	1422.0	1368.0	6094.0	3.0	86.5	0.519	0.527
1b	479.6	1124.0	552.0	2990.0	304.7	1446.0	1362.0	6102.7	3.5	101.1	0.517	0.525
2a	494.0	1122.0	566.0	2998.0	354.0	1456.0	1352.0	6160.0	3.5	101.4	0.531	0.539
2b	478.1	1118.8	575.0	2953.8	320.0	1464.0	1334.6	6072.4	3.5	99.9	0.516	0.524
3a	498.0	1122.0	584.0	2974.0	314.0	1478.0	1329.2	6095.2	3.5	100.6	0.530	0.538
3b	486.3	1130.0	575.0	2928.0	387.6	1433.5	1372.0	6121.1	3.5	99.0	0.518	0.526
4a	493.7	1128.0	562.0	2978.9	336.0	1482.0	1343.5	6140.5	3.5	100.7	0.521	0.529
4b	498.0	1130.0	575.0	2968.8	319.3	1442.0	1360.0	6090.1	3.5	100.4	0.530	0.538
5a	494.1	1120.0	582.0	2996.0	322.0	1476.0	1346.0	6140.0	3.5	101.3	0.532	0.540
5b	492.0	1136.0	575.0	3020.0	344.0	1430.5	1378.0	6172.5	3.5	102.1	0.523	0.531
6a	493.9	1120.0	548.0	2994.0	348.3	1468.0	1346.0	6156.3	3.5	101.2	0.531	0.539
6b	496.0	1120.0	575.0	2962.0	374.0	1419.6	1338.2	6093.8	3.5	100.2	0.532	0.540
7a	477.7	1138.0	575.0	2996.0	385.8	1470.0	1404.0	6255.8	3.5	101.3	0.508	0.516
7b	496.0	1130.0	546.0	2970.0	374.0	1445.8	1356.0	6145.8	3.5	100.4	0.528	0.536
8a	496.0	1126.0	575.0	2998.0	626.0	1147.5	1311.3	6082.8	3.5	101.4	0.531	0.539
8b	490.0	1126.0	575.0	2979.0	324.0	1450.0	1368.0	6121.0	3.5	100.7	0.525	0.533
9a	492.6	1126.0	536.0	2970.7	332.0	1453.1	1336.0	6091.8	3.5	100.5	0.527	0.535
9b	510.0	1116.4	575.0	2984.0	330.0	1418.5	1342.3	6074.7	3.5	100.9	0.547	0.555
10a	491.8	1125.5	528.0	2978.0	318.0	1446.0	1346.0	6088.0	3.5	100.7	0.526	0.534
10b	496.0	1146.0	575.0	2959.2	348.0	1500.0	1360.0	6167.2	3.5	100.1	0.520	0.528
11a	491.8	1126.0	562.0	2978.0	372.0	1445.4	1340.0	6135.4	3.5	100.7	0.526	0.534
11b	492.0	1128.0	575.0	2960.9	292.8	1449.2	1338.0	6040.9	3.5	100.1	0.525	0.533
12a	489.3	1134.0	546.0	3001.7	322.0	1468.0	1350.0	6141.7	3.5	101.5	0.521	0.529
12b	489.7	1128.0	575.0	2979.0	354.0	1476.0	1380.0	6189.0	3.5	100.7	0.523	0.531
13a	479.9	1150.0	564.0	2966.0	328.0	1444.0	1354.0	6092.0	3.5	100.3	0.505	0.512
13b	494.0	1130.0	575.0	2948.6	346.0	1448.0	1320.7	6063.3	3.5	99.71	0.525	0.533
14a	493.4	1130.0	540.0	2984.0	332.0	1459.0	1344.0	6119.0	3.5	100.9	0.526	0.534
14b	479.0	1114.1	575.0	2992.0	312.0	1468.0	1345.9	6117.9	3.5	101.2	0.521	0.529
15a**				2998.0		1462.0		4460.0				
15b	480.1	1132.0	575.0	2950.0	313.0	1441.3	1343.7	6048.0	3.5	99.76	0.512	0.520
16a	479.6	1120.4	542.0	2969.1	348.8	1484.0	1338.0	6139.9	3.5	100.4	0.518	0.526
16b	483.3	1130.0	575.0	2960.9	318.0	1436.8	1340.1	6055.8	3.5	100.1	0.516	0.524
17a	483.0	1122.0	532.0	2972.0	338.0	1467.3	1352.0	6129.3	3.5	100.5	0.520	0.528
17b	494.0	1144.0	575.0	2952.0	340.0	1460.0	1336.4	6088.4	3.5	99.83	0.519	0.527
18a	469.9	1126.0	526.0	3012.0	344.0	1436.0	1376.0	6168.0	3.5	101.9	0.508	0.516
18b	488.0	1130.0	575.0	2970.0	330.0	1449.8	1336.0	6085.8	3.5	100.4	0.521	0.529
19a	492.0	1138.0	524.0	2992.0	330.0	1478.0	1346.0	6146.0	3.5	101.2	0.521	0.529
19b	483.2	1128.0	575.0	2931.1	378.0	1458.0	1343.7	6110.8	3.5	99.12	0.516	0.524
20a	498.0	1118.0	546.0	2980.0	318.0	1504.0	1340.0	6142.0	3.5	100.8	0.536	0.544
20b	500.0	1130.0	575.0	2976.0	375.0	1424.0	1347.6	6122.7	3.5	100.6	0.532	0.540
21a	488.6	1129.0	575.0	3000.0	330.0	1436.4	1384.0	6150.4	3.5	101.4	0.523	0.531
21b	500.0	1132.0	575.0	3012.3	314.6	1443.8	1352.0	6122.6	3.5	101.9	0.532	0.540
22a	494.0	1150.0	556.0	2952.0	322.0	1458.0	1345.1	6077.1	3.5	99.83	0.516	0.524
22b	504.0	1138.0	575.0	2958.0	323.5	1456.0	1372.0	6109.5	3.5	100	0.531	0.539

* w:c ratio excluding water of admixtures.
**Most of the data is missing for mix 15a.
*** Moisture is calculated only for the 0–4 mm aggregate fraction.

Table A-14. Differences between target and actual amounts (kg) for concrete to the walls.

			Aggregates				
Batch	**Water**	**Cement**	**0–4 mm**	**4–8 mm**	**8–16 mm**	**16–22 mm**	**Total**
1a	−15.9	−10.7	13.9	19.0	−30.5	27.5	29.9
1b	−11.4	4.0	19.6	−10.3	−6.5	21.5	24.3
2a	2.9	2.0	27.6	39.0	3.5	11.5	81.6
2b	−13.0	−1.2	−16.7	5.0	11.5	−5.9	−6.0
3a	6.9	2.0	3.6	−1.0	25.5	−11.3	16.8
3b	−4.8	10.0	−42.4	72.6	−19.0	31.5	42.7
4a	2.7	8.0	8.5	21.0	29.5	3.0	62.0
4b	6.9	10.0	−1.6	4.3	−10.5	19.5	11.6
5a	3.1	0.0	25.6	7.0	23.5	5.5	61.6
5b	0.9	16.0	49.6	29.0	−22.0	37.5	94.0
6a	2.9	0.0	23.6	33.3	15.5	5.5	77.8
6b	4.9	0.0	−8.4	59.0	−32.9	−2.3	15.3
7a	−13.3	18.0	25.6	70.8	17.5	63.5	177.4
7b	4.9	10.0	−0.4	59.0	−6.7	15.5	67.4
8a	4.9	6.0	27.6	311.0	−305.0	−29.2	4.3
8b	−1.1	6.0	8.6	9.0	−2.5	27.5	42.6
9a	1.6	6.0	0.3	17.0	0.6	−4.5	13.4
9b	19.0	−3.6	13.6	15.0	−34.0	1.8	−3.7
10a	0.7	5.5	7.6	3.0	−6.5	5.5	9.6
10b	4.9	26.0	−11.3	33.0	47.5	19.5	88.7
11a	0.7	6.0	7.6	57.0	−7.1	−0.5	56.9
11b	0.9	8.0	−9.6	−22.2	−3.3	−2.5	−37.5
12a	−1.7	14.0	31.3	7.0	15.5	9.5	63.3
12b	−1.4	8.0	8.6	39.0	23.5	39.5	110.6
13a	−11.2	30.0	−4.4	13.0	−8.5	13.5	13.6
13b	2.9	10.0	−21.9	31.0	−4.5	−19.8	−15.1
14a	2.3	10.0	13.6	17.0	6.5	3.5	40.5
14b	−12.0	−5.9	21.6	−3.0	15.5	5.4	39.5
15a*			27.6		9.5		
15b	−10.9	12.0	−20.4	−2.0	−11.2	3.2	−30.4
16a	−11.5	0.4	−1.4	33.8	31.5	−2.5	61.4
16b	−7.7	10.0	−9.6	3.0	−15.7	−0.4	−22.7
17a	−8.1	2.0	1.6	23.0	14.8	11.5	50.9
17b	2.9	24.0	−18.4	25.0	7.5	−4.1	9.9
18a	−21.2	6.0	41.6	29.0	−16.5	35.5	89.6
18b	−3.1	10.0	−0.4	15.0	−2.7	−4.5	7.4
19a	0.9	18.0	21.6	15.0	25.5	5.5	67.6
19b	−7.9	8.0	−39.3	63.0	5.5	3.2	32.4
20a	6.9	−2.0	9.6	3.0	51.5	−0.5	63.6
20b	8.9	10.0	5.6	60.0	−28.5	7.1	44.2
21a	−2.5	9.0	29.6	15.0	−16.1	43.5	72.0
21b	8.9	12.0	41.8	−0.4	−8.7	11.5	44.2
22a	2.9	30.0	−18.4	7.0	5.5	4.6	−1.4
22b	13.0	18.0	−12.4	8.5	3.5	31.5	31.1

*Most of the data is missing for mix 15a.

Table A-15. Differences between target and actual amounts (%) for concrete to the walls.

			Aggregates				
Batch	**Water**	**Cement**	**0–4 mm**	**4–8 mm**	**8–16 mm**	**16–22 mm**	**Total**
1a	−3.1	−1.0	0.5	6.0	−2.1	2.1	0.5
1b	−2.3	0.4	0.7	−3.3	−0.4	1.6	0.4
2a	0.6	0.2	0.9	12.4	0.2	0.9	1.3
2b	−2.6	−0.1	−0.6	1.6	0.8	−0.4	−0.1
3a	1.4	0.2	0.1	−0.3	1.8	−0.8	0.3
3b	−1.0	0.9	−1.4	23.0	−1.3	2.3	0.7
4a	0.5	0.7	0.3	6.7	2.0	0.2	1.0
4b	1.4	0.9	−0.1	1.4	−0.7	1.5	0.2
5a	0.6	0.0	0.9	2.2	1.6	0.4	1.0
5b	0.2	1.4	1.7	9.2	−1.5	2.8	1.5
6a	0.6	0.0	0.8	10.6	1.1	0.4	1.3
6b	1.0	0.0	−0.3	18.7	−2.3	−0.2	0.3
7a	−2.7	1.6	0.9	22.5	1.2	4.7	2.9
7b	1.0	0.9	0.0	18.7	−0.5	1.2	1.1
8a	1.0	0.5	0.9	98.7	−21.0	−2.2	0.1
8b	−0.2	0.5	0.3	2.9	−0.2	2.1	0.7
9a	0.3	0.5	0.0	5.4	0.0	−0.3	0.2
9b	3.9	−0.3	0.5	4.8	−2.3	0.1	−0.1
10a	0.1	0.5	0.3	1.0	−0.4	0.4	0.2
10b	1.0	2.3	−0.4	10.5	3.3	1.5	1.5
11a	0.1	0.5	0.3	18.1	−0.5	0.0	0.9
11b	0.2	0.7	−0.3	−7.0	−0.2	−0.2	−0.6
12a	−0.4	1.3	1.1	2.2	1.1	0.7	1.0
12b	−0.3	0.7	0.3	12.4	1.6	2.9	1.8
13a	−2.3	2.7	−0.1	4.1	−0.6	1.0	0.2
13b	0.6	0.9	−0.7	9.8	−0.3	−1.5	−0.2
14a	0.5	0.9	0.5	5.4	0.4	0.3	0.7
14b	−2.4	−0.5	0.7	−1.0	1.1	0.4	0.6
15a*			0.9		0.7		
15b	−2.2	1.1	−0.7	−0.6	−0.8	0.2	−0.5
16a	−2.3	0.0	0.0	10.7	2.2	−0.2	1.0
16b	−1.6	0.9	−0.3	1.0	−1.1	0.0	−0.4
17a	−1.6	0.2	0.1	7.3	1.0	0.9	0.8
17b	0.6	2.1	−0.6	7.9	0.5	−0.3	0.2
18a	−4.3	0.5	1.4	9.2	−1.1	2.6	1.5
18b	−0.6	0.9	0.0	4.8	−0.2	−0.3	0.1
19a	0.2	1.6	0.7	4.8	1.8	0.4	1.1
19b	−1.6	0.7	−1.3	20.0	0.4	0.2	0.5
20a	1.4	−0.2	0.3	1.0	3.5	0.0	1.0
20b	1.8	0.9	0.2	19.1	−2.0	0.5	0.7
21a	−0.5	0.8	1.0	4.8	−1.1	3.2	1.2
21b	1.8	1.1	1.4	−0.1	−0.6	0.9	0.7
22a	0.6	2.7	−0.6	2.2	0.4	0.3	0.0
22b	2.6	1.6	−0.4	2.7	0.2	2.3	0.5
MIN	−4.3	−1.0	−1.4	−7.0	−21.0	−2.2	−0.6
MAX	3.9	2.7	1.7	98.7	3.5	4.7	2.9
AVG	−0.2	0.8	0.2	9.1	−0.3	0.8	0.7

*Most of the data is missing for mix 15a.

Appendix B

Coefficient of thermal expansion

B1 Mature concrete

The linear coefficient of thermal expansion (CTE) was determined for well matured concrete (age approx. 1 year), using a not standardized test method. There is no standardized test method for concrete available at present time. Shrinkage beams with dimensions of $100 \times 100 \times 400$ mm were used. These beams were produced while casting the slab and the walls. After completion of the shrinkage test, the length of the beams was determined at 20 °C. The beams were heated up to 80 °C and the length was measured again. After cooling to 20 °C, the length was determined a third time. The weight was determined before and after the heating process. The results are summarised in Table B-1.

Table B-1. Coefficient of thermal expansion.

Sample	Length change at 80 C (mm/m)	Length change after cooling to 20 °C (mm/m)	Weight change after cooling to 20 °C (%)	Calculated α_t (1/K)
Slab-1	0.436	0.00	−1.26	
Slab-2	0.428	−0.03	−1.32	
Slab-3	0.418	−0.01	−1.35	
Average	**0.428**		**−1.31**	**7.13×10^{-6}**
Walls-1	0.370	0.00	−1.26	
Walls-2	0.271*	−0.01	−1.24	
Walls-3	0.395	0.01	−1.28	
Average	**0.383**		**−1.26**	**6.38×10^{-6}**
Total average				**6.75×10^{-6}**

*Result unreasonably low, not considered in calculation of average and α_t.

The linear coefficient of thermal expansion was determined to be 6.75×10^{-6} 1/K. According to the literature (Neville 1995, Ljungkrantz et al. 1994), air cured concrete with granitic aggregate should have a CTE of around $8.5–9.5 \times 10^{-6}$ 1/K. Observe that the tested samples were stored for approximately one year at 50 % RH. One may assume that the samples have an internal RH of approx. 50 %. In Neville (1995) the CTE for concrete with RH of 50 % is given with around 8×10^{-6} 1/K. The determined values are somewhat lower than the values stated in the literature but not unreasonably low. Observe that in engineering practice, a value of 10×10^{-6} 1/K is usually assumed for the CTE.

B2 Young concrete

In young (hardening) concrete, the CTE is $9.5–11 \times 10^{-6}$ 1/K during the heating phase according to Ljungkrantz et al. (1994). During subsequent cooling, the CTE is given with $7.0–9.0 \times 10^{-6}$ 1/K. The exact values depend strongly on the composition of the concrete. The determination in experiments is difficult and there is no standard available describing a procedure. According to Ljungkrantz et al. (1994), the difference of thermal expansion and contraction is only occurring during the hardening of the concrete (hydration). In mature concrete, this difference has not been found.

Appendix C

Heat calculations and thermal crack risk calculations

The caissons in 2BMA shall be made of unreinforced concrete with the requirement of a maximum crack width or joint is 0.1 mm. In order to reduce the extent of thermal cracking in a structure where reinforcement cannot be used, two possibilities can be identified. The primary option is to cast the base slab and the walls in one uninterrupted sequence. This limits the risk for thermal cracks during hardening as there will be no joints in the structure, but imposes very strict requirements on the formwork.

The second option is to cast the base slab first and the walls later. This simplifies construction but increases the risk for crack formation caused by restraint between the different parts of the structure. The mature slab will prevent the movements of the walls during hardening of the concrete with an increased risk for crack formation as a consequence. In order to reduce the risk for crack formation, the base slab will need to be pre-heated prior to casting of the walls. Pre-heating causes the base slab to expand and through simultaneous cooling down of walls and base slab the risk for thermal cracks is reduced.

The required heating effect and heating time needs to be calculated prior to casting the walls in order to meet the requirements on the risk of cracking.

C1 Background thermal cracking

Tensile stresses and resulting cracks in a concrete structure may develop from loading or from restrained load-independent deformations such as those emanating from the heat of hydration of the concrete during hardening (see Figure C-1). The thermal shrinkage of the newly cast element may be restrained by inner restraint (risk of surface cracks) or adjacent structures (external restraint, risk of through-cracks). Autogenous deformations (self-desiccation and chemical shrinkage) of the hardening concrete add to the thermal shrinkage when cooling takes place after the hydration process.

The cracking which may result from this type of deformation is of special importance for massive structures (generally defined as a structure with a thickness of more than 800 mm). This is a result of the more pronounced temperature rise inside the structure during hardening and also the comparably lower amount of reinforcement in massive structures. Early age cracking due to heat of hydration and early autogenous deformations will be denoted temperature cracking in the following as a simplification. It is not to be confused with stresses and cracks resulting from external temperature loads such as seasonal temperature variations.

The basic mechanism of temperature cracking is explained in the section below (Hedlund 2000, Hösthagen 2017).

Figure C-1. *Early age cracks in retaining walls, left picture: Anders Hösthagen, BOSTEK, right picture: Jonatan Paulsson-Tralla, BOSTEK.*

During hardening (hydration) of concrete, heat is generated due to the exothermal cement hydration processes. Usually, the temperature varies within the cross section; it is lower in the surface layers than in the centre. This temperature difference leads to a differential movement, i.e. the inner parts expand more than the outer parts in the so-called expansion phase of the hydration. If the temperature difference between inner and outer parts is large, the developing stresses may exceed the tensile strength of the young concrete and surface cracks may form. This principle is illustrated in Figure C-2.

The tensile stresses in the surface of the cross section will later turn to compression, thus reducing the crack width. However, due to a certain interlocking effect of the cracked surfaces, a complete crack closure will not be achieved. Later developing through-cracks are related to the average volume decrease due to both temperature drop and the relatively homogenous basic shrinkage during the critical contraction phase, as illustrated in Figure C-2. Typically, through-cracks are generated over the entire cross section as a result of the restraint from the adjacent existing structural concrete or subgrade.

Depending on dimensions and other prevailing conditions, the cracks may appear weeks, months and in extreme cases even years after a section has been casted. The critical time period for later through cracks starts from the point of "zero stress" shortly after the temperature maximum (see Figure C-2) and continues until cracking occurs or until the ratio between the maximum tensile stresses to tensile strength has been reached. Cracks formed in the cooling phase tend to remain open permanently. Prevailing drying shrinkage will increase the crack width with time. Therefore, through-cracks are often considered as being more critical than surface cracks, concerning appearance and durability.

The consequences of these restrained early movements lead to cracks more often than expected. Even relatively thin cross sections generate enough heat to cause early age cracking, as stated in Bamforth (2007): "As a rule of thumb, any concrete element cast against an adjacent element of the same thickness or greater, and which achieves a temperature rise in excess of about 20 °C, has a significant risk of early thermal cracking if the length of the joint exceeds about 5 m. A 20 °C rise would typically be achieved in a 300 mm thick wall cast in plywood formwork using C30/37 concrete with CEM I."

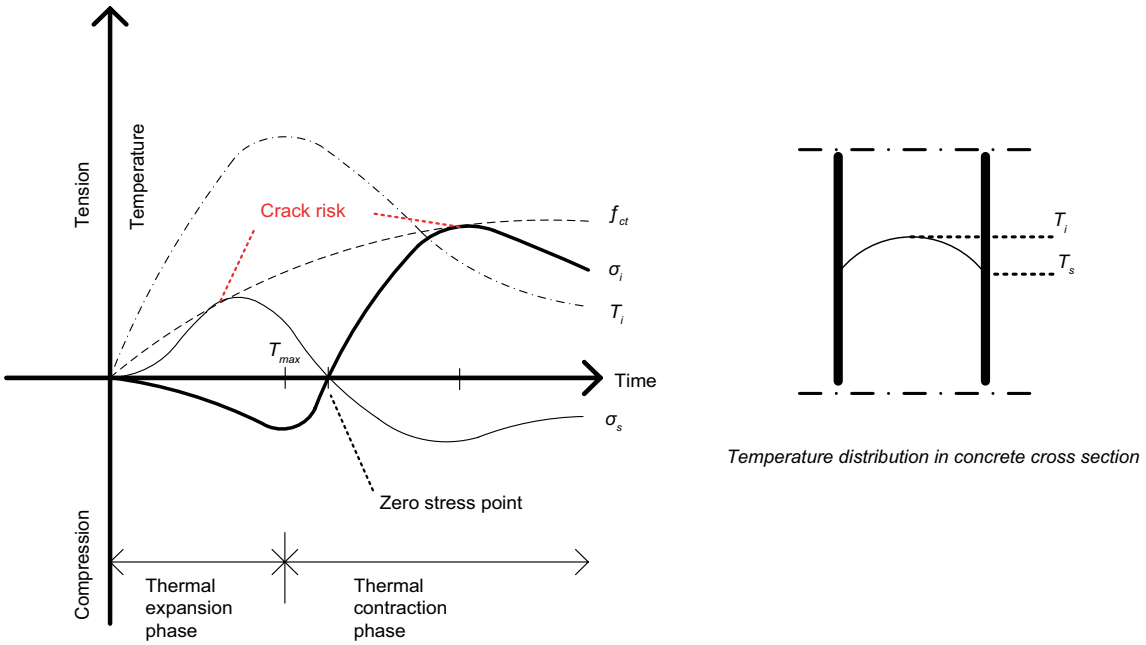

Figure C-2. *Schematic demonstration of the stress development at the surface and the interior of a concrete construction, and the development of surface tensile strength. Stress development showed is representative for a freely cast construction or an undisturbed (i.e. no cooling or heating) part of a construction. T_s and T_i is the surface and interior temperature, s_s and s_i is the surface and interior stress and f_{ct} is the surface tensile strength (Hösthagen 2017).*

Common measures to control the heat development and thus temperature cracking are adjustment of the concrete mix design, use of special cements, and replacement of cement or active measures such as cooling of newly cast structures with cast in cooling pipes. The margins of the stresses developing depend not only on the heat development but also on the degree of restraint. The dimensions, especially the length, of the newly cast structural member, but also the dimensions of the restraining structures are of importance.

Temperature cracks in concrete structures may also be limited by means of reinforcement. However, reinforcement may only help to control the crack width for the actual exposure acceptable crack widths, never avoid cracking in general. For massive structures, this results in technically and economically unrealistic amounts of reinforcement; especially for small crack widths (Leonhardt 1988, Eckfeldt 2005).

The topic of temperature cracks was first described in literature in the 1920s when the construction of several massive concrete dams was initiated in the USA. During the construction of the Hoover dam in the 1930s, the importance of the heat of hydration of young concrete was noted and the Hoover dam was constructed using cast-in cooling pipes (Arizona Leisure 2018).

Early calculations and design of measures to control the risk of temperature cracks were based on tabularized values of heat- and strength development or simple temperature restrictions. The first attempt to use the strain development in concrete to characterize the crack risk was done by Löfquist (1946). Later, the importance of the restraint was realized, and first attempts were made to calculate the stresses resulting from restrained thermal movements and to compare those with the developing tensile strength of the hardening concrete (Springenschmid 1998). In recent time, the use of 2D and 3D finite element analysis (FEA) has become increasingly common to evaluate the risk of early age cracking.

C2 Parametrisation of test results

C2.1 Theoretical background and formulas

In order to be able to perform numerical calculations of early age cracking in FEA, the mechanical properties of the concrete material need to be transformed into material parameters as input. The parametrization required for software ConTest Pro is described in e.g. Jonasson et al. (2001). For a complete setup of material parameters, a number of tests have to be performed in order to determine material properties to be used in temperature and stress calculations. The following properties have to be evaluated based on tested data:

- Maturity functions,
- heat of hydration,
- strength growth at variable temperature,
- Young´s modulus and early age creep,
- free deformation at variable temperature, and
- stress growth at totally restraint conditions.

The following section is extracted from Jonasson et al. (2001) Hösthagen (2017) and Vogt et al. (2009) and corresponding references therein. In this report only the most essential formulas are given.

Maturity function

$$t_e = \beta_\Delta \int_t \beta_T \cdot dt + t_{e,0} \qquad \text{(C-1)}$$

where β_Δ = adjustment factor to be used for different admixtures [-], here = 1, β_T = temperature sensitivity factor [-], see further Equation (1-2), t = clock time [h], and $t_{e,0}$ = starting time of t_e (at $t = 0$) to be used for different admixtures [-], here = 0.

β_T is often called the maturity function, which can be expressed by:

$$\beta_T = \begin{cases} \exp\left[\theta \cdot \left(\frac{1}{293} - \frac{1}{T+273}\right)\right] & \text{for T} > -10\ ^\circ C \\ 0 & \text{for T} \le -10\ ^\circ C \end{cases} \quad \text{(C-2)}$$

where θ = "activation temperature" [K] = (formally:) activation energy divided by general gas constant, which here is expressed by:

$$\theta = \theta_{ref} \cdot \left(\frac{30}{T+10}\right)^{\kappa_3} \quad \text{(C-3)}$$

where θ_{ref} [K] and κ_3 are fitting parameters according to best fit with test data.

Heat of hydration

$$W_B = \frac{W_{tot}}{B} = W_U \cdot \exp\left[-\lambda_1 \cdot \left(\ln(1+\frac{t_e}{t_1})\right)^{\kappa_1}\right] \quad \text{(C-4)}$$

where W_B = generated heat by weight of binder as a function of equivalent time [J/kg], B = binder content, here the sum of cement and fly ash content [kg/m^3], W_{tot} = generated heat at testing [J], W_U = ultimate generated heat by weight of binder [J/kg], and l_1 [-], t_1 [h] and k_1 [-] are fitting parameters.

Strength growth

The growth of the compressive strength for a series of equivalent points of time can be expressed by:

$$f_{cc}\left(t_e(i)\right) = \frac{\eta_i}{1000} \cdot f_{cc,28d} \quad \text{(C-5)}$$

The compressive strength is given for the following points of time:

$t_e(i)$ = [4, 6, 8, 12, 18, 24, 72, 168, 672 h]$^{-1}$

Thus, the strength development starts formally at t_e = 4 h and is always related to t_e = 28 d, which results in

$\eta_1 = 0$
$\eta_9 = 1000$

Young's modulus and early age creep

The Young's modulus at loading age t_0, $E(t_0)$, can be expressed by:

$$E\left(t_0\right) = \frac{1}{J(\Delta t_0, t_0)} = \frac{1}{J(0.001, t_0)} \quad \text{(C-6)}$$

where $J(0.001,t_0)$ is the measured deformation 0.001d (≈ 1.5 minutes) after loading [1/Pa], and t_0 = equivalent age at loading [d].

The total deformation, $J(\Delta t_{load},t_0)$, can now be expressed by:

$$J(\Delta t_{load}, t_0) = \frac{1}{E_0(t_0)} + \Delta J(\Delta t_{load}, t_0) \quad \text{(C-7)}$$

where $\Delta l_{load} = t - t_0$ = load duration, [d], $\Delta J(\Delta t_{load},t_0)$ = "creep" part of the total deformation [1/Pa].

The Young's modulus is expressed by:

$$E_c(t_0) = \left[\exp\left\{ s_E \cdot \left(1 - \sqrt{\frac{28 - t_{SE}}{t_0 - t_{SE}}} \right) \right\} \right]^{0.5} \cdot E_{28d} \tag{C-8}$$

where t_0 = equivalent age at loading [d], t_{SE} = equivalent time, where deformations start to create stresses [d], E_{28} = Young's modulus at equivalent time = 28d [GPa], and s_E = shape parameter for the growth of the Young's modulus [-].

With two straight lines in the logarithmic time scale the creep portion can be formulated as:

$$\Delta J(\Delta t_{load}, t_0) = \begin{cases} a_1 \cdot \log\left(\dfrac{\Delta t_{load}}{\Delta t_0} \right) & \text{for } \Delta t_0 \le \Delta t_{load} < \Delta t_1 \\ a_1 \cdot \log\left(\dfrac{\Delta t_1}{\Delta t_0} \right) + a_2 \cdot \log\left(\dfrac{\Delta t_{load}}{\Delta t_1} \right) & \text{for } \Delta t_{load} \ge \Delta t_1 \end{cases} \tag{C-9}$$

where Δt_1 = time duration for the distinct break point in the creep behaviour [d], a_1 and a_2 are inclinations, dependent on the loading ages, in the linear-logarithmic plot of the creep behaviour [10^{-12}/(Pa log-unit)].

Free deformation at variable temperature

The model for free deformation at variable temperature is expressed by:

$$\varepsilon_{\text{tot}} = \varepsilon_T^o + \varepsilon_{SH}^o \tag{C-10}$$

$$\varepsilon_T^o = \Delta T \cdot \alpha_{\text{T}} \tag{C-11}$$

$$\varepsilon_{SH}^o = \begin{cases} 0 & \text{for } t_e \le t_{s1} \\ \dfrac{t_e - t_{s1}}{t_{s2} - t_{s1}} \cdot \varepsilon_{s1} & \text{for } t_{s1} < t_e \le t_{s2} \\ \varepsilon_{s1} + \exp\left[-\left(\dfrac{t_{SH}}{t_e - t_{s2}} \right)^{\eta_{SH}} \right] \cdot \varepsilon_{s2} & \text{for } t_e > t_{s2} \end{cases} \tag{C-12}$$

where ε_{tot} = the measured strain [-], ε_T^o = the stress free strain related to changes in temperature [-], ε_{SH}^o = the stress free strain not related to changes in temperature [-], ΔT = change in temperature [ºC], α_T = thermal dilation coefficient [1/°C], t_{s1} [h], t_{s2} [h], ε_{s1} [-] ε_{s2} [-], t_{SH} [h] and η_{SH} [-] are fitting parameters.

Stress growth at full restrained conditions

The tensile strength is related to the compressive strength according to:

$$f_{ct} = (f_{cc} / f_{cc}^{ref})^{\beta_1} \cdot f_{ct}^{ref} \tag{C-13}$$

where f_{ct} = tensile strength [MPa], f_{cc}^{ref} = reference compressive strength [MPa], f_{ct}^{ref} = reference tensile strength [MPa}, and β_1 = exponent [-].

The stress-strain curve used in the calculation is illustrated in Figure C-3 and α_{ct} denotes the upper limit of the linear stress-strain at 1st loading. Remaining denotations in Figure C-3 are: σ = (uniaxial) stress in the concrete [MPa], ε_m = strain related to stresses in concrete (= "material" strain) [-], ε_0 is the strain related to a linear behaviour all the way up to $\sigma = f_{ct}$.

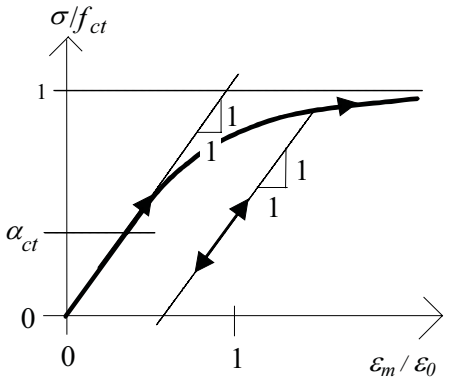

Figure C-3. *Non-linear stress-strain curve for the concrete in tension.*

C3 Material parameters

C3.1 Basis for material parameters

For the present investigation, the material parameters of the actual concrete were not determined from laboratory investigations. This was due to logistical and economic reasons in the present step of the material development. Moreover, any required change in concrete composition due to observations from the test casting would result in time consuming and expensive re-testing. Instead, the material parameters of a comparable concrete were chosen as basis (self-compacting concrete with limestone filler, Anläggningscement Degerhamn and w/c = 0.47). These material parameters were modified when evaluating the test casting in TAS05 (Mårtensson and Vogt 2019), see the following section. The modified parameters are used for all re-calculations in this report. Observe that there might be a slight deviation since the w/c was somewhat increased for the concrete used in TAS08.

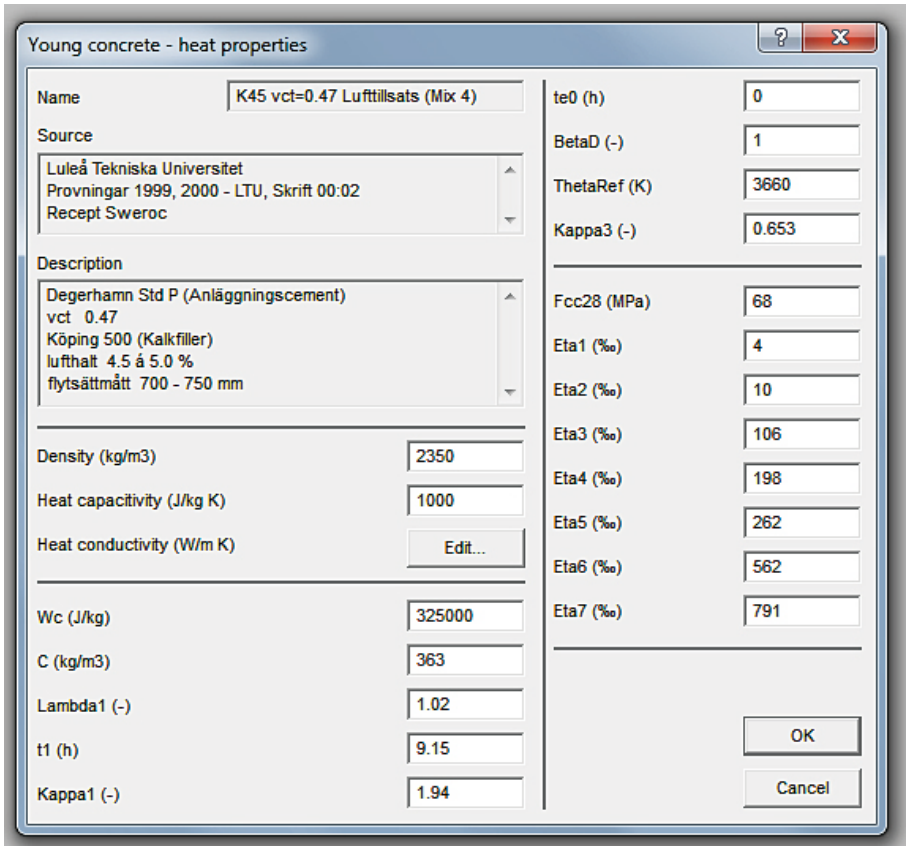

Figure C-4. *Original heat parameters for SCC with w/c of 0.47. For denotation, see previous section.*

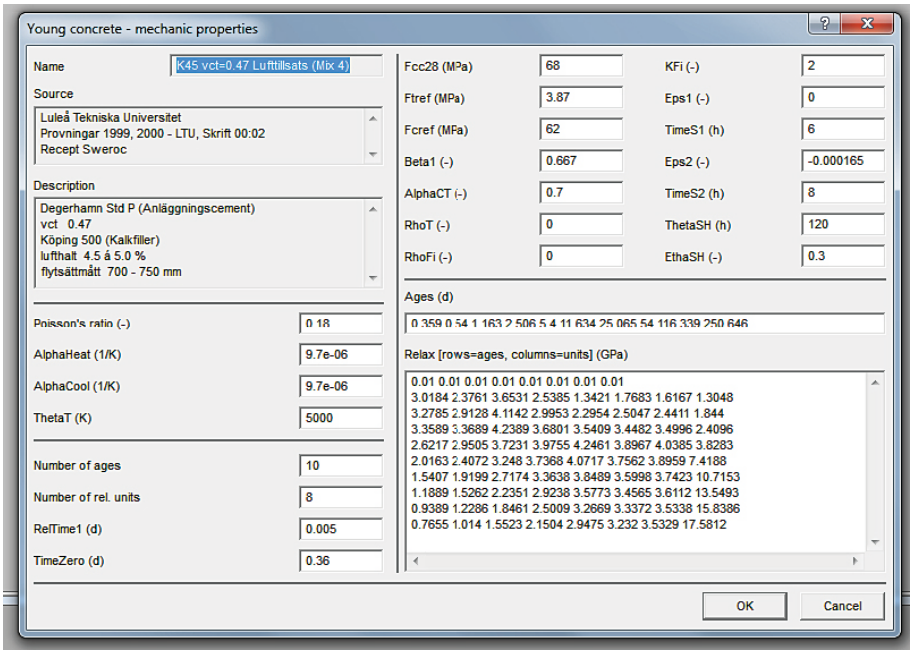

Figure C-5. *Original stress parameters for SCC with w/c of 0.47. For denotation, see previous section.*

C3.2 Heat parameters from TAS05 casting

The heat development of the concrete from the test in TAS05 could be simulated with the parameters in Figure C-6 with satisfying results, see also Mårtensson and Vogt (2019). These parameters were used for the re-calculation of the castings in TAS08.

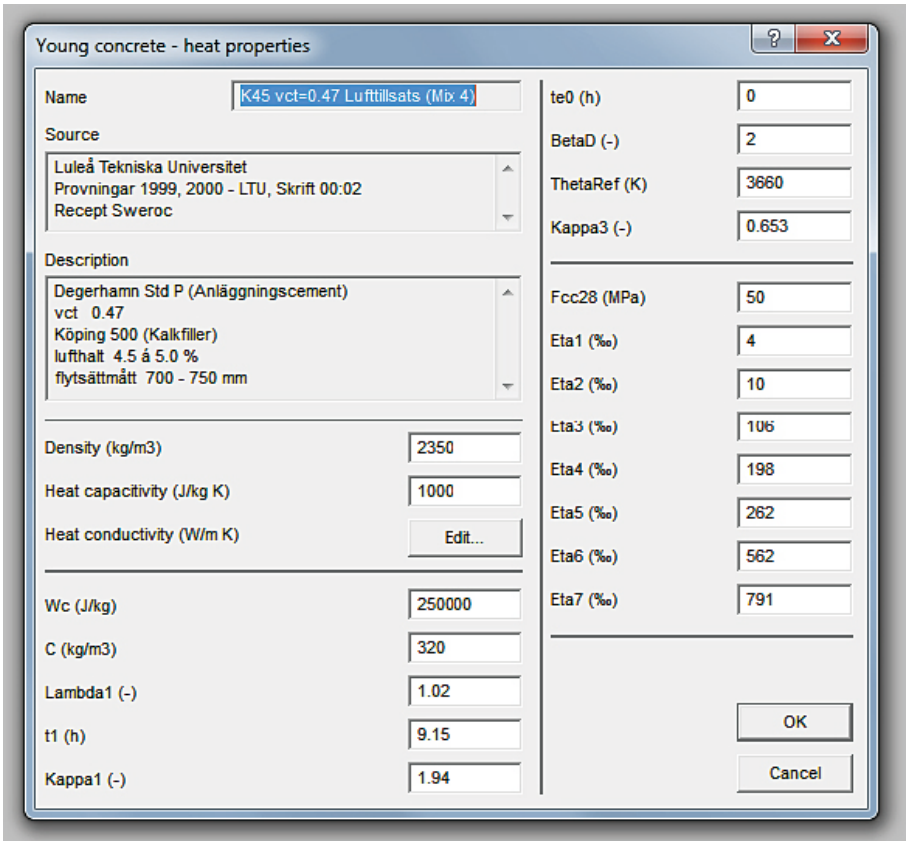

Figure C-6. *Deduced heat parameters for the young concrete.*

C3.3 Final stress parameters

The parameters for stress development in the concrete, deduced from the test in TAS05 are displayed in Figure C-7; see also Mårtensson and Vogt (2019). These parameters were used for the re-calculation of the castings in TAS08.

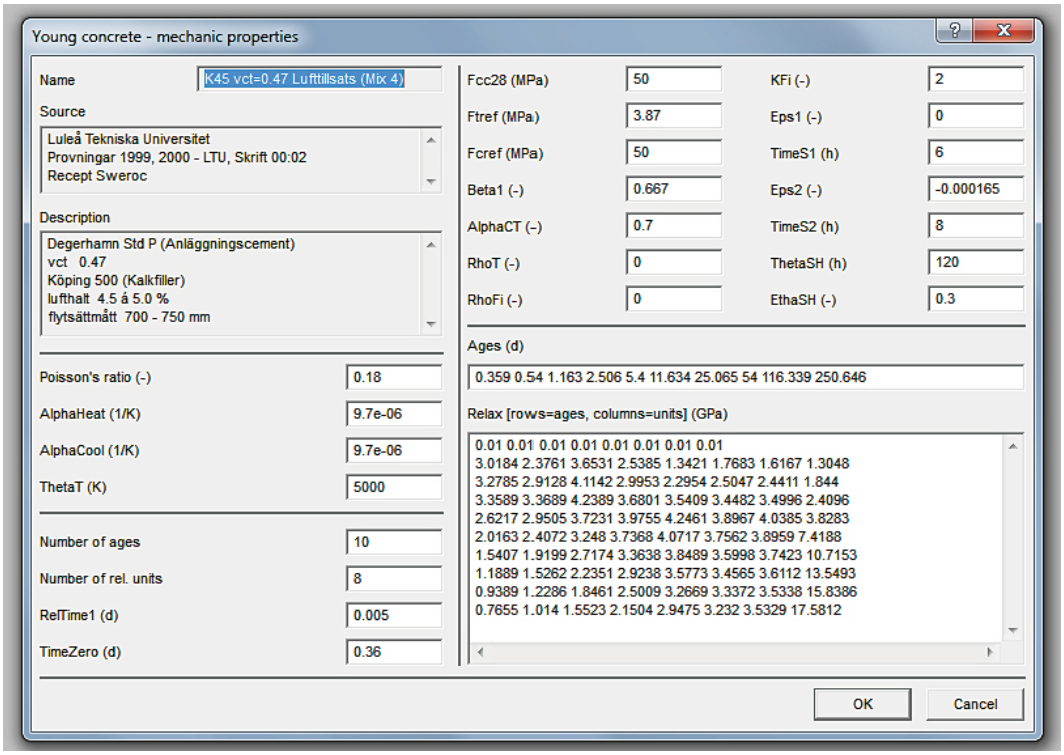

Figure C-7. *Deduced stress parameters.*

C4 Input data and chosen measurements

C4.1 Geometry and boundary conditions

The exact dimensions of the test casting were modelled and meshed in Software ConTest Pro. More details can be found in Appendix D. Figures C-8 and C-9 display the FE-mesh for the slab and walls respectively.

The boundary conditions in the simulation are summarised in Table C-1. The thermal properties of the fresh concrete are displayed in Figure C-6.

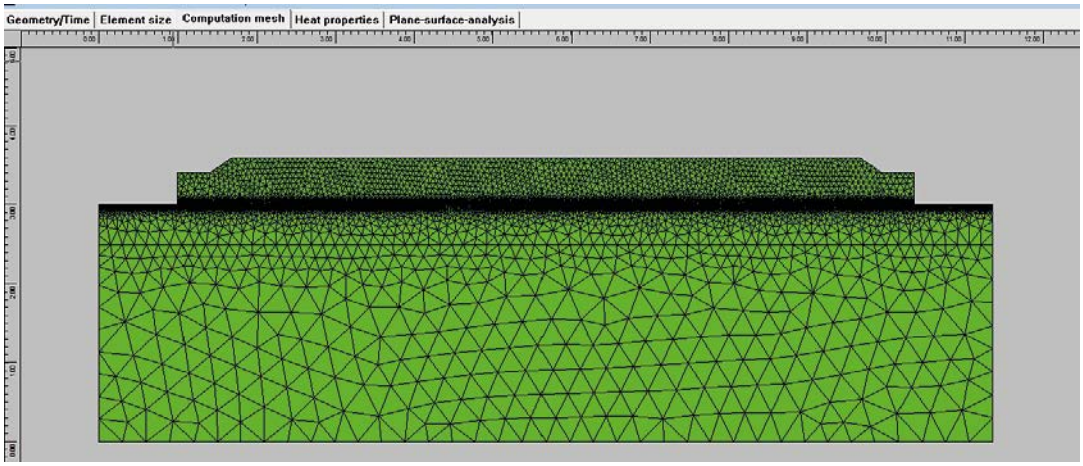

Figure C-8. *FE-mesh in the models for the slab.*

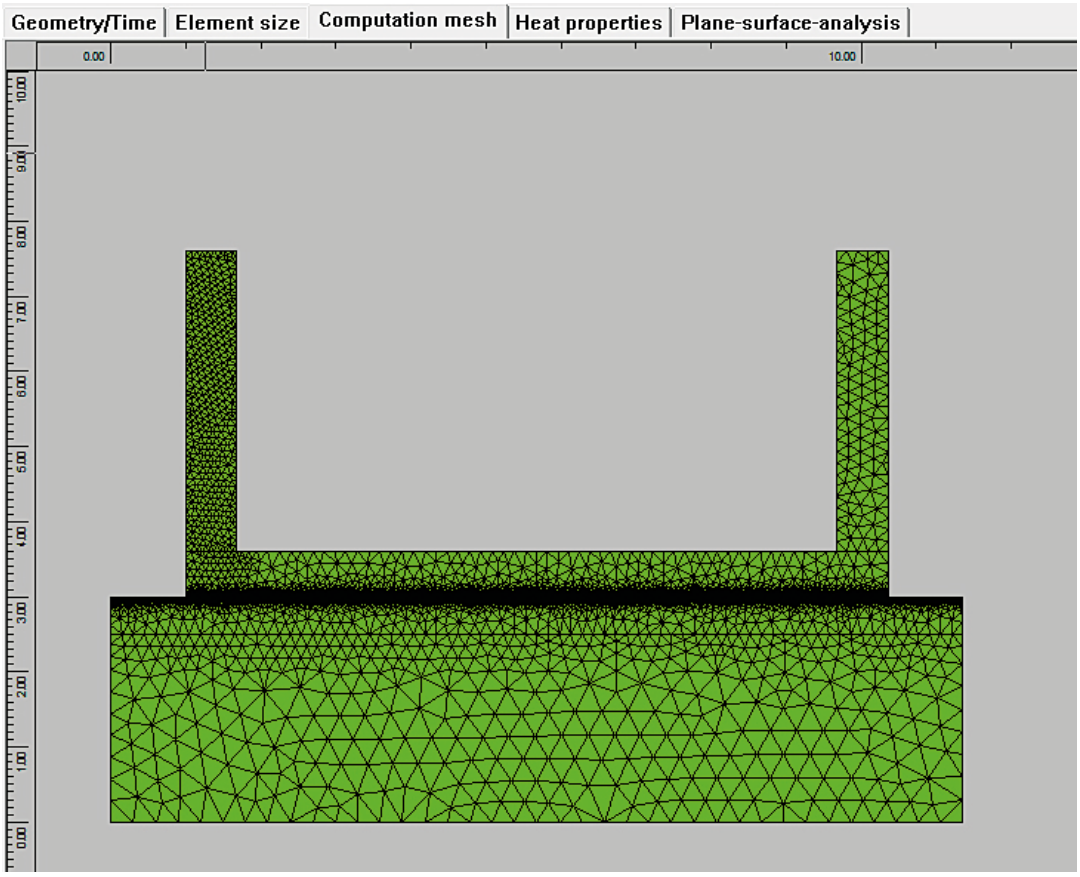

Figure C-9. *FE-mesh in the models for the walls.*

Table C-1. Boundary conditions for the analysis.

Boundary/material	Thickness (mm)	Wind speed (m/s)	Conductivity/HTC (W/m K)/(W/m^2 K)	Density (kg/m^3)	Heat capacitivity (J/kg K)
Free surface / plastic foil	-	1	7.24		
Plywood 21 mm (sides of the slab and wall)	21	1	3.93		
Plywood 12 mm (box-out for the walls)	18	1	5.25		
Rock	-	-	3.7	2650	850
Gravel	-	-	2.1	2200	1400
Mature concrete	-	-	1.7	2350	1000
Foil, double layer	-	-	0.1	250	1500

C5 Casting of the slab

Temperature

The temperature measurement results from the thermocouple setup were used for comparison; see Table C-2, Figure C-10 and Figure C-11. The recorded temperature differs between the different measuring positions (see Chapter 10) and therefore the average for each measuring position is chosen for evaluation. The difference can be explained with different starting temperatures in the fresh concrete and different casting speed for different sections of the slab. A certain temperature increase for the boundaries after casting until 72 hours after casting is assumed due to heat from hydration of the cement and machinery (as observed for the test casting in TAS05 as well).

Table C-2. Temperatures used in the analysis. Linear interpolation is done automatically in the used software. Calculation time 1 000 h.

Boundary	Time (h)	Temperature (°C)
Air, formwork	0	18
	24	20
	48	20
	72–1 000	16
Rock, gravel, mature slab	0–1 000	16
Fresh concrete	0	19

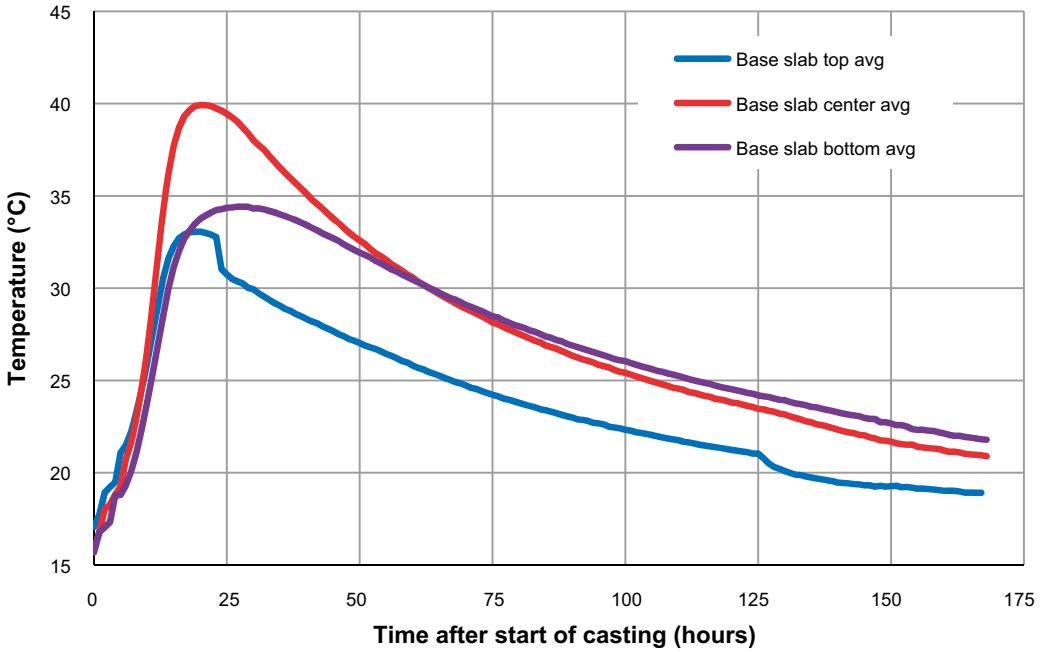

Figure C-10. *Temperature evolution in the slab until 168 hours after casting started. Average of sensors #1 to #6.*

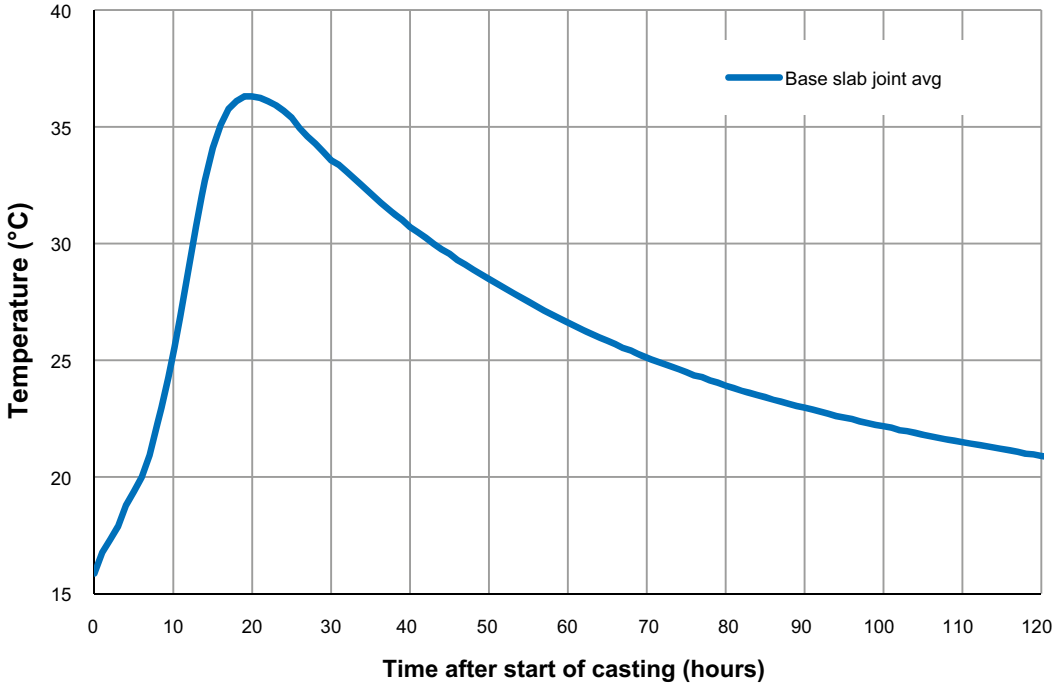

Figure C-11. *Temperature evolution in the slab 50 mcm under the joint to the wall until 120 hours after casting started. Average of sensors #10 to #14.*

Strain

The results from the strain measurement show certain variations for different sensors, see Chapter 10. This is not unusual when measuring strain in hardening concrete and this type of measurement tends to be difficult to evaluate. Some sensors show strong fluctuations at the beginning of the measurement, indicating probable contact with pokers or falling concrete. Other sensors drift with time or show sudden fluctuations after a certain time. No sensor shows the typical indication of cracking, i.e. a sudden jump from a high level of tensile strain towards lower tensile strain.

For this test casting, the function of the sensors was tested in uninsulated and insulated beams (see Chapter 6). These beams are not restrained and thus, the results can be assumed to present the specific strain that each sensor type registers in a unrestrained situation. The registered strain curves were zeroed and the results for the manufactured strain transducers were corrected for temperature (as described in the manual for the strain gauges). The commercial strain transducers do not need to compensated for temperature. Figure C-12 shows the results.

The strain measurements with the least disturbance were zeroed (strain #1), corrected for temperature (only the manufactured strain transducers) and the measured strain in the beams (from function test of the sensors) was subtracted from the measured strain in the structure. Figure C-13 shows the strain measured in the structure and after subtraction of the measured strain in the beams (no restraint).

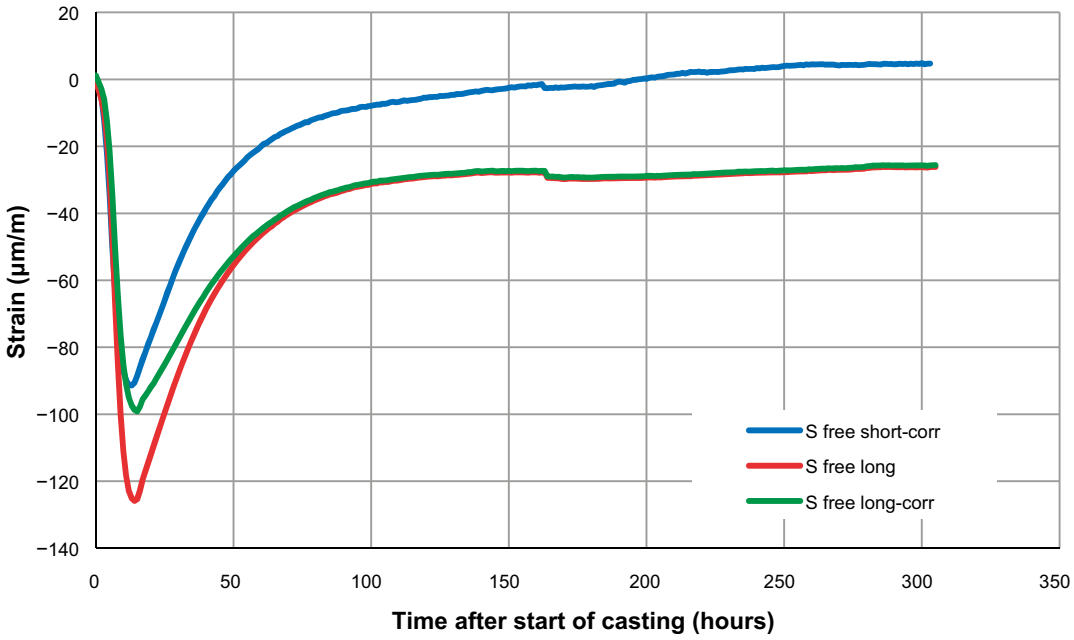

Figure C-12. *Corrected strain results for the sensors in the not insulated test beam. Short sensor = commercial strain transducer, long sensor = manufactured strain transducer.*

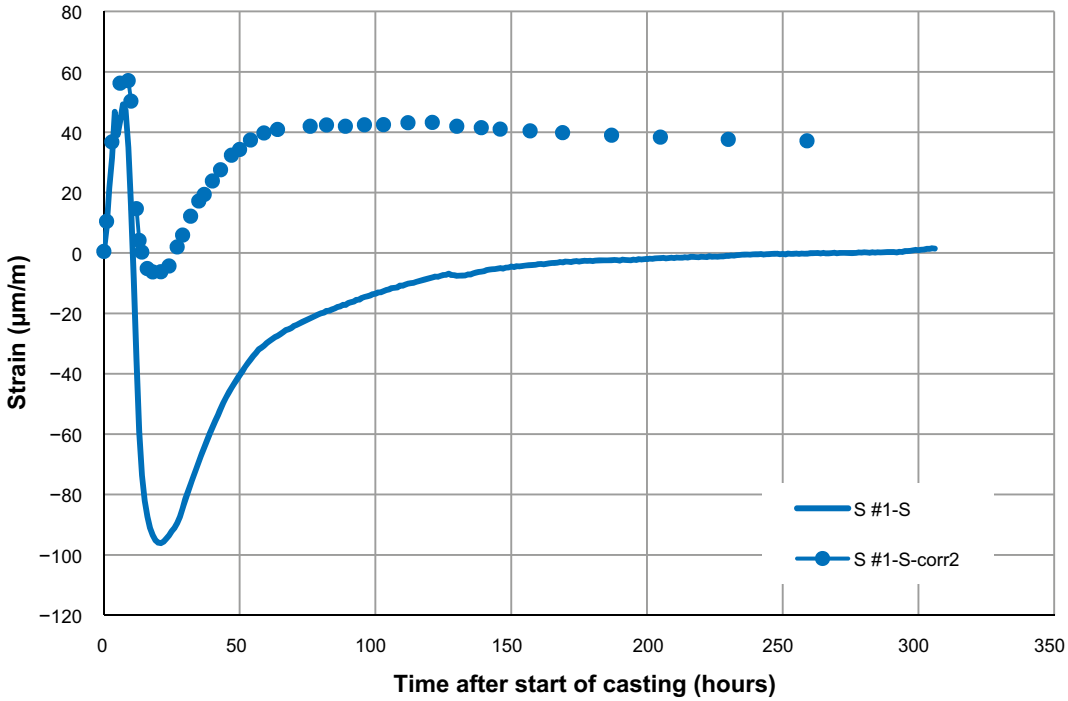

Figure C-13. *Strain and compensated strain for the slab.*

C6 Heating of the slab

Temperature

The temperature measurement results from the thermocouple setup was used for evaluation, see Figure C-14. The recorded temperature differs between the different measuring positions (see Section 10.2) and the average for each measuring position is chosen for evaluation. The difference can be explained with different placement of heating mats and insulation. The heating mats had to be placed in between the struts for the platform, so heating and insulation may have differed between the different positions.

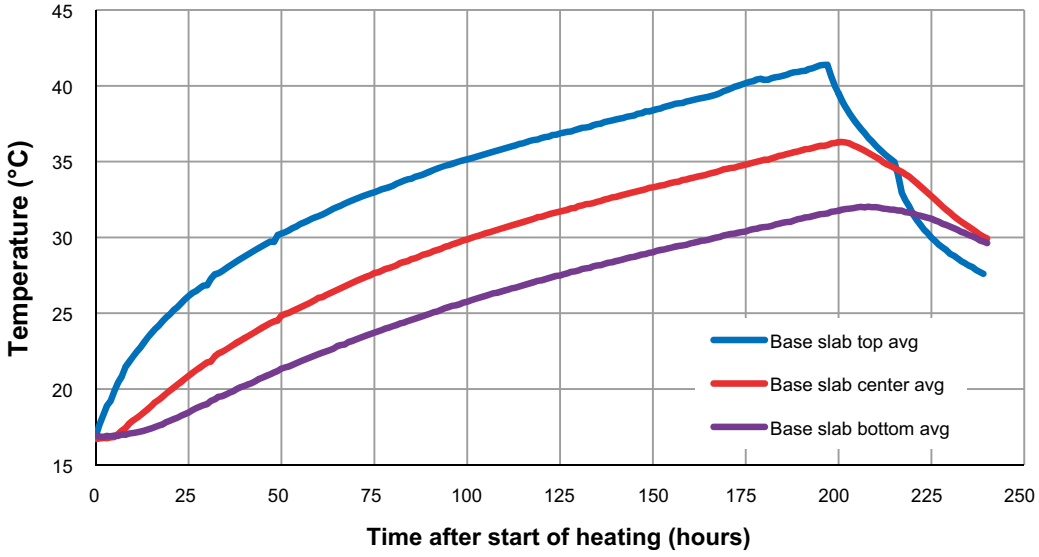

Figure C-14. *Temperature variations for the slab during heating and after casting of the wall. Average of sensors #1 to #6. Casting of the walls starts at approximately 168 h.*

Deformation

The total elongation of the 18 m long slab was 2.2 mm. The slab was heated up from +17 ºC to +36 ºC (in the centre). This should give a theoretical expansion of 3.44 mm (1.72 mm for each LVDT) when assuming the CTE according to engineering practice to 10×10^{-6} 1/K.

However, the CTE determined for dry concrete with an age of over one year was 6.75×10^{-6} 1/K (Appendix B) which gives a theoretical expansion of 2.32 mm (1.16 mm for each LVDT). According to literature, a CTE of 8×10^{-6} 1/K is more realistic for the present situation giving an expansion of 2.75 mm.

The difference between theoretical and actual expansion may be caused by friction between the slab and the foundation may hinder expansion to a certain degree but also by that the LVDT was placed at half the height of the slab and not at the top which experienced the highest temperature. Since the slab was warmed from top, it may have warped which gives smaller expansion in the neutral fibre (half the height). That effect cannot be determined with the actual placement of the LVDT.

C7 Casting of the walls

Temperature

The temperature measurement results from the thermocouple setup was used for comparison, see Table C-3 and Figure C-15. The maximum temperature differs between the different measuring positions (see Chapter 11) and therefore the average for each measuring position is chosen for evaluation. The difference can be explained with different starting temperatures in the fresh concrete and different temperatures in the surrounding environment.

The temperature at the inside of the walls is about 4 ºC higher than at the outside. Clearly, the warming of the slab with heating mats has resulted in a heated space under the platform. A certain temperature increase for the outside boundaries after casting until 72 hours after casting is assumed due to heat from hydration of the cement and machinery (as observed for the test casting in TAS05 as well).

The small temperature increase at 50 h after casting may be explained by that the tie rods were released at that time. This gives a very thin air layer between concrete and formwork which can increase insulation. Also, removal of insulation from the slab may contribute as heat is released from the warm slab.

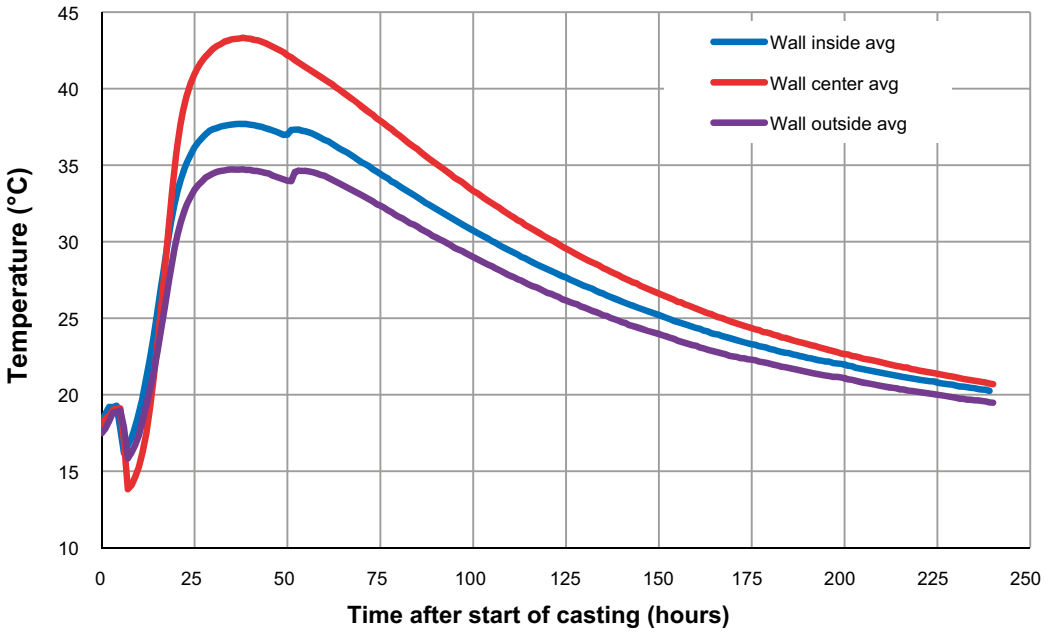

Figure C-15. *Temperature in the walls until 240 hours after casting started. Average of sensors #7 to #12.*

Table C-3. Temperatures used in the analysis. Linear interpolation is done automatically in the used software. Calculation time was 1 000 h.

Boundary	Time (h)	Temperature (°C)
Air, formwork outside	0	18
	24	20
	48	20
	72–1 000	16
Formwork inside	0	25
	24	26
	48	26
	72	25
	96–1 000	16
Rock, gravel, mature slab	0–1 000	16
Fresh concrete	0	16

Strain

The results from the strain measurement show certain variations for different sensors, see Chapter 11. This is not unusual when measuring strain in hardening concrete and this type of measurements tends to be difficult to evaluate. Some sensors show strong fluctuations at the beginning of the measurement, indicating probable contact with pokers or falling concrete. Other sensors drift with time or show sudden variations after a certain time. No sensor shows the typical reaction to cracking, i.e. a sudden jump from a high level of tensile strain towards lower tensile strain.

The strain measurements with the least disturbance were zeroed (strain #6 & #10 for the long wall and #4 & #11 for the short wall), corrected for temperature (only the manufactured strain transducers) and the measured strain in the beams was subtracted from the measured strain in the structure. Figure C-16 and Figure C-17 shows the strain measured in the structure and after subtraction of the measured strain in the beams (no restraint).

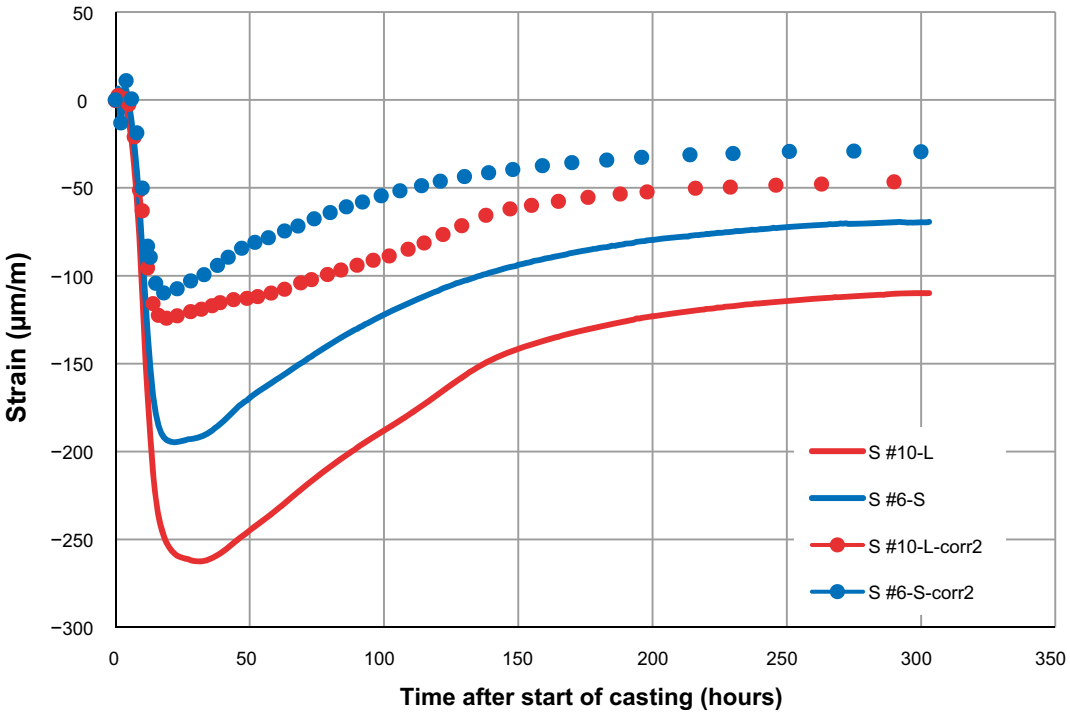

Figure C-16. *Strain and compensated strain for the long wall.*

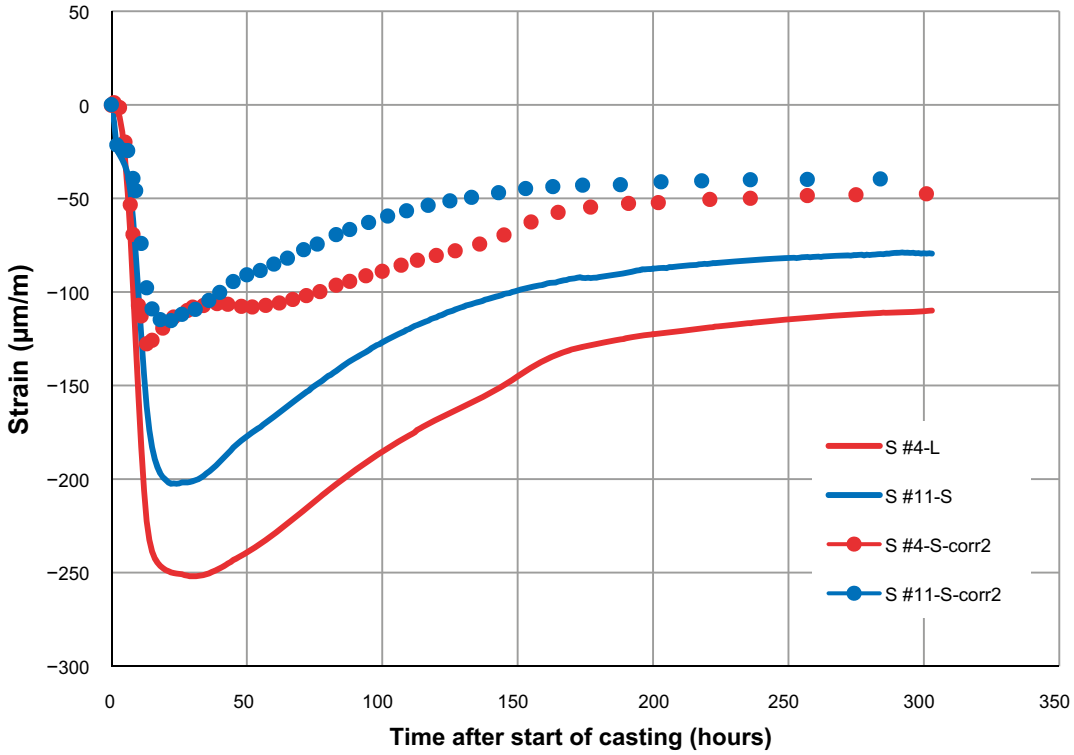

Figure C-17. *Strain and compensated strain for the short wall.*

All sensors show a rapid increase of compressive strain with increasing temperature in the initial stages of hydration. This is typical for strain measurements on hardening concrete. The corrected values for strain fit the registered temperature increase of about 25 °C, assuming 50–60 % restraint. At full restraint, this temperature increase would equal a maximum possible strain of about −250 µm/m. However, the wall is not subjected to 100 % restraint. According to the restraint analysis, the restraint at the position of the strain transducer is about 50 %.

After the initial increase of compression, the compression decreases. However, tensile strain is never reached. The curves level out at −50 to −25 µm/m. That would imply that the wall remains compressed after cooling down.

C8 Heat calculation and comparison with measurements

C8.1 Casting of the slab

Calculated and measured temperatures are compared in Figure C-18 and Figure C-19. The fit for the central, joint and the bottom sensors is good. A somewhat larger difference is noted for the sensor close to the top of the slab. This is not uncommon when comparing measured and calculated values. It seems to be due to the effects of spraying the surface with cold water at several occasions after casting (water curing). This effect is difficult to incorporate into a simulation.

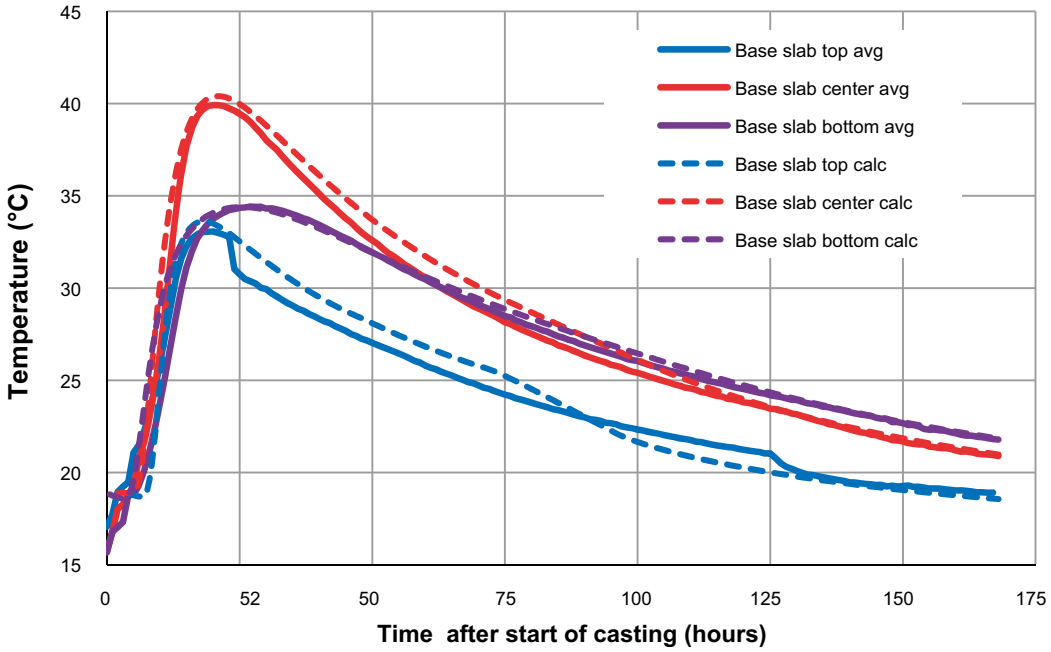

Figure C-18. *Comparison of measured and calculated temperature for the slab.*

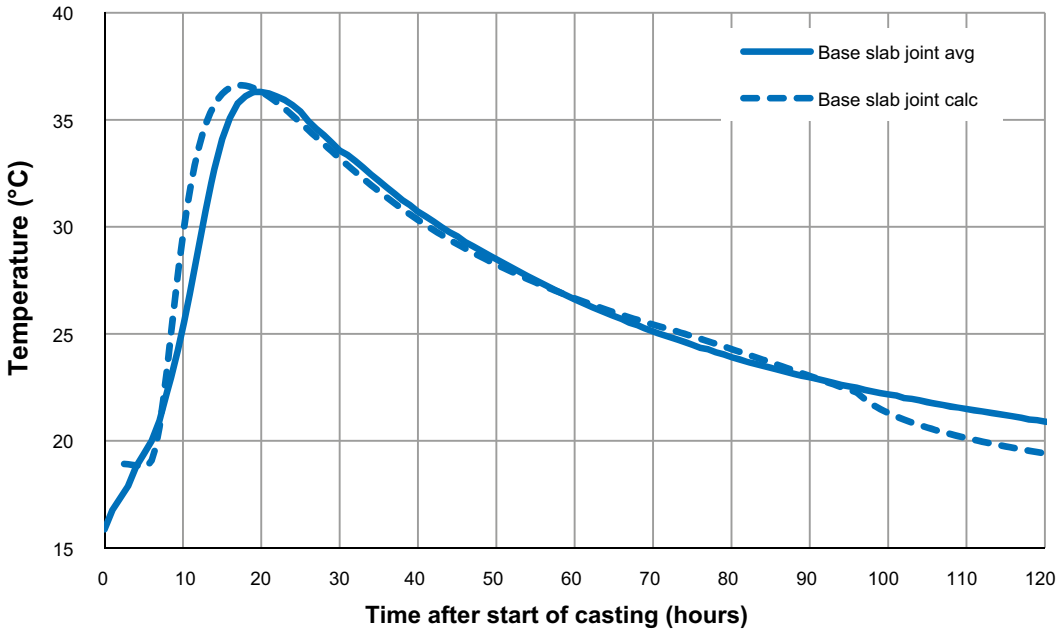

Figure C-19. *Comparison of measured and calculated temperature for the slab, 50 mm below the joint to the wall.*

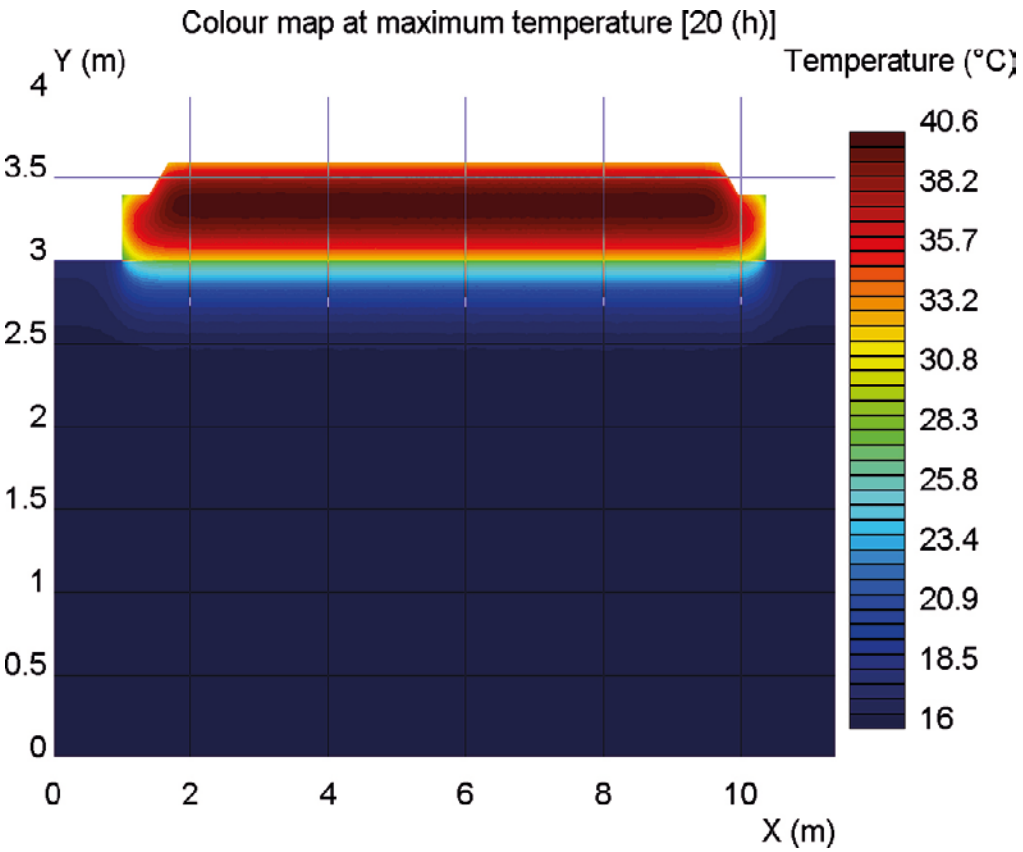

Figure C-20. *Simulated maximum temperature in the slab.*

C8.2 Heating of the slab

Calculated and measured temperatures are compared in Figure C-21. The fit for the average temperature is good. A larger deviation is noted for the sensors close to the top and bottom of the slab. This is not uncommon when comparing measured and calculated values. A possible explanation for the deviations is that the placement of the heating mats and insulating mats in relation to the thermocouples differ between different measuring positions. These effects are difficult to incorporate in a simulation.

Figure C-22 shows the simulated temperature when casting starts.

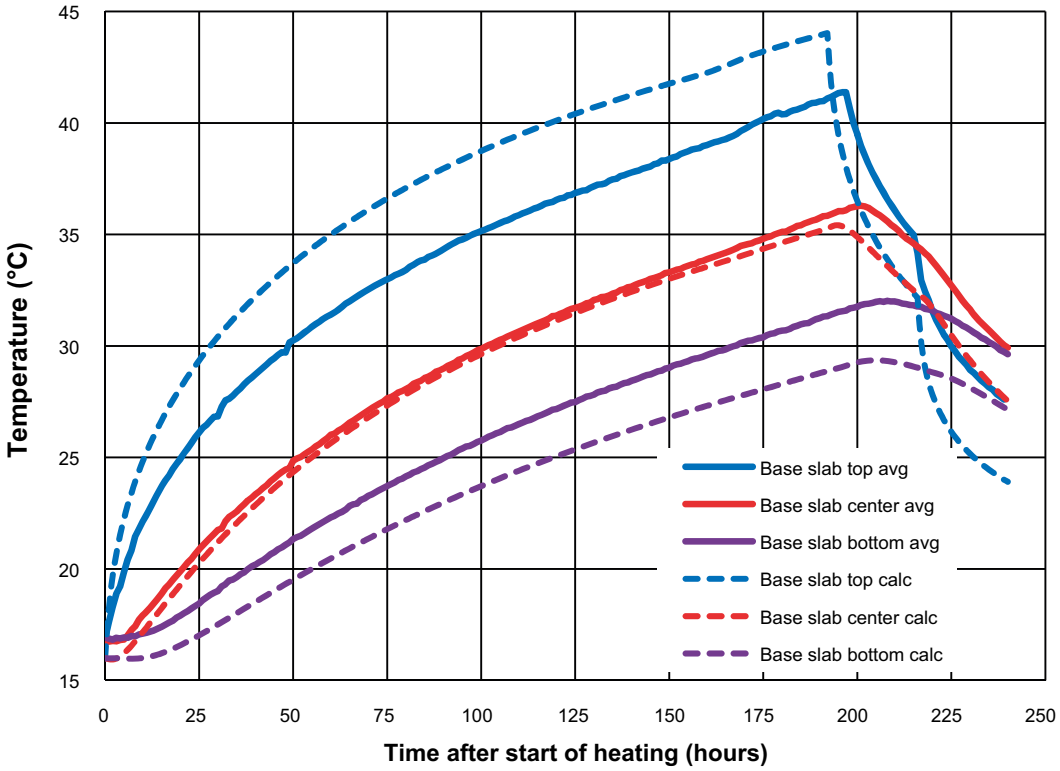

Figure C-21. *Comparison of measured and calculated temperature for the slab during heating and after casting of the wall.*

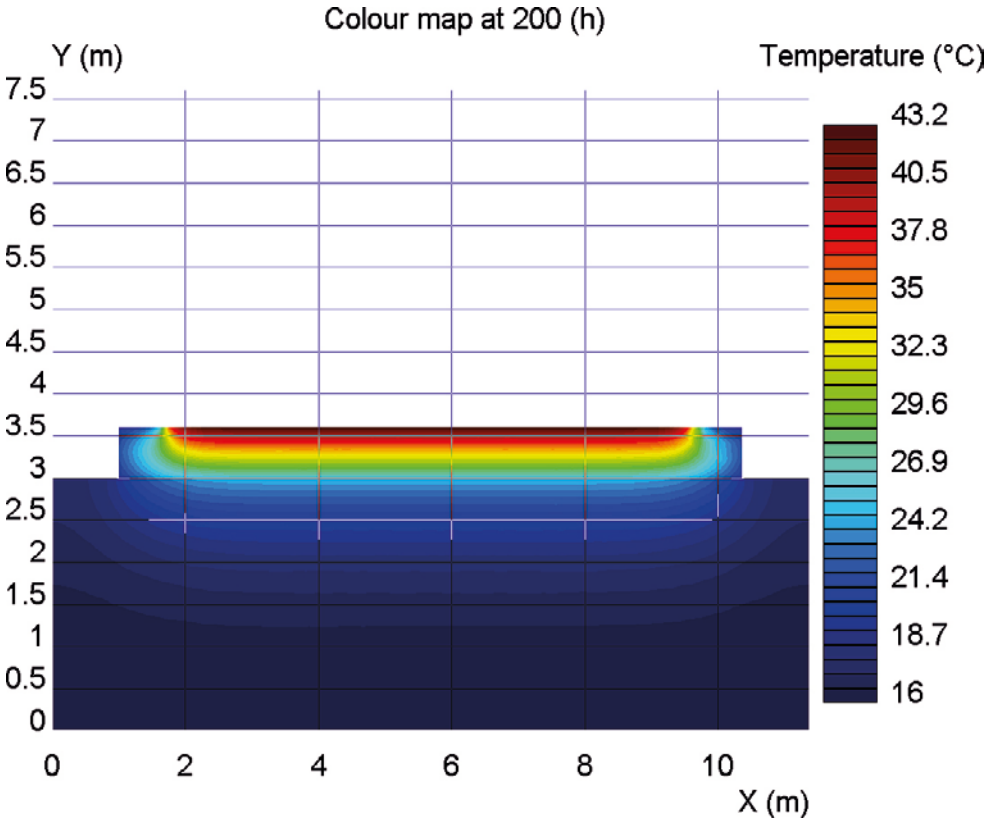

Figure C-22. *Simulated temperature in the slab when starting to cast the walls (168 hours after warming starts).*

C8.3 Casting of walls

The simulation of the temperature evolution in the walls shows certain deviations compared to the measured data. The simulated maximum temperature is about 1.5 ºC lower than the measured value.

For the slab, the fit is much better. A possible reason may be the fact that the concrete used in the walls did not contain any retarder which may influence the heat development. The deviation close to the formwork is smaller for inside and outside. Note that the inside was presumably warmer than the outside due to entrapped heat from heating the slab. No recorded data for the inside air temperature was available for comparison.

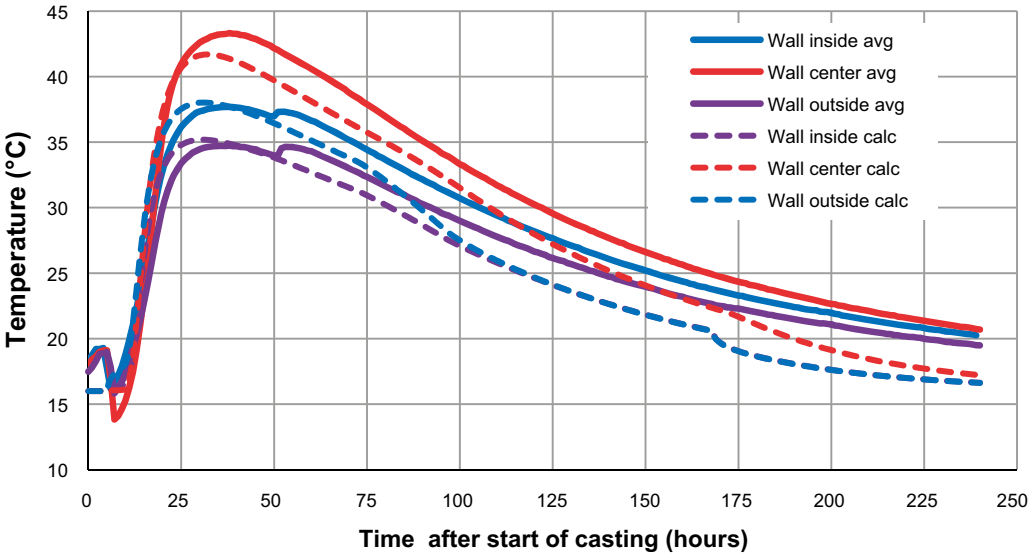

Figure C-23. *Comparison of measured and calculated temperature in the walls.*

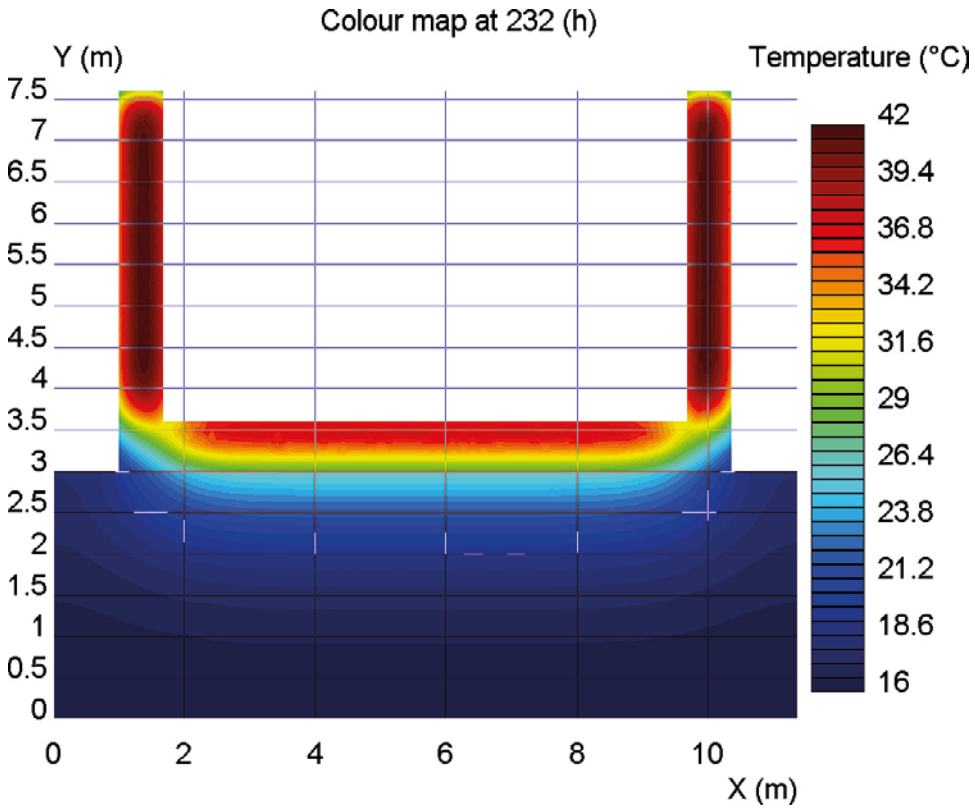

Figure C-24. *Simulated maximum temperature in the walls.*

C9 Strain calculation and comparison with measurements

No cracks have yet been observed neither through visual inspections nor by evaluation of the strain measurements, where cracking would have been indicated by sudden decrease in the measured (tensile) strain.

C9.1 Restraint situation for the walls

The restraint situation of the test casting has been assessed, using elastic 3D FEM calculations. The restraint situation for the walls of the full-scale caisson structure and the scaled component in TAS08 was analysed. Figure C-25 displays the calculated degree of restraint for different walls. The displayed degrees of restraint in Figure C-25 are extracted for the section of the wall where the wall is subjected to the highest restraint, typically at half the length (compare Figure C-26). Figure C-26 illustrates the distribution of the restraint in the walls.

The calculations show that the degree of restraint for the short wall of the component in TAS08 is almost identical to the restraint of the walls in the full-scale caisson. The long wall in the TAS08 component has a somewhat higher degree of restraint than in the full-scale caisson, due to the identical length of 18.1 m and the lower height (thus higher L/H ratio).

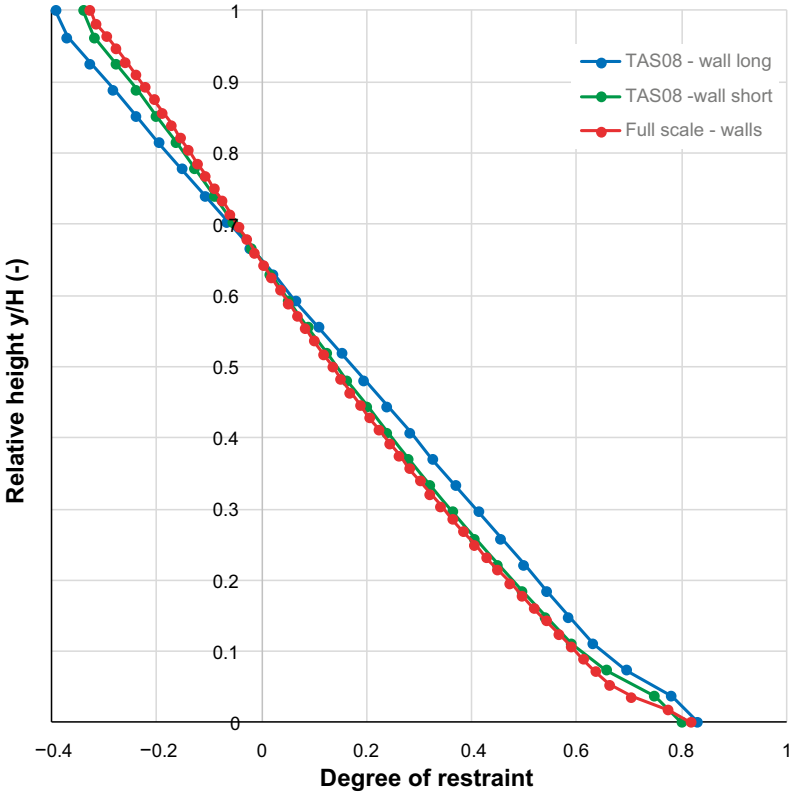

Figure C-25. *Calculated restraint for full-scale caisson and component in TAS08. The y-axis displays the relative height of the wall, with 0 = the joint to the slab and 1 = top of the wall.*

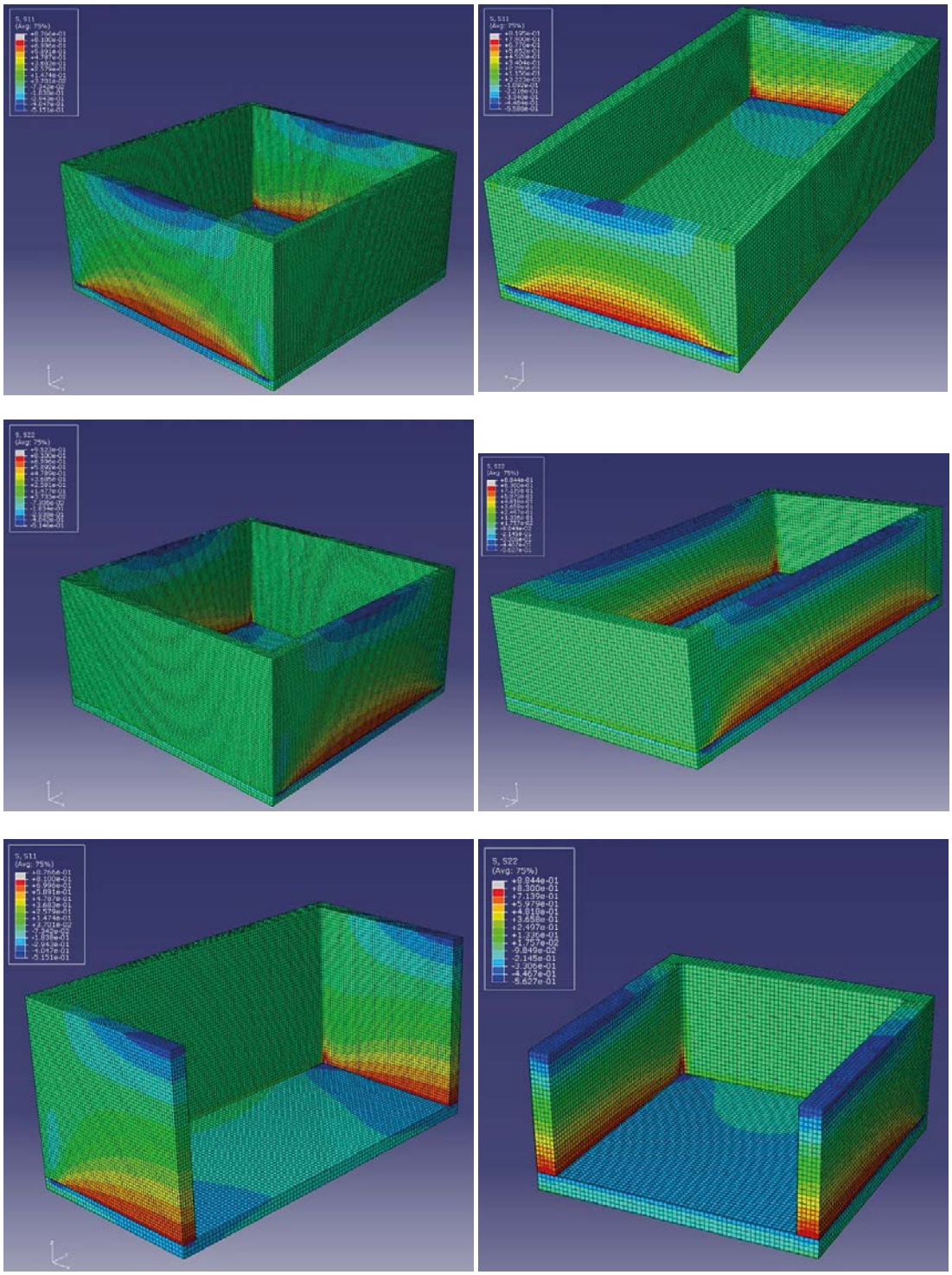

Figure C-26. *Colour plots of the calculated degree of restraint for full-scale caisson (left column) and component in TAS08 (right column).*

C9.2 Slab

Due to the difficulties with the evaluation of the strain measurements, only an indicative comparison of measurement and simulation is possible.

The restraint situation for the slab was modelled with very low restraint from the underlying concrete. This is justified by that the smooth surface of the underlying slab in combination with the plastic sheet placed on top of the foundation prevents the adhesion between these 2 parts. A rough calculation of the ratio between friction force and force due to temperature expansion/contraction can be used to estimate the translation restraint for the slab. This ratio was determined to be approximately 0.08, thus a translation restraint of 0.08 was used in the strain calculation. Rotation was assumed to be free.

In the simulation, the strain is expressed as strain ratio, i.e. the ratio between actual strain and strain capacity of the concrete for in a timeline. Figure C-27 and Figure C-28 show the results.

The general shape alignment of the measured and simulated curves differs to a certain degree, especially in time. Both curves show an early tensile strain, followed by a decrease of the tensile strain towards compression. Both curves show a remaining low tensile strain or strain ratio. The low strain (ratio) is consistent with the absence of cracks.

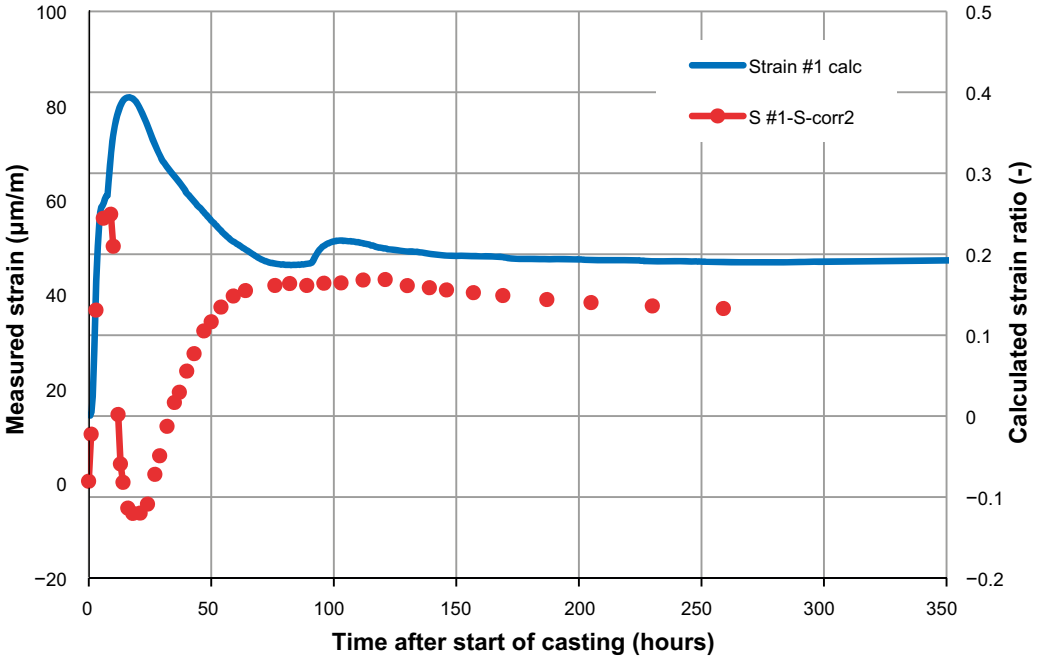

Figure C-27. *Comparison between measured and calculated strain for the slab.*

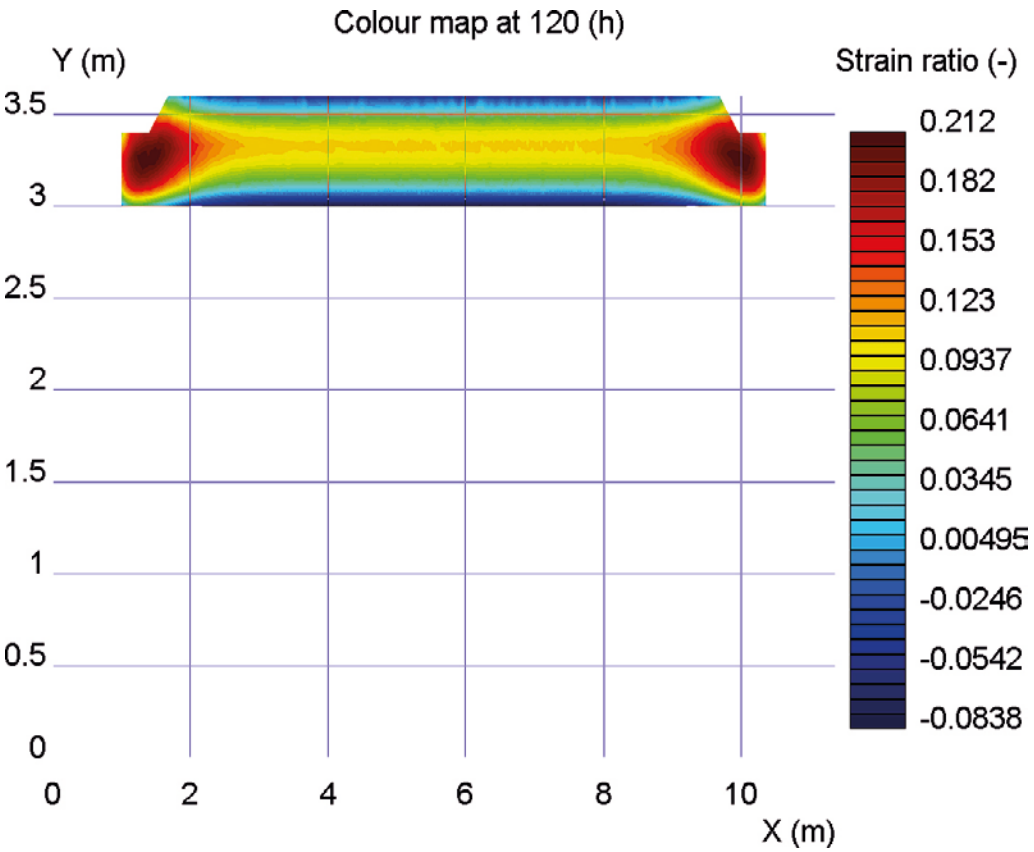

Figure C-28. *Simulated strain ratio in the cross section 120 h after casting.*

C9.3 Walls

The restraint for the walls was modelled according to the 3D analysis of the restraint, see earlier in this chapter. The restraint was imported into ConTest using a so called ERM model (equivalent restraint method), see Hösthagen (2017).

The comparison of simulation and measurement is displayed in Figure C-29 and Figure C-30. The general shape of the measured and simulated curves is similar with a rapid increase of compression immediately after casting, followed by a slow decrease of compression. In the simulation, a strain ratio of 0.50 is calculated which would equal 45 to 60 µm/m in tensile strain (the tensile strain capacity of concrete is 90 to 120 µm/m according to Bamforth (2007) and Ljungkrantz et al. 1994). On the contrary, the measurement shows only compression, −50 to −25 µm/m. That would imply that the wall remains compressed after cooling down. The exact reasons for the deviations between measurement and simulation could not be assessed further within the context of this work.

The calculated strain ratio in the lower part of the wall is around 0.50. It is known from experience that structures tend to crack if the strain ratio exceeds 0.80. Thus, both simulation and measurements are consistent with the absence of cracks. It is however questionable if there really is no tension in the structure as most of the measurements indicate.

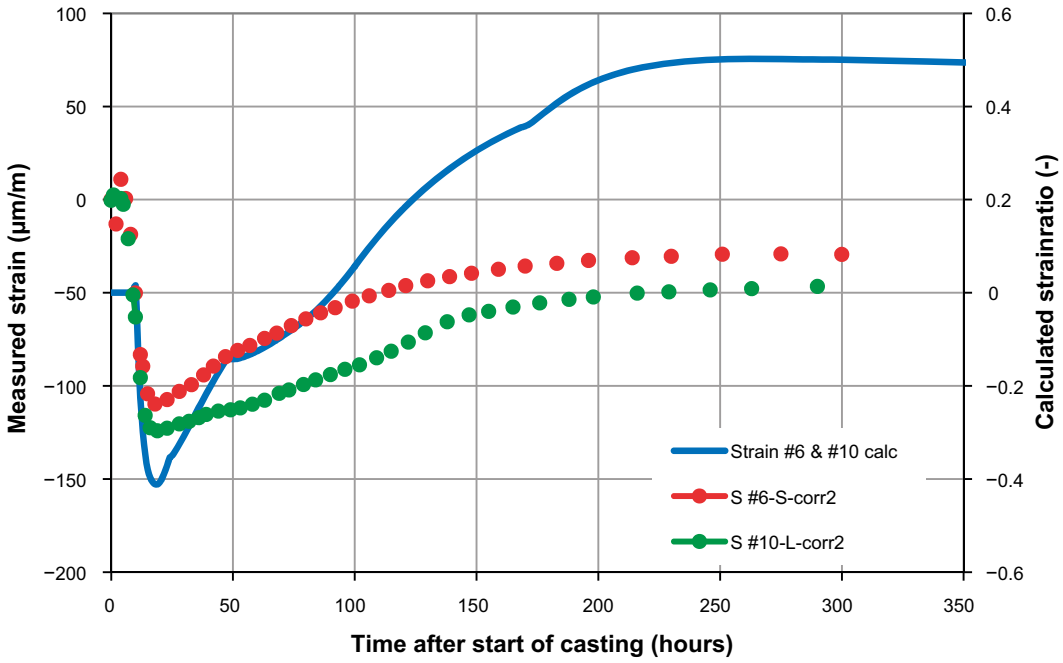

Figure C-29. *Comparison between measured and calculated strain for the long wall, 0.8 m above the slab.*

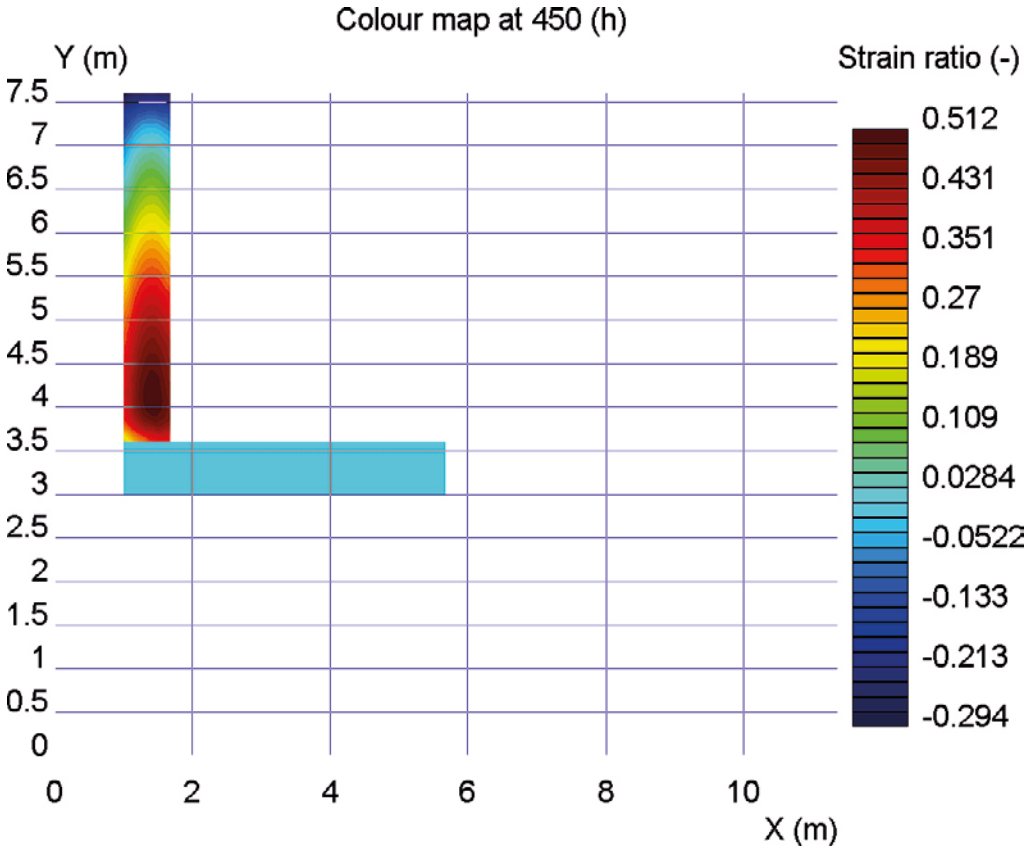

Figure C-30. *Simulated maximum strain ratio in the cross section of the long wall.*

C9.4 Discussion of strain measurement

Strain measurements in hardening concrete are generally regarded difficult to execute and evaluate (see e.g. Bamforth 2007 and Jonasson et al. 2009). The measuring setup chosen in this project is based on a setup used in Vogt et al. (2010). The results from this project can be summarized as follows. The control measurement in the external beam (unrestrained) resulted in a curve that showed zero strain in the beginning and changed with time (several days after casting) slowly to compression which is explained by the autogenous shrinkage of the used concrete. However, no rapid increase of compression directly after casting was measured. The measurement on the real structure (restrained) gave results consistent with accepted theory with compression building up initially after casting. With time and cooling down of the concrete, compression changed slowly to tension.

Typical for all strain measurements in the present study is the rapid increase in compression immediately after casting. At least for the beams, one could expect a measured curve as described above. The recorded compressive strain is for a number of strain gauges larger than theoretically possible by temperature increase in a completely restrained situation (the beams and the slab are definitely not highly restrained). There is no good explanation for this behavior since the strain gauges are temperature compensated (full bridge). Jonasson et al. (2009) reports that the early creep in the expansion phase of the hardening concrete results in a strain measurement which gives too high compression readings. Thus, attempts were made to correct the recorded strain values in the structure with the measurements from the beams. It is assumed that the values determined on the beams represent the reaction of the strain gauges in an unrestrained situation (kind of an “eigen-strain” of the strain gauges in the actual concrete). When subtracting the measured strain in the beams from the strain in the structure, the resulting curves are closer to what can be expected according to theory. However, no tension occurs after cooling down in the walls which is not according to theory. Within the context of this work, there is no possibility to further investigate the reason for the somewhat unexplainable strain measurements. The manufacturer of the strain gauges, the person who set up the system described in Vogt et al. (2010) and other experts were consulted. Regrettably, no attempt proved conclusive.

Appendix D

E:\Work__PE\SKB\TAS_08\TAS08_BPL.CPR: Report

D1 Software & Project Information

D1.1 Software

System name: ConTeSt

System version: 1.0

Developed by: JEJMS Concrete AB

D1.2 Project

Original filename: D:\Work\SKB\TAS05\TAS05_et1_T.CPR

Created: 2018.06.01 12.34.11

Created by: swecvo on CNU21810QY

Current filename: E:\Work__PE\SKB\TAS_08\TAS08_BPL.CPR

Last change: 2020.02.06 17.41.11

Last change by: swecvo on PC0MLZ09

D2 Geometry & Time

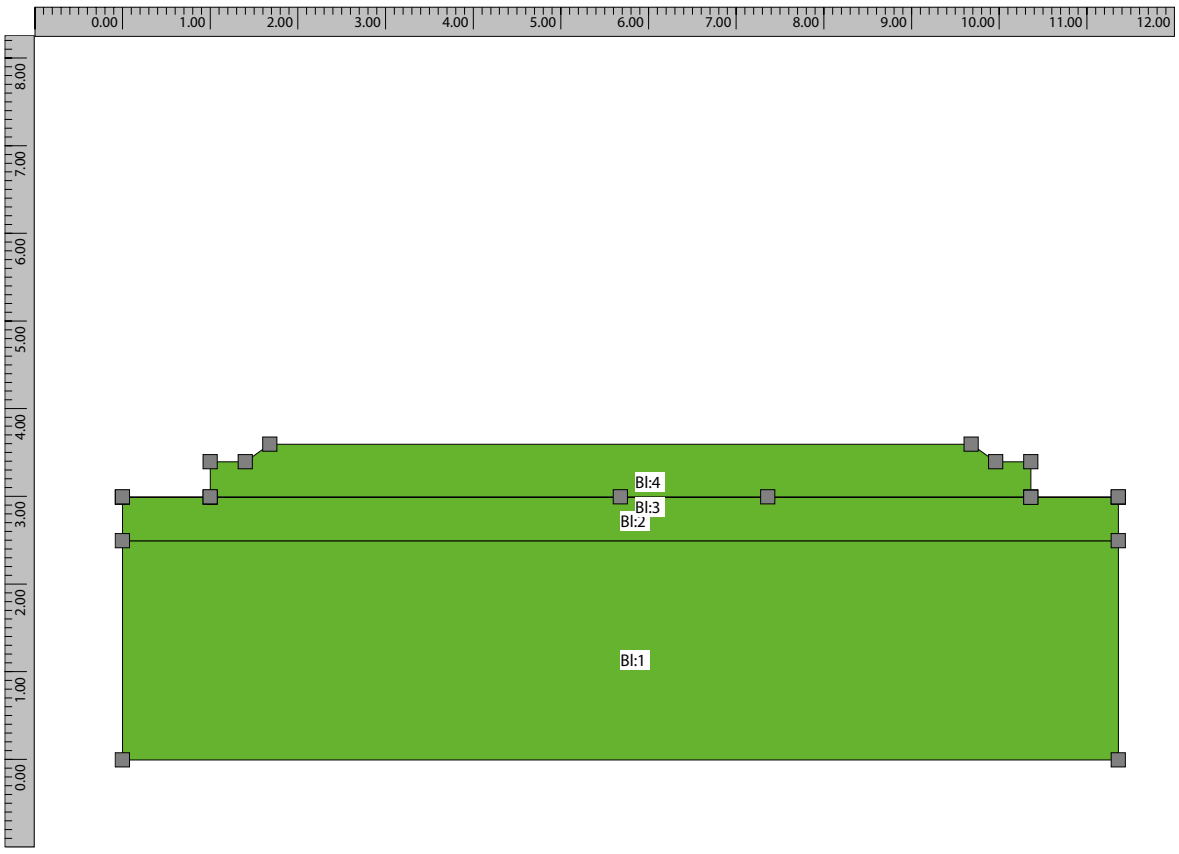

Figure D-1. *Geometry of the base slab.*

D2.1 Description

D2.1.1 Blocks

Block 1: (11.360;0.000) - (11.360;2.500) - (0.000;2.500) - (0.000;0.000)

Block 2: (0.000;2.500) - (11.360;2.500) - (11.360;2.995) - (10.360;2.995) - (1.000;2.995) - (0.000;2.995)

Block 3: (0.000;2.995) - (1.000;2.995) - (10.360;2.995) - (11.360;2.995) - (11.360;3.000) - (10.360;3.000) - (7.360;3.000) - (5.680;3.000) - (1.000;3.000) - (0.000;3.000)

Block 4: (5.680;3.000) - (7.360;3.000) - (10.360;3.000) - (10.360;3.400) - (9.960;3.400) - (9.680;3.600) - (1.680;3.600) - (1.400;3.400) - (1.000;3.400) - (1.000;3.000)

D2.1.2 Computation time

Total time length: 1 000 (h)

D3 Element Size

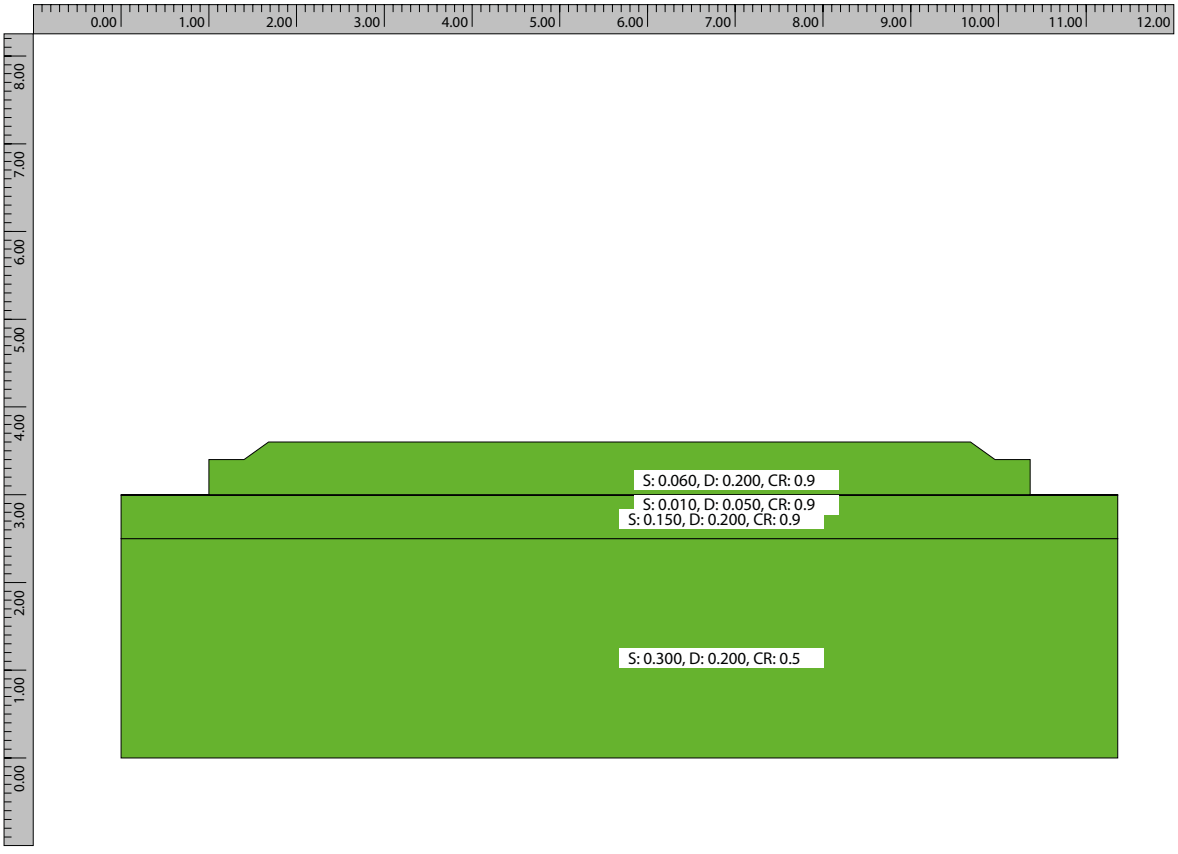

Figure D-2. *Element size for the meshing of the base slab.*

D4 Computation Mesh

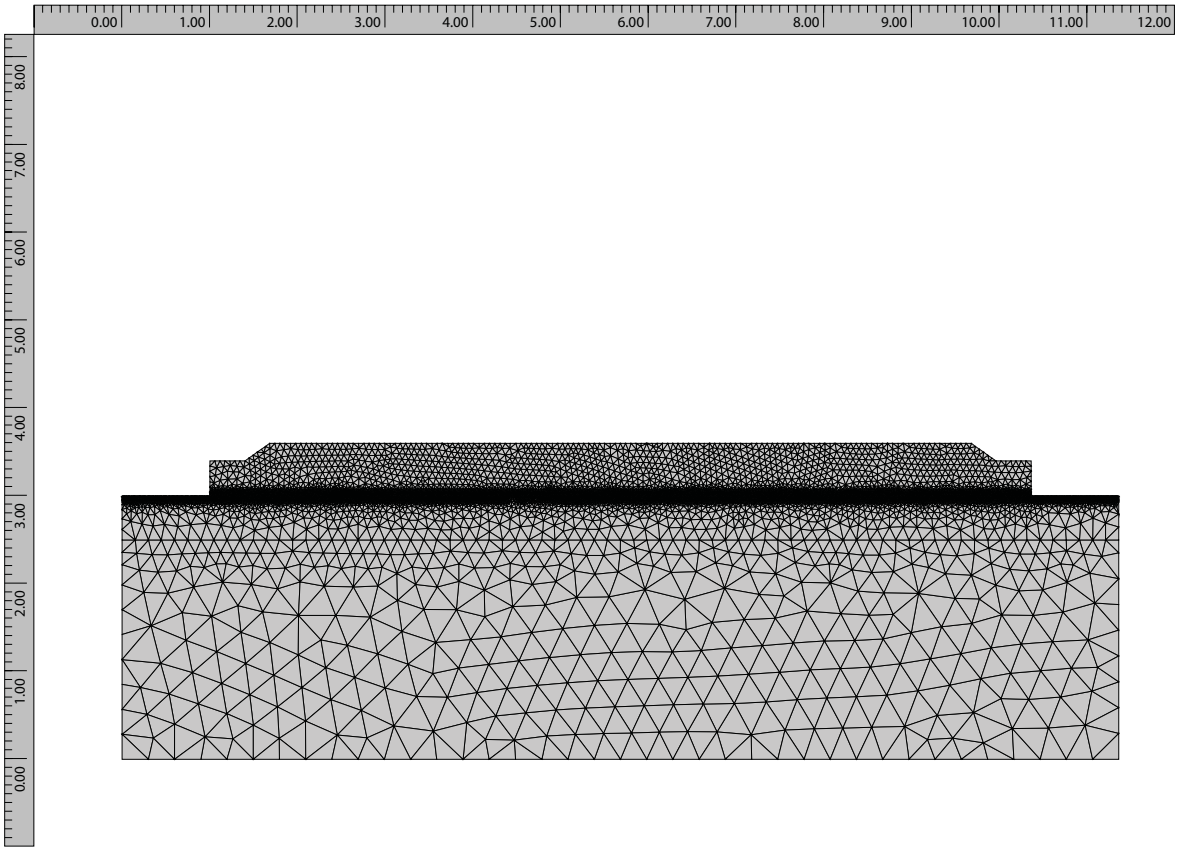

Figure D-3. *Finite element mesh for the base slab.*

D5 Heat Properties

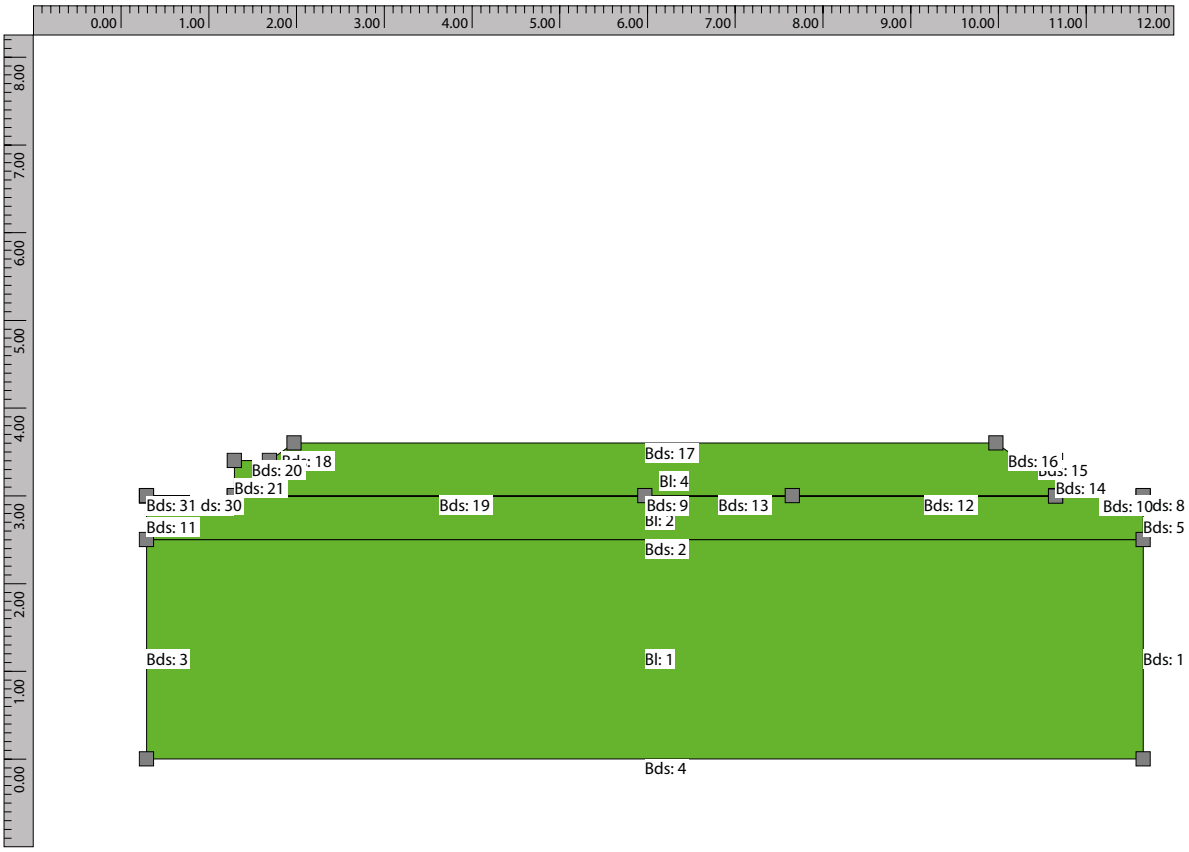

Figure D-4. *List of boundaries for the base slab.*

D5.1 Description

D5.1.1 Block type list

SCC-mod-TAS05: Young concrete

Start temperature

Constant: 19.0

Material definition: K45 vct = 0.47 Lufttillsats (Mix 4) (str)

Source

Luleå Tekniska Universitet

Provningar 1999, 2000 – LTU, Skrift 00:02

Recept: Sweroc

Description

Degerhamn Std P (Anläggningscement)

vct 0.47

Köping 500 (Kalkfiller)

lufthalt 4.5 á 5.0 %

flytsättmått 700–750 mm

Original material parameters

Density: 2 350 (kg/m³), Heat cap. 1 000 (J/(kg·K))

Heat cond. (W/m²K) as piece-wise linear function of equivalent time of maturity (h), (equ. time; heat cond.): (0;2.1), (12;2.1), (24;1.7), (10000;1.7)

C 363 (kg/m³), Wc 325 000 (J/kg), Lambda1 1.02 (-), t1 9.15 (h), Kappa1 1.94 (-)

te0 0 (h), BetaD 1 (-), ThetaRef 3 660 (K), Kappa3 0.653 (-)

Eta6 4 (‰), Eta8 10 (‰), Eta12 106 (‰), Eta18 198 (‰), Eta24 262 (‰), Eta72 562 (‰), Eta168 791 (‰)

Fcc28 68 (MPa)

Following material parameters are changed by the user

C 320 (kg/m³)

Wc 250 000 (J/kg)

te0 −2 (h)

BetaD 2 (-)

Fcc28 50 (MPa)

Mature concrete: Other material

Start temperature

Constant: 16.0

Material definition: Mature C35/45 w0/C = 0.40 AEA (str)

Source

Luleå University of Technology, Sweden.

Tests during 1995 to 2004

Adjustment to a “general” data base 2006

Description

Moderate heat cement (Degerhamn OPC) from Cementa AB in Sweden.

Primarily aimed for use in civil engineering structures.

Original material parameters

Density: 2 350 (kg/m³), Heat cap. 1 000 (J/(kg·K))

Heat cond. (W/m²K) as piece-wise linear function of equivalent time of maturity (h), (equ. time; heat cond.): (0;1.7), (12;2.1), (24;1.7), (10000;1.7),

Blinding: Other material

Start temperature:

1D-linear

18.0 (°C) at (0.000;2.995)

16.0 (°C) at (0.000;2.500)

Material definition: Mature C28/35 w0/C = 0.55 AEA (str)

Source

Luleå University of Technology, Sweden,

Tests during 1995 to 2004

Adjustment to a “general” data base 2006

Description

Moderate heat cement (Degerhamn OPC) from Cementa AB in Sweden.

Primarily aimed for use in civil engineering structures.

Original material parameters

Density: 2 350 (kg/m³), Heat cap. 1 000 (J/(kg·K))

Heat cond. (W/m²K) as piece-wise linear function of equivalent time of maturity (h), (equ. time; heat cond.): (0;1.7), (12;2.1), (24;1.7), (10000;1.7),

Rock: Other material

Start temperature

Constant: 16.0

Material definition: Rock (str)

Source

Luleå University of Technology 1997

Description

Original material parameters

Density: 2 650 (kg/m³), Heat cap. 850 (J/(kg·K))

Heat cond. 3.7 (W/m²K)

Folie: Other material

Start temperature

Constant: 15.0

Material definition: Insulation material

Source

Luleå University of Technology 1999

Description

Cellular plastic

Original material parameters

Density: 25 (kg/m³), Heat cap. 1 500 (J/(kg·K))

Heat cond. 0.036 (W/m²K)

Following material parameters are changed by the user

Density: 250 (kg/m³)

Heat cond. 0.1 (W/m²K)

New_old Bpl: Young concrete

Start temperature

Constant: 16.0

Material definition: C40/50 w0/C = 0.38 Air entrainment (str)

Source

Luleå University of Technology, Sweden,

Tests during 1995 to 2004

Adjustment to a “general” data base 2006/2008

Description

Moderate heat cement (Degerhamn OPC) from Cementa AB in Sweden.

Primarily aimed for use in civil engineering structures.

Original material parameters

Density: 2 350 (kg/m³), Heat cap. 1 000 (J/(kg·K))

Heat cond. (W/m²K) as piece-wise linear function of equivalent time of maturity (h), (equ. time; heat cond.): (0;2.1), (96;2.1), (120;1.7), (10000;1.7), C 435 (kg/m³), Wc 325 000 (J/kg), Lambda1 2.2 (-), t1 4.75 (h), Kappa1 1.65 (-) te0 0 (h), BetaD 1 (-), ThetaRef 4 200 (K), Kappa3 0.5 (-) s 0.331 (-), tS 5.556 (h), tA 8.334 (h), nA 1.148 (-), Lambda2 0 (-), Tr2 1 (°C), Kappa2 0 (-) Fcc28 58 (MPa)

Following material parameters are changed by the user

C 0 (kg/m³)

te0 1 000 (h)

D5.1.2 Block connection list

Block 1: Rock

Block 2: Blinding

Block 3: Folie

Block 4: SCC-mod-TAS05, simulate filling

D5.1.3 Boundary type list

Free surface

Temperature

Piece-wise linear (time (h);temp. (°C))

(0;18) (24;18) (48;20) (72;20) (96;16)

Wind velocity:

Constant 1 (m/s)

Heat transfer coefficient:

Constant 30 (W/m²K)

Supplied heat:

Constant 0 (W/m²)

Rock

Temperature:

Constant 16 (°C)

Heat transfer coefficient:

Constant 80 (W/m²K)

Supplied heat:

Constant 0 (W/m²)

Form wall 21 mm kvar

Temperature:

Piece-wise linear (time (h);temp. (°C))
(0;18) (24;18) (48;20) (72;20) (96;16)

Wind velocity:

Constant 1 (m/s)

Heat transfer coefficient:

Piece-wise constant (time (h);htc (W/m²K))
(0:6.66667)
Wood 0.021 (m):
(672:500)
Free Surface

Supplied heat:

Constant 0 (W/m²)

Form corner 40 mm

Temperature:

Piece-wise linear (time (h);temp. (°C))
(0;18) (24;18) (48;20) (72;20) (96;16)

Wind velocity:

Constant 2 (m/s)

Heat transfer coefficient:

Piece-wise constant (time (h);htc (W/m²K))
(0:3.5)
Wood 0.04 (m)
(168:500)
Free Surface

Supplied heat:

Constant 0 (W/m²)

Form boxout 12 mm 4d

Temperature:

Piece-wise linear (time (h);temp. (°C)),
(0;18) (24;18) (48;20) (72;20) (96;16)

Wind velocity:

Constant 1 (m/s)

Heat transfer coefficient:

Piece-wise constant (time (h);htc (W/m²K)),
(0:11.6667)
Wood 0.012 (m),
(96:500)
Free Surface

Supplied heat:

Constant 0 (W/m²)

Form slab boxout 40 mm

Temperature:

Piece-wise linear (time (h);temp. (°C));
(0;18) (24;20) (48;20) (72;17)

Wind velocity:

Constant 2 (m/s)

Heat transfer coefficient:

Piece-wise constant (time (h);htc (W/m²K)),
(0:3.5)
Wood 0.04 (m),
(168:500)
Free Surface

Supplied heat:

Constant 0 (W/m²)

varmematta 7d

Temperature:

Constant 16 (°C)

Wind velocity:

Constant 2 (m/s)

Heat transfer coefficient:

Piece-wise constant (time (h);htc (W/m²K)),
(0:2)
Expanded polyethylene 0.02 (m),
(248:500)
Free Surface

Supplied heat:

Piece-wise constant (time (h);power (W/m²)),
(0;0) (32;100) (224;0)

isol insida form

Temperature:

Constant 15 (°C)

Wind velocity:

Constant 1 (m/s)

Heat transfer coefficient:

Piece-wise constant (time (h);htc (W/m²K)),
(0:4)
Expanded polyethylene 0.01 (m), (199:500)
Free Surface

Supplied heat:

Constant 0 (W/m²)

Moving Boundary: Moving boundary

Temperature:

Constant 18 (°C)

Wind velocity:

Constant 1 (m/s)

Heat transfer coefficient:

Constant 500 (W/m²K)

Free Surface

Supplied heat:

Constant 0 (W/m²)

D5.1.4 Boundary connection list

Boundary segment 1: adiabatic (no heat flow)

Boundary segment 2: inner segment (full thermal contact)

Boundary segment 3: adiabatic (no heat flow)

Boundary segment 4: Rock

Boundary segment 5: adiabatic (no heat flow)

Boundary segment 6: inner segment (full thermal contact)

Boundary segment 7: inner segment (full thermal contact)

Boundary segment 8: adiabatic (no heat flow)

Boundary segment 9: inner segment (full thermal contact)

Boundary segment 10: free surface

Boundary segment 11: adiabatic (no heat flow)

Boundary segment 12: inner segment (full thermal contact)

Boundary segment 13: inner segment (full thermal contact)

Boundary segment 14: Form wall 21 mm kvar

Boundary segment 15: Form boxout 12 mm 4d

Boundary segment 16: Form boxout 12 mm 4d

Boundary segment 17: free surface

Boundary segment 18: Form boxout 12 mm 4d

Boundary segment 19: inner segment (full thermal contact)

Boundary segment 20: Form boxout 12 mm 4d

Boundary segment 21: Form wall 21 mm kvar

Boundary segment 30: free surface

Boundary segment 31: adiabatic (no heat flow)

D5.1.5 Inner point type list

D5.1.6 Simulation of filling process for young concrete

Surface position as a piece-wise linear func. of time (time (h); y-coord. (m))

(0;3), (4;3.6),

D6 Plane-Surface Analysis

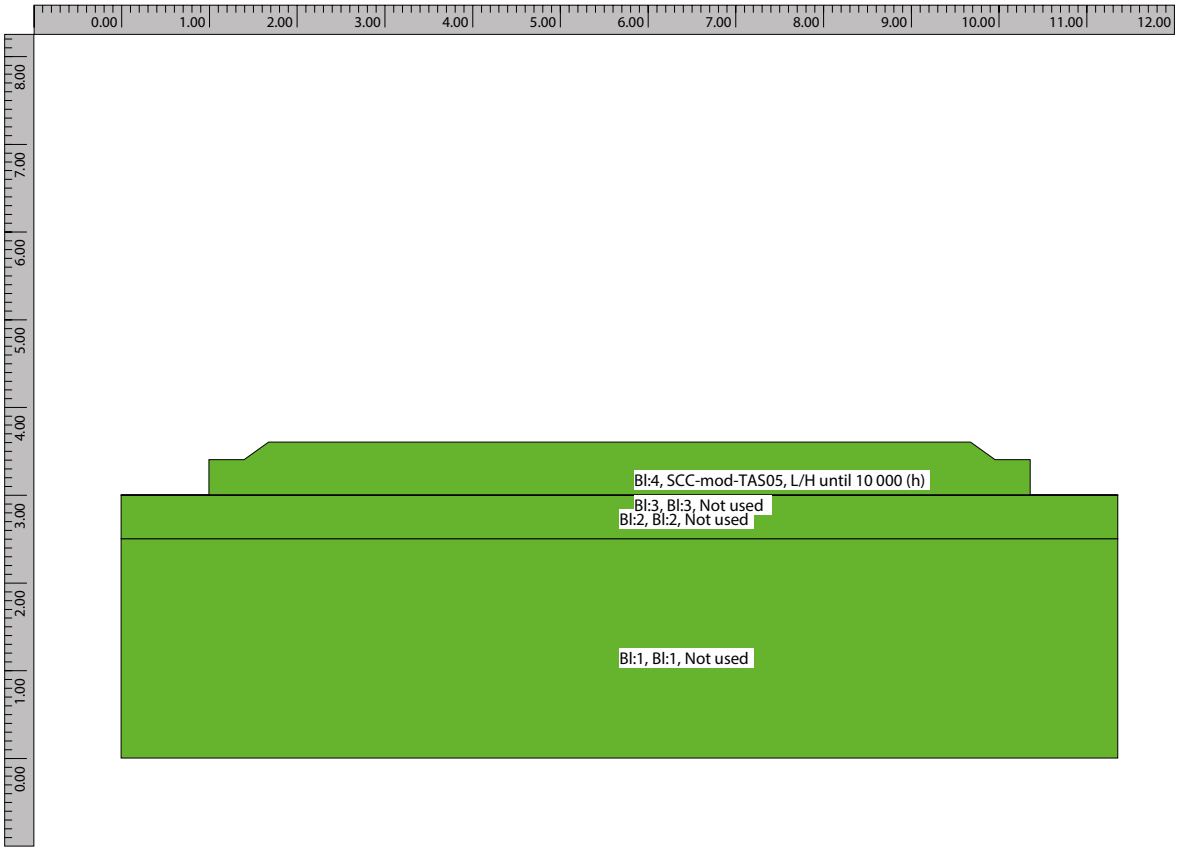

Figure D-5. *Blocks used in the base slab stress calculations.*

D6.1 Description

D6.1.1 Stress case

Default time stepping

Translation

Constant = 0.080

Rotation around X-axis:

Free (0.000)

Rotation around Y-axis:

Full restraint (1.000)

D6.1.2 Block data list

Block 4: SCC-mod-TAS05, L/H until 10 000 (h)

D6.1.3 Block type list

SCC-mod-TAS05: Young concrete

Material definition: K45 vct = 0.47 Lufttillsats (Mix 4) (str)

Source

Luleå Tekniska Universitet

Provningar 1999, 2000 – LTU, Skrift 00:02

Recept Sweroc

Description

Degerhamn Std P (Anläggningscement)

vct 0.47

Köping 500 (Kalkfiller)

lufthalt 4.5 á 5.0 %

flytsättmått 700–750 mm

Original material parameters

Po-ratio 0.18 (-), AlfaHeat 9.7e−06 (1/K), AlfaCool 9.7e−06 (1/K)

ThetaT 5 000 (K), RelaxTime1 0.005 (d), TimeZero 0.36 (d)

Fcc28 68 (MPa), Fcref 62 (MPa), Ftref 3.87 (MPa)

Beta1 0.667 (-), Alfact 0.7 (-), RaaT 0 (-), RaaFi 0 (-)

KFi 2 (-), Eps1 0 (-), TimeS1 6 (h)

Eps2 −0.000165 (-), TimeS2 8 (h), ThetaSH 120 (h), EthaSH 0.3 (-)

Relax: Age 0.359 (d), Units (GPa) 0.01 0.01 0.01 0.01 0.01 0.01 0.01 0.01

Relax: Age 0.54 (d), Units (GPa) 3.0184 2.3761 3.6531 2.5385 1.3421 1.7683 1.6167 1.3048

Relax: Age 1.163 (d), Units (GPa) 3.2785 2.9128 4.1142 2.9953 2.2954 2.5047 2.4411 1.844

Relax: Age 2.506 (d), Units (GPa) 3.3589 3.3689 4.2389 3.6801 3.5409 3.4482 3.4996 2.4096

Relax: Age 5.4 (d), Units (GPa) 2.6217 2.9505 3.7231 3.9755 4.2461 3.8967 4.0385 3.8283

Relax: Age 11.634 (d), Units (GPa) 2.0163 2.4072 3.248 3.7368 4.0717 3.7562 3.8959 7.4188

Relax: Age 25.065 (d), Units (GPa) 1.5407 1.9199 2.7174 3.3638 3.8489 3.5998 3.7423 10.7153

Relax: Age 54 (d), Units (GPa) 1.1889 1.5262 2.2351 2.9238 3.5773 3.4565 3.6112 13.5493

Relax: Age 116.339 (d), Units (GPa) 0.9389 1.2286 1.8461 2.5009 3.2669 3.3372 3.5338 15.8386

Relax: Age 250.646 (d), Units (GPa) 0.7655 1.014 1.5523 2.1504 2.9475 3.232 3.5329 17.5812

Following material parameters are changed by the user
Fcc28 50 (MPa)
Fcref 50 (MPa)

mature concrete: Other material
Material definition: Mature C35/45 w0/C = 0.40 AEA (str)
Source
Luleå University of Technology, Sweden
Tests during 1995 to 2004
Adjustment to a “general” data base 2006
Description
Moderate heat cement (Degerhamn OPC) from Cementa AB in Sweden.
Primarily aimed for use in civil engineering structures.
Original material parameters
Po-ratio 0.18 (-), E-modulus 34.4 (GPa), AlfaHeat 1e−05 (1/K)
Fcc 53 (MPa), Ftref 3.68 (MPa)

Blinding: Other material
Material definition: Mature C28/35 w0/C = 0.55 AEA (str)
Source
Luleå University of Technology, Sweden
Tests during 1995 to 2004
Adjustment to a “general” data base 2006
Description
Moderate heat cement (Degerhamn OPC) from Cementa AB in Sweden.
Primarily aimed for use in civil engineering structures.
Original material parameters
Po-ratio 0.18 (-), E-modulus 32.6 (GPa), AlfaHeat 1e−05 (1/K)
Fcc 43 (MPa), Ftref 3.21 (MPa)

Rock: Other material
Material definition: Rock (str)
Source
Luleå University of Technology 1997
Description
Original material parameters
Po-ratio 0.2 (-), E-modulus 30 (GPa), AlfaHeat 1e−05 (1/K)
Fcc 30 (MPa), Ftref 3 (MPa)

New_old Bpl: Young concrete
Material definition: C40/50 w0/C = 0.38 Air entrainment (str)
Source
Luleå University of Technology, Sweden
Tests during 1995 to 2004
Adjustment to a “general” data base 2006/2008
Description
Moderate heat cement (Degerhamn OPC) from Cementa AB in Sweden.
Primarily aimed for use in civil engineering structures.

Original material parameters

Po-ratio 0.18 (-), AlfaHeat 1.1e−05 (1/K), AlfaCool 9e−06 (1/K)

ThetaT 5 000 (K), RelaxTime1 0.005 (d), TimeZero 0.25 (d)

Fcc28 58 (MPa), Fcref 58 (MPa), Ftref 3.91 (MPa)

Beta1 0.667 (-), Alfact 0.9 (-), RaaT 0 (-), RaaFi 0.9 (-)

KFi 2 (-), Eps1 0 (-), TimeS1 6 (h)

Eps2 −0.000164 (-), TimeS2 24 (h), ThetaSH 120 (h), EthaSH 0.3 (-)

Relax: Age 0.249 (d), Units (GPa) 0.01 0.01 0.01 0.01 0.01 0.01 0.01 0.01

Relax: Age 0.5 (d), Units (GPa) 0.857221 0.256405 3.50511 1.16388 0.786528 0.439177 0.122558 0.101706

Relax: Age 1.077 (d), Units (GPa) 2.67304 4.80813 9.03774 3.7919 4.01799 2.19963 0.705556 0.754292

Relax: Age 2.321 (d), Units (GPa) 2.11587 4.25012 8.20966 7.23161 6.34904 3.5086 1.10078 0.684051

Relax: Age 5 (d), Units (GPa) 1.26691 2.75358 5.95473 8.32677 7.27362 3.96807 1.25504 3.14366

Relax: Age 10.772 (d), Units (GPa) 0.801966 1.78874 4.18532 7.43422 7.50287 4.12974 1.31843 7.05465

Relax: Age 23.208 (d), Units (GPa) 0.539145 1.25091 2.9427 6.22062 7.65742 4.43895 1.40975 9.90401

Relax: Age 50 (d), Units (GPa) 0.399024 0.941339 2.22694 5.08507 7.71281 5.01355 1.56935 11.4966

Relax: Age 107.722 (d), Units (GPa) 0.327423 0.75879 1.85384 4.2392 7.64612 5.8679 1.86341 11.9331

Relax: Age 232.079 (d), Units (GPa) 0.290016 0.655347 1.65703 3.71388 7.45375 6.88487 2.37315 11.4866

Following material parameters are changed by the user

D7 Heat Computation Results

D7.1 Temperature curves

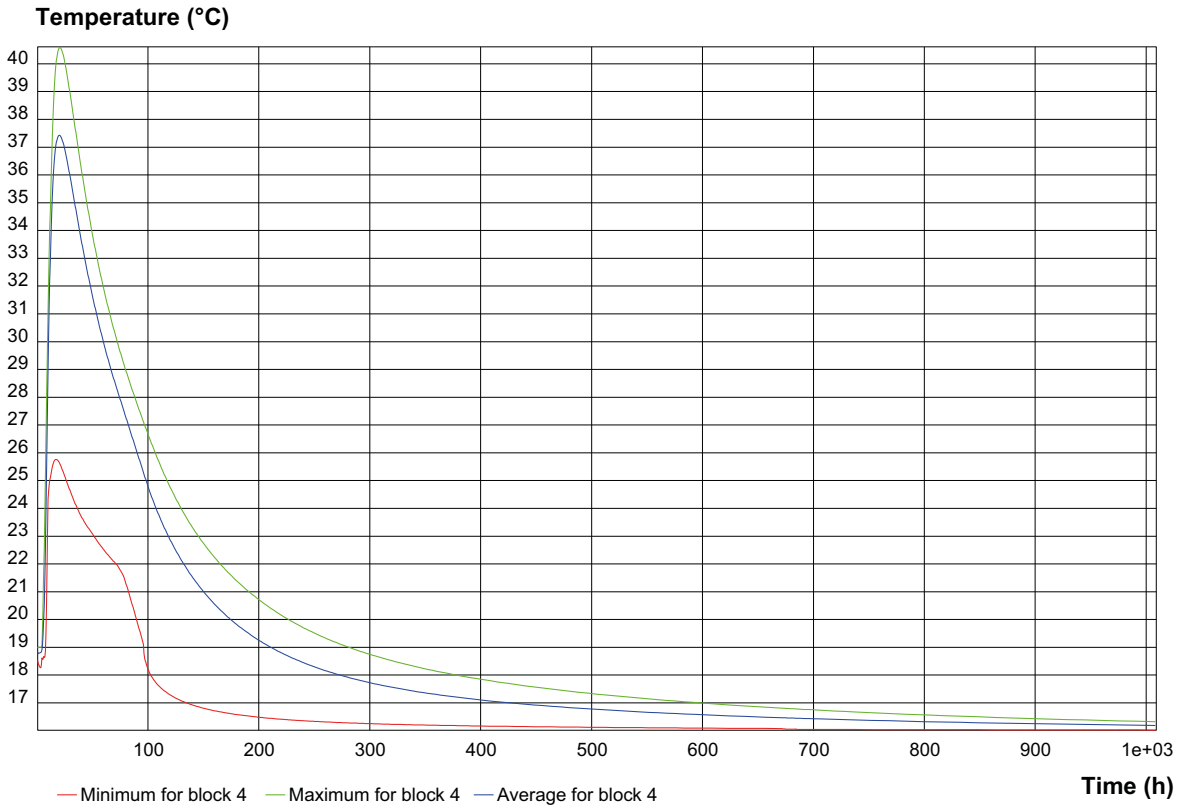

Figure D-6. *Temperature evolution in the base slab (minimum, maximum and average).*

D7.2 Temperature max

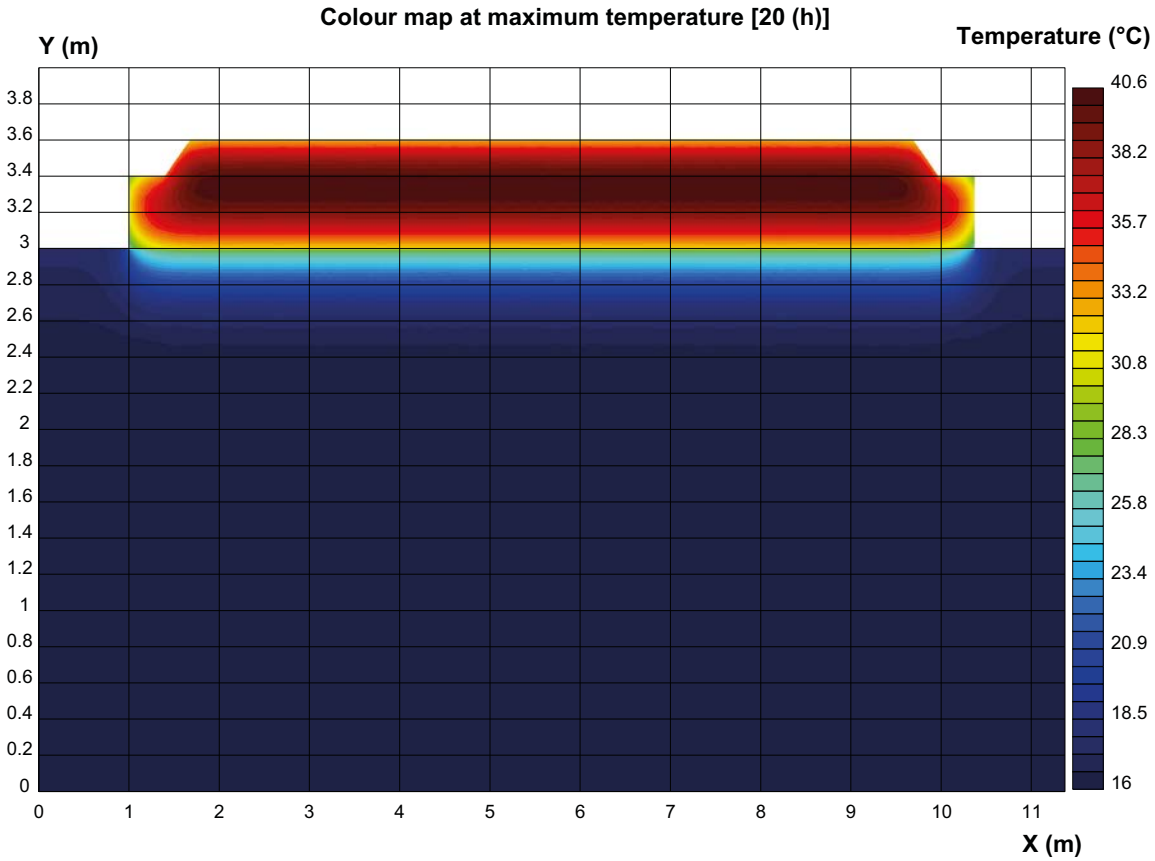

Figure D-7. *Maximum temperature in the base slab at 20 hours after start of casting.*

D7.3 Temperature points

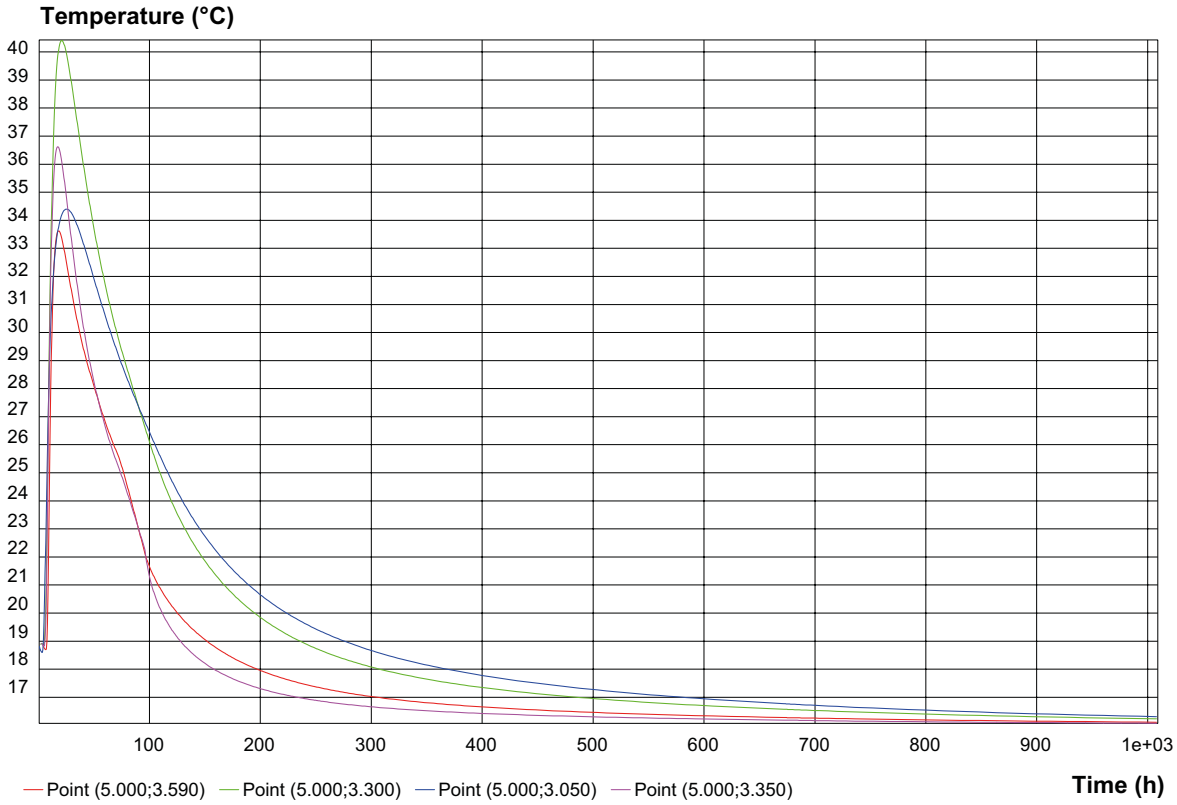

Figure D-8. *Temperature evolution in 4 different positions in the base slab during the first 1 000 hours after start of casting.*

D8 Plane-Surface Computation Results

D8.1 Strain-ratio curves

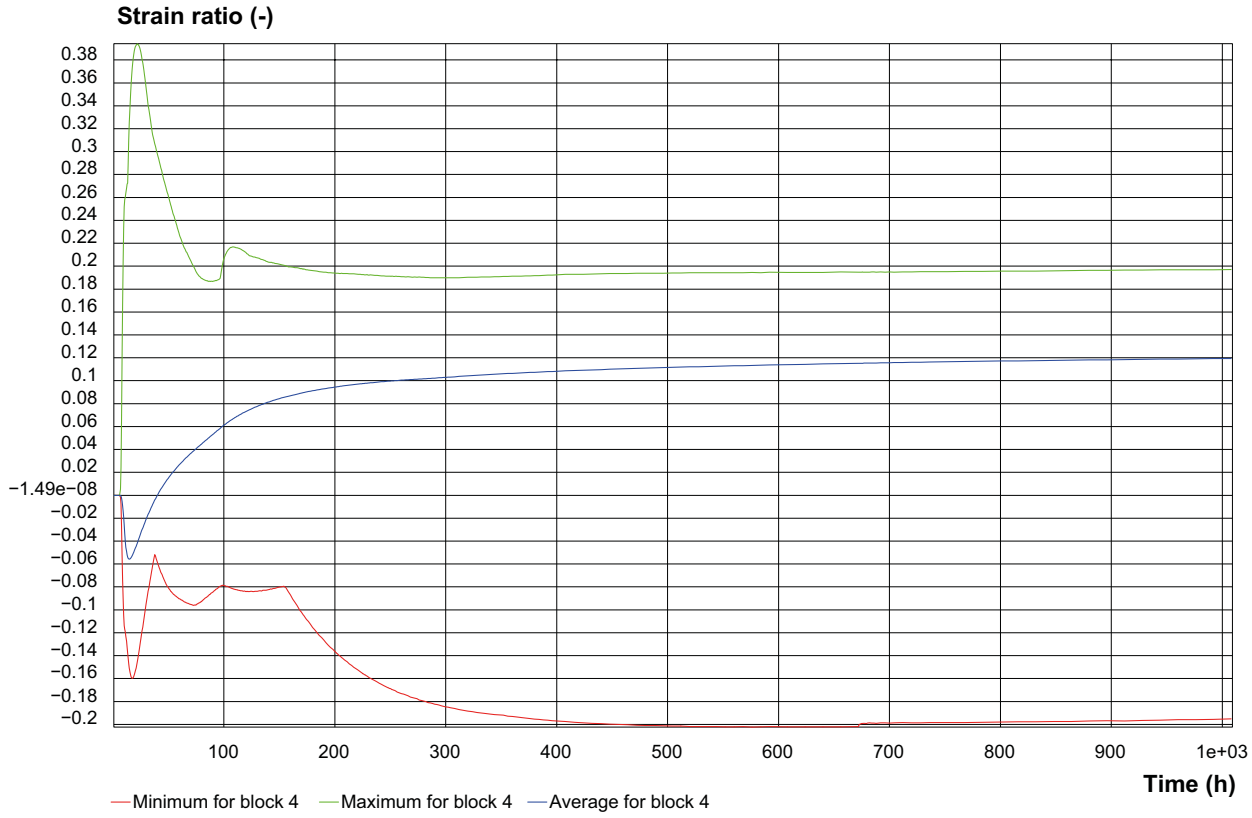

Figure D-9. *Calculated strain ratio in the base slab (minimum, maximum and average).*

D8.2 Strainratio max

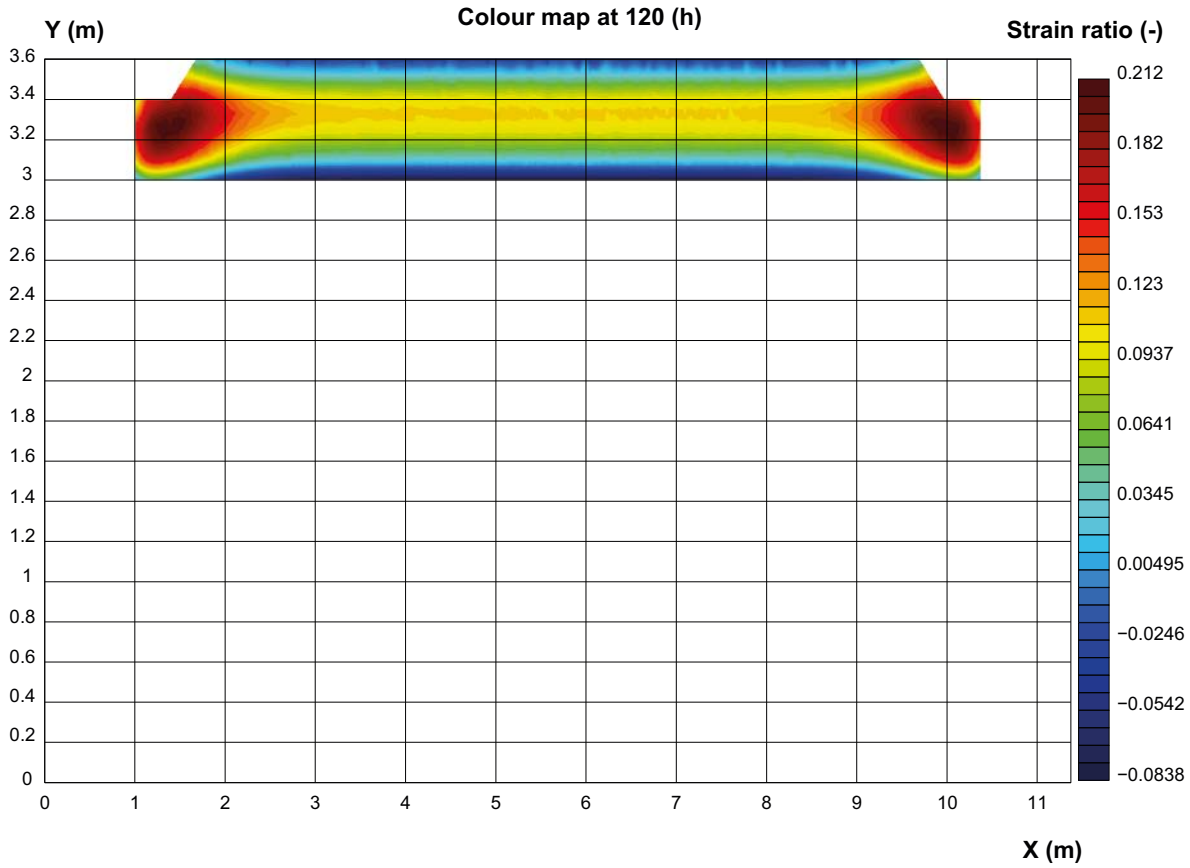

Figure D-10. *Maximum strain ratio in the base slab at 120 hours after start of casting.*

Appendix E

E:TAS08_Wall.CPR: Report

E1 Software & Project Information

E1.1 Software

System name: ConTeSt

System version: 1.0

Developed by: JEJMS Concrete AB

E1.2 1.2 Project

Original filename: D:\Work\SKB\TAS05\TAS05_et1_T.CPR

Created: 2018.06.01 12.34.11

Created by: swecvo on CNU21810QY

Current filename: E:\Work__PE\SKB\TAS_08\TAS08_B15_S16_varm7d_2.CPR

Last change: 2020.02.06 20.54.22

Last change by: swecvo on PC0MLZ09

E2 Geometry & Time

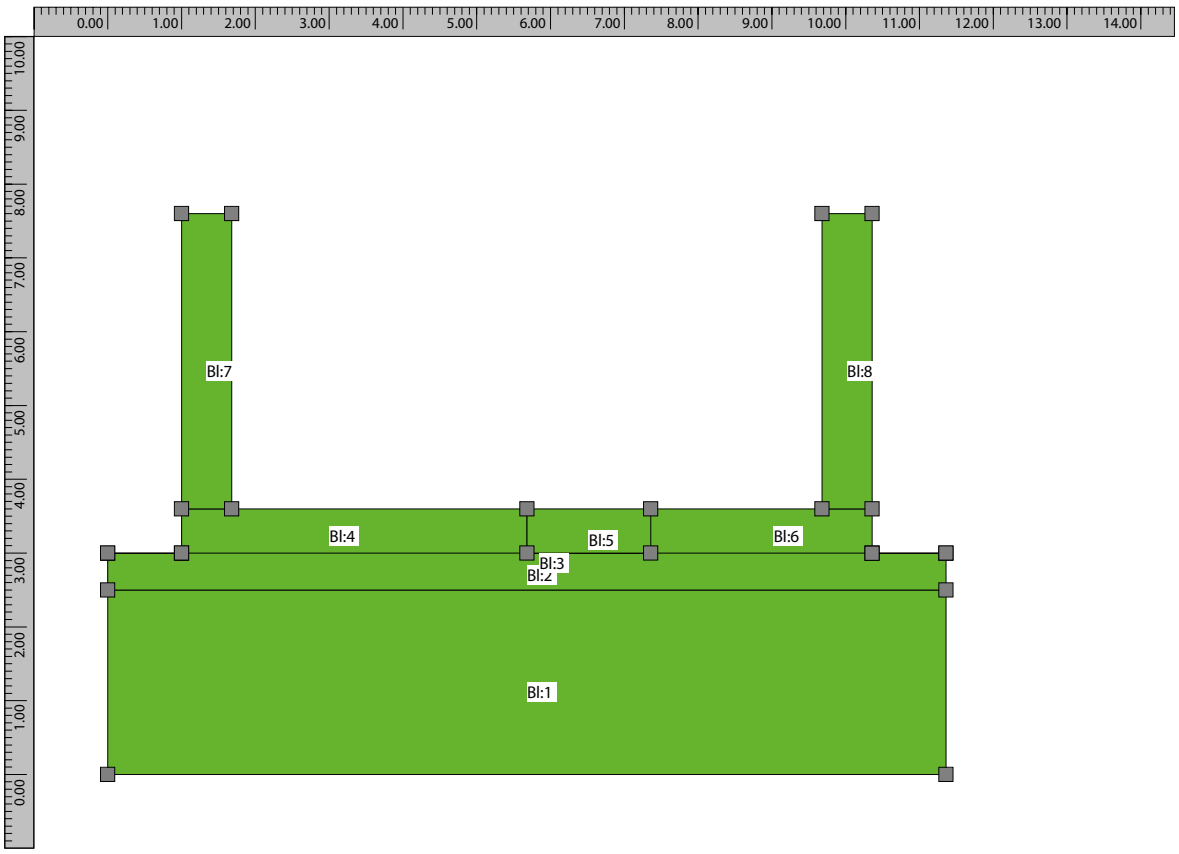

Figure E-1. *Geometry of the base slab and walls.*

E2.1 Description

E2.1.1 Blocks

Block 1: (11.360;0.000) - (11.360;2.500) - (0.000;2.500) - (0.000;0.000)

Block 2: (0.000;2.500) - (11.360;2.500) - (11.360;2.995) - (10.360;2.995) - (1.000;2.995) - (0.000;2.995)

Block 3: (0.000;2.995) - (1.000;2.995) - (10.360;2.995) - (11.360;2.995) - (11.360;3.000) - (10.360;3.000) - (7.360;3.000) - (5.680;3.000) - (1.000;3.000) - (0.000;3.000)

Block 4: (5.680;3.000) - (5.680;3.600) - (1.680;3.600) - (1.000;3.600) - (1.000;3.000)

Block 5: (7.360;3.000) - (7.360;3.600) - (5.680;3.600) - (5.680;3.000)

Block 6: (7.360;3.000) - (10.360;3.000) - (10.360;3.600) - (9.680;3.600) - (7.360;3.600)

Block 7: (1.680;3.600) - (1.680;7.600) - (1.000;7.600) - (1.000;3.600)

Block 8: (10.360;3.600) - (10.360;7.600) - (9.680;7.600) - (9.680;3.600)

E2.1.2 Computation time

Total time length: 1 000 (h)

E3 Element Size

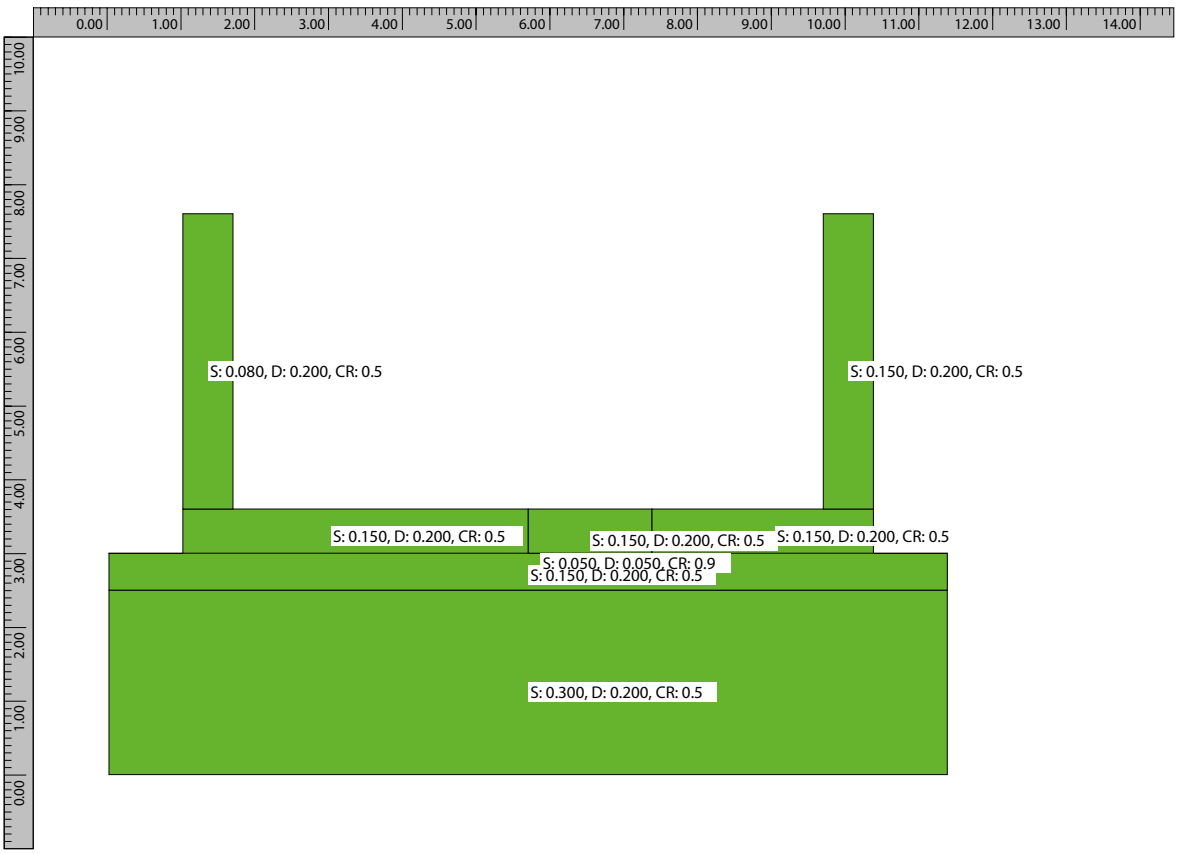

Figure E-2. *Element size for the meshing of the base slab and walls.*

E4 Computation Mesh

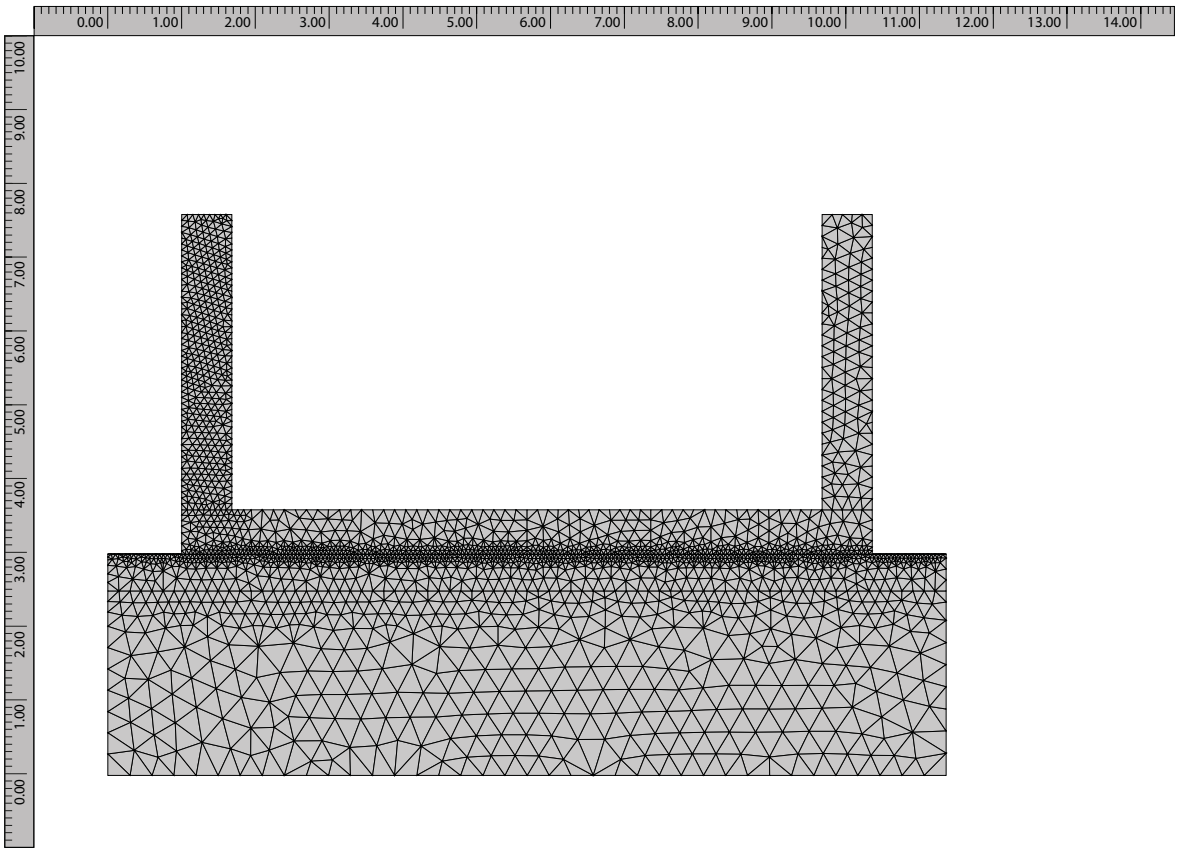

Figure E-3. *Finite element mesh for the base slab and walls.*

E5 Heat Properties

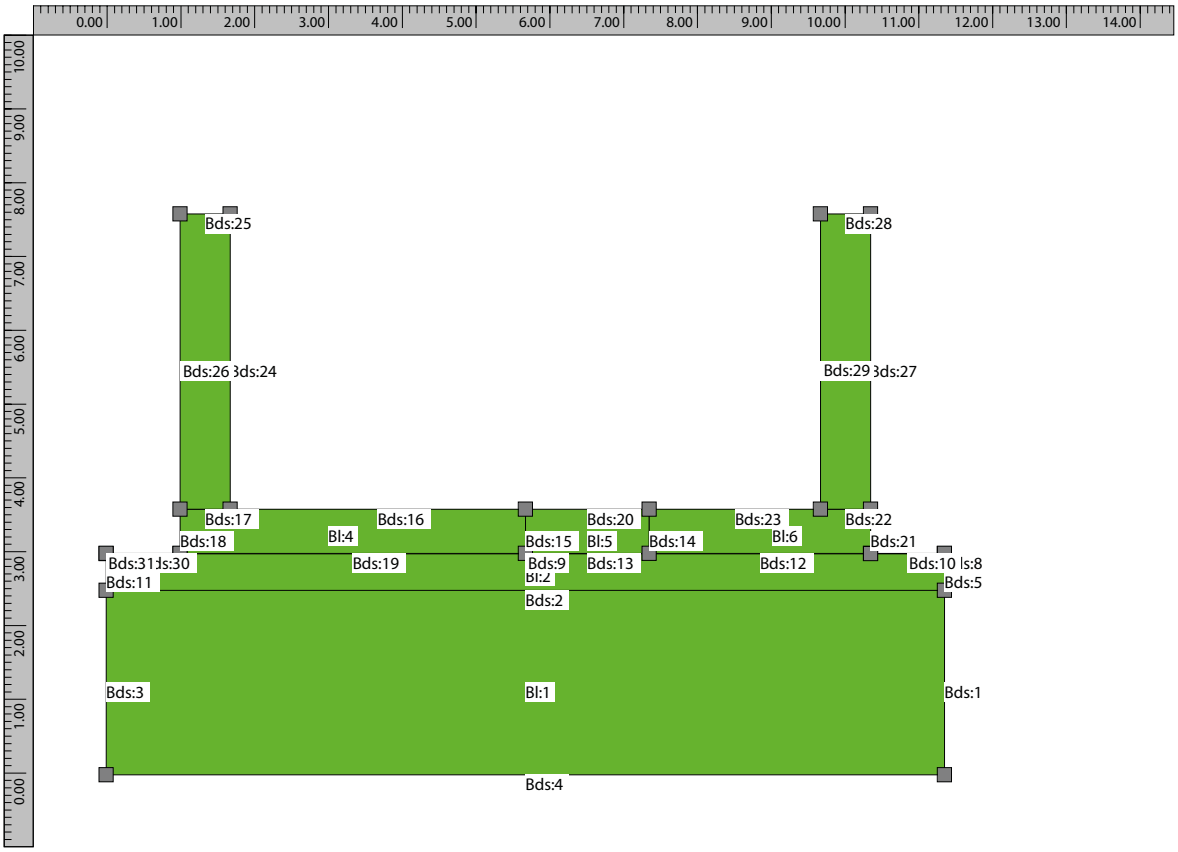

Figure E-4. *List of boundaries for the base slab and walls.*

E5.1 Description

E5.1.1 Block type list

SCC-mod-TAS05: Young concrete

Start temperature:

Constant: 16.0

Material definition: K45 vct = 0.47 Lufttillsats (Mix 4) (str)

Source

Luleå Tekniska Universitet

Provningar 1999, 2000 – LTU, Skrift 00:02

Recept Sweroc

Description

Degerhamn Std P (Anläggningscement)

vct 0.47

Köping 500 (Kalkfiller)

lufthalt 4.5 á 5.0 %

flytsättmått 700–750 mm

Original material parameters

Density: 2 350 (kg/m³), Heat cap. 1 000 (J/(kg·K))

Heat cond. (W/m²K) as piece-wise linear function of equivalent time of maturity (h), (equ. time; heat cond.): (0;2.1), (12;2.1), (24;1.7), (10000;1.7),

C 363 (kg/m³), Wc 325 000 (J/kg), Lambda1 1.02 (-), t1 9.15 (h), Kappa1 1.94 (-)

te0 0 (h), BetaD 1 (-), ThetaRef 3 660 (K), Kappa3 0.653 (-)

Eta6 4 (‰), Eta8 10 (‰), Eta12 106 (‰), Eta18 198 (‰), Eta24 262 (‰), Eta72 562 (‰), Eta168 791 (‰)

Fcc28 68 (MPa)

Following material parameters are changed by the user

C 320 (kg/m³)

Wc 250 000 (J/kg)

te0 −4 (h)

BetaD 2 (-)

Fcc28 50 (MPa)

Mature concrete: Other material

Start temperature:

Constant: 16.0

Material definition: Mature C35/45 w0/C = 0.40 AEA (str)

Source

Luleå University of Technology, Sweden

Tests during 1995 to 2004

Adjustment to a “general” data base 2006

Description

Moderate heat cement (Degerhamn OPC) from Cementa AB in Sweden.

Primarily aimed for use in civil engineering structures.

Original material parameters

Density: 2 350 (kg/m³), Heat cap. 1 000 (J/(kg·K))

Heat cond. (W/m²K) as piece-wise linear function of equivalent time of maturity (h), (equ. time; heat cond.): (0;1.7), (12;2.1), (24;1.7), (10000;1.7),

Blinding: Other material

Start temperature:

Constant: 16.0

Material definition: Mature C28/35 w0/C = 0.55 AEA (str)

Source

Luleå University of Technology, Sweden

Tests during 1995 to 2004

Adjustment to a “general” data base 2006

Description

Moderate heat cement (Degerhamn OPC) from Cementa AB in Sweden.

Primarily aimed for use in civil engineering structures.

Original material parameters

Density: 2 350 (kg/m³), Heat cap. 1 000 (J/(kg·K))

Heat cond. (W/m²K) as piece-wise linear function of equivalent time of maturity (h), (equ. time; heat cond.): (0;1.7), (12;2.1), (24;1.7), (10000;1.7),

Rock: Other material

Start temperature:

Constant: 16.0

Material definition: Rock (str)

Source

Luleå University of Technology 1997

Description

Original material parameters

Density: 2 650 (kg/m³), Heat cap. 850 (J/(kg·K))

Heat cond. 3.7 (W/m²K)

C35/45 ERM: Young concrete

Start temperature:

Constant: 15.0

Material definition: C35/45 w0/C = 0.40 Air entrainment (str)

Source

Luleå University of Technology, Sweden

Tests during 1995 to 2004

Adjustment to a “general” data base 2006

Description

Moderate heat cement (Degerhamn OPC) from Cementa AB in Sweden.

Primarily aimed for use in civil engineering structures.

Original material parameters

Density: 2 350 (kg/m³), Heat cap. 1 000 (J/(kg·K))

Heat cond. (W/m²K) as piece-wise linear function of equivalent time of maturity (h), (equ. time; heat cond.): (0;2.1), (96;2.1), (120;1.7), (10000;1.7), C 430 (kg/m³), Wc 325 000 (J/kg), Lambda1 2.2 (-), t1 4.75 (h), Kappa1 1.65 (-) te0 0 (h), BetaD 1 (-), ThetaRef 4 200 (K), Kappa3 0.5 (-) s 0.331 (-), tS 5.556 (h), tA 8.334 (h), nA 1.148 (-) Lambda2 0 (-), Tr2 1 (°C), Kappa2 0 (-) Fcc28 53 (MPa)

Following material parameters are changed by the user

C 400 (kg/m³)

Foil double: Other material

Start temperature:

Constant: 15.0

Material definition: Insulation material

Source

Luleå University of Technology 1999

Description

Cellular plastic

Original material parameters

Density: 25 (kg/m³), Heat cap. 1 500 (J/(kg·K))

Heat cond. 0.036 (W/m²K)

Following material parameters are changed by the user

Density: 250 (kg/m³)

Heat cond. 0.1 (W/m²K)

E5.1.2 Block connection list

Block 1: Rock

Block 2: Rock

Block 3: Foil double

Block 4: mature concrete

Block 5: mature concrete

Block 6: mature concrete

Block 7: SCC-mod-TAS05, simulate filling

Block 8: SCC-mod-TAS05, simulate filling

E5.1.3 Boundary type list

free surface

Temperature

Piece-wise linear (time (h);temp. (°C))

(0;18) (200;18) (224;18) (248;20) (272;20) (296;16)

Wind velocity

Constant 1 (m/s)

Heat transfer coefficient

Constant 30 (W/m²K)

Supplied heat

Constant 0 (W/m²)

Rock

Temperature

Constant 16 (°C)

Heat transfer coefficient

Constant 80 (W/m²K)

Supplied heat

Constant 0 (W/m²)

Form wall 21 mm
- Temperature
  - Piece-wise linear (time (h);temp. (°C))
    (0;18) (200;18) (224;18) (248;20) (272;20) (296;16)
- Wind velocity
  - Constant 1 (m/s)
- Heat transfer coefficient
  - Piece-wise constant (time (h);htc (W/m²K))
    (0:6.66667)
      Wood 0.021 (m)
    (368:500)
      Free Surface
- Supplied heat
  - Constant 0 (W/m²)

Form corner 40 mm
- Temperature
  - Piece-wise linear (time (h);temp. (°C))
    (0;18) (24;18) (48;20) (72;20) (96;16)
- Wind velocity
  - Constant 2 (m/s)
- Heat transfer coefficient
  - Piece-wise constant (time (h);htc (W/m²K))
    (0:3.5)
      Wood 0.04 (m)
    (168:500)
      Free Surface
- Supplied heat
  - Constant 0 (W/m²)

Form slab top 12 mm
- Temperature
  - Piece-wise linear (time (h);temp. (°C))
    (0;18) (24;20) (48;20) (72;17)
- Wind velocity
  - Constant 2 (m/s)
- Heat transfer coefficient
  - Piece-wise constant (time (h);htc (W/m²K))
    (0:11.6667)
      Wood 0.012 (m)
    (30:500)
      Free Surface
- Supplied heat
  - Constant 0 (W/m²)

Form slab boxout 40 mm
- Temperature
  - Piece-wise linear (time (h);temp. (°C))
    (0;18) (24;20) (48;20) (72;17)
- Wind velocity
  - Constant 2 (m/s)
- Heat transfer coefficient
  - Piece-wise constant (time (h);htc (W/m²K))
    (0:3.5)
      Wood 0.04 (m)
    (168:500)
      Free Surface
- Supplied heat
  - Constant 0 (W/m²)

varmematta 7d
- Temperature
  - Constant 18 (°C)
- Wind velocity
  - Constant 1 (m/s)
- Heat transfer coefficient
  - Piece-wise constant (time (h);htc (W/m²K))
    (0:2)
      Expanded polyethylene 0.02 (m)
    (248:500)
      Free Surface
- Supplied heat
  - Piece-wise constant (time (h);power (W/m²))
    (0;0) (32;100) (224;0)

Form wall 21 mm in
- Temperature
  - Piece-wise linear (time (h);temp. (°C))
    (0;18) (190;18) (200;25) (224;26) (248;26) (272;25) (296;16)
- Wind velocity
  - Constant 1 (m/s)
- Heat transfer coefficient
  - Piece-wise constant (time (h);htc (W/m²K))
    (0:6.66667)
      Wood 0.021 (m)
    (368:500)
      Free Surface
- Supplied heat
  - Constant 0 (W/m²)

Moving Boundary: Moving boundary

Temperature

Constant 18 (°C)

Wind velocity

Constant 1 (m/s)

Heat transfer coefficient

Piece-wise constant (time (h);htc (W/m²K))

(0:2)

Expanded polyethylene 0.02 (m)

(177:500)

Free Surface

Supplied heat

Piece-wise constant (time (h);power (W/m²))

(0;0) (32;100) (177;0)

E5.1.4 Boundary connection list

Boundary segment 1: adiabatic (no heat flow)

Boundary segment 2: inner segment (full thermal contact)

Boundary segment 3: adiabatic (no heat flow)

Boundary segment 4: Rock

Boundary segment 5: adiabatic (no heat flow)

Boundary segment 6: inner segment (full thermal contact)

Boundary segment 7: inner segment (full thermal contact)

Boundary segment 8: adiabatic (no heat flow)

Boundary segment 9: inner segment (full thermal contact)

Boundary segment 10: free surface

Boundary segment 11: adiabatic (no heat flow)

Boundary segment 12: inner segment (full thermal contact)

Boundary segment 13: inner segment (full thermal contact)

Boundary segment 14: inner segment (full thermal contact)

Boundary segment 15: inner segment (full thermal contact)

Boundary segment 16: varmematta 7d

Boundary segment 17: inner segment (full thermal contact)

Boundary segment 18: Form wall 21 mm

Boundary segment 19: inner segment (full thermal contact)

Boundary segment 20: varmematta 7d

Boundary segment 21: Form wall 21 mm

Boundary segment 22: inner segment (full thermal contact)

Boundary segment 23: varmematta 7d

Boundary segment 24: Form wall 21 mm in

Boundary segment 25: free surface

Boundary segment 26: Form wall 21 mm

Boundary segment 27: Form wall 21 mm

Boundary segment 28: free surface

Boundary segment 29: Form wall 21 mm in

Boundary segment 30: free surface

Boundary segment 31: adiabatic (no heat flow)

E5.1.5 Inner point type list

E5.1.6 Simulation of filling process for young concrete

Surface position as a piece-wise linear func. of time (time (h); y-coord. (m)) (0;3.6), (200;3.6), (210;7.6),

E6 Plane-Surface Analysis

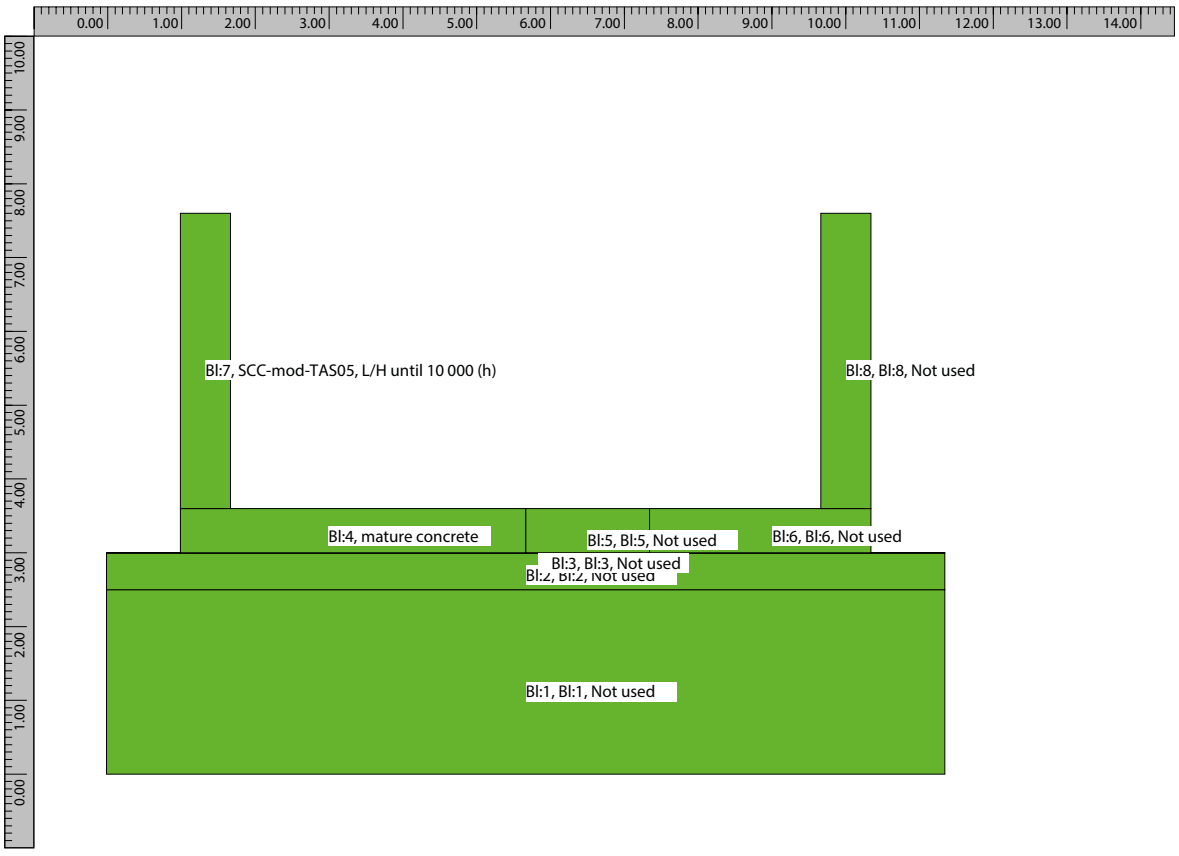

Figure E-5. *Blocks used in the calculations of stresses in the walls and base slab.*

E6.1 Description

E6.1.1 Stress case

Default time stepping

Translation

Constant = 0.170

Rotation around X-axis

Free (0.000)

Rotation around Y-axis

Full restraint (1.000)

Resilience: LH-based

Structure length: 18.100 (m)

Data source: Standard

Resilience reduction length and width dependent

Data source: External file C:\Program Files (x86)\ConTeSt\redH4.0m.rrt

Length = 0.000 (m) : [width(m),red]
(0.400;0.500) (0.800;0.500) (1.200;0.500)
Length = 4.000 (m) : [width(m),red]
(0.400;0.500) (0.800;0.500) (1.200;0.500)
Length = 8.000 (m) : [width(m),red]
(0.400;0.720) (0.800;0.750) (1.200;0.780)
Length = 20.000 (m) : [width(m),red]
(0.400;1.000) (0.800;1.000) (1.200;1.000)

E6.1.2 Block data list

Block 4: mature concrete

Block 7: SCC-mod-TAS05, L/H until 10 000 (h)

E6.1.3 Block type list

SCC-mod-TAS05: Young concrete

Material definition: K45 vct = 0.47 Lufttillsats (Mix 4) (str)

Source

Luleå Tekniska Universitet
Provningar 1999, 2000 – LTU, Skrift 00:02
Recept Sweroc

Description

Degerhamn Std P (Anläggningscement)
vct 0.47
Köping 500 (Kalkfiller)
lufthalt 4.5 á 5.0 %
flytsättmått 700–750 mm

Original material parameters

Po-ratio 0.18 (-), AlfaHeat 9.7e−06 (1/K), AlfaCool 9.7e−06 (1/K)
ThetaT 5 000 (K), RelaxTime1 0.005 (d), TimeZero 0.36 (d)
Fcc28 68 (MPa), Fcref 62 (MPa), Ftref 3.87 (MPa)
Beta1 0.667 (-), Alfact 0.7 (-), RaaT 0 (-), RaaFi 0 (-)

KFi 2 (-), Eps1 0 (-), TimeS1 6 (h)

Eps2 −0.000165 (-), TimeS2 8 (h), ThetaSH 120 (h), EthaSH 0.3 (-)

Relax: Age 0.359 (d), Units (GPa) 0.01 0.01 0.01 0.01 0.01 0.01 0.01 0.01

Relax: Age 0.54 (d), Units (GPa) 3.0184 2.3761 3.6531 2.5385 1.3421 1.7683 1.6167 1.3048

Relax: Age 1.163 (d), Units (GPa) 3.2785 2.9128 4.1142 2.9953 2.2954 2.5047 2.4411 1.844

Relax: Age 2.506 (d), Units (GPa) 3.3589 3.3689 4.2389 3.6801 3.5409 3.4482 3.4996 2.4096

Relax: Age 5.4 (d), Units (GPa) 2.6217 2.9505 3.7231 3.9755 4.2461 3.8967 4.0385 3.8283

Relax: Age 11.634 (d), Units (GPa) 2.0163 2.4072 3.248 3.7368 4.0717 3.7562 3.8959 7.4188

Relax: Age 25.065 (d), Units (GPa) 1.5407 1.9199 2.7174 3.3638 3.8489 3.5998 3.7423 10.7153

Relax: Age 54 (d), Units (GPa) 1.1889 1.5262 2.2351 2.9238 3.5773 3.4565 3.6112 13.5493

Relax: Age 116.339 (d), Units (GPa) 0.9389 1.2286 1.8461 2.5009 3.2669 3.3372 3.5338 15.8386

Relax: Age 250.646 (d), Units (GPa) 0.7655 1.014 1.5523 2.1504 2.9475 3.232 3.5329 17.5812

Following material parameters are changed by the user

Fcc28 50 (MPa)

Fcref 50 (MPa)

mature concrete: Other material

Material definition: Mature C35/45 w0/C = 0.40 AEA (str)

Source

Luleå University of Technology, Sweden

Tests during 1995 to 2004

Adjustment to a “general” data base 2006

Description

Moderate heat cement (Degerhamn OPC) from Cementa AB in Sweden.

Primarily aimed for use in civil engineering structures.

Original material parameters

Po-ratio 0.18 (-), E-modulus 34.4 (GPa), AlfaHeat 1e−05 (1/K)

Fcc 53 (MPa), Ftref 3.68 (MPa)

Blinding: Other material

Material definition: Mature C28/35 w0/C = 0.55 AEA (str)

Source

Luleå University of Technology, Sweden

Tests during 1995 to 2004

Adjustment to a “general” data base 2006

Description

Moderate heat cement (Degerhamn OPC) from Cementa AB in Sweden.

Primarily aimed for use in civil engineering structures.

Original material parameters

Po-ratio 0.18 (-), E-modulus 32.6 (GPa), AlfaHeat 1e−05 (1/K)

Fcc 43 (MPa), Ftref 3.21 (MPa)

Rock: Other material

Material definition: Rock (str)

Source

Luleå University of Technology 1997

Description

Original material parameters

Po-ratio 0.2 (-), E-modulus 30 (GPa), AlfaHeat 1e−05 (1/K)

Fcc 30 (MPa), Ftref 3 (MPa)

C35/45 ERM: Young concrete

Material definition: C35/45 w0/C = 0.40 Air entrainment (str)

Source

Luleå University of Technology, Sweden

Tests during 1995 to 2004

Adjustment to a “general” data base 2006

Description

Moderate heat cement (Degerhamn OPC) from Cementa AB in Sweden.

Primarily aimed for use in civil engineering structures.

Original material parameters

Po-ratio 0.18 (-), AlfaHeat 1.1e−05 (1/K), AlfaCool 9e−06 (1/K)

ThetaT 5 000 (K), RelaxTime1 0.005 (d), TimeZero 0.25 (d)

Fcc28 53 (MPa), Fcref 53 (MPa), Ftref 3.68 (MPa)

Beta1 0.667 (-), Alfact 0.9 (-), RaaT 0 (-), RaaFi 0.9 (-)

KFi 2 (-), Eps1 0 (-), TimeS1 6 (h)

Eps2 −0.0001368 (-), TimeS2 24 (h), ThetaSH 120 (h), EthaSH 0.3 (-)

Relax: Age 0.249 (d), Units (GPa) 0.01 0.01 0.01 0.01 0.01 0.01 0.01 0.01

Relax: Age 0.5 (d), Units (GPa) 0.857221 0.256405 3.50511 1.16388 0.786528 0.439177 0.122558 0.101706

Relax: Age 1.077 (d), Units (GPa) 2.67304 4.80813 9.03774 3.7919 4.01799 2.19963 0.705556 0.754292

Relax: Age 2.321 (d), Units (GPa) 2.11587 4.25012 8.20966 7.23161 6.34904 3.5086 1.10078 0.684051

Relax: Age 5 (d), Units (GPa) 1.26691 2.75358 5.95473 8.32677 7.27362 3.96807 1.25504 3.14366

Relax: Age 10.772 (d), Units (GPa) 0.801966 1.78874 4.18532 7.43422 7.50287 4.12974 1.31843 7.05465

Relax: Age 23.208 (d), Units (GPa) 0.539145 1.25091 2.9427 6.22062 7.65742 4.43895 1.40975 9.90401

Relax: Age 50 (d), Units (GPa) 0.399024 0.941339 2.22694 5.08507 7.71281 5.01355 1.56935 11.4966

Relax: Age 107.722 (d), Units (GPa) 0.327423 0.75879 1.85384 4.2392 7.64612 5.8679 1.86341 11.9331

Relax: Age 232.079 (d), Units (GPa) 0.290016 0.655347 1.65703 3.71388 7.45375 6.88487 2.37315 11.4866

Following material parameters are changed by the user

E7 Heat Computation Results

E7.1 Temperature curves

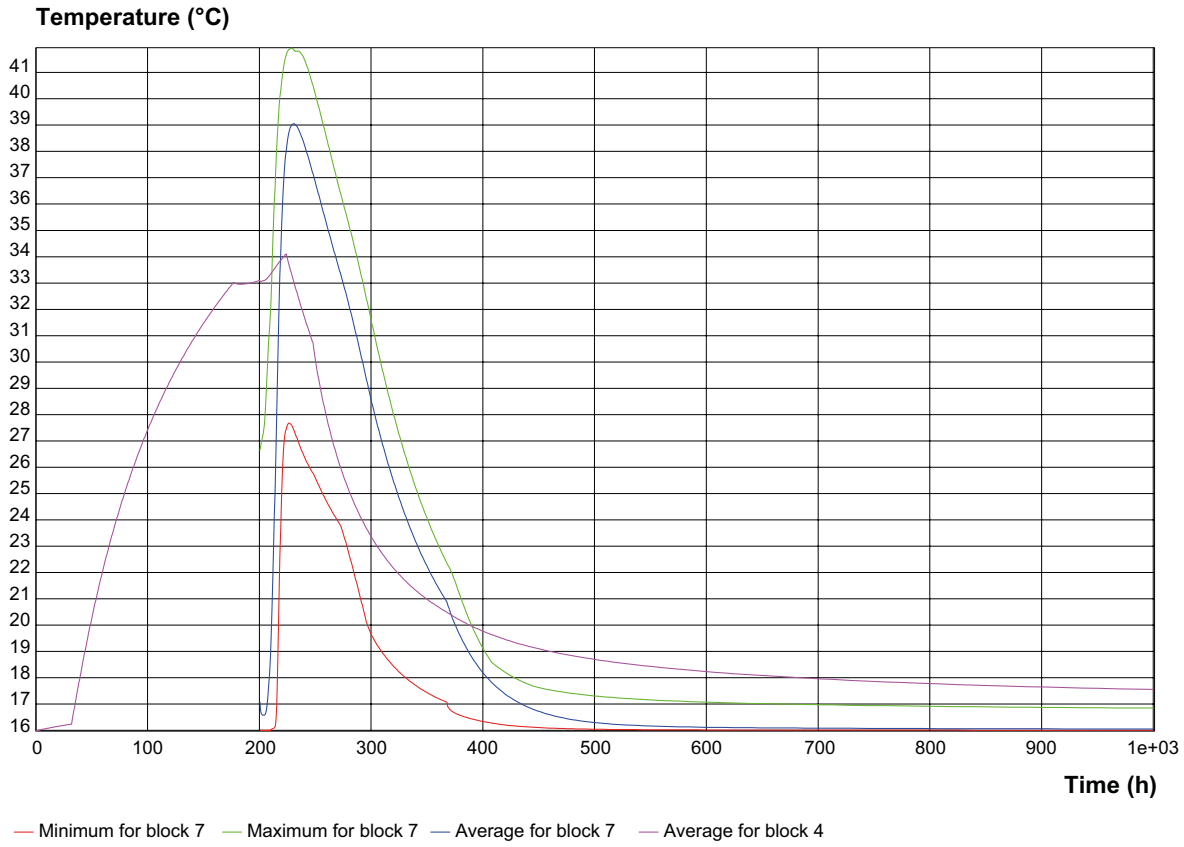

Figure E-6. *Temperature evolution in the walls (minimum, maximum and average).*

E7.2 Temp gjutstart

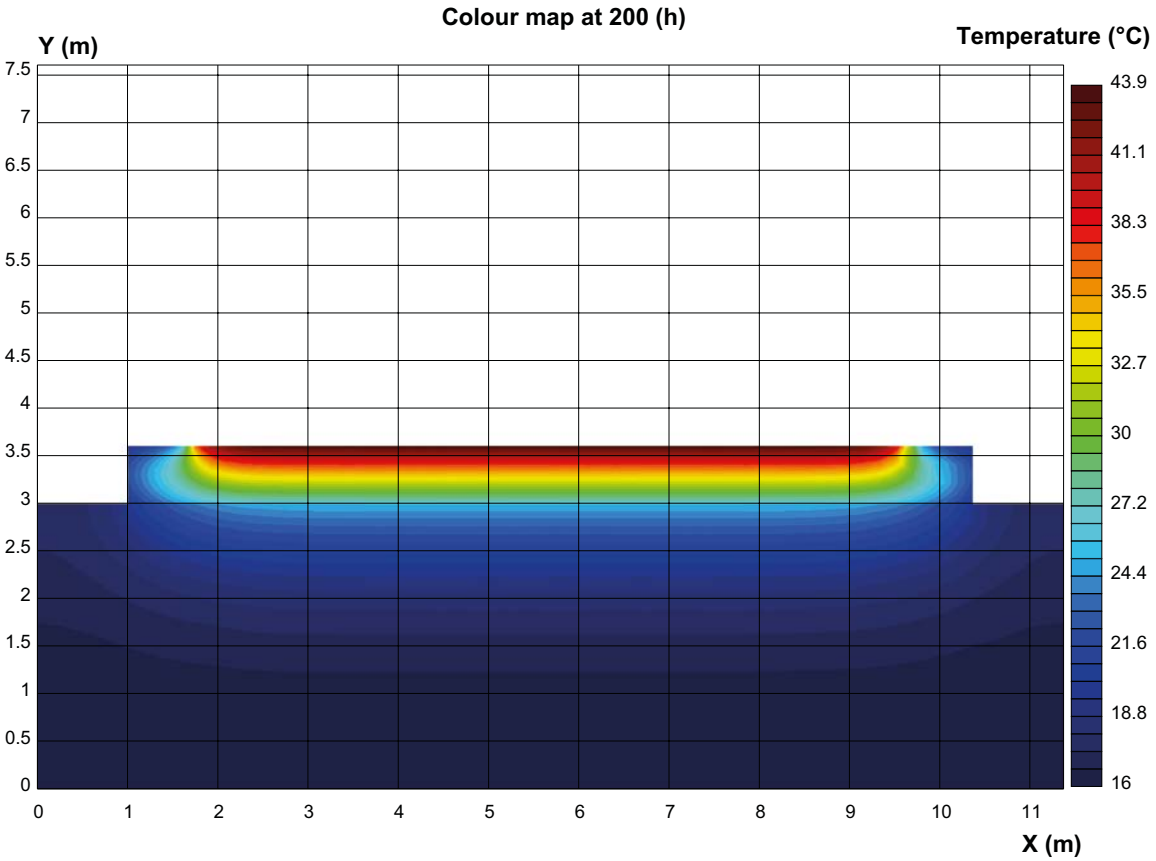

Figure E-7. *Temperature in the base slab after heating for 1 week.*

7.3 Temp max

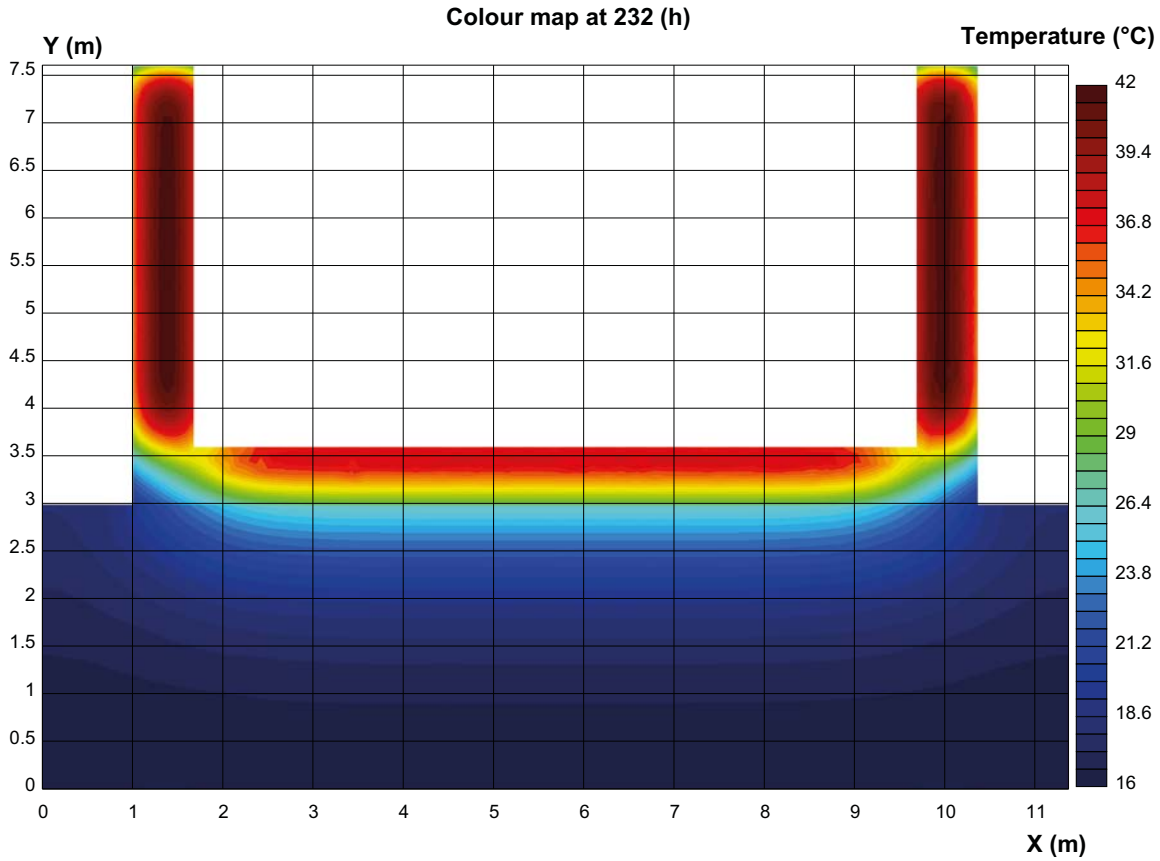

Figure E-8. *Maximum temperature in the walls and base slab.*

7.4 Tempcurves slab

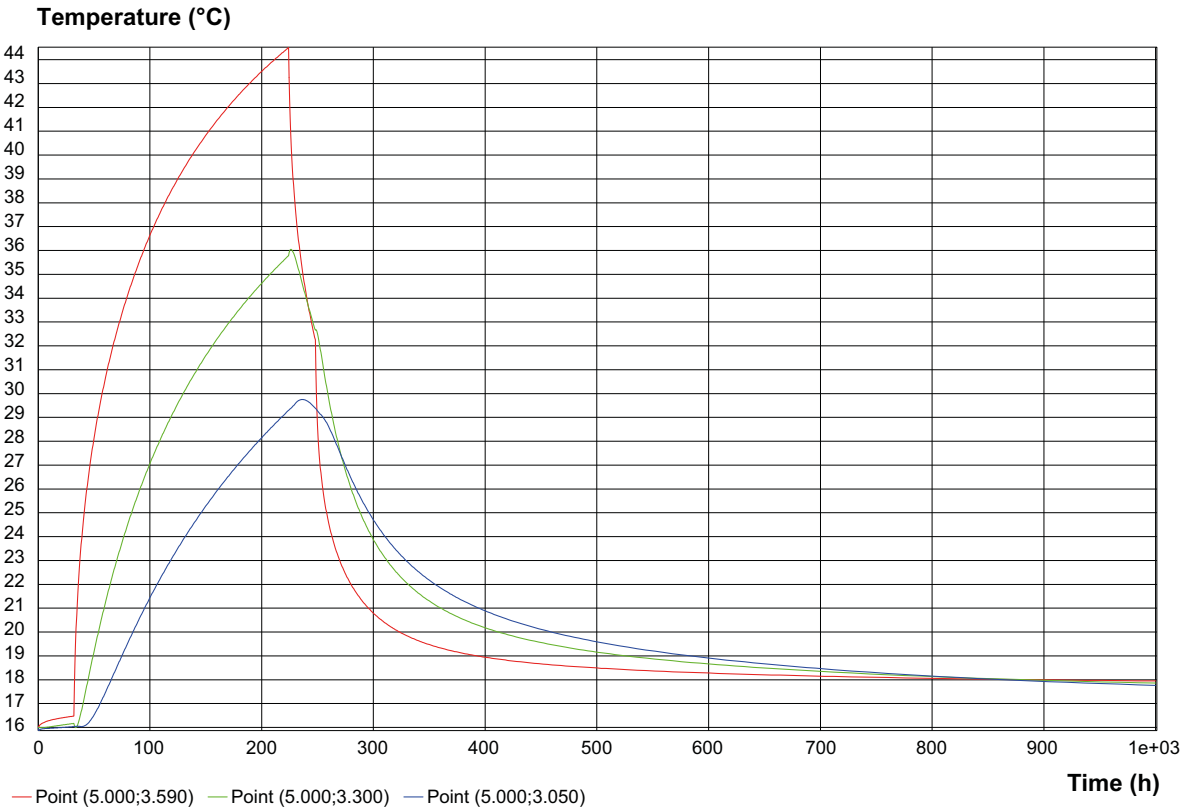

Figure E-9. *Temperature evolution in 3 different points in the base slab.*

7.5 Tempcurves wall

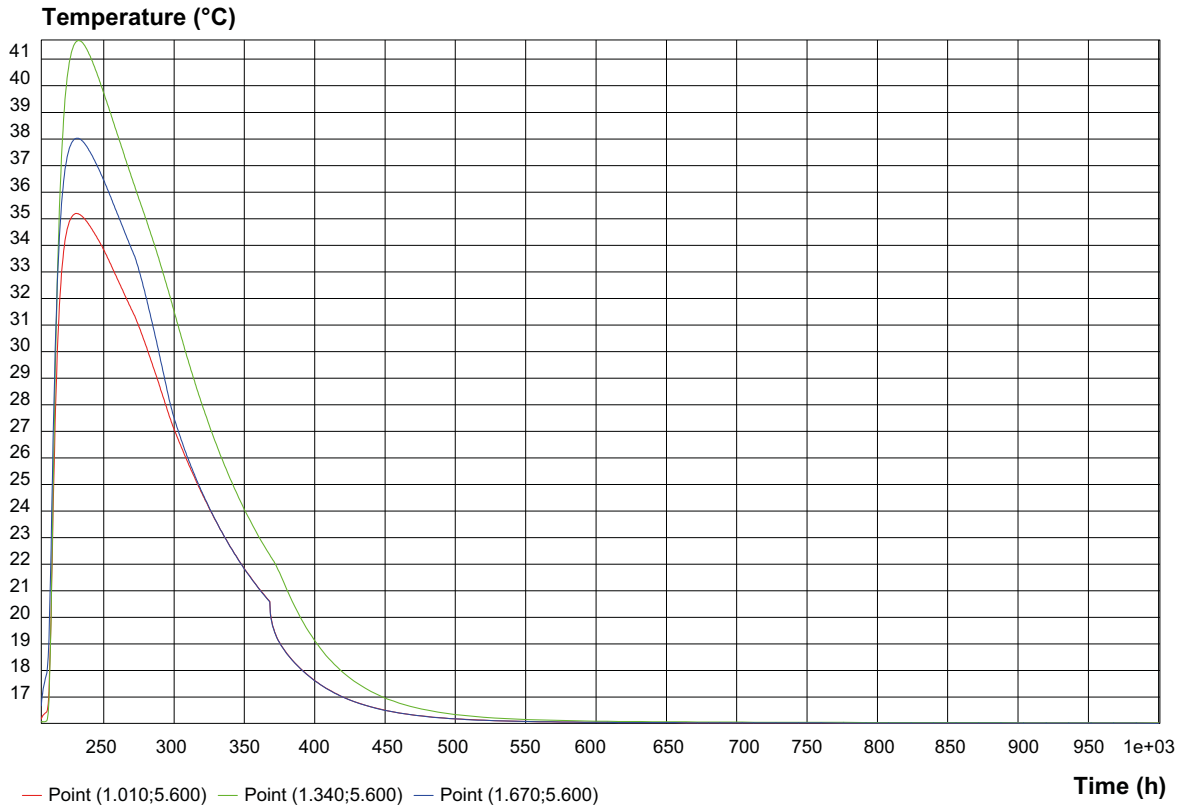

Figure E-10. *Temperature evolution in 3 different points in the walls.*

E8 Plane-Surface Computation Results

E8.1 Strain-ratio curves

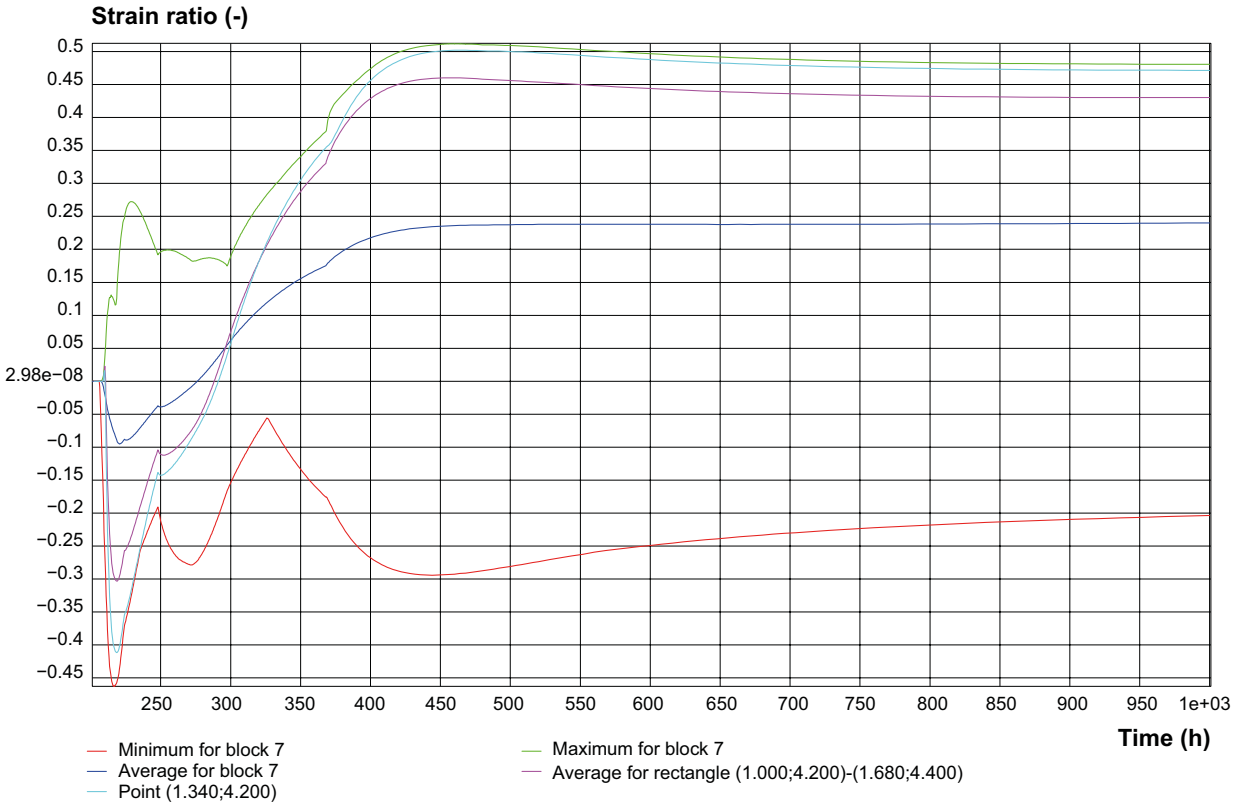

Figure E-11. *Calculated strain ratio in the walls.*

E8.2 Strainratio max

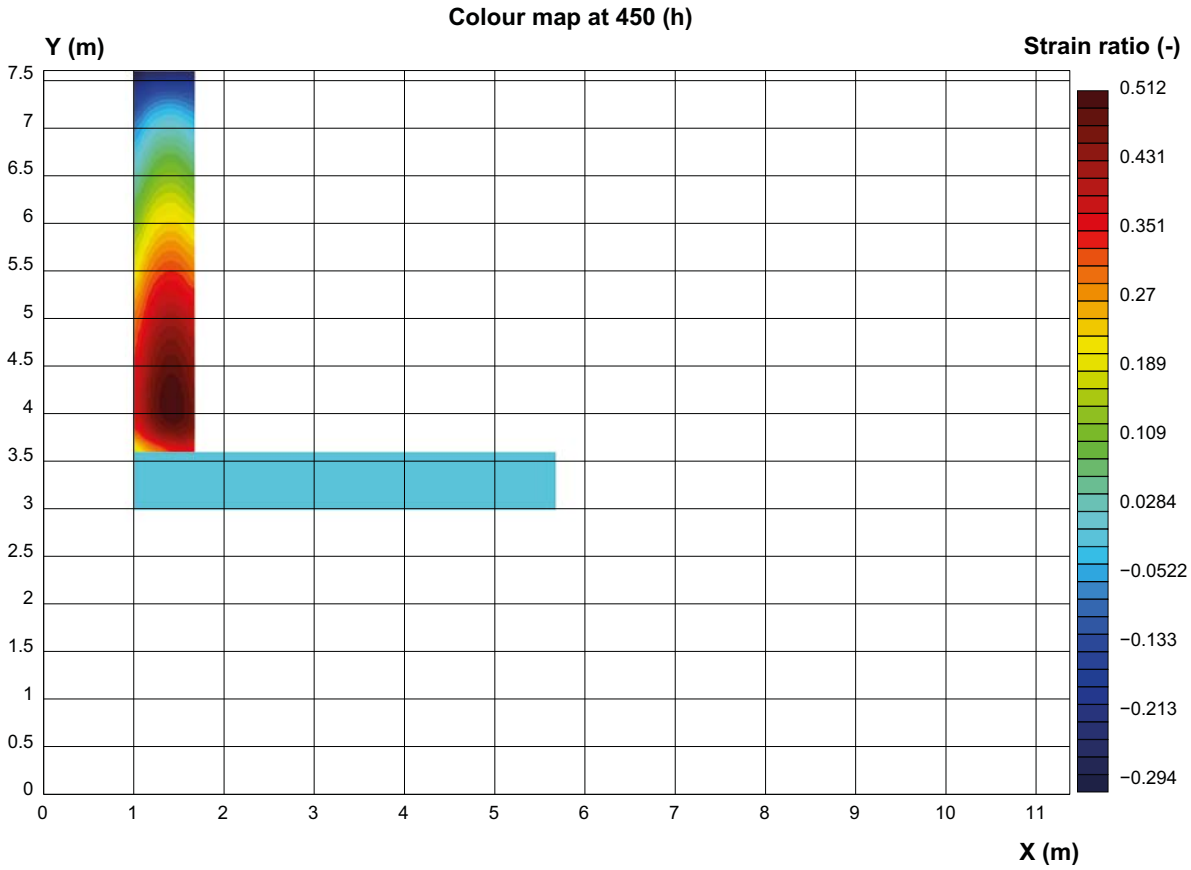

Figure E-12. *Maximum calculated strain ratio in the walls.*

Arkitektkopia AB, Bromma, 2020

SKB is responsible for managing spent nuclear fuel and radioactive waste produced by the Swedish nuclear power plants such that man and the environment are protected in the near and distant future.

skb.se